Peeling the onion

Unravelling the biology of fungal onion pathogens causing leaf blight, neck rot and white rot

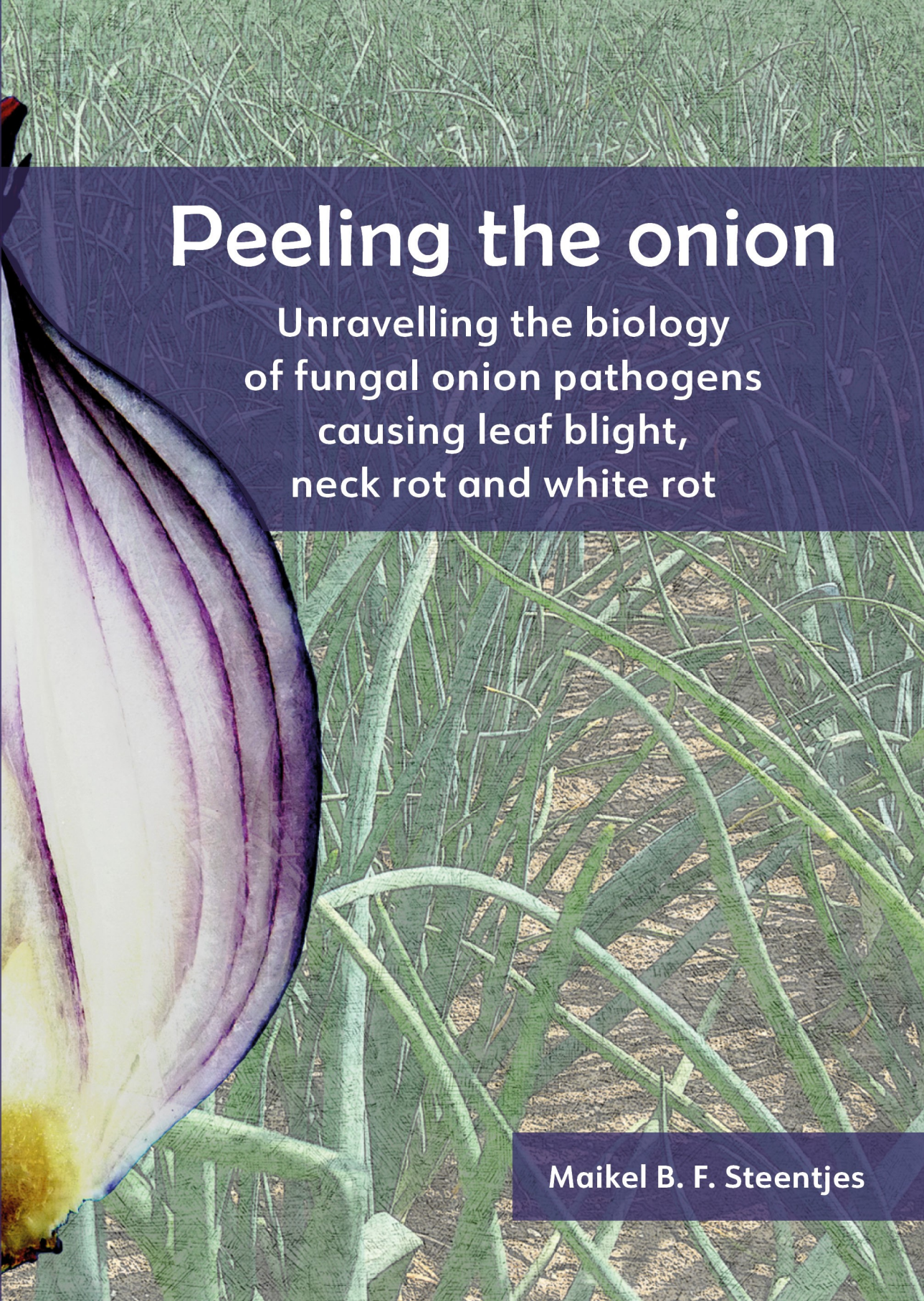

Maikel B. F. Steentjes

Propositions

1. *Botrytis* is not a genus of necrotrophic fungi.
   (this thesis)

2. The host range of *Botrytis* species is a polygenic trait.
   (this thesis)

3. Evaluating research proposals on applicability hampers scientific progress.

4. The craving of biologists to classify observations into confined categories limits scientific creativity.

5. Governmental regulation of the price of meat is required to enable sustainable livestock farming.

6. Wildlife rescue operations weaken animal populations by interfering with natural selection.

Propositions belonging to the thesis, entitled

Peeling the onion – Unravelling the biology of fungal onion pathogens causing leaf blight, neck rot and white rot

Maikel B. F. Steentjes
Wageningen, 28 June 2021

Peeling the onion

Unravelling the biology of fungal onion pathogens causing leaf blight, neck rot and white rot

Maikel B. F. Steentjes

Thesis committee

Promotor
Dr Jan A.L. van Kan
Associate Professor at the Laboratory of Phytopathology
Wageningen University & Research

Co-promotor
Dr Olga E. Scholten
Senior Researcher at Plant Breeding
Wageningen University & Research

Other members
Prof. Dr Gerlinde B. de Deyn, Wageningen University & Research
Prof. Dr Guido F.J.M. van den Ackerveken, Utrecht University
Dr Jürgen Köhl, Wageningen University & Research
Dr Daniele Liberti, BASF Vegetable Seeds, El Ejido, Spain

This research was conducted under the auspices of the Graduate School Experimental Plant Sciences

Peeling the onion

Unravelling the biology of fungal onion pathogens causing leaf blight, neck rot and white rot

Maikel B. F. Steentjes

Thesis
submitted in fulfilment of the requirements for the degree of doctor
at Wageningen University
by the authority of the Rector Magnificus,
Prof. Dr A.P.J. Mol,
in the presence of the
Thesis Committee appointed by the Academic Board
to be defended in public
on Monday 28 June 2021
at 4 p.m. in the Aula.

Maikel B. F. Steentjes
Peeling the onion - Unravelling the biology of fungal onion pathogens causing leaf blight, neck rot and white rot, 186 pages.

PhD thesis, Wageningen University, Wageningen, the Netherlands (2021)
With references, with summaries in English and Dutch

ISBN 978-94-6395-818-9
DOI https://doi.org/10.18174/546836

Table of contents

Chapter 1

General introduction

Parts of this chapter are published as:

Steentjes, M. B., Scholten, O. E., & van Kan, J. A. (2021). Peeling the onion: Towards a better understanding of *Botrytis* diseases of onion. Phytopathology, 111(3), 464-473.

Background

Onion (*Allium cepa*) is one of the most important vegetable crops worldwide. It is grown for its edible bulbous organs, which have a high nutritional value and give a specific pungent flavour to the diets of many people worldwide. For the production of bulbs, onion is cultivated as an annual crop that can either be sown from seed or planted from pre-grown sets that enable early harvest. For the production of seed however, onion is cultivated as a biennial crop since inflorescences are formed in the second year. After harvest, bulbs can be consumed directly or processed but some varieties are also well-suited for storage which makes onion available all year round. In 2018, nearly 100 million tonnes of onion were produced worldwide, on a total production area of more than 5 million hectares (FAOSTAT 2020).

As for many other vegetable crops, the production of onion bulbs is threatened by numerous pathogens and pests from a wide variety of taxa (Schwartz and Mohan 2008). Notorious threats are the insect pest *Thrips tabaci*, the fungal disease *Fusarium* basal rot caused predominantly by *Fusarium oxysporum* f. sp. *cepae*, and the Iris yellow spot virus. All are capable of causing serious diseases that can strongly affect yield (Cramer 2000; Gent et al. 2006; Gill et al. 2015). Remarkably, there are two closely related fungal genera, *Botrytis* and *Stromatinia*, that contain as many as five species that are able to cause multiple distinct diseases on all organs of the onion plant; roots, bulbs and leaves.

The Ascomycete genus *Botrytis* consists of approximately 35 species that are known as necrotrophic plant pathogens (Garfinkel et al. 2019; Hyde et al. 2014). The most well-known and extensively studied model species is *B. cinerea,* which is able to infect over 1400 plant species (Elad et al. 2016). Phylogenetic analysis of *Botrytis* has divided the genus into two clades. *B. cinerea* and *B. pseudocinerea*, both pathogens with a broad host range, belong to clade 1, while the species in clade 2 are mostly host-specific to one or a few taxonomically related plant species (Hyde et al. 2014; Staats et al. 2005). As many as eight *Botrytis* species are pathogenic exclusively on plants in the genus *Allium*. In addition to *B. squamosa*, *B. aclada*, *B. allii* and *B. byssoidea,* that exclusively infect onion (*A. cepa*), four other species are host specific to other *Allium* species. *B. porri* is a pathogen of leek and garlic (*A. porrum*, *A. sativum*), *B. sphaerosperma* is pathogenic on three-cornered leek (*A. triquetrum*), *B. globosa* causes disease on wild garlic (*A. ursinum*) and *B. sinoallii* is a pathogen of Japanese bunching or Welsh onion (*A. fistulosum*) (Chilvers and du Toit 2006; Elad et al. 2016; Zhang et al. 2010).

Stromatinia is a closely related genus of *Botrytis* in the family of Sclerotiniaceae and like *Botrytis* contains plant-associated species (Xu et al. 2010). One species of the genus, *Sclerotium cepivorum*, is considered a host-specific pathogen of onion and garlic. The onion pathogenic *Botrytis* species and *S. cepivorum* cause a variety of distinct but severe

diseases that all have a different etiology and require different control strategies (Table 1). This thesis will focus on the interaction of *S. cepivorum* and *Botrytis* species with their host plant onion.

Table 1. Overview of the different *Botrytis* species and *Sclerotium cepivorum* with names of diseases they cause on onion with the corresponding host tissues.

Species	Disease	Host tissue
B. squamosa	Leaf blight	Leaves
B. aclada	Neck rot	Bulbs
B. allii	Neck rot	Bulbs
B. byssoidea	Neck rot	Bulbs
S. cepivorum	White rot	Roots and bulbs

Leaf blight

Pathology

Botrytis leaf blight is a foliar disease of onion caused by *Botrytis squamosa*. This fungus was first described in 1925 and was reported to cause a disease of onion named small sclerotial neck rot (Walker 1925a). Several decades later, *B. squamosa* was isolated from diseased leaves and the species was recognized as the causal agent of onion leaf blight (Hickman and Ashworth 1943; Page 1953). When artificially inoculated on mature onion leaves, *B. cinerea* is also able to cause symptoms. However, the superficial leaf flecks caused by *B. cinerea* never grow into the intercellular spaces of the leaf and do not cause blighting (Hancock and Lorbeer 1963). Occasionally *B. cinerea* is detected on plants showing symptoms of leaf blight, but it is usually accompanied by *B. squamosa* and is thus not considered the causal agent of the disease (Hickman and Ashworth 1943; Misawa and Takeuchi 2015). Leaf blight is a major disease in almost all onion production areas worldwide, including Europe, Asia, Australia and North and South America (Carisse et al. 2011). Although information on yield losses caused by leaf blight is limited, in untreated plots losses up to 30% have been reported (De Visser 1996; Shoemaker and Lorbeer 1977b).

The symptomatology and histopathology of *Botrytis squamosa* have been reviewed in the past (Lacy and Lorbeer 2008b; Lorbeer 1992; Lorbeer et al. 2007) and will be summarized here. When a conidium of *B. squamosa* lands on the surface of an onion leaf, it can germinate and form a germ tube. At the tip of the germ tube an appressorium develops that is able to penetrate the leaf cuticle. The appressorium is often formed on top of anticlinal walls of epidermal cells and enables the fungus to enter the leaf tissue by growing through the middle lamella that separates the anticlinal walls. Alternatively,

germ tubes grow into the leaf tissue directly by entering via stomata. Upon leaf entry, hyphae grow mostly intercellularly and enter the cavity of the hollow onion leaf. The collapse of epidermal and mesophyll cells results in the first characteristic symptoms of leaf blight that can be observed as small necrotic spots on the onion leaves (Figure 1). The subsequent spreading of hyphae results in the expansion of the lesion. The lesions are often surrounded by a chlorotic halo and sometimes a characteristic longitudinal slit develops within the lesion. In a later stage of the infection leaves start to blight, leading to early leaf senescence and consequently reduced plant growth. On necrotic plant tissue the fungus produces new conidia that are dispersed by wind to other leaves and initiate a new infection cycle providing a source of secondary inoculum.

Besides conidia, *B. squamosa* produces sclerotia on colonized plant parts, especially under conditions that are not conducive for conidiation. Sclerotia can last on decomposing plant material for several months and function as overwintering structures (Ellerbrock and Lorbeer 1977b). When the new growing season starts, sclerotia are able to form apothecia which play a role in the sexual reproduction of the fungus (Bergquist and Lorbeer 1972). Alternatively, sclerotia can produce new conidia as a primary source of inoculum (Ellerbrock and Lorbeer 1977a). Other sources of primary inoculum include conidia grown on colonized leaves of sprouted bulbs in cull piles, onion plants in seed production fields, and volunteer onion plants that grow around bulb production fields and remain from bulbs from the previous year (Ellerbrock and Lorbeer 1977a; Lorbeer 1992; Lorbeer et al. 2007).

Figure 1. Symptoms of leaf blight on a mature onion leaf caused by *B. squamosa* showing necrotic leaf spots.

The severity of a leaf blight epidemic is strongly influenced by environmental factors. For development of lesions a temperature of around 20°C is optimal and a leaf wetness period of at least 6 to 8 hours is required for initiation of infection (Alderman and Lacy 1983; Alderman et al. 1985; Sutton et al. 1984). Longer leaf wetness periods of up to 48 hours increase the number of lesions (Shoemaker and Lorbeer 1977a). Conidiation on colonized plant parts is promoted by moderate temperatures of 14°C to 20°C, and also requires moist conditions in the form of leaf wetness or high relative humidity (Lorbeer et al. 2007; Sutton et al. 1983; Sutton et al. 1978).

Control

Due to the fast progression of the disease, onion growers heavily rely on preventative fungicides applied at 7- to 10-day intervals for up to 14 sprays per growing season (Carisse et al. 2011; Carisse and Tremblay 2007). Forecasting models for leaf blight help growers to time their fungicide sprays based on weather conditions and the amount of airborne conidia above the onion canopy measured by spore traps (Carisse et al. 2012; Carisse et al. 2008; Lacy and Pontius ; Sutton et al. 1986; Vincelli and Lorbeer 1989). Forecasting models allow fungicides to be used more efficiently, reducing the total number of sprays per growing season (Carisse et al. 2005; De Visser 1996). Increasing awareness of the negative effects of fungicide use on the environment, as well as the risk of resistance development in the target fungus, has resulted in restrictions in the number of admitted fungicides. Nowadays, there are strains of *B. squamosa* that have become insensitive to active ingredients that have been used for control of leaf blight such as iprodione. Due to cross-resistance, these strains have also become insensitive to vinclozolin which, like iprodione, belongs to the dicarboximide fungicides (Carisse et al. 2011; Carisse and Tremblay 2007; Presly and Maude 1982; Tremblay et al. 2003). Currently, fungicides against leaf blight are based on active ingredients from different classes such as mancozeb (dithiocarbamate), prothioconazole (triazole) and fluoxastrobin (strobilurin), and using these products in tandem reduces the probability of resistant *B. squamosa* populations. However, relying on fungicide treatments alone is not a durable strategy to combat leaf blight. Some studies have focussed on biocontrol of *B. squamosa* by supressing its sporulation using antagonists, but this has not led to commercially available products against leaf blight (Köhl et al. 1992; Köhl et al. 2003).

To reduce the reliance on fungicides, scientists and breeders are searching for sources of natural resistance against *Botrytis* leaf blight. In general, all commercial onion varieties are susceptible to leaf blight (Bergquist and Lorbeer 1971; Tremblay et al. 2003), but variation has been observed in levels of susceptibility among cultivars (Araújo et al. 2018). Strong resistance to *B. squamosa* has been reported in a wild relative of onion, *Allium roylei*. Resistance was determined to be conferred by a single gene (named *Bs1*), that behaved in

a partially dominant manner and resulted in high levels of resistance in progeny plants of *A. cepa* × *A. roylei* (de Vries et al. 1992; van der Meer and de Vries 1991). A QTL for resistance to *B. squamosa* from *A. roylei* was identified on chromosome 6 using SNP markers in an interspecific three-way cross population [*A. cepa* x F1(*A. roylei* x *A. fistulosum*)] segregating for resistance (Scholten et al. 2016). The large size of the QTL region indicated that, apart from the *Bs1* gene, minor genes from *A. roylei* or *A. fistulosum* may have affected resistance levels in plants of this population. Backcrossing of the *Bs1* resistance gene into *A. cepa* resulted in lines that resemble cultivated onion with a quantitative level of resistance against leaf blight (Hyde et al. 2015). A second source of resistance was found in another relative of onion, the Japanese bunching or Welsh onion (*Allium fistulosum*) (Bergquist and Lorbeer 1971; Currah and Maude 1984).

Onion related *Allium* species may be used in breeding programmes to breed for resistance (Kik 2002), however crossing *Allium* species that range in genome sizes may result in low fertility in progeny plants (Labani and Elkington 1987; Van Raamsdonk et al. 2003). An example of a successful introgression of disease resistance is the introgression of downy mildew resistance from *A. roylei* into onion. After many years of backcrossing and subsequent selfing, breeding has led to the development and release of downy mildew resistant onion varieties (Scholten et al. 2007). For optimal exploitation of related species in breeding programmes, it is important to gain a better understanding of the molecular mechanisms underlying leaf blight resistance, for which a lot of research is still needed.

Neck rot

Pathology

Botrytis neck rot is a serious disease of onion bulbs that causes post-harvest losses. As the name suggests, it results in rotting of the neck area of the onion bulb where tissue softens and turns brown while it decays (Figure 2). Often, sclerotia develop between the rotting scales of the bulb. Additionally, mycelium and grey conidia can be observed on the outer surface of the neck area (Lacy and Lorbeer 2008a; Lorbeer et al. 2007). Although infection takes place in the field, symptoms of neck rot are typically observed after bulbs are taken from storage (Maude and Presly 1977a). Neck rot is reported in all major onion production areas worldwide and yield losses can reach up to 50% yet losses heavily vary between years (Chilvers and du Toit 2006; Chilvers et al. 2004; Hwang et al. 2016; Khan et al. 2013; Maude and Presly 1977a, b).

Multiple *Botrytis* species are known to be associated with neck rot. *B. allii* and *B. aclada* are considered to be the main causal agents (Chilvers and du Toit 2006). Also *B. byssoidea* can cause neck rot, but since the disease usually displays more pronounced mycelial growth

and less sclerotia and conidia formation, the disease caused by *B. byssoidea* is sometimes referred to as mycelial neck rot (Lacy and Lorbeer 2008a; Lorbeer et al. 2007; Owen et al. 1950). *B. squamosa* has also been associated with a neck rot disease of onion as can be seen from the original description of the name 'small sclerotial neck rot' (Walker 1925a), which is nowadays sporadically observed in onion plants and is more regarded as a late stage symptom of severe leaf blight infections (Lorbeer et al. 2007). Occasionally, *B. cinerea* is isolated from rotting onion necks, often together with *B. allii* or *B. aclada* (Rod 1984) and is therefore not considered as a causal agent of the disease (Yohalem et al. 2003). Furthermore, *B. cinerea* is able to cause brown stain, a rarely observed superficial discoloration of the outer dry scales of bulbs that is not causing problems in bulb production (Clark and Lorbeer 1973a, b).

B. aclada and *B. allii* occupy the same ecological niche and the morphological differences between them are subtle. Therefore, *B. aclada* and *B. allii* were not distinguished for a long time and their names were used synonymously for one species causing onion neck rot (Hennebert 1973). Based on chromosome number and size of conidia, two subgroups could be distinguished, one subgroup which has 16 chromosomes, like other *Botrytis* species, and one subgroup which has 32 chromosomes with conidia approximately double in volume (Shirane et al. 1989). Molecular fingerprinting studies confirmed the existence of two subgroups and showed that both differ from *B. byssoidea* (Nielsen et al. 2001). Sequencing of DNA fragments elucidated that the subgroup containing 32 chromosomes was the result of a hybridization event with one ancestor from the subgroup containing 16 chromosomes and the other ancestor being *B. byssoidea* (Nielsen and Yohalem 2001). The subgroup with 16 chromosomes was named *B. aclada* and the subgroup with 32 chromosomes *B. allii* (Yohalem et al. 2003). Since *B. aclada* and *B. allii* were used synonymously until 2003, literature until 2003 could refer to either one of them. Sequence analysis of phylogenetically informative gene sequences of two *B. allii* isolates revealed that these isolates arose from independent hybridization events (Staats et al. 2005).

Figure 2. Symptoms of neck rot on a sliced onion bulb.

Botrytis neck rot typically remains symptomless during the growing season of onion plants. First symptoms are generally observed after bulbs have been harvested and stored. The asymptomatic infection makes it difficult to predict yield losses and to develop control strategies that can be applied in the field to mitigate the damage. To unravel the infection biology of neck rot and to elucidate how the fungus reaches the neck area without causing symptoms, several hypotheses about the infection strategy have been proposed.

One of the infection strategies proposed is a symptomless infection of the leaves followed by endophytic growth towards the bulb. A study by Tichelaar (1967) suggests that conidia of *B. allii* are able to germinate and penetrate the surface of onion leaves without causing a plant response. The hyphae grow in the epidermis and when the leaves senesce the fungus colonizes the underlying mesophyll tissue without causing symptoms (Tichelaar 1967). In this way, the fungus will grow through the leaves towards the bulb, resulting in latent infection of the neck area. By contrast, other studies have reported that inoculation of onion leaves with spores of *B. allii* triggers leaf flecks and sometimes expanding lesions are observed (Presly 1985; Stewart and Mansfield 1984). Since such symptoms are not observed in the field, artificial inoculations may arguably not be representative for studying the infection biology of neck rot in the field.

Another infection strategy which potentially highly contributes to the incidence of neck rot, is infection through seed. *B. allii* was detected in commercial onion seed batches with up to 71% of seed samples being infected (du Toit et al. 2004; Maude and Presly 1977a; Stewart and Franicevic 1994). The fungus was detected externally on the seed coat as well as internally, and was found able to survive for up to 3 years (du Toit et al. 2004; Maude and Presly 1977a). *B. allii* was reported to spread from the infected seed to the seedling, first being detected in the cotyledon, later in the true leaves, and eventually in the neck of the mature onion (Maude and Presly 1977a; Stewart and Franicevic 1994). Although growth of the fungus throughout living plant tissue was always symptomless, conidiophores were observed after colonized leaf tissue senesced and turned necrotic, indicating that seed transmission is not the only way of spread of the disease (Maude and Presly 1977a; Tichelaar 1967). Although several studies reported a high correlation between the percentage of infected seed and the incidence of neck rot in storage (Maude 1983; Maude and Presly 1977b; Stewart and Franicevic 1994), in a wet growing season the incidence of bulbs with neck rot was greater than the occurrence of infection in seeds (Maude and Presly 1977b). During storage, no further spread of the fungus was observed from infected to healthy bulbs, suggesting that infection occurs only in the field (Maude and Presly 1977b).

In addition to infection through seed and latent infection of leaves, it is hypothesised that bulb infection occurs just before harvest at the moment the foliage is cut , leaving a wound above the neck area providing a perfect point of entry for germinating conidia of neck rot fungi (Maude et al. 1984).

Control

In order to reduce the incidence of neck rot in storage, several control strategies have been developed that aim to reduce infection during onion cultivation. Application of preventative fungicides for the control of neck rot is a common practice in onion cultivation (Kritzman 1983; Presly 1984), but has also led to *B. allii* populations that have become resistant against active compounds such as benomyl and carbendazim (Gladders et al. 1994; Kritzman 1983; Viljanen-Rolinson et al. 2007). Nowadays, fungicide sprays with the active ingredients fluopyram, tebuconazole, boscalid and pyraclostrobin, are commonly applied in onion cultivation and are simultaneously effective against leaf blight as well as against neck rot. Fungicides are also applied on seeds to reduce the level of seed borne inoculum. Treatment of seeds has been reported to drastically reduce the incidence of neck rot, but its effectiveness can be countervailed by spread of the disease in the field under favourable weather conditions (Maude and Presly 1977b). To prevent seed as a source of neck rot, nowadays, seed batches are tested for the presence of *Botrytis* spp. and contaminated batches are disinfected. Also, after harvest, bulbs can be treated with fungicides to reduce fungal growth inside the bulbs and decrease the incidence of neck rot in storage (Ali and El Shabrawy 1979; Grinstein et al. 1992).

As an alternative to fungicides, several studies have focussed on biological control of neck rot. Rod (1984) explored the potential of antagonistic fungi as biocontrol agents to inhibit the growth of *B. allii* and identified several candidates. Different strains of *Trichoderma viride* were found to have an inhibitory effect on growth of *Botrytis* spp. (Morris and Lane 1990; Roulston and Lane 1988). Köhl et al. (1997) reported that amongst others *Ulocladium atrum* could be used as a potential biocontrol agent against neck rot. Sporulation of *Botrytis aclada* on necrotic leaf tissue could be suppressed by competition for tissue colonization by the antagonistic fungus, but growth into living leaf tissue could not be stopped (Köhl et al. 1999; Köhl et al. 1995; Yohalem et al. 2004).

Breeding for onion varieties resistant against neck rot is difficult because of the different causal agents and the complexity of performing biologically relevant disease assays. There are differences in susceptibility between onion varieties and the few studies that focussed on resistance breeding against neck rot concluded that susceptibility is a quantitative trait that shows continuous variation and is at least in part heritable (Lin et al. 1995; Vik and Aastveit 1984).

Also cultural control methods are applied to limit the chances of neck rot infection in bulb storage. To prevent infection through the wound that arises after cutting the leaves, bulbs are lifted from the soil and left on the field to dry for several days, a process called curing. During that process, the top of the onion dries, making it more difficult for fungi to grow into the neck of the bulb (Maude et al. 1984). To speed up that process and to further

inhibit fungal growth, bulbs are often cured using heated air (Gunkel et al. 1971; Harrow and Harris 1969; Maude et al. 1984; Walker 1925b).

Despite the development of control strategies, neck rot remains difficult to control and is thus a major problem in storage of onions. The latent nature of the infection makes it difficult to predict the incidence of neck rot in storage. However, diagnostic methods have been developed that detect the presence of neck rot fungi in seeds, plants or bulbs with the aim to predict the incidence of neck rot in storage. The first method that was developed is based on the outgrowth of fungi on selective media in which only *Botrytis* species are capable to grow (Kritzman and Netzer 1978; Lorbeer and Tichelaar 1970). Subsequently, the different neck rot species can be distinguished based on their macro- and microscopic morphological characteristics. An accurate guideline for fungal isolation and characterisation of species is described by Chilvers and du Toit (2006). To be able to use diagnostic tools for the prediction of disease incidence, a more efficient and direct method than traditional fungal isolation is preferred. Nielsen et al. (2002) developed a diagnostic tool to detect and distinguish *B. aclada*, *B. allii* and *B. byssoidea*. This method, based on PCR followed by restriction fragment length polymorphism (RFLP), enables detection of *B. aclada* in symptomless onion leaves (Nielsen et al. 2002). An adaptation of the PCR protocol by using a magnetic capture hybridization (MCH-PCR) increased speed and sensitivity of the detection (Walcott et al. 2004). A real-time PCR (qRT-PCR) method to quantify the amount of *Botrytis* neck rot fungi in onion seed was developed by Chilvers et al. (2007). This assay uses specific primer pairs that are optimized to only anneal to *B. aclada*, *B. allii* and *B. byssoidea* while not targeting other *Botrytis* species or other fungi commonly detected on onion seed. In addition to this qRT-PCR method, which was based on SYBR Green chemistry, another qRT-PCR was developed for determining the quantity of *B. aclada* in bulb tissue based on TaqMan probe-based chemistry (Coolong et al. 2008). Khan et al. (2013) developed a high-resolution melting analysis assay that allowed fast and simple discrimination between neck rot species. Alternatively to DNA-based detection, an ELISA assay was developed to detect *B. allii* using polyclonal antisera (Linfield et al. 1995). Also volatiles produced by infected bulbs can be used in metabolite profiling to detect neck rot in bulbs (Li et al. 2011). More specifically, Prithiviraj et al. (2004) distinguished bulbs infected with *B. allii* from uninfected bulbs, and also from bulbs infected with other fungi and bacteria. Bulbs infected with *Botrytis allii*, *Burkholderia cepacia* and mock treated bulbs could be distinguished based on their volatile profile (Li et al. 2011). Although several methods for the detection and identification of neck rot fungi have been developed, either for detecting latent leaf infection or contaminated seed, sampling is the most problematic factor. Optimization of sample size, distribution of samples and timing are difficult to assess in advance, though they are essential for an accurate prediction of the incidence of neck rot in storage. The latent nature of neck rot infection remains a significant problem in developing strategies to mitigate neck rot.

White rot

Pathology

White rot is an important and widespread disease of onion caused by *Sclerotium cepivorum*. Due to its soil-borne nature, the disease is difficult to control and can be destructive for continued onion cultivation. Apart from onion, *S. cepivorum* is also able to cause white rot disease in the related *Allium* crop garlic. White rot poses a threat to all major onion production areas worldwide and is reported in countries of all continents including Mexico, Ethiophia, Hungary, Australia, the USA and India (Amin et al. 2014; Bakonyi et al. 2011; Gupta and Bharat 2017; Lupien et al. 2013; Metcalf et al. 1997; Perez-Moreno et al. 1999).

Since white rot is a soil-borne disease, infection of onion plants starts at their roots. In the initial phase of infection, the above ground parts do not show symptoms yet and are seemingly healthy. Only when the fungus grows into the basal plate of the onion bulb symptoms become apparent (Crowe and Hall 1980b). Symptoms of foliage include premature yellowing and dying of older leaves followed by stunting. Severe infection of plants can lead to complete dead of all foliage (Crowe 2008). When onion production fields contain areas in which the soil is contaminated with *S. cepivorum*, symptomatic plants can be observed in clusters (Crowe et al. 1980). Although such clusters may initially be small, they can expand since neighbouring plants can get infected by the fungus due to physical contact of their root systems (Crowe et al. 1980). In soils that are heavily contaminated, symptomatic plants appear in larger areas of the field and symptoms are more severe. In addition to foliar symptoms, patches of white mycelium can be observed around the base of the bulb (Figure 3). Once the basal plate and scales of the bulb are infected they start to rot. On the decaying bulb tissue, many small black sclerotia are formed (Crowe 2008).

In contrast to *Botrytis* species, *S. cepivorum* does not produce asexual spores to spread and establish disease but uses sclerotia to infect and proliferate. The fungus is able to produce microconidia that can germinate but their role in virulence and spread of the disease requires further investigation (Coley-Smith 1960; Gindro and L'Hoste 1997). Genetic comparison of worldwide field populations revealed that the fungus was clonally disseminated within countries, but also provided evidence for (possibly meiotic) recombination that occurred before migration of the populations (Couch and Kohn 2000). Whether *S. cepivorum* indeed is capable of sexual reproduction remains to be elucidated as there are no reports of apothecia for this species (Sammour et al. 2011).

The sclerotia of *S. cepivorum* are thick walled and relative small with a diameter of approximately 0.2-0.5 mm, although variation in size exists between sampled strains (Backhouse and Stewart 1987). Sclerotia formed on decaying bulb tissue end up in the

soil when the infected onion plant senesces and decomposes. Once in soil, sclerotia of *S. cepivorum* can survive and stay dormant for many years (Coley-Smith et al. 1990). When a suitable host plant grows nearby, sclerotia germination is induced by *Allium*-specific root exudates and volatiles (Coley-Smith 1960; Coley-Smith and Holt 1966; Davis et al. 2007). Hyphae emerging from the sclerotia infect the root by formation of appressorium-like structures or infection cushions (also known as compound appressoria) (Abd-El-Razik et al. 1973; Stewart et al. 1989b). The fungus spreads throughout the roots and eventually colonizes the basal plate and bulb tissue (Crowe 2008; Stewart et al. 1989a).

Figure 3. Symptoms of white rot caused by *S. cepivorum* on the outside of an onion bulb.

There are a many factors that influence the intensity of white rot infection. Temperature influences the progression of the disease with favourable temperatures for the pathogen ranging from 6 to 24°C, and elongated periods of soil temperatures over 22°C can completely eliminate *S. cepivorum* (Crowe and Hall 1980a; Entwistle et al. 1991). Another environmental factor that influences the severity of infection is soil moisture (Leggett and Rahe 1985). The most important variable however, is the density of sclerotia present in the soil (Crowe et al. 1980). Since white rot is considered to be solely propagated by sclerotia, spread of the disease is mostly mediated by human handling. Contaminated equipment or soil that contains sclerotia are often considered as initial sources of inoculum. Also movement of diseased plant material or even grazing animals have been considered to spread the disease (Mikhail et al. 1974). When a field is contaminated with a relatively low amount of sclerotia, the progression of the disease is slow and the distribution patchy (Crowe 2008). However, if infested fields are continuously used for *Allium* cultivation, the spread and number of sclerotia will rapidly increase over subsequent years (Crowe et al. 1980). Since sclerotia can stay dormant in the soil in absence of host plants for over

20 years and remain viable, *Allium* production in infested fields is not feasible anymore (Coley-Smith et al. 1990).

Control

The most crucial element of control strategies against white rot is to prevent the introduction of the disease into production fields. Especially movement of contaminated equipment from infested fields and introduction of diseased plant material should be prevented (Crowe 2008). Once symptomatic plants are observed, they can be removed to prevent spread of the disease and accumulation of sclerotia. In addition, removal of neighbouring asymptomatic plants should be considered since their root system may have been in contact with the diseased plants and therefore can be infected as well (Crowe 2008; Crowe et al. 1980). Although removal of plant material does not eliminate white rot, it does help to stop the spread and the increase in number of sclerotia.

Several strategies have been developed to reduce the number of viable sclerotia in the soil. Inundation of contaminated soil reduced the number of vital sclerotia since they cannot stand prolonged soil saturation conditions. The efficacy of inundation was dependent on temperature but predominantly controlled by the duration and time of year (Banks and Edgington 1989; Leggett and Rahe 1985). Inundation greatly reduces the number of viable sclerotia, with a decline of up to 93% in heavily invested fields, but it does not result in complete eradication and therefore onions grown in the subsequent year are still affected (Coley-Smith et al. 1990; Crowe et al. 2005). Alternatively to inundation, soil solarization has been tested to eradicate viable sclerotia by heat (Entwistle et al. 1991). Although laboratory-based trials were successful, solarization is not widely adopted as a method in the control of white rot (McLean et al. 2001).

In addition to water and heat, also chemicals are used to reduce the number of viable sclerotia by soil fumigation. Chemicals like methyl bromide were shown to eliminate nearly all viable sclerotia. However, soil fumigation is not cost effective and has side effects on the microbial soil community (Crowe 2008; Sammour et al. 2011). As an alternative to chemicals, compounds that do not directly kill sclerotia, but induce germination in the absence of host plants have been tested for their efficacy to eliminate viable sclerotia in soil. Natural products such as *Allium* root extracts or garlic power were shown to induce sclerotia germination (Coley-Smith and Holt 1966; Esler and Coley-Smith 1983). Also synthetic compounds that stimulate germination like diallyl disulphide (DADS) or di-N-propyl disulfide have been tested for their efficacy to eradicate viable sclerotia (Coley-Smith and Parfitt 1986). In field trials with DADS, over 90% of all sclerotia germinated, which is comparable to the reduction of viable sclerotia using chemical fumigation (Davis et al. 2007; Hovius and McDonald 2002). However, the few remaining sclerotia still cause severe plant damage and yield losses when onions are grown on the treated plot.

Instead of preventing infection by eradication sclerotia from soil, other control strategies focus on preventing infection or slowing down the progression of the disease. Like for onion diseases caused by *Botrytis* species, fungicide sprays are regularly used against white rot. Because of the soil-borne nature of the disease however, foliar applied fungicides cannot prevent infection. Fungicide applications to seeds or planting onion do inhibit fungal growth in the initial phase of root growth, but cannot prevent infection of developing root systems (Banks and Edgington 1989; Miñambres et al. 2010). Still, spraying mature plants with fungicide does help to slow down the progression of the disease and the amount of new sclerotia produced (Crowe 2008; Fletcher et al. 1971; Sammour et al. 2011).

As an alternative to chemical treatments, the antagonistic effects of several soil microbes on white rot have been tested (Entwistle et al. 1991; Wong and Hughes 1986). Amongst others the potential of *Trichoderma* spp. as biocontrol agents of *S. cepivorum* was evaluated. In vitro studies showed extensive growth inhibition of *S. cepivorum*, but field application had only very limited effects (Metcalf and Wilson 2001; Rivera-Mendez et al. 2020). Also the microparasite *Coniothyrium minitans* was assessed for its potential as biocontrol agent and was shown to effectively control white rot under laboratory conditions (Ahmed and Tribe 1977), but biocontrol is not commonly used in onion cultivation to control white rot.

Several studies focussed on host variation in white rot susceptibility. Many of those screens found differences in disease incidence between *Allium* species and between commercial onion cultivars (Bansal and Broadhurst 1992; Brix and Zinkernagel 1992; Hovius and Goldman 2004; Utkhede and Rahe 1978; van der Meer et al. 1983). The observed differences might indicate levels of quantitative resistance that can be potentially exploited for breeding purposes. Some of the differences were proposed to originate from differential ability of genotypes to stimulate sclerotium germination (Bansal and Broadhurst 1992; Hovius and Goldman 2004). However, resistant plants have not been further characterized and contradicting levels of susceptibility were reported for the same cultivars or species. For example, onion cultivar Ailsa Craig showed relatively low infection incidences in one study, while in a second study this cultivar did not show any sign of reduced white rot susceptibility (Brix and Zinkernagel 1992; Utkhede and Rahe 1978). Similarly, the onion cultivar Pukekohe Longkeeper was found to be most resistant in one study, but belonged to the group of most susceptible cultivars in another (Bansal and Broadhurst 1992; van der Meer et al. 1983). Differences in resistance levels were also found between seed lots of the same cultivars (Utkhede and Rahe 1984). These inconsistencies illustrate the difficulty in assessing of and breeding for white rot resistance. Lack of standardized inoculation methods and variation in plant and fungal material compromises the comparability of resistance screens. Additionally, strong environmental effects impair the detection of presumably low quantitative differences (Utkhede et al. 1982). Better controllable laboratory trials that correlate with disease incidence in the field might improve the sensibility of screens for resistance and enable future breeding efforts (Hovius and Goldman 2004).

Thesis outline

Research on leaf blight, neck rot and white rot in onion has a long history and most of the work described was performed several decades ago. It is remarkable how little progress has been made in the past two decades in increasing our knowledge of the interaction between *Botrytis* species and *S. cepivorum* with their host onion, which can be exploited to rationally develop novel concepts for controlling these diseases in onion. New approaches are required to acquire a better fundamental understanding of the biology and ecology of these fungi. In this thesis, we studied the genetic, biochemical, molecular and cellular aspects of the interaction of *Botrytis* species and *S. cepivorum* with their host onion. New insights are essential to reveal leads for resistance breeding in onion as a durable solution against leaf blight, neck rot and white rot in onion cultivation.

In **chapter 2**, I describe a study on the biology of the early phases of onion infection for leaf blight, neck rot and white rot. Using GFP-labelled transformants of *B. squamosa*, *B. aclada* and *S. cepivorum*, we visualized the first contact with host tissue and traced the fungi during infection. We revealed that all three pathogens have distinct infection strategies, which has consequences for the development of control measures and breeding approaches.

Plants protect themselves against microbial invaders by the production of antimicrobial compounds. In **chapter 3**, I report on the effect of onion-specific saponins called ceposides on *B. aclada* and *S. cepivorum*. Furthermore, we studied candidate genes that were potentially involved in the detoxification of ceposides.

The genetic elements underlying differences in host range between *Botrytis* species are unknown. In **chapter 4**, I describe an attempt to resolve the host specificity of *Botrytis* species infecting *Allium* using comparative genomics. By sequencing the genomes of onion pathogenic *Botrytis* species and *S. cepivorum*, as well as closely related *Botrytis* species pathogenic on other hosts, we searched for genetic elements underlying onion pathogenicity. Amongst other secreted proteins and secondary metabolite gene clusters were analysed in all sequenced species. By performing synteny analysis we were able to provide insight in the evolution of *Botrytis* genomes.

In **chapter 5**, I describe a study that was focussed on effector proteins of *B. squamosa*. Using a combination of proteomics and genome-wide effector prediction, we identified candidate effectors. By heterologous production of proteins in two independent expression systems, we were able to test the cell death-inducing activity of candidate effectors. The role of candidate effectors in virulence of *B. squamosa* on onion was assessed using knockout mutants obtained by CRIPSR-Cas9-mediated transformation.

One of the *B. squamosa* effectors identified in chapter 5 that was able to induce cell death in onion was necrosis- and ethylene-inducing protein 1 (Nep1). In **chapter 6**, I report a more detailed study of microbial Nep1-like proteins on monocot plants including onion, and assessed the contribution of *Bs*Nep1 to virulence of *B. squamosa*. By infiltrating pure protein in an interspecific *Allium* hybrid population, we were able to identify a QTL for *Bs*Nep1 insensitivity that co-localized to a previously identified QTL for *B. squamosa* resistance.

In **chapter 7**, I integrate all aspects of the interaction of *Botrytis* species and *S. cepivorum* with their host onion that are studied in this thesis. I relate facets of pathogenicity to the host specificity of onion-pathogenic *Botrytis* species. Furthermore I discuss the perspectives to incorporate our insights into resistance breeding strategies in order to generate onions with increased resistance against leaf blight, neck rot and white rot.

Chapter 2

Visualization of three Sclerotiniaceae species pathogenic on onion reveals distinct biology and infection strategies

Maikel B. F. Steentjes [1]
Sebastian Tonn [1]
Hilde Coolman [1]
Sander Langebeeke [1]
Olga E. Scholten [2]
Jan A. L. van Kan [1]

[1] Laboratory of Phytopathology, Wageningen University, Wageningen 6708 PB, The Netherlands
[2] Plant Breeding, Wageningen University, Wageningen 6708 PB, The Netherlands

This chapter is published as:

Steentjes, M. B., Tonn, S., Coolman, H., Langebeeke, S., Scholten, O. E., & van Kan, J. A. (2021). Visualization of three Sclerotiniaceae species pathogenic on onion reveals distinct biology and infection strategies. *International journal of molecular sciences*, *22*(4), 1865.

Abstract

Botrytis squamosa, *Botrytis aclada* and *Sclerotium cepivorum* are three fungal species of the family Sclerotiniaceae that are pathogenic on onion. Despite their close relatedness, these fungi cause very distinct diseases, respectively called leaf blight, neck rot and white rot, which pose serious threats to onion cultivation. The infection biology of particularly neck rot and white rot is poorly understood. In this study, we used GFP-expressing transformants of all three fungi to visualize the early phases of infection. *B. squamosa* entered onion leaves by growing either through stomata or into anticlinal walls of onion epidermal cells. *B. aclada,* known to cause post-harvest rot and spoilage of onion bulbs, did not penetrate the leaf surface but instead formed superficial colonies which produced new conidia. *S. cepivorum* entered onion roots via infection cushions and appressorium-like structures. In the non-host tomato, *S. cepivorum* also produced appressorium-like structures and infection cushions, but upon prolonged contact with the non-host the infection structures died. With this study, we have gained understanding in the infection biology and strategy of each of these onion pathogens. Moreover, by comparing the infection mechanisms we were able to increase insight into how these closely related fungi can cause such different diseases.

Introduction

Onion is an important vegetable crop that is cultivated worldwide but its production is threatened by pathogens and pests. There are three main onion diseases that are caused by species of the fungal family Sclerotiniaceae. *Botrytis squamosa* is the causal agent of onion leaf blight, while *Botrytis aclada*, *Botrytis byssoidea* and *Botrytis allii* cause neck rot, and *Sclerotium cepivorum* causes onion white rot. Although the species are related, the diseases they cause are distinct and have their own etiology.

The most notorious disease is *Botrytis* leaf blight, caused by the necrotroph *B. squamosa*. The fungus was first described nearly 100 years ago and even today leaf blight is still a major disease in almost all onion cultivation areas worldwide (Araújo et al. 2018; Carisse et al. 2011; Tanović et al. 2019). The disease is characterized by small necrotic spots on onion leaves that expand at a later stage leading to blighting of leaves and early leaf senescence, eventually resulting in a reduction of plant growth and bulb yield and quality (Lacy and Lorbeer 2008a; Steentjes et al. 2021a). Compared to neck rot and white rot, the disease cycle of leaf blight is relatively well studied. Spores of *B. squamosa* are dispersed by wind and upon landing on the onion leaf surface, the spores germinate to penetrate the surface and enter the leaf tissue. Once inside the leaf, the fungus spreads intercellularly and proliferates by obtaining nutrients from killed host cells. Infected onion leaves turn necrotic and on the outside new conidia are produced that can initiate a new disease cycle (Lorbeer 1992; Lorbeer et al. 2007).

Botrytis neck rot is a disease that results in rotting of the neck of the onion bulb. Although infection is initiated in the field, symptoms are observed only after bulbs have been harvested and stored, making neck rot a post-harvest disease (Lacy and Lorbeer 2008b; Steentjes et al. 2021a). Neck rot is caused by a complex of the three species *Botrytis aclada*, *B. byssoidea* and a hybrid species of the former two, called *B. allii* (Chilvers and du Toit 2006; Nielsen and Yohalem 2001). Since the disease remains asymptomatic during the growing season of onion plants, it is difficult to study its etiology. In the past, symptomless infection of leaves has been hypothesized to lead to an endophytic growth of the fungus towards the bulb (Tichelaar 1967). Also endophytic growth from contaminated seed has been suggested as an infection strategy, as correlations between the numbers of infected seed and the incidence of neck rot in storage were reported (Maude 1983; Maude and Presly 1977a; Stewart and Franicevic 1994). Despite these hypotheses, the infection process of neck rot still remains unclear.

White rot of onion is caused by the soil-borne pathogen *Sclerotium cepivorum*, which mainly colonizes roots, basal plate and bulb of the onion plant. Symptoms of infected plants are premature yellowing, dieback, wilting of older leaves, and stunting of plants followed by death of all foliage and sometimes root rot (Crowe 2008; Sammour et al. 2011).

Unlike *Botrytis* species, *S. cepivorum* does not produce spores to spread and establish disease. Instead, spread occurs through sclerotia formed on infected hosts which can remain dormant in soil for up to many years. Root exudates of *Allium* plants have been reported to stimulate sclerotia to germinate and infect the roots (Coley-Smith 1960, 1986; Davis et al. 2007; Tyson et al. 2000). Once a production field is infested with *S. cepivorum*, onion cultivation is no longer possible.

Although all three diseases pose a serious threat to onion cultivation, the infection biology of these fungi, especially the ones causing neck rot and white rot is still poorly understood. To provide insight into the early infection biology and to understand the interaction between plant and fungus, we developed GFP-expressing transformants of *B. squamosa*, *B. aclada* and *S. cepivorum* and visualized the infection process on onion. Using epifluorescence and confocal microscopy, we were able to visualize the interaction between these fungi and onion, and colonization of the host tissues. By comparing infection strategies of the three related fungi, we aimed to determine how they cause such distinct diseases on the same host and aimed to provide insights for the development of new control strategies.

Material and methods

Fungal isolates and culture conditions

B. squamosa isolate MUCL31421, *B. aclada* isolate 633 and *S. cepivorum* isolate UFL were used as recipient strains for transformation. Spores of *B. squamosa* were obtained by growth on autoclaved onion leaves on top of water agar (Oxoid) at a temperature of 20°C in the dark for 3 days. After 3 days, plates were transferred to 16/8h day/night rhythm of white light supplemented with UV light (330-370nm, Sylvania F15T8/BLB) at a temperature of 20°C for 4 days. Spores of *B. aclada* were produced by growth on MEA (Oxoid) in the dark at 20°C for 7 days, after which plates were exposed to 16/8h day/night rhythm of white light supplemented with UV light (360-380nm, Phillips TLD 18W/08) for 3 days. Sclerotia of *S. cepivorum* were obtained by growth on MEA (Oxoid) plates in the dark at 20°C. For long term storage, spores of *B. squamosa* and *B. aclada* were kept in 15% glycerol at -80°C and sclerotia of *S. cepivorum* were stored at room temperature.

Fungal transformation

To fluorescently label the fungi, a gene cassette containing *gfp* (codon optimized for *B. cinerea*) under control of a *oliC* promotor, together with a hygromycin resistance marker was amplified from plasmid pNDH-OGG (Schumacher 2012). Using a PEG-mediated protoplast transformation (Have et al. 1998), the construct was inserted into the genomes of *B. squamosa*, *B. aclada* and *S. cepivorum*. Protoplasts of *B. squamosa* and *B. aclada* were obtained by digestion of overnight germinated spores in 1% Malt Extract (Difco) using Glucanex (Sigma-Aldrich). For *S. cepivorum*, mycelium was grown on PDA (Oxoid) covered with cellophane for 3 days after which the mycelium was isolated and homogenized (Kinematica CH-6010). The suspension of mycelial fragments was incubated overnight in 1% Malt Extract (Difco) before protoplasting using Glucanex (Sigma-Aldrich). Transformed protoplasts were selected using an initial hygromycin concentration of 30µg/ml for *B. squamosa* and *B. aclada* and 75µg/ml for *S. cepivorum*. Transformant colonies were assessed for their capacity to fluoresce and the integration of the *gfp* gene and resistance cassette was confirmed by PCR. Virulence of transformants was checked by inoculation on onion leaves and bulb scales, and growth speed was assessed by measuring diameter of five replicate colonies per strain on MEA plates and calculating growth rates using trendlines.

Plant material and inoculation

All onion plants used in this study were grown in a climate chamber with 12h light, 70% relative humidity, 18°C day temperature and 16°C night temperature.

For inoculation assays of *B. squamosa*, young but fully grown leaves of 2-4 month onion plants cv. Manesco were used. Detached leaves were placed in humid boxes and the cuticula of leaves was gently wiped with tissue paper to facilitate inoculation. Spores were suspended in 12g/L PDB (Difco) to a final concentration of $5x10^4$ or 10^5 spores/ml and inoculated in 1µl droplets.

For inoculation assays of *B. aclada*, leaves of 4-6 weeks old onion plants from sets of cv. Cupido were used. Spores were suspended in 12g/L PDB to a final concentration of 10^4 or 10^5 spores/ml and inoculated in droplets of 1µl. For the long term infection assay, 6 week old onion sets cv. Cupido were inoculated with one inoculation droplet of 1µl per leaf with 10^4 spores/ml in 12g/L PDB. On weekly intervals, leaves were segmented into 10mm wide segments and placed on MEA plates with 100µg/ml hygromycin. Inoculation on non-host plants species was performed on tomato cv. Motelle, *Nicotiana benthamiana* and a lily Oriental x Asiatic hybrid cultivar.

For inoculation of *S. cepivorum*, seedlings of onion cv. Stuttgarter Riesen, tomato cv. Moneymaker and white cabbage cv. Express, were placed on object glasses with fixed

cover slips with roots and part of the hypocotyl in between the glass slides. The prepared slides were placed upright in 0.25 Murashige & Skoog basal salt mixture (Duchefa). For inoculation, sclerotia were cleaned and pregerminated on droplets of MEA before they were placed directly onto the seedling. Inoculated seedlings were placed back in nutrient solution and visualized at regular intervals.

Fluorescence microscopy and germ tube measurements

For determining fluorescence of the transformant colonies, images were captured with a Nikon Eclipse 90i fluorescence microscope mounted with a Nikon cooled camera head DS-5Mc using a Plan Fluor 4x/0.13 lens. For visualization of the *S. cepivorum* infection process, Plan Fluor 10x/0.30 and 40x/0.75 lenses were used. With a Nikon Intensilight mercury lamp, GFP-expressing fungi were visualized using a FGP(R)-BP filter (exitation:460-500nm, dichroic mirror: 505, barrier wavelength: 500-550nm). For visualization of the *B. squamosa* and *B. aclada* infection, a Zeiss LSM 510-META confocal laser scanning microscope equipped with a mmi DCA252cF-K07 CellCamera was used with EC Plan-Neofluor 40x/1.30 Oil DIC and Plan Apochromat 63x/1.4 Oil DIC objectives. An Argon laser 488nm was used for excitation with the GFP signal passing through a BP 505-530 filter and the chloroplast autofluorescence and propidium iodide signal passing through an LP 615 filter. To visualize the epidermal cell walls, inoculated leaf segments were stained in 0.05mg/L propidium iodide. For the visualization of leaf surface penetration, Z-stacks of optical sections including pathogen, leaf surface, epidermal cells and mesophyll cells were acquired. 3D-projects of Z-stacks were made using the image analysis tool imageJ. For the *B. squamosa* germ tube measurements of different nutrient concentrations in the inoculum, in total 24 inoculation spots with 4 replicates per nutrient concentration were imaged resulting in 448 measurable germ tubes. Using imageJ, a segmented line was manually drawn from the base of the spore until the apex of the germ tube and length, fluorescence (measured as average intensity) and curvature (calculated as the ratio feret value/length) were measured per germ tube. Spore size and germ tube width were measured similarly using 22 images of germinated spores for both *B. squamosa* and *B. aclada*.

Statistical analysis

All statistical analysis was performed in GraphPad 9.0 (Prism). WT and GFP-transformants' growth rates were pairwise compared for *B. squamosa*, *B. aclada* and *S. cepivorum* using unpaired *t*-tests. Germ tube length, curvature and fluorescence intensity at different concentrations PDB in the inoculum were side-by-side analyzed using unpaired *t*-tests. Differences were considered to be statistically significant with two-tailed P values ≤ 0.05.

Results

Transformation of *B. squamosa*, *B. aclada* and *S. cepivorum* with gfp yields fluorescently labeled fungi

To visualize the infection process of the three different fungi in onion, we used fluorescently labeled transformants. A GFP (green fluorescent protein) encoding gene was inserted into the genomes of the fungi using a polyethylene glycol-mediated protoplast transformation, resulting in multiple GFP-expressing transformants of each fungal species. Transformants did not show abnormalities in morphology and pathogenicity, and were able to fluoresce (Figure 1A). Furthermore, transformants were not reduced in growth speed as compared to WT (Figure 1B). For each species, one fluorescent transformant with normal morphological appearance and growth rate was selected to study the infection biology.

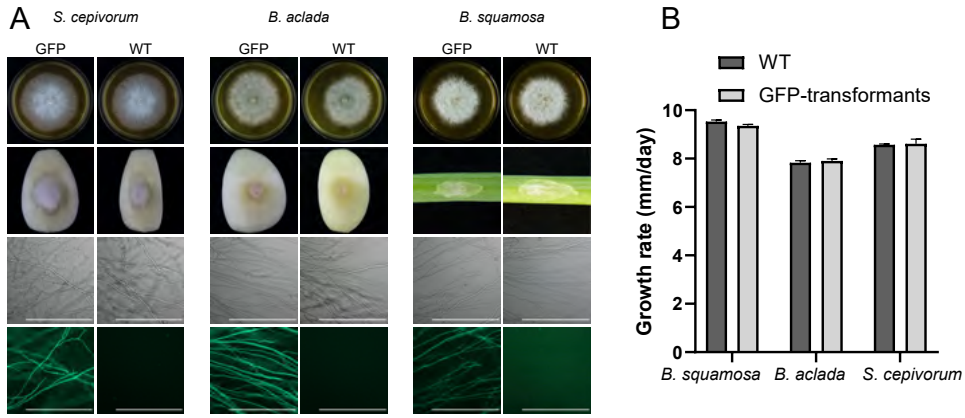

Figure 1. Evaluation of WT and GFP-expressing transformants of *B. squamosa*, *B. aclada* and *S. cepivorum*. (**A**) No differences were observed between WT and transformants based on morphology and growth on agar plates (first row) and pathogenicity on host tissue (second row), and only transformant strains are able to fluoresce (third and fourth row). Scale bar=500µm. (**B**) No difference was observed in growth rate between WT and transformants (unpaired *t*-test, $p>0.05$, error bars representing standard error).

B. squamosa enters the onion leaf by growth through stomata or into anticlinal walls

The average width and length of *B. squamosa* conidia measured 15.6µm and 22.6µm respectively, which is in accordance with previously published measurements (Presly 1985). Spores of *B. squamosa* applied to the surface of onion leaves germinated within the first two hours after inoculation (Figure 2A). The majority of spores germinated unipolar (Figure 2B) but also bipolar germination from opposing sides of the spore was observed (Figure 2C). Occasionally, germ tubes growing over the onion leaf surface branched, mostly with one but sometimes with two opposing lateral branches (Figure 2D). The width of germ tubes measured on average 5.5µm. The length depended on the nutrient concentration applied in the inoculum, with higher nutrient concentrations resulting in longer germ tubes at 8 hours post inoculation (HPI) on the onion leaf surface (Figure 2E). Spores inoculated without nutrients in the inoculum did not germinate and did not show fluorescence. In addition to length, also the curvature of germ tubes and the fluorescence intensity varied with nutrient concentration in the inoculum (Supplemental figure 1A, 1B).

Most of the germ tubes that penetrated the onion leaf surface did so by entering through stomata (Figure 2F, 2G). Alternatively, *B. squamosa* was observed to enter the onion leaf by growing into anticlinal cell walls of the onion epidermis (Figure 2H, 2I). In several cases, germ tubes were observed to grow over stomata, presumably when they were closed, instead of growing through them. Likewise, germ tubes very often grew over anticlinal walls of onion epidermal cells as compared to growth into anticlinal walls towards mesophyll tissue, suggesting leaf penetration by growth into the epidermal layer might be triggered by external stimuli.

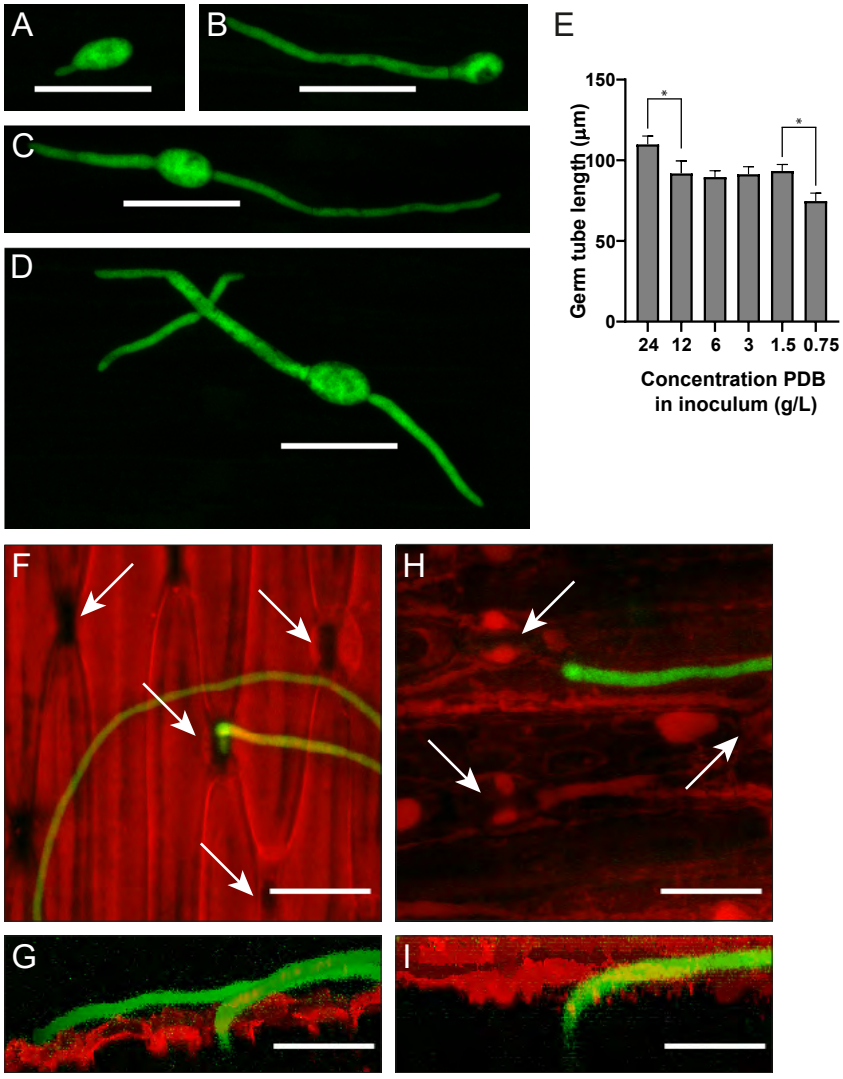

Figure 2. *B. squamosa* growth on and penetration of the onion leaf surface. Fluorescence microscope images of spores germinating (**A**, **B**) unipolar and (**C**) bipolar, and (**D**) a branching germ tube. (**E**) The effect of nutrient concentration in the inoculum on germ tube length at 8 HPI on the onion leaf surface, (unpaired *t*-test, * $p<0.05$, error bars representing standard error). Confocal laser scanning microscopy images of *B. squamosa* penetrating the onion leaf surface. (**F**) Top view and (**G**) front view of a 3D projection of stomatal penetration. (**H**) Top view and (**I**) front view of a 3D projection of growth into anticlinal walls of epidermal cells. All scale bars represent 50µm, arrows indicate stomata, *B. squamosa*-GFP in green and PI stained onion cell walls in red.

Botrytis aclada reproduces asexually without penetrating the onion leaf surface

Botrytis neck rot is a storage disease of onion that does not display symptoms in the field. To resemble field conditions, inoculations of *B. aclada* were performed with spore densities that did not result in disease symptoms or other plant responses. Inoculation of *B. aclada* spores on onion leaves resulted in germination within a similar timeframe and with comparable polarity and branching patterns as for *B. squamosa*. The conidia of *B. aclada* however, measured on average 5.2µm wide and 7.0µm long which is similar to previous reports (Nielsen et al. 2001; Yohalem et al. 2003). This is over three times smaller in size, and therefore approximately 30 times smaller in volume as compared to *B. squamosa*. Also germ tubes were smaller than germ tubes of *B. squamosa*, measuring on average 3.2µm wide. Germ tubes of *B. aclada* were observed to grow exclusively over the surface of the onion leaf. Even while we examined inoculated leaf samples up to 48 HPI, we neither observed penetration of the onion leaf surface by growth into the epidermal cell layer nor through stomata, even when hyphae grew along or over stomata (Figure 3A, 3B). Instead, the hyphae branched and developed conidiophores with new conidia from 72 HPI onwards (Figure 3C). No lesion, discoloration, or any other plant response was observed, while the newly developed conidia could be seen by eye (Figure 3D, 3E). To ensure that the development of conidiophores was not an artifact of nutrients used in the inoculum for synchronized spore germination, spores were pre-incubated in nutrient solution to initiate germination and washed with water before inoculation. Germination, growth and formation of conidiophores was similar to non-washed inoculum, indicating that the nutrients for developing conidiophores are acquired from another source than the inoculum. In addition to inoculating *B. aclada* on its host plant onion, we also inoculated non-host plants. Production of new conidia without necrotic symptoms was observed on leaves of tomato and lily, but not on *Nicotiana benthamiana* (Supplemental figure 2).

In order to follow the development of the fungus over a longer time period, onion leaves were inoculated and sampled at weekly intervals, and divided into 10mm segments to examine outgrowth of *B. aclada*. The fungus could never be isolated from any leaf segment other than the segment on which it was inoculated (Supplemental figure 3). *B. aclada* could be isolated from the segment with the initial inoculation spot for up to 50 days post inoculation (DPI) even when leaves were already naturally withered of age, suggesting regrowth from newly produced conidia instead of outgrowth of invasive hyphae since the dry and withered leaves unlikely sustain hyphal growth.

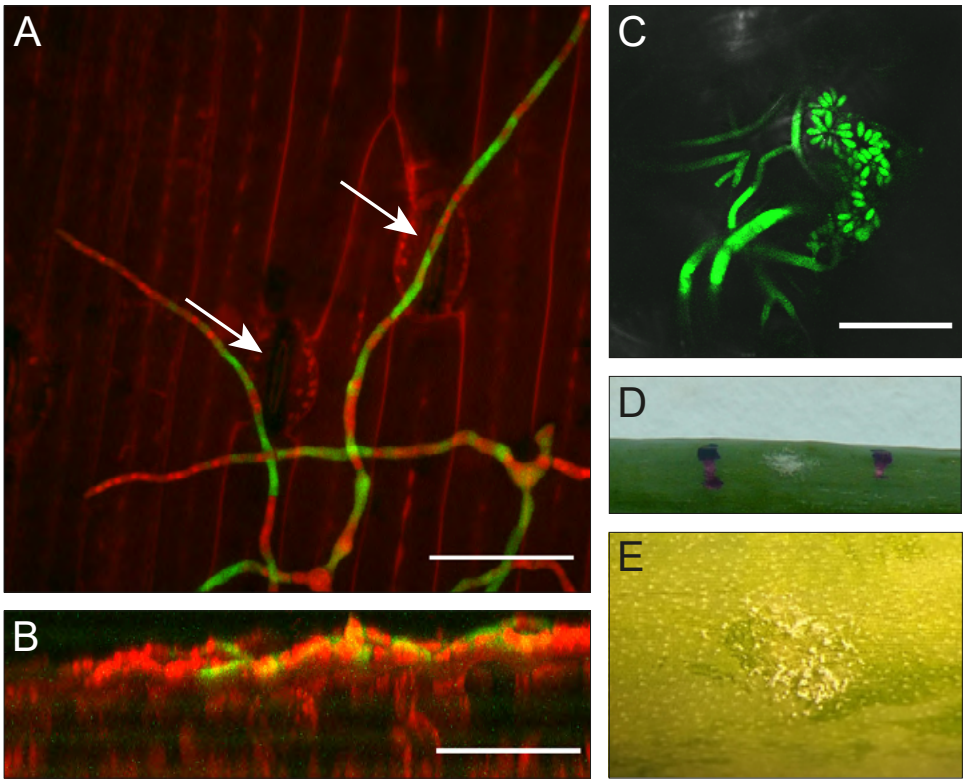

Figure 3. *B. aclada* on onion leaves. (**A**) Top view and (**B**) front view of a 3D projection of confocal laser scanning microscopy images of hyphae growing over and along stomata of an onion leaf. Scale bars represent 50µm, arrows indicate stomata, *B. aclada*-GFP in green and PI stained onion cell walls in red. Conidiophores with newly formed spores of *B. aclada* on the surface of an onion leaf observed by (**C**) fluorescence microscopy (scale bar 200µm), (**D**) on a macroscopic scale, and (**E**) using binocular microscope.

Sclerotium cepivorum infects onion by formation of appressorium-like structures and infection cushions

To study the infection process of *S. cepivorum,* onion seedlings were inoculated with pre-germinated sclerotia of *S. cepivorum*. During germination of sclerotia the hard shell burst followed by outgrowth of multiple branched hyphae (Figure 4A). No targeted growth towards or away from the host plant root was observed. At early time points (12 to 24 HPI) *S. cepivorum* hyphae attached to the root epidermis of the onion seedling and developed infection structures. Both appressorium-like structures, formed by swelling of the tip of a single hypha (Figure 4B), and infection cushions (also referred to as compound appressoria), formed by one or two branched and curled hyphae resulting in a bundle of

intertwined hyphae (Figure 4C), were observed. Approximately 10 to 12 hours after the formation of the infection structures, invasive hyphae were observed growing inside the onion root (Figure 4D, 4E).

Once inside the root, hyphae grew in cortical tissue while epidermis and hypodermis remained intact (Figure 4F). Hyphae progressing towards the root tip were also observed to grow in or around vascular tissue. In advanced stages the cortical root tissue developed cavities that were enriched with hyphae. Eventually, the fungus exited the root by growing through the root tip (Figure 4G).

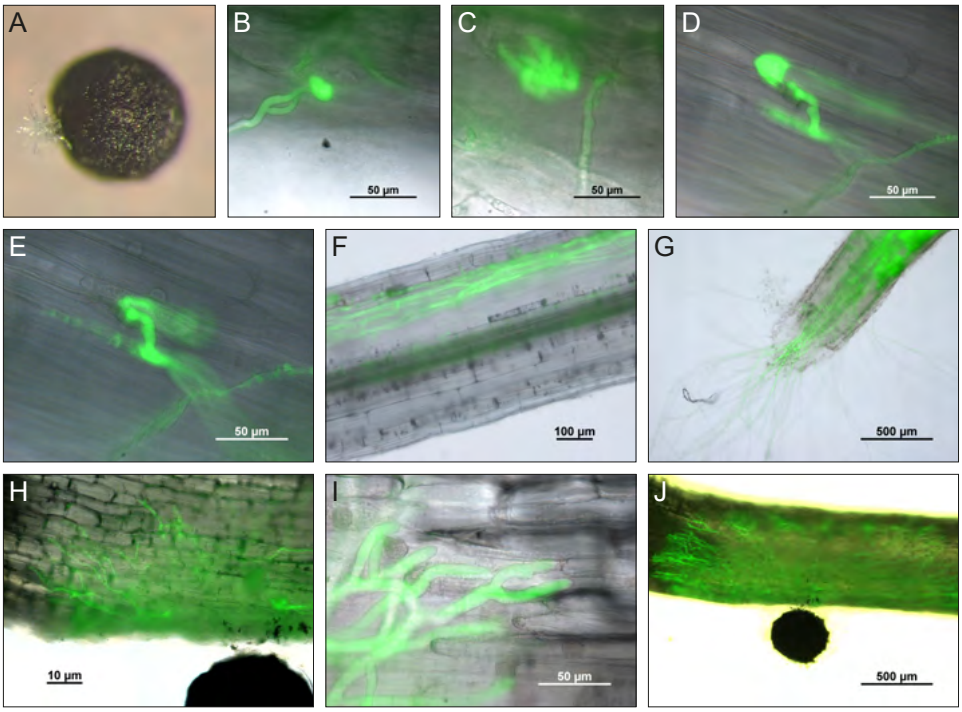

Figure 4. *S. cepivorum* on onion. (**A**) Binocular microscope image of a germinating sclerotium with outgrowth of hyphae. *S. cepivorum* attaching to host surface by forming (**B**) an appressorium-like structure and (**C**) an infection cushion observed by fluorescence microscopy. (**D**, **E**) Invasive hyphae growing inside the onion root 10 hours after the formation of an appressorium-like structure. (**F**) Hyphae growing through cortical root tissue and (**G**) eventually growing through the root tip. (**H**) Spreading infection through an onion leaf, with (**I**) disintegrating onion tissue around leading hyphae. (**J**) Hyphae growing over the full width of an onion leaf 36 HPI.

Inoculation of *S. cepivorum* on the basal part of the leaf resulted in different fungal growth patterns than inoculation on root tissue. After penetration, hyphae grew rapidly throughout the plant. Approximately 24 HPI, hyphae in the epidermal and subepidermal layers had grown from the initial infection site towards all directions (Figure 4H). Host tissue appeared to be macerated around and in front of the leading hyphae (Figure 4I).

The fungus further colonized and spread across the width of the basal part of the leaf and grew both towards leaf as well as root tissue (Figure 4J). Approximately 5 DPI the fungus grew into the roots while all other plant parts were already fully colonized and macerated.

In addition to visualizing the interaction between *S. cepivorum* and its host plant onion, we tested the host specificity of *S. cepivorum* by inoculating seedlings of non-host plants cabbage and tomato. On cabbage, hyphae grew around plant tissue but no formation of infection structures was observed (data not shown). On tomato seedlings however, hyphae that emerged from sclerotia attached to the epidermis of roots and root hairs and formation of appressoria and infection cushions was observed within 24 hours after inoculation (Figure 5A, 5B, 5C). Both appressoria and infection cushions morphologically resembled the structures observed on onion seedlings. In all cases however, the infection structures lost fluorescence within 10 to 24 hours upon contact with the non-host, indicating dying of the infection structure (Figure 5D, 5E, 5F). Only the apical cells that were in direct physical contact with the tomato root epidermis or root hairs died, while other hyphae retained their fluorescence and continued growing. In none of the observed cases, hyphae could be detected that had penetrated the tomato root tissue.

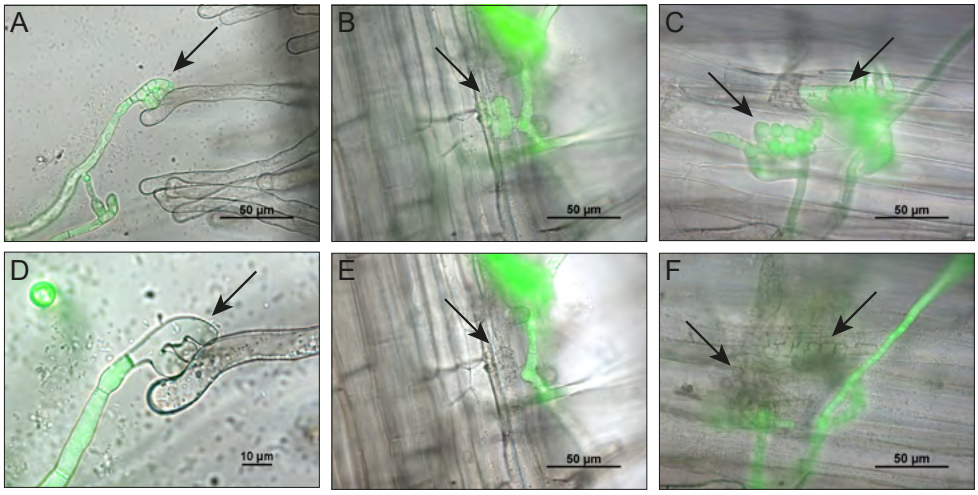

Figure 5. Unsuccessful infection of tomato roots by *S. cepivorum*. Fluorescent microscopical images of (**A**) branching hyphae attached to a tomato root hair, (**B**) an appressorium-like structure and (**C**) an infection cushion attached to the tomato root epidermis. (**D**) 12 hours, (**E**) 10 hours and (**F**) 24 hours later, infection structures lost their fluorescence, indicated by arrows.

Discussion

In this study, we transformed *B. squamosa*, *B. aclada* and *S. cepivorum* to obtain fluorescently labeled fungi that allowed accurate visualization of the infection processes in onion tissues. This is the first report of transformation of *B. aclada* and *S. cepivorum*, and although *B. squamosa* was the first *Botrytis* species that had been transformed (Huang et al. 1989), this is also the first report on GFP-expressing *B. squamosa*. Although the *gfp* cassette was ectopically integrated, the successful protoplast transformation paves the way for molecular studies using knock-out mutants of these fungi, possibly by adapting the CRISPR-Cas9 protocol developed for *B. cinerea* (Leisen et al. 2020).

When *B. squamosa* was inoculated on onion leaves, two modes of penetration were observed: 1) growth through stomata and 2) growth into anticlinal walls of epidermal cells. This is in accordance with previous observations (Clark and Lorbeer 1976; Lorbeer 1992; Lorbeer et al. 2007), but formation of distinct appressoria was not observed by us. *Botrytis* species, including *B. squamosa*, are known to secrete plant cell wall degrading enzymes such as cutinases, pectinases and cellulases that facilitate progressive growth of germ tubes penetrating the leaf surface, thereby diminishing the need to develop distinct appressoria (Hancock et al. 1964; Kars and van Kan 2007; Mansfield and Richardson 1981). When inoculating *B. squamosa* on onion leaves, we observed that the higher the nutrient concentration in the inoculum the longer the germ tube and the higher the fluorescence intensity, whereas in water spores did not germinate at all. The availability of nutrients likely influenced the basal metabolism of the fungus, thereby affecting the speed of polarized growth as well as expression of the *gfp* gene. The activity of the *Aspergillus nidulans oli*C promotor that was used to control *gfp* might be influenced by sugar availability, since the *Oli*C gene encodes a mitochondrial ATP synthase subunit (Ward et al. 1988).

Botrytis neck rot is a post-harvest disease of onion that is initiated in the field but only becomes apparent upon storage of the bulbs for several weeks or months, as is typically done for Dutch long day onions (Lacy and Lorbeer 2008b; Steentjes et al. 2021a). From our leaf infection assays for microscopy, as well as from the long term infection and resampling assays, we did not observe penetration of the onion leaf surface nor did we obtain evidence of asymptomatic, endophytic growth of *B. aclada* through onion leaves. This is in contrast to a study performed by Tichelaar et al. (Tichelaar 1967) who reported germ tubes growing through stomata of onion leaves. In contrast to the latter study, we typically used whole leaves and whole plants in our experimental setup to ensure biologically relevant conditions. Remarkably, we could observe germ tubes growing through stomata after the epidermal layer of the onion leaf was peeled off and placed on agar medium before inoculation (data not shown). The isolation of the single cell layer likely resulted in cell death and dis-functioning of stomata, providing an artificial host substrate that *B. aclada* was able to penetrate.

Necrotrophs like most *Botrytis* species are presumed to destruct host cells to obtain nutrients and proliferate. The formation of conidiophores without penetrating the leaf surface and killing host cells suggests that *B. aclada* obtains nutrients from another source. Several fungal plant pathogens, such as certain *Colletotrichum* species and *Rhynchosporium secalis*, have a subcuticular growth phase in which they grow under the cuticle and within the periclinal and anticlinal walls of epidermal cells (Carisse et al. 2000; De Silva et al. 2017). Our results suggest that *B. aclada* has a similar growth, in which the nutrients required for developing new conidia might be acquired from the cuticle, consisting of a layer of cutin with embedded polysaccharides and an overlying layer of waxes, or the polysaccharides from the outer periclinal cell wall of epidermal cells (Yeats and Rose 2013).

There is no consensus about the way in which *B. aclada* ends up in the neck area of the onion bulb. It has been hypothesized that the neck area could be reached through endophytic growth from contaminated seed (Maude and Presly 1977b; Stewart and Franicevic 1994), through endophytic or epiphytic growth from asymptomatic infection of leaves (Tichelaar 1967), or by growth into wounds in the onion bulbs, neck or leaves (Maude et al. 1984). The conidia production that we observed on green leaves of onion and even other plant species may play an important role in the disease cycle. This may especially be the case just before the harvest of onion bulbs, when relatively dry foliage is cut from the bulbs creating a wound just above the neck area and thus providing a potential entry point for conidia of *B. aclada* during the period the bulbs remain on the field (Maude et al. 1984). Moreover, the cutting and thus movement of foliage will facilitate spores to become airborne. The simultaneous induction of a temporary high spore pressure and the availability of entry points to the onion bulb might result in the initiation of infection. The capacity of *B. aclada* to also grow and sporulate on the surface of other plants which are considered to be non-hosts (e.g. tomato and lily) might also generate a reservoir of spores that may be present in the vicinity of the crop at the moment that the foliage is cut and bulb tissue becomes exposed to the air. To what extent non-host plants serve as a source of *B. aclada* inoculum is a challenging question to address.

To study the infection biology of *S. cepivorum*, onion seedlings were inoculated using pregerminated sclerotia. In the field, sclerotia remain dormant in the soil until a host plant growing nearby secretes root exudates that induce germination (Coley-Smith 1986; Coley-Smith and King 1969; Davis et al. 2007; Esler and Coley-Smith 1983). However, several studies have reported that sclerotia can spontaneously germinate without root exudates in sterile conditions, suggesting that root exudates do not directly induce germination but instead might abolish suppression of germination by antagonistic soil microbes (Allen and Young 1968; Coley-Smith et al. 1987).

To facilitate visualisation of the infection process, onion seedlings were grown in liquid and inoculated with germinated sclerotia. Infection progressed rapidly and the infection process observed is in accordance with previous descriptions (Abd El-Razik et al. 1974; Metcalf and Wilson 1999; Stewart et al. 1989b; Stewart et al. 1989a). Penetration of the epidermis occurred after formation of appressorium-like structures and infection cushions. On roots of cabbage seedlings, no formation of infection structures was observed, possibly because the cuticle composition or the absence of specific root exudates did not induce infection structure formation (El-Samra et al. 1981; Podila et al. 1993; Tsuba et al. 2002). On tomato seedlings *S. cepivorum* formed infection structures similar to those on onion seedlings, although they did not result in successful invasion of the tomato root system. The abrupt loss of fluorescence of the apical cells of the infection structures indicates that a successful tomato defense response prevented infection, probably because it triggered fungal cell death in infection structures, however without affecting the neighboring hyphal cells of *S. cepivorum*. The cell death in the infection structure suggests a preinvasive mode of defense, possibly by antifungal secondary metabolites or antifungal proteins. For example, *Arabidopsis thaliana* produces upon infection the phytoalexin camalexin which is able to induce programmed cell death in *B. cinerea* (Shlezinger et al. 2011). Likewise, the tomato saponin α-tomatine is known to kill cells of *Fusarium oxysporum* by inducing programmed cell death (Ito et al. 2007). Moreover, tomato roots are known to contain chitinases and ß-1,3-glucanases with strong inhibitory activity on fungal hyphae, especially on growing tips. However, the observation that infection structures still contained a seemingly intact outer wall devoid of cytoplasm and GFP, would argue against the involvement of hydrolytic enzymes in the successful defense in tomato roots and root hairs against *S. cepivorum*.

Our research clearly shows that the infection process of onion by *B. squamosa*, *B. aclada* and *S. cepivorum* involves three completely different infection strategies. Even the sister taxa *B. aclada* and *B. squamosa* showed a completely different biology, despite their close relatedness and their similar genome structure and gene content, with respect to secondary metabolites and effector genes (Valero-Jiménez et al. 2020). It is clear that although *B.* squamosa, *B. aclada* and *S. cepivorum* are related fungal pathogens of onion, they all have their own unique biology and infection strategy and cause distinct diseases. When developing control strategies or breeding for onion cultivars resistant against leaf blight, neck rot and white rot, it is important to consider the fundamental differences between the causal agents.

Acknowledgements

Authors are thankful to Jeff Rollins (University of Florida, Gainesville, USA) and Jürgen Köhl (Wageningen Plant Research, Bio-Interactions, the Netherlands) for providing fungal isolates, as well as to Jyotsna Nepal for developing inoculation protocols. This research is supported by the Dutch Technology Foundation STW, which is part of the Netherlands Organisation for Scientific Research (NWO), and which is partly funded by the Ministry of Economic Affairs (Project 15003).

Supplemental figures

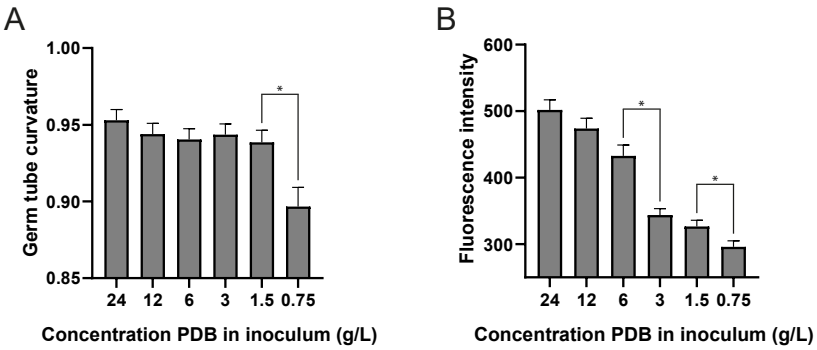

Supplemental figure 1. The effect of nutrient concentration in the inoculum on (**A)** curvature and (**B**) intensity of fluorescence of germ tubes of *B. squamosa* at 8 HPI on the onion leaf surface. Error bars representing standard error, unpaired *t*-test, * p<0.05.

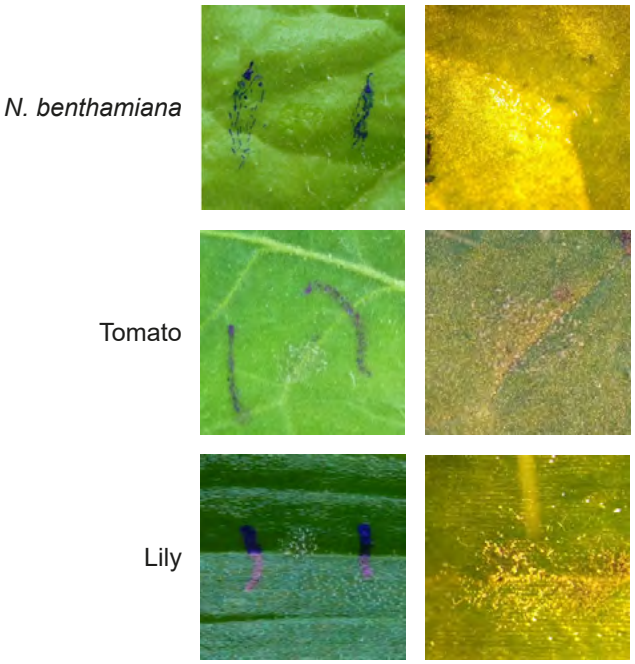

Supplemental figure 2. Different plant species inoculated with *B. aclada* at 72 HPI. Not only onion but also non-host plants tomato and lily show sporulation.

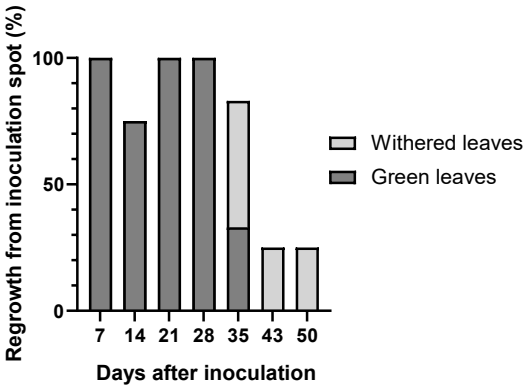

Supplemental figure 3. *B. aclada* long term infection assay. Regrowth from inoculated leaf segments over time.

Chapter 3

Fungal growth inhibitory effect and potential detoxification of ceposides

Maikel B. F. Steentjes [1]
Michele C. Malvestiti [1]
Sebastian Tonn [1]
Hilde Coolman [1]
Yaohua You [1]
Olga E. Scholten [2]
Jan A. L. van Kan [1]

[1] Laboratory of Phytopathology, Wageningen University, Wageningen 6708 PB, The Netherlands
[2] Plant Breeding, Wageningen University, Wageningen 6708 PB, The Netherlands

Abstract

Plants are able to defend themselves against pathogens and pests by producing antimicrobial secondary metabolites that prevent or slow down infection. Plant pathogens have evolved ways to circumvent the antimicrobial action of these toxins, often by enzymatically degrading the host-specific metabolite. Onion is reported to contain a variety of antimicrobial compounds, including a group of saponins called ceposides. We propose that onion pathogenic fungi such as *Sclerotium cepivorum* and *Botrytis aclada*, causal agents of respectively white rot and neck rot, are able to detoxify these antifungal metabolites in order to be virulent on onion. In this work, we compared the growth inhibitory effect of onion bulb extract on host-specific onion bulb pathogens *S. cepivorum* and *B. aclada*, and the generalist pathogen *B. cinerea*. Furthermore we tested 10 *B. aclada* isolates for differences in sensitivity to the onion bulb extract. In addition, we identified genes that encode enzymes which are potentially involved in the detoxification of ceposides by their capacity to hydrolyse the terminal sugar residues rhamnose and xylose. The expression of these candidate genes upon exposure to onion bulb extract was analysed to investigate their involvement in ceposides detoxification. Finally, the putative role of the xylosidase as potential ceposides detoxifying enzyme was studied by analysing *B. cinerea* knock-out and overexpression mutants for their sensitivity to bulb extract and their virulence on onion bulb.

Introduction

Growth of plants and production of crops is hampered by pathogens and pests that parasitize on host plants for their own benefit. As a consequence, plants have evolved defence mechanisms against pathogens that actively or passively counteract colonization. Pathogens in turn, need to overcome these defence mechanisms in order to colonize and reproduce on host plants. One plant defence mechanism is the production of secondary metabolites with antimicrobial activity that prevent or slow down infection. These antimicrobial compounds can be produced and accumulate upon pathogen attack (phytoalexins), or they can be preventatively present (phytoanticipins) (Tiku 2020). In the evolutionary arms race of attack, defence and counterattack, some pathogens have evolved ways to circumvent the antimicrobial action of toxic metabolites of host plants by enzymatically degrading the toxin (Mansfield 2000; Osbourn 1996).

There are several well-studied examples of species-specific antifungal secondary metabolites that inhibit plant colonization and pathogens that have evolved ways to overcome these defence mechanisms. Oat, for example, produces the antimicrobial saponin avenacin, while wheat cannot produce this compound. Isolates of the cereal pathogen *Gaeumannomyces graminis* originating from infected oat (*G. graminis* var. *avenae*, GGA) produce an enzyme called avenacinase that detoxifies avenacin, while isolates originating from infected wheat (*G. graminis* var. *tritici*, GGT) cannot detoxify avenacin and therefore cannot infect oat. Knock-out mutants of GGA confirmed that the presence of the avenacinase gene determines host pathogenicity on oat (Bowyer et al. 1995). Moreover, mutant oat lines deficient in avenacin production are compromised in their basal resistance to a variety of fungal pathogens, including GGT (Haralampidis et al. 2001; Papadopoulou et al. 1999).

Similarly, tomato produces the saponin α-tomatine that is known for its antimicrobial and antinutritional activity. Pathogens of tomato have evolved ways to detoxify α-tomatine with at least three distinct types of enzymes that all enzymatically hydrolyze different glycosidic moieties of the α-tomatine structure (You and van Kan 2021). Isolates of the generalist pathogen *B. cinerea* pathogenic on tomato can detoxify α-tomatine, while an isolate collected from grapevine (M3a) cannot degrade α-tomatine and is therefore not virulent on tomato (Quidde et al. 1998). The *B. cinerea* tomatinase was produced in liquid cultures in the presence of α-tomatine. From breakdown products it was derived that the tomatinase is a β-xylosidase that is present in tomato infecting isolate B05.10 but not in isolate M3a (Quidde et al. 1998).

Crop species of the family *Allium* such as onion (*A. cepa*), shallot (*A. cepa* var. *aggregatum*) and garlic (*A. sativum*) possess a variety of compounds that are known for their bioactive, cytotoxic or antimicrobial activity (Abdelrahman et al. 2019; Lanzotti et al. 2014). Many

of these bioactive compounds of *Allium* are sulphur-containing metabolites such as allicin, a volatile thiosulfinate from garlic that is formed after disruption of tissue due to an enzymatic reaction of alliinase and the precursor molecule alliin (Lanzotti 2006). Allicin has a variety of antimicrobial effects, including antibacterial activity against a wide range of Gram-negative and Gram-positive bacteria and antifungal activity against *Candida* and *Cryptococcus* spp. among others (Ankri and Mirelman 1999; Kyung 2012). In addition to thiosulfinates, also many species-specific saponins have been reported, such as voghierosides isolated from the garlic variety Voghiera, ceposides isolated from onion and Alliospiroside A from shallot (Abdelrahman et al. 2017; Lanzotti et al. 2012a; Lanzotti et al. 2012b; Sobolewska et al. 2016). Alliospiroside A is a shallot-specific saponin that inhibits growth of the fungal onion pathogen *Fusarium oxysporum* f.sp. *cepa*, the causal agent of *Fusarium* basal rot in onion. The biosynthetic and regulatory genes responsible for the production of Alliospiroside A are present on chromosome 2A of shallot. Monosomic addition lines of Japanese bunching onion (*Allium fistulosum*) with shallot chromosome 2A produced Alliospiroside A resulting in an increased resistance against *F. oxysporum* f.sp. *cepa*, demonstrating the potency of using antifungal compounds in resistance breeding (Abdelrahman et al. 2017; Vu et al. 2012). Ceposides are onion-specific saponins that have been identified in three forms (A, B and C) with minor changes in terminal sugar residues. All three forms showed antifungal activity against several plant pathogens including *B. cinerea* (Lanzotti et al. 2012b). The antifungal effect of individual ceposides increased with their concentration and a synergistic effect was observed upon applying all three ceposides in combination against *B. cinerea* and *Trichoderma atroviride* (Lanzotti et al. 2012b).

Although onion possesses various antimicrobial compounds there are also several pathogens and pests that are capable of infecting onion bulbs. Two major host-specific fungi of onion are *Sclerotium cepivorum* and *Botrytis aclada*, causing white rot and neck rot, respectively (Crowe 2008; Lacy and Lorbeer 2008; Sammour et al. 2011; Steentjes et al. 2021a). It seems logical to suggest that pathogens specialized on onion bulbs have evolved ways to deal with antifungal compounds released from their host cells during infection. In this study, we aimed to provide insight in the antifungal effect of ceposides on the onion bulb-specific pathogens *S. cepivorum* and *B. aclada* compared to the closely related generalist pathogen *B. cinerea*. To do so, we tested the inhibitory effect of bulb extracts on fungal growth. Moreover, we identified candidate genes for the enzymatic hydrolysis of ceposides and performed expression analysis and infection assays of mutant strains to evaluate the involvement of these candidate genes in ceposides detoxification.

Material and methods

Fungal isolates and growth conditions

Fungal isolates *B. aclada* 633, *S. cepivorum* UFL, and *B. cinerea* strain B05.10 were used to assess the inhibitory growth effect of bulb extract. To assess differences in sensitivity between *B. aclada* isolates, next to strain 633 also strains 501, 513, 518, 543, 559, 633, 651, 654, 662 and 673 were used which were all isolated from infected onion bulbs in 2015 and 2016 in The Netherlands or New Zealand. To assess the role of *B. cinerea* βXYL in bulb extract sensitivity and onion bulb virulence, strains B05.10, M3a, and mutant strains B05.10ΔβXYL and M3a+βXYL were used. All fungi were grown on PDA (Oxoid) in the dark at 20°C and for long term storage conidia of *B. aclada* and *B. cinerea* were stored at -80°C in 15% glycerol and sclerotia of *S. cepivorum* were stored at room temperature. For preparing liquid cultures of *B. aclada* to assess gene expression and to perform infection assays with *B. cinerea*, conidia were produced. Conidia of *B. aclada* and *B. cinerea* were obtained by growth on MEA (Oxoid) at a temperature of 20°C in the dark for 6 days. After 6 days, plates were exposed to UV light (360-380nm, Phillips TLD 18W/08) for 24 hours. After approximately 4 days of conidia development in the dark at 20°C, conidia were harvested.

Ceposides-containing onion bulb extract

To detect ceposides using thin layer chromatography, a crude bulb extract was made by blending 50 g of fresh bulb scales in 500 mL water. The suspension was centrifuged and the supernatant was filter sterilized and subsequently freeze dried until 100 mL remained. To test the growth inhibitory effect of ceposides against *S. cepivorum*, *B. cinerea* and *S. cepivorum*, and to assess the expression of genes potentially involved in detoxification of ceposides, crude extracts of onion bulb reportedly containing ceposides were prepared following the procedure described by Lanzotti et al. (Lanzotti et al. 2012b). Onion tissue (150 g fresh bulb of yellow onions) was blended in 100 mL of water and 200 mL acetone was added while stirring before the suspension was filtered over filter paper. The remaining onion tissue was suspended in a second aliquot of 200 mL acetone while stirring, and was filtered. The filtrates were combined and the acetone was evaporated overnight using a nitrogen flow. The watery residue was mixed with an equal volume of ethyl acetate and after phase separation the watery phase was collected. The watery phase was then partitioned with an equal volume of n-butanol. The butanol layer was collected and evaporated using nitrogen flow to obtain a powdery residue. This residue was dissolved in 25 ml Milli-Q water, filter sterilized and stored at 4°C.

Thin layer chromatography, chemical staining, and *C. cucumerinum* growth assay

TLC plates (Silica gel 60-F254) were used to separate onion metabolites and to confirm the presence of ceposides in bulb extract. 150 µl of crude water extract was evaporated using a speed vacuum and the remaining compounds were dissolved in 120 µl EtOH/H_2O (70:30, v/v). To prevent diffusion of samples on the plate before migration, samples were loaded in four aliquots of 30 µl with intervals of a few minutes to allow drying of the plate. Plates were placed in solvent BuOH/AcOH/H_2O (60:15:25, v/v) for 8.5 hours until the mobile phase reached the top of the plate, and were subsequently dried. For the detection of ceposides, plates were sprayed with p-anisaldehyde (SigmaAldrich) in H_2SO_4 and glacial AcOH. Plates were incubated for 5 minutes at 110°C, and spots that stained red were indicative for the presence of triterpenes such as saponins (Oleszek et al. 2008). To test the fungal growth inhibitory effect of the metabolites separated on the TLC plate, plates were spray inoculated with a spore suspension of *Cladosporium cucumerinum* of 10^7 spores per ml in PDB (30 g/L). Plates were incubated in the dark in boxes with water to ensure high relative humidity, though plates were prevented of making direct contact with water by placing them on floral foam. Five days after inoculation plates were assessed for growth of *C. cucumerinum*.

Growth inhibition assays

Agar plugs (5 mm diameter) from the edges of growing colonies on PDA (Oxoid) were transferred to the center of PDA plates containing different bulb extract concentrations (0%, 1%, 5% or 10% v/v). The volume of water used to prepare the PDA was adjusted according to the volume of bulb extract to be added to avoid diluting the PDA concentration and maintain equal nutrient levels over the different treatments. Colony diameter was measured at consecutive days until plates were fully grown and growth rates were calculated using trendlines.

Identification of candidates genes for the detoxification of ceposides

To identify putative αRHAs in the genome of *S. cepivorum* UFL, protein sequences of αRHAs from *S. sclerotiorum* 1980 UF-70 were obtained from EnsemblFungi (fungi.ensembl.org) and BLASTed against the genome assembly of *S. cepivorum* UFL (Valero-Jiménez et al. 2020). The best hit for each of the four genes was selected as putative αRHA. For the identification of αRHAs in the genome of *B. aclada* 633, genes annotated as αRHAs in the genome of *B. cinerea* B05.10 in the CAZy database as well as the four αRHAs of *S. cepivorum* were BLASted against the *B. aclada* 633 genome (Valero-Jiménez et al. 2020). A total of 8 *B. aclada* genes were identified as putative αRHAs. The ßXYL from *B. aclada* was identified

by BLASTing the *B. aclada* 633 genome for homologues of the *B. cinerea* B05.10 potential tomatinase gene identified by You et al. (unpublished). All candidate genes are listed in Supplemental table 1.

Expression analysis αRHAs of *S. cepivorum*

To assess the expression of putative αRHA genes in *S. cepivorum* in response to bulb extract, liquid cultures from blended mycelium were prepared. Mycelium was harvested from two plates of Gamborg B5 (basal salt mixture, Duchefa) + 0.1 M fructose agar covered with cellophane sheets, homogenized (Kinematica CH-6010) in 25 mL liquid Gamborg B5 + 0.1 M fructose and transferred to a conical glass flask with a total of 70 ml medium. Liquid cultures were incubated at 22°C at 120 rpm. After one hour, the liquid culture was divided in two conical flasks. To one flask 1 mL of the onion bulb extract was added, to the other flask 1 mL of the liquid medium was added as a control. In total, three replicates were performed, each time combining two colonies from separate petri dishes to start the liquid culture. Mycelium was collected from liquid cultures at 2 and 8 hours after adding the onion extract or the control. Mycelium was filtered over nylon mesh, frozen and freeze dried. To isolate RNA, samples were grinded, incubated in Trizol (Ambion, Life Technologies) and treated with chloroform. Ethanol was added to the aqueous phase and the mixture was used as input for an RNeasy Plant Mini Kit (Qiagen). This RNA was used as template for cDNA synthesis following the protocol of M-MLV Reverse Transcriptase (Promega). A CFX96 Touch™ Real-Time PCR Detection System (Bio-Rad) using SensiMix SYBR Hi-ROX (Bioline) was used to determine the relative expression of the αRHA genes in three technical replicates. Averaging quantification cycle (Cq) values for technical replicates per biological replicate resulted in one Cq value per biological replicate. These averages were used for subsequent calculations. Primer pair specific amplification efficiencies were calculated per gene using the LinRegPCR software (Ramakers et al. 2003). Relative expression ratios of αRHA genes were calculated from Cq values as described by Pfaffl (2001) using using Actin A and β-tubulin A as reference genes for normalization. Fold change expression values refer to the expression change in samples treated with bulb extract compared to the untreated control samples at the same timepoint.

Expression analysis αRHAs and βXYL from *B. aclada*

To evaluate the expression of αRHA genes and the βXYL gene from *B. aclada* in response to bulb extract, liquid cultures of *B. aclada* were prepared using 50 ml liquid Gamborg B5 + 0.1 M fructose and 10^6 conidia per ml medium. Cultures were grown for 24 hour at 20°C and 120 rpm. An aliquot of mycelium was harvested at timepoint 0 hours, and 2 ml of bulb extract and 50 ml extra medium were added to the remaining culture. 2, 4 and 24 hours after adding the extract, mycelium was harvested as well. Processing of mycelium, isolation

of RNA and cDNA synthesis were performed as described for *S. cepivorum*. The obtained cDNA was used as template for semi-quantitative PCR to assess the expression levels of candidate genes. Primers for candidate genes were designed to yield approximately 500bp amplicons and were preferably spanning an intron. Primers of all candidate genes and reference gene Actin A were used to amplify the cDNA of timepoint 0h, 2h, 4h and 24h for 45 cycles. PCR products were visualized on a 2% agarose gel.

Onion bulb infection assay

B. cinerea strains B05.10, M3a, and mutant strains B05.10ΔβXYL and M3a+βXYL were assessed for their virulence on onion bulb scales. Bulbs of yellow onion were cut into quarters, the outermost and innermost scales were removed and individual scales were prepared for inoculation. On all scales a scratch on the surface of 1 mm deep and 10 mm wide was made using a scalpel. Scales were inoculated using 10^6 spores per ml in 15mM sucrose + Gamborg B5 basal salt mixture buffered at pH 6.0 with 10mM KPO_4. Droplets of 2 µl were inoculated evenly over the 10mm wide scratch with 12 replicates per *B. cinerea* strain. Onion bulb scales were incubated in boxes with wet filter paper to ensure high relative humidity, though scales were prevented of making direct contact with water by placing them on petri dishes. Lesion sizes were measured on 3 consecutive days and lesion growth rates were calculated using trendlines.

Statistical analysis

Statistical analysis of fungal growth rates and lesion growth rates was performed in SPSS Statistics 25.0 (IBM). A one-way ANOVA with Tukey Post Hoc analysis for multiple comparisons assuming equal variance was performed to assess if differences were significant ($p \leq 0.05$). For growth rates of *S. cepivorum*, *B. aclada* and *B. cinerea,* and *B. cinerea* B05.10, B05.10ΔβXYL, M3a and M3a+OliCβXYL, significance of differences between extract concentrations was determined per species or per strain. Differences in growth rates of different *B. aclada* strains were evaluated only on 10% extract concentration. Statistical analysis to test significance of the differences in *S. cepivorum* αRHA genes expression in response to bulb extract between treatment and control was performed using the Relative expression software tool REST (Pfaffl et al. 2002).

Results

Detection of ceposides from onion bulbs using thin layer chromatography

Since ceposides are not commercially available and cannot easily be purified, ceposides-containing onion bulb extracts were produced. By lack of an internal standard the concentrations of individual compounds in these extracts were not determined. Thin layer chromatography (TLC) of a crude water extract yielded a spot with an Rf value of 0.82 that stained red upon treatment of the TLC plate with p-anisaldehyde which is indicative for triterpenes such as saponins (Figure 1A). Spraying the TLC plate with a spore suspension of *Cladosporium cucumerinum* in nutrient medium and incubating the plate under humid conditions facilitated *C. cucumerinum* growth on the entire plate except at the place where the spot was located (Figure 1B). LC-MS of one extract confirmed the presence of ceposides A, B and C and identified an additional ceposide, designated ceposide D, which is an isomer of ceposide C (Figure 1C). These results confirmed the presence of ceposides in onion bulbs, and the growth inhibitory activity of ceposides on fungi. Since we used onion bulbs of unknown cultivars in different seasons, the different batches of extract produced in this study could differ in chemical composition and ceposide content.

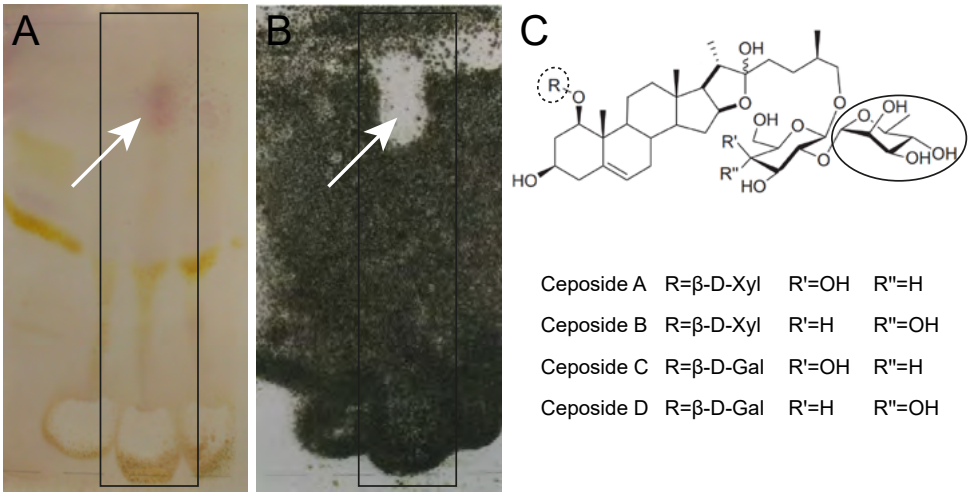

Figure 1. Isolation of ceposides from onion bulb extract. (**A)** TLC plate stained with p-anisaldehyde reagent. Arrow marks a red spot indicative of the presence of triterpenes such as saponins. (**B)** TLC plate spray-inoculated with *C. cucumerinum* assessed at 5 DPI. Arrow indicates area with growth inhibitory activity. (**C)** Chemical structure of ceposides with the three ceposide-specific residues depicted as R, R' and R''. The rhamnose present in all four ceposides is indicated with a circle and the xylose present in ceposide A and B is indicated with a dashed circle. Adapted from Lanzotti et al. (2012b).

The growth inhibitory effect of bulb extract on *S. cepivorum*, *B. aclada* and *B. cinerea*

The antifungal effect of bulb extract was assessed in a radial growth assay with the two onion-specific pathogenic fungi *S. cepivorum* and *B. aclada,* and the generalist pathogen *B. cinerea*. Colony diameters were measured at consecutive days in order to calculate growth rates. Relative to controls without bulb extract, both *S. cepivorum* and *B. cinerea* showed a reduction in growth rate of up to 25% at 10% bulb extract concentration, while *B. aclada* was inhibited by <10% (Figure 2A, 2B). On control plates as well as on plates with 5% and 10% bulb extract, all species eventually fully covered the plates after which sclerotia (*S. cepivorum* and *B. cinerea*) or spores (*B. aclada*) were formed.

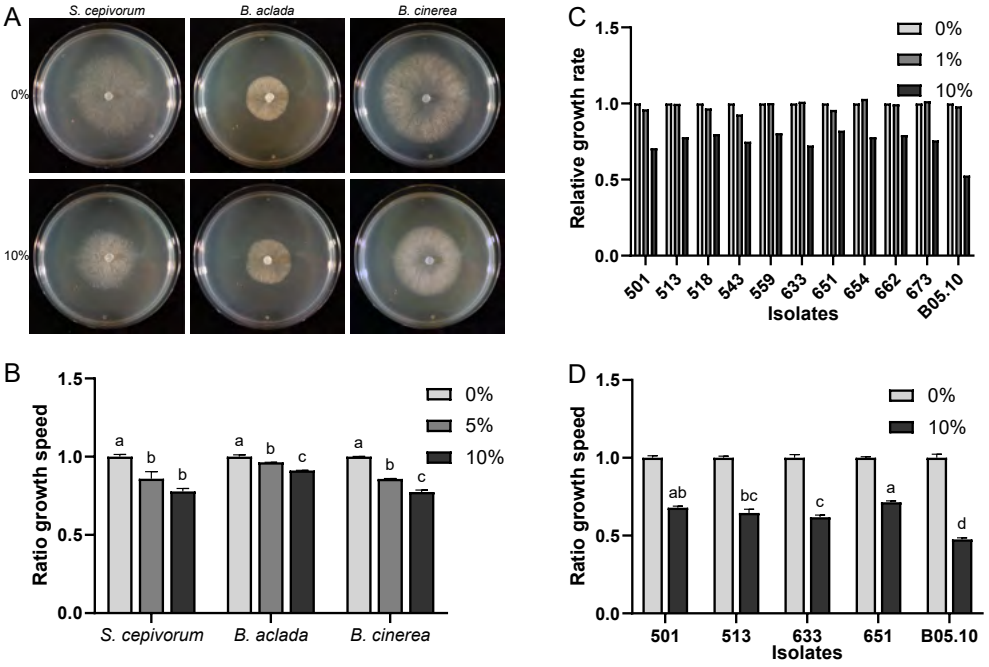

Figure 2. The effect of different concentrations of bulb extract on growth of *S. cepivorum*, *B. aclada* and *B. cinerea*. (**A)** Colonies of *S. cepivorum*, *B. aclada* and *B. cinerea* on 0% and 10% bulb extract at 2 days after inoculation. (**B)** Growth rate of *S. cepivorum*, *B. aclada* and *B. cinerea* on 5% and 10% bulb extract relative to controls lacking bulb extract. Values are averages of two replicates and different letters within each fungus indicate significant differences (Tukey Post Hoc analysis). (**C)** Growth rate of 10 *B. aclada* isolates and *B. cinerea* on 1% and 10% bulb extract compared to control. (**D)** Growth rate of *B. aclada* isolates 501, 513, 633 and 651, and *B. cinerea* on 10% bulb extract relative to 0%. Values are averages of three replicates and significant differences are indicated with letters for 10% bulb extract concentration (Tukey Post Hoc analysis).

Since *B. aclada* appeared less sensitive to bulb extract than *S. cepivorum* and *B. cinerea*, we aimed to test for variation between multiple *B. aclada* isolates in their sensitivity to bulb

extract. To do so, the growth inhibitory effect of bulb extract was assessed on 10 strains isolated in 2015 and 2016 in The Netherlands and New Zealand. As a control, *B. cinerea* strain B05.10 was included since it showed a relatively high sensitivity in the previous assay. As expected, *B. cinerea* showed the highest growth inhibition with a reduction in growth rate of almost 50% at an extract concentration of 10% compared to the control without extract. All 10 *B. aclada* isolates showed a comparable inhibition in growth. At 10% extract concentration, growth inhibition ranged from 30% for isolate 501 to 18% for isolate 651 relative to growth of controls without extract (Figure 2C). The latter two isolates together with isolate 513 and 633 were selected for further analysis using more replicates per isolate. Again, *B. cinerea* showed the largest reduction in growth rate while all four *B. aclada* isolates were comparably inhibited in growth (Figure 2D). Of all *B. aclada* isolates, isolate 633 showed the largest growth inhibition with a growth inhibition of 40% relative to the control.

Expression of *S. cepivorum* and *B. aclada* alpha-L-rhamnosidase genes, encoding candidate enzymes for ceposides detoxification

To enable fungal growth in presence of antifungal compounds, production of fungal enzymes involved in the detoxification is often induced in response to the presence of these compounds. All ceposides contain a terminal rhamnose at the same position, while other moieties differ between the individual ceposides (Figure 1C). A single rhamnosidase that is able to remove terminal rhamnoses might be sufficient to detoxify all three ceposides and to contribute to pathogenesis of onion bulb pathogens. Rhamnose-specific glycosidases are classified as alpha-L-rhamnosidases (αRHAs) (Yanai and Sato 2000), and in the genome of *S. cepivorum* four putative αRHAs were identified (Supplemental table 1). To evaluate if any of the putative αRHAs is involved in detoxifying ceposides, expression of these four genes in *S. cepivorum* cultures exposed to bulb extract was compared to expression in medium without bulb extract. Relative expression of each candidate gene was determined 2 and 8 hours after adding the bulb extract to the liquid medium (Figure 3A). αRHA2 showed the highest upregulation 2 hours after adding the extract. The average of three biological replicates measured an almost 4-fold higher expression as compared to the control at the same timepoint without bulb extract. However, none of the expression levels was significantly different for any of the candidates at either time point.

To assess whether expression of αRHAs of *B. aclada* is induced upon contact with ceposides, we first identified the αRHAs of *B. aclada* strain 633 (Supplemental table 1). A semi-quantitative RT-PCR was performed on mycelium that was harvested at 2h, 4h and 24h after adding bulb extract to the medium with t=0h representing mycelium in absence of bulb extract. Amplicons were obtained for all αRHA transcripts except αRHA5 and bands were of expected sizes, suggesting expression of seven of the eight genes (Figure

3B). For αRHA3 and αRHA4 double bands were observed, likely as a result of splicing variants. All αRHA transcripts that we detected were already expressed in absence of the bulb extract (t=0h) and none showed clear upregulation at any timepoint in response to the extract. Since every bulb extract is unique, the extract used for the αRHA expression study in *B. aclada* was tested for its antifungal activity. The inhibitory effect on the growth of *S. cepivorum*, *B. aclada* and *B. cinerea* was similar as observed before (Supplemental figure 1). The observation that αRHA transcript levels in both *S. cepivorum* and *B. aclada* were not upregulated upon bulb extract exposure does not imply a role for αRHAs in the detoxification of ceposides.

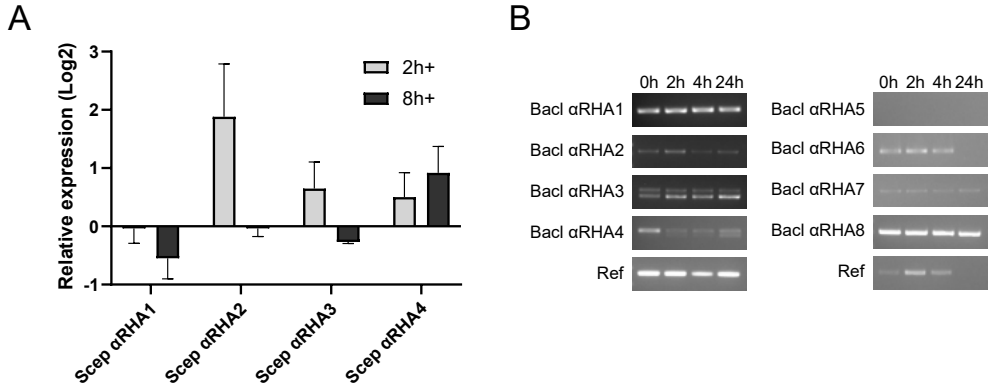

Figure 3. Expression of alpha-L-rhamnosidases of *S. cepivorum* and *B. aclada* in response to bulb extract. (**A)** Relative expression of the four αRHAs of *S. cepivorum* at 2 and 8 hours after adding bulb extract as compared to control medium without extract at the corresponding timepoints using Actin A and β-tubulin A as reference genes. Each bar represents the average of three biological replicates with three technical replicates respectively. **(B)** Expression of eight αRHAs of *B. aclada* assessed by semi-quantitative RT-PCR with Actin A as reference gene at 0, 2, 4 and 24 hours after exposure to bulb extract.

β-xylosidase as a candidate enzyme for the detoxification of ceposides

B. cinerea is able to detoxify the tomato saponin α-tomatine using a β-xylosidase (βXYL) (Quidde et al. 1998). The gene encoding this βXYL is strongly upregulated upon contact with α-tomatine, and is not present in the genome of the *B. cinerea* grapevine isolate M3a that is not virulent on tomato (You et al. unpublished data). The tomatinase gene is not widely distributed in *Botrytis* species; apart from *B. cinerea* homologues are only present in *B. calthae* and *B. aclada* (Supplemental table 1). Two ceposides contain a terminal xylose and we considered that the βXYL present in *B. aclada* might be able to remove the xylose moiety of ceposides and thereby play a role in their detoxification (Figure 1C).

To evaluate if the βXYL of *B. aclada* is upregulated upon contact with ceposides, expression analysis was performed on mycelium exposed to bulb extract using a semi-

quantitative RT-PCR. The βXYL amplicon was detected at 2h, 4h and 24h after adding the ceposides containing extract as well as in absence of extract (t=0h), suggesting there is no upregulation upon contact with ceposides (Figure 4A).

Because of the role of *B. cinerea* βXYL in the detoxification of α-tomatine, knockout mutants of strain B05.10 that naturally possesses βXYL and overexpression mutants of strain M3a that naturally lacks the βXYL gene, have been made (You et al. unpublished data). To assess the capacity of *B. cinerea* βXYL to detoxify ceposides, wild type strains and mutants of *B. cinerea* were tested for their sensitivity to the presence of different concentrations bulb extract. All tested *B. cinerea* strains showed a comparable growth inhibition to increasing concentrations of bulb extract (Figure 4B).

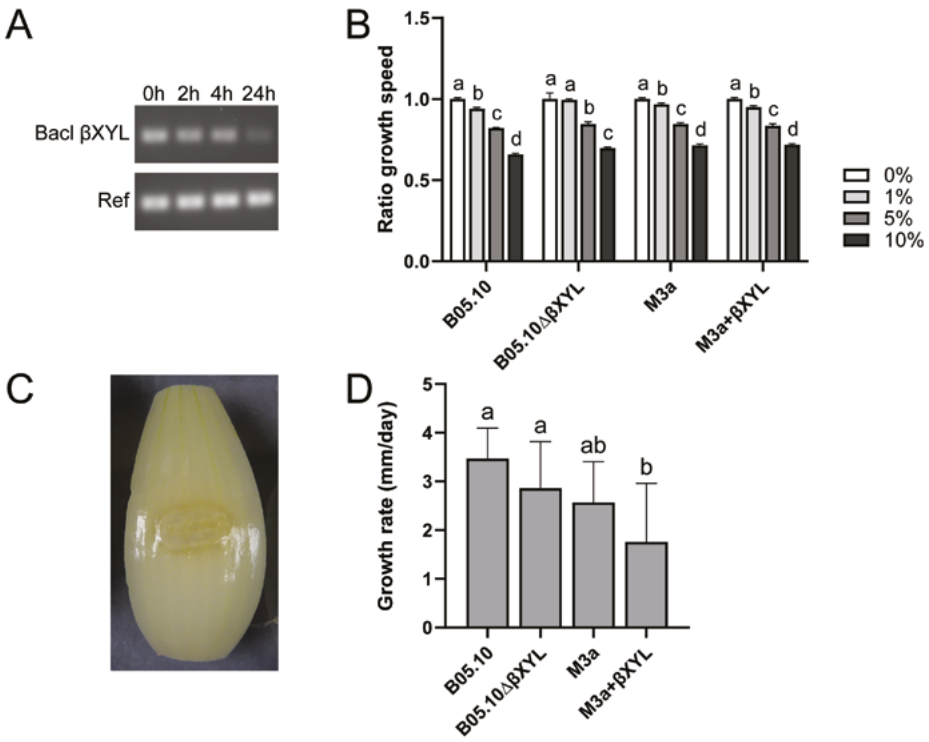

Figure 4. The role of βXYL in detoxification of ceposides and virulence on onion bulbs. (**A)** Expression analysis of *B. aclada* βXYL assessed by semi-quantitative RT-PCR using Actin A as reference gene at 0, 2, 4 and 24 hours after exposure to bulb extract. (**B)** Growth rates of *B. cinerea* strains B05.10, B05.10ΔβXYL, M3a and M3a+βXYL on increasing concentrations of bulb extract relative to controls without extract. Values are averages of two replicates and different letters within each fungus indicate significant differences (Tukey Post Hoc analysis). (**C)** Onion bulb scale infected by *B. cinerea* showing an expanding lesion. (**D)** Lesion growth of *B. cinerea* strains B05.10, B05.10ΔβXYL, M3a and M3a+βXYL on onion bulb scales. Values are averages of twelve replicates and significant differences are indicated with different letters (Tukey Post Hoc analysis).

The contribution of the *B. cinerea* βXYL activity to pathogenesis on onion bulb was tested in an infection assay using a set of strains that differed in the possession of the βXYL gene. Spores of the strains B05.10, deletion mutant B05.10ΔβXYL, M3a and overexpression mutant M3a+βXYL were inoculated on wounded onion bulb scales and lesion diameters were measured at consecutive days in order to calculate lesion growth rates (Figure 4C). Although there was variation in lesion growth between strains, lesion growth rates did not significantly differ between isogenic strains containing or lacking the βXYL gene (Figure 4D). Altogether, the steady expression level of *B. aclada* βXYL upon exposure to bulb extract and the unaltered sensitivity to bulb extract, as well as the virulence on onion bulbs of *B. cinerea* strains with and without βXYL suggest that βXYL does not participate in the detoxification of ceposides.

Discussion

Bulbs of onion were used as source for the isolation of ceposides by extraction and partition. According to Lanzotti et al. (2012b), only a small fraction of the bulb extract consists of the onion-specific saponins called ceposides. Moreover, there is no information about variation in ceposide production between onion cultivars nor is it known whether ceposide levels decrease during long term storage of bulb, which is common practise in Dutch onion trade. Since the quantity and purity of ceposides in bulb extract used in our experiments may have varied between extracts, it is difficult to compare the effects of different extracts. Moreover, the bulb extract likely contained other metabolites and other saponins that possibly also have antimicrobial activity. Lanzotti et al. (2012b) tested the growth inhibitory effect of ceposides on a number of fungi, including *B. cinerea* and *S. cepivorum*. Almost all tested fungi were inhibited in growth, but the onion bulb pathogen *S. cepivorum* was not affected in their study. In our growth assays we did observe an inhibitory effect on *S. cepivorum*, suggesting that next to ceposides possibly other antifungal compounds were present in our bulb extract as well. Alternatively, different isolates of *S. cepivorum* may display different sensitivity to ceposides.

We speculated that ceposides could be detoxified by hydrolysis of terminal sugar residues, similar to detoxification of other saponins (Bowyer et al. 1995; Quidde et al. 1998), although no information is available about degradation products of ceposides and their effect on fungal growth. We assessed the expression of αRHAs of *S. cepivorum* and *B. aclada* and βXYL of *B. aclada* upon exposure to bulb extract. Most candidate genes were already expressed in absence of bulb extract, and none of them showed significantly increased transcript levels in presence of the extract. It is commonly known that the expression of fungal enzymes capable of hydrolysing antifungal saponins is induced upon exposure to their target compound. For example, tomatinase activity from *B. cinerea, Fusarium*

oxysporum f.sp. *lycopersici* and *Cladosporium fulvum* is highly induced upon exposure to α-tomatine (Ökmen et al. 2013; Pareja-Jaime et al. 2008; Quidde et al. 1998). The enzymatic activity required for detoxification of other phytoalexins such as pisatin from pea and resveratrol from grapevine is also rapidly and strongly induced upon contact with their target compound (Hirschi and VanEtten 1996; Schouten et al. 2002). Expression profiles of the selected genes considered to be candidates for the detoxification of ceposides did not match the pattern expected for true ceposidases.

To assess the role of βXYL in ceposides detoxification, we not only evaluated *B. aclada* βXYL expression levels, but also tested wild type and mutant strains of *B. cinerea* that differed in their ability to produce βXYL for sensitivity to bulb extract and their virulence on onion bulbs. There are numerous examples that fungal mutants lacking a host saponin detoxifying enzyme are more sensitive to the saponin and often reduced in host virulence. *G. graminis* mutants with a disrupted avenacinase gene lost complete virulence on the avenacin containing host oat (Bowyer et al. 1995). *F. oxysporum* f. sp. *lycopersici* tomatinase-disrupted mutants were reduced in virulence on tomato and were more sensitive to α-tomatine (Pareja-Jaime et al. 2008). *Septoria lycopersici* tomatinase deficient mutants were more sensitive to α-tomatine however, were not affected in their ability to cause disease (Martin-Hernandez et al. 2000). We observed that *B. cinerea* strains lacking βXYL were not altered in sensitivity to bulb extract and not affected in virulence on onion bulbs, suggesting that βXYL does not contribute to detoxification of ceposides. However, despite the fact that *B. cinerea* and *B. aclada* βXYL display 85% amino acid identity, βXYL mutants of *B. aclada* are required to confirm that βXYL does not play a role in ceposides detoxification and virulence of *B. aclada*.

In addition to ceposides, onion bulbs are known to contain many other bioactive metabolites such as characteristic organosulfur volatiles. These thiosulfinates are released upon cellular damage of onion bulb tissue and have antimicrobial activity (Lanzotti et al. 2014). In *Pantoea ananatis*, a bacterial pathogen of onion that causes center rot, a gene cluster was identified that encodes tolerance to thiosulfinates via sulfur redox genes (Stice et al. 2020). The plasmid-borne allicin tolerance (*alt*) gene cluster facilitates growth of *P. ananatis* in onion extract and promotes onion bulb colonization. Likewise, a gene cluster was identified in *Pseudomonas fluorescens* isolated from garlic that confers resistance to allicin, and *Pseudomonas salominii* strains isolated from garlic were reported to contain similar clusters as well (Borlinghaus et al. 2020; Gardan et al. 2002). Since thiosulfinate metabolites like allicin inhibit both bacteria and fungi (Borlinghaus et al. 2014; Leontiev et al. 2018), it seems logical to propose that onion pathogenic fungi like *S. cepivorum* and *B. aclada* possess tolerance mechanisms to these compounds. Bioinformatic analysis may reveal thiosulfinate tolerance genes or gene clusters homologous to those identified in bacteria or new genes based on annotation as sulphur redox genes. Alternatively, RNA sequencing of fungi grown in the presence of pure antifungal onion metabolites, whether

organosulfur compounds or saponins, may be an effective way to identify genes or gene clusters involved in tolerance or detoxification of antifungal metabolites.

Acknowledgements

Authors thank Jeff Rollins (University of Florida, Gainesville, USA) and Jürgen Köhl (Wageningen Plant Research, Bio-Interactions, the Netherlands) for providing fungal isolates as well as Bert Schipper (Wageningen Plant Research, Bioscience, the Netherlands) for performing LC-MS analysis. This research is supported by the Dutch Technology Foundation STW, which is part of the Netherlands Organisation for Scientific Research (NWO), and which is partly funded by the Ministry of Economic Affairs (Project 15003).

Supplemental tables and figures

Supplemental table 1. Names and gene identifiers for genes of *S. cepivorum* and *B. aclada* used in this study.

	Name	Gene ID
S. cepivorum	αRHA1	SCEP_033g00080
	αRHA2	SCEP_007g02780
	αRHA3	SCEP_030g00730
	αRHA4	SCEP_029g01180
B. aclada	αRHA1	BACL_001g00160
	αRHA2	BACL_003g06650
	αRHA3	BACL_003g09000
	αRHA4	BACL_005g05350
	αRHA5	BACL_007g02540
	αRHA6	BACL_008g01030
	αRHA7	BACL_010g04470
	αRHA8	BACL_010g04840
	βXYL	BACL_015g04100

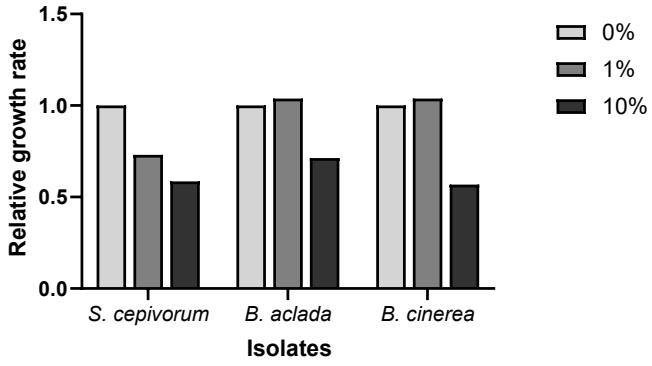

Supplemental figure 1. Relative growth rates of *S. cepivorum*, *B. aclada* and *B. cinerea* on 1% and 10% onion bulb extract as compared to 0%. The extract used for this assay was also used to study the expression of αRHAs and βXYL in *B. aclada*.

Chapter 4

Dynamics in secondary metabolite gene clusters in otherwise highly syntenic and stable genomes in the fungal genus *Botrytis*

Claudio A. Valero-Jiménez [1]
Maikel B. F. Steentjes [1]
Jason C. Slot [2]
Xiaoqian Shi-Kunne [1]
Olga E. Scholten [3]
Jan A. L. van Kan [1]

[1] Laboratory of Phytopathology, Wageningen University, Wageningen 6708 PB, The Netherlands
[2] Department of Plant Pathology, The Ohio State University, Columbus, OH 43210, USA
[3] Plant Breeding, Wageningen University, Wageningen 6708 PB, The Netherlands

This chapter is published as:

Valero-Jiménez, C. A., Steentjes, M. B., Slot, J. C., Shi-Kunne, X., Scholten, O. E., & van Kan, J. A. (2020). Dynamics in secondary metabolite gene clusters in otherwise highly syntenic and stable genomes in the fungal genus *Botrytis*. *Genome biology and evolution* 12(12), 2491-2507.

Abstract

Fungi of the genus *Botrytis* infect >1,400 plant species and cause losses in many crops. Besides the broad host range pathogen *Botrytis cinerea*, most other species are restricted to a single host. Long-read technology was used to sequence genomes of eight *Botrytis* species, mostly pathogenic on *Allium* species, and the related onion white rot fungus, *Sclerotium cepivorum*. Most assemblies contained <100 contigs, with the *Botrytis aclada* genome assembled in 16 gapless chromosomes. The core genome and pan-genome of 16 *Botrytis* species were defined and the secretome, effector, and secondary metabolite repertoires analyzed. Among those genes, none is shared among all *Allium* pathogens and absent from non-*Allium* pathogens. The genome of each of the *Allium* pathogens contains 8–39 predicted effector genes that are unique for that single species, none stood out as potential determinant for host specificity. Chromosome configurations of common ancestors of the genus *Botrytis* and family Sclerotiniaceae were reconstructed. The genomes of *B. cinerea* and *B. aclada* were highly syntenic with only 19 rearrangements between them. Genomes of *Allium* pathogens were compared with ten other *Botrytis* species (nonpathogenic on *Allium*) and with 25 Leotiomycetes for their repertoire of secondary metabolite gene clusters. The pattern was complex, with several clusters displaying patchy distribution. Two clusters involved in the synthesis of phytotoxic metabolites are at distinct genomic locations in different *Botrytis* species. We provide evidence that the clusters for botcinic acid production in *B. cinerea* and *Botrytis sinoallii* were acquired by horizontal transfer from taxa within the same genus.

Introduction

Fungi have great societal impact because of their utility for nutritional, industrial, and medical purposes, as well as their pathogenic behavior on humans and plants. In recent years, the sequencing of fungal genomes has progressed at tremendous pace thanks to their small genome size and decreases in sequencing costs (Spatafora et al. 2017). Many species of industrial fungi from the genera *Aspergillus*, *Penicillium*, and *Trichoderma* have been sequenced e.g., de Vries et al. (2017), whereas for human pathogens such as *Cryptococcus neoformans*, *Candida* spp., or *Aspergillus fumigatus*, numerous isolates were sequenced to obtain insight in population diversity (e.g., Ashton et al. (2019); Lind et al. (2017)). Similarly, many dozens of plant pathogenic fungi species have been sequenced in order to gain insight into their evolution and the traits that enable the infection of plants (Möller and Stukenbrock 2017). Studies on plant pathogenic fungi have provided evidence for evolutionary adaptations that confer dynamics and plasticity on the genome, such as the presence of repeat-rich, gene-poor genomic regions or the possession of entire "dispensable" or "lineage-specific" chromosomes that contain effector genes which confer the capacity to specifically infect certain host plant species or plant genotypes (Bertazzoni et al. 2018; Dong et al. 2015; Presti and Kahmann 2017; Sipos et al. 2017).

The fungal genus *Botrytis* comprises ~35 recognized species that all are pathogenic on plants (Garfinkel et al. 2017; Hyde et al. 2014) with the exception of *Botrytis deweyae*, which colonizes *Hemerocallis* (daylily) as an endophyte (Grant-Downton et al. 2014). *Botrytis* spp. are notorious pathogens with a necrotrophic infection behavior, that is, they kill host cells and invade the dead cells to acquire nutrients. Two species that have been extensively studied are *Botrytis cinerea* and *Botrytis pseudocinerea*, morphologically indistinguishable taxa that cause gray mold on >1,400 host plant species (Elad et al. 2016). Other *Botrytis* species are considered to be restricted to a single host or a small number of taxonomically related hosts (Elad et al. 2016; Staats et al. 2005). In these cases, each host plant usually is infected by its own specialized *Botrytis* species. There are two exceptions in the pattern of specialized host–pathogen relationships within the genus: as many as eight *Botrytis* species can infect onion (*Allium cepa*) or other *Allium* species (Staats et al. 2005), and a recent study reported as many as 15 previously unknown, phylogenetically distinct *Botrytis* taxa sampled from peony in Alaska (Garfinkel et al. 2019). Phylogenetic analysis separated the genus *Botrytis* into two distinct clades, and *Botrytis* species that infect *Allium* are widely dispersed throughout the largest clade (Garfinkel et al. 2019; Hyde et al. 2014; Staats et al. 2005). Their closest relatives are often pathogenic on hosts that are phylogenetically distant from *Allium*. For example, the closest relatives of *Botrytis squamosa* (onion leaf blight) are the lily pathogen *Botrytis elliptica* and *Hemerocallis* endophyte *B. deweyae*. Furthermore, the closest relative of *Botrytis aclada* (onion neck rot) is the peony pathogen *Botrytis paeoniae*. By contrast, *Botrytis globosa* and *Botrytis sphaerosperma* are sister taxa

and both able to infect *Allium* hosts. The fact that *Allium* pathogens are dispersed over the phylogeny of the genus *Botrytis* suggests that the capacity to infect *Allium* has either been acquired multiple times or lost multiple times, independently, during evolution in the genus.

Pathogens with a necrotrophic lifestyle such as *Botrytis* spp. actively manipulate the cell death balance in their host plant, and in the necrotrophic phase exploit the host cell death machinery by secreting cell death-inducing metabolites and effector proteins (Veloso and van Kan 2018). In the necrotrophic wheat pathogen *Parastagonospora nodorum*, several cell death-inducing effector proteins were identified that contribute to pathogenicity only on wheat genotypes carrying a cognate receptor for these effectors, following an inverse gene-for-gene interaction (Faris et al. 2010; Liu et al. 2009; Liu et al. 2012; Shi et al. 2015; Shi et al. 2016). Each effector–receptor pair contributes in a quantitative manner to disease severity. At least one of the *Parastagonospora nodorum* effector genes has been horizontally transferred between distinct fungi pathogenic on wheat and barley (Friesen et al. 2006; McDonald et al. 2019).

The genome of the generalist *B. cinerea* has been extensively studied in the past decade. A gapless genome assembly was generated comprising 18 contigs, representing (near-)full-length chromosomes. Two contigs are minichromosomes (209 and 247 kb, respectively) with few genes and neither seems relevant for plant infection (van Kan et al. 2017), indicating that the core genome of *B. cinerea* consists of 16 chromosomes. Light microscopic studies by Shirane et al. (1989) showed that five *Botrytis* species (*B. aclada*, *B. byssoidea*, *B. cinerea*, *B. squamosa*, and *B. tulipae*) all contain 16 mitotic chromosomes. The *B. cinerea* reference assembly was supported by a genetic and optical map (van Kan et al. 2017) and a manually curated community annotation (Ensembl Fungi; Pedro et al. 2019). In a follow-up study, we analyzed the genomes of nine *Botrytis* species, mainly pathogens on flower bulb crops, using short-read sequence technology (Valero-Jiménez et al. 2019). In the present study, we sequenced the genomes of eight additional host-specific *Botrytis* species and one *Sclerotium* species, most of which are pathogenic on *Allium*, in order to compare their predicted proteome content and possibly identify host range determinants. The comparison focused on genes that are present in (and possibly shared among) *Allium* pathogens and absent from the non-*Allium* pathogens. The genome assemblies were of sufficiently high quality to analyze chromosome architecture and synteny and to infer the genome organization of ancestors of the genus *Botrytis* and the family Sclerotiniaceae. Furthermore, analysis of secondary metabolite (SM) biosynthetic gene clusters (BGCs) in Sclerotiniaceae and 25 other fungi within the Leotiomycetes showed a patchy distribution of these clusters and provided evidence for two horizontal transfer events of an SM BGC within the genus *Botrytis*.

Materials and methods

Strains and culture conditions

The fungal isolates that were sequenced are listed in Supplemental table 1. For long-term storage, all *Botrytis* species were kept as conidial suspensions in 15% glycerol at −80 °C, whereas *Sclerotium cepivorum* was stored as sclerotia at room temperature. The fungi were grown on malt extract plates at 20 °C before DNA extraction.

DNA and RNA isolation

High molecular weight DNA was isolated from freeze-dried and grinded mycelium upon treatment with cell lysis solution (Qiagen), proteinase K, and protein precipitation solution (Qiagen). DNA was precipitated using isopropanol, redissolved in Tris–ethylenediaminetetraacetic acid buffer, and treated with RNase A. The obtained DNA was cleaned using a Salt: chloroform wash (Pacific Biosciences shared protocol).

RNAs used for producing RNA-Seq libraries were pools of RNA isolated from different sources: 1) 5-day old mycelia grown on malt extract plates supplemented with blended onion leaves, 2) conidia, 3) sclerotia, 4) infected onion bulbs, and 5) infected onion leaves. For isolation of RNA, freeze-dried, grinded samples were incubated in Trizol (Ambion, Life Technologies) and treated with chloroform. After adding ethanol to the aqueous phase, the mixture was used as input for an RNeasy Plant Mini Kit (Qiagen) to isolate RNA.

Sequencing and assembly

All genomes were sequenced with one Pacbio SMRT cell using the Sequel instrument at Keygene N.V. (Wageningen, the Netherlands). De novo assembly was done with HGAP (Chin et al. 2013) and CANU (Koren et al. 2017) using default settings. The resulting assemblies were combined with quickmerge (Chakraborty et al. 2016), then two steps of corrections were done with Arrow, and erroneously merged contigs (based on inspection of mapped reads coverage) were manually corrected. Completeness of the genome assembly was assessed by the Benchmarking Universal Single-Copy Orthologs (BUSCO) (Simão et al. 2015). The transcriptome of each genome was sequenced using strand-specific paired-end libraries with a read length of 2× 150 bp using an Illumina HiSeq-X sequencer at the Beijing Genome Institute (BGI, Hongkong, China).

Genome annotation

Genome annotation was performed using the FUNGAP pipeline (Min et al. 2017), which included the annotation by MAKER (Cantarel et al. 2008), AUGUSTUS (Stanke et al. 2006), and BRAKER (Hoff et al. 2016). The gene prediction tools were supported with RNA-Seq libraries. Gene models of the manually curated genome of *B. cinerea* (van Kan et al. 2017), and all the fungal proteins available in the Swissprot database were provided as evidence for gene prediction. Furthermore, the predicted proteins were manually inspected and curated. The genome curation was done in Webapollo (Dunn et al. 2019), and each gene was inspected to confirm that prediction was supported by the evidence tracks (RNA-Seq, *B. cinerea* as reference and the Swissprot proteins); for instance, some gene models were deleted if they were overlapping a repetitive region, whereas other gene models were changed to have a correct Methionine start, or correct splice junctions. The manual curation was done to all the predicted proteins of *B. aclada*, *B. squamosa*, and *S. cepivorum*, and to the secretome of all other genomes. The predicted proteins were functionally annotated using the funannotate pipeline (Love 2019).

Phylogenetic and phylogenomic analysis

The phylogenetic relationships of the *Botrytis* genus and other related species of Sclerotiniaceae were determined between all species sequenced in this study and including the previously sequenced species *B. cinerea* B05.10 (van Kan et al. 2017), and other *Botrytis* species (Valero-Jiménez et al. 2019). The other species that were included were *Sclerotinia sclerotiorum* and *Sclerotinia borealis*, and *Marssonina brunnea* as the outgroup of the tree. The tree was constructed using 4,746 single-copy ortholog genes, identified with Orthofinder (Emms and Kelly 2015). The protein sequence for each gene was aligned and concatenated into a single matrix using MAFFT (Katoh and Standley 2013), and a maximum-likelihood phylogenetic tree was inferred with RAxML v.8.2.10 (Stamatakis 2014) using a generalized time reversible plus GAMMA amino acid substitution model with 100 rapid bootstraps. A pan-genome analysis was done to calculate the number of core genes and was estimated using OrthoMCL (Li et al. 2003) implemented in GET_HOMOLOGUES-EST (Contreras-Moreira and Vinuesa 2013) with *e*-value $1e^{-5}$ and 75% coverage. For the pan-genome analysis, only the orthogroups present in at least two species were included.

Secretome and effector prediction

Genes encoding putatively secreted proteins were identified for each genome using several prediction tools. Signal-P v4.1 (Petersen et al. 2011) was initially used to screen for a signal peptide, followed by TMHMM v.2.0 (Krogh et al. 2001) to identify putative

transmembrane domains. Proteins that did not have a signal peptide or that had a transmembrane domain (a single transmembrane domain in the first 60 amino acids was allowed) were discarded. TargetP was used to predict protein localization (Emanuelsson et al. 2007). Effectors were predicted using the EffectorP tool v1.0 and v2.0 (Sperschneider et al. 2016).

Ancestral genome reconstruction

The ancestral genome of *Botrytis* was constructed using the CHROnicle package that comprises SynChro, ReChro, and Anchro (Vakirlis et al. 2016). In order to identify conserved synteny blocks, pairwise comparisons between the genomes were done with SynChro. Subsequently, reconstruction of the ancestral chromosome gene order was done with Anchro.

SM gene cluster analysis

Putative gene clusters that are predicted to be involved in biosynthesis of SMs were identified using antiSMASH using default settings (antibiotics and Secondary Metabolite Analysis SHell) version 4.0.1 (Weber et al. 2015). The data set used for this analysis included 45 genomes from the order Leotiomycetes that were publicly available and published (Supplemental table 3). BiG-SCAPE version 20181005 (Navarro-Muñoz et al. 2020) was used to analyze all the SMs clusters predicted by antiSMASH. In the BiG-SCAPE analysis, a cutoff of 0.65 as well as the MIBiG parameter that included the MIBiG repository version 1.4 of annotated SMC was used (Medema et al. 2015). The output of BiG-SCAPE was visualized using Cytoscape version 3.7.1 (Shannon et al. 2003).

Reconstruction of BGC evolution

Presence/absence and additional fragmented homologs of BOT and BOA genes for each species was confirmed by TBlastN against the genome assemblies. Pseudogenes were manually identified by inspection of TBlastN reports for in-frame stop codons, and interrupted reading frames and truncations that could not be explained by novel intron sites.

Phylogenetic analyses were performed on all BGC genes, both with and without pseudogenes and outgroup taxa. Outgroup taxa were obtained by searching a database of 529 genome annotations (Gluck-Thaler and Slot 2018) using BlastP. Protein sequence data sets for each gene were aligned using mafft v. 7.221 (Katoh and Standley 2013), and ambiguously aligned characters were removed using TrimAl v. 1.4 (Capella-Gutiérrez et al. 2009). Maximum-likelihood analysis was performed in RAxML v. 8.2.9 (Stamatakis 2014) with automated model selection and topological robustness was assessed by 100

bootstrap replicates. In order to evaluate alternative hypotheses versus inferred horizontal gene transfer (HGT) events, we applied minimal topological constraints to exclude putative transferred genes from the donor clade. Constrained trees were built with automated model selection and their likelihoods were compared using the Approximately Unbiased test with 10,000 multiscale bootstrap replicates (Shimodaira 2002) as implemented in IQ-TREE v. 1.6.12 (Nguyen et al. 2015).

In order to determine synteny in the BOT and BOA loci, each locus including up to ten genes on either side of the BOA/BOT genes of interest (if present) was combined and assigned to a homology group using usearch cluster_agg method with a minimum linkage identity of 0.6 in usearch v. 8.0.1517 (Edgar 2010). The loci were then manually aligned according to their homology group and manual blasts were performed to confirm true orthology where ambiguous.

Ancestral state reconstructions were performed using a substitution matrix weighted against gain of functional genes and pseudogenes, except where HGT was already determined by gene trees and synteny analysis for BOA clusters in Mesquite v 3.6 (Maddison and Maddison 2019).

Results

Sequencing and assembly

Eight *Botrytis* species and *S. cepivorum* (Supplemental table 1) were sequenced using long-read single-molecule technology at 34–120× coverage. The genome assembly sizes ranged from 42.98 to 61.28 Mb (Table 1). The genomes of six species are similar in size to the previously described genome of *B. cinerea* (43.5 Mb; (van Kan et al. 2017)), whereas genomes of *B. squamosa*, *B. sinoallii*, and *S. cepivorum* exceed a size of 54 Mb. The *B. aclada* genome could be assembled into 16 distinct chromosomes, with eight chromosomes containing telomeric repeats at both ends, and six containing a telomeric repeat on one end.

The most fragmented assembly of the nine species is that of *B. elliptica*, despite its genome size of <48 Mb, with 137 contigs and a contig N50 of 652 kb. BUSCO analysis indicated that all genomes had a high level of completeness (98.0–99.2%). Prediction of gene models was performed using the FunGAP pipeline and supported by RNA-Seq data (from in vitro samples and infected plant material) and by alignment to the manually curated genome of *B. cinerea* B05.10 (van Kan et al. 2017). After prediction by this pipeline, proteomes of *B. aclada*, *B. squamosa*, and *S. cepivorum* were entirely manually curated, whereas for the other six species, only the (predicted) secreted proteins were manually curated. The curated proteomes of the nine species contain between 11,107 and 12,480 genes (Table 1).

Table 1. Assembly and gene prediction information of *Botrytis* spp. genomes from this study. Taxa in the table are ordered as they appear in the phylogenetic tree in Figure 1.

Species	Contigs	Assembly size (Mb)	Largest contig (Kb)	N50 (Kb)	BUSCO complete/ partial	Predicted genes	Secretome size	% of secreted proteins
B. byssoidea	59	42.98	2599	1263	98.0 (99.3)	12212	898	7.35
B. globosa	27	45.68	4093	2511	98.0 (99.0)	12073	864	7.16
B. elliptica	137	47.66	2119	652	99.2 (99.9)	12442	932	7.49
B. squamosa	29	54.60	4659	2938	98.7 (99.1)	11963	897	7.5
B. deweyae	76	44.36	243	1076	98.0 (99.0)	12480	942	7.55
B. sinoallii	47	61.28	6466	2252	98.3 (99.5)	12281	885	7.21
B. porri	31	46.78	4253	2706	98.2 (98.9)	12088	888	7.35
B. aclada	16	48.31	4155	3028	99.1 (99.3)	11870	867	7.30
S. cepivorum	48	55.66	4533	1651	98.2 (99.5)	11107	790	7.11

Phylogenetics and phylogenomics

A phylogenetic tree was constructed based on a concatenated amino acid alignment of 4,746 conserved core genes totaling 409,576 positions, using *Marssonina brunnea* (order Helotiales, family Dermataceae) as the outgroup (Figure 1). The relationship among the *Botrytis* species is fully concordant with previous studies (Hyde et al. 2014; Staats et al. 2005), which divided the genus in two clades based on three protein-coding genes (G3PDH, HSP60, and RPB2). All *Botrytis* species newly sequenced in this study group in Clade 2, which contains taxa that mostly infect monocot host plants (only *B. paeoniae* infects dicots). A pan-genome analysis for 16 *Botrytis* species (eight species sequenced in this study, seven species previously sequenced with short-read technology (Valero-Jiménez et al. 2019), and the previously sequenced *B. cinerea* B05.10 (van Kan et al. 2017) indicated that the core genome of *Botrytis* spp. consists of 7,524 orthogroups (>60% of genes within any individual species) (Supplemental figure 1A), whereas the pan-genome consists of 13,856 orthogroups (Supplemental figure 1B).

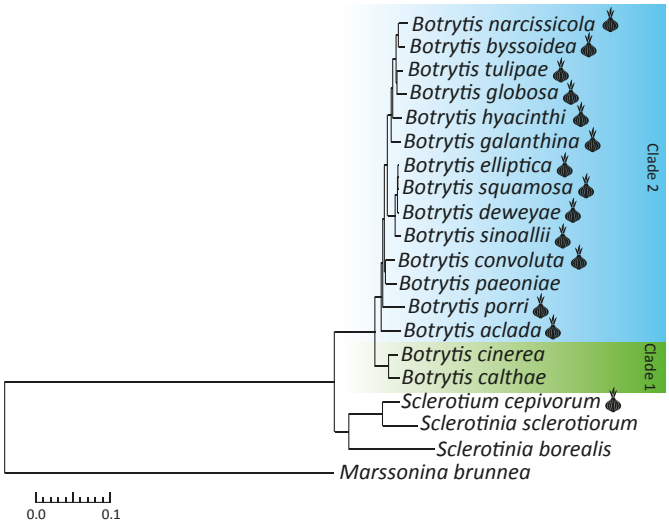

Figure 1. Phylogenetic tree based on single-copy orthologous genes of different *Botrytis* species and three Sclerotiniaceae, with *Marssonina brunnea* as the outgroup to root the tree. All branches have a high bootstrap support (ML > 90). Two clades previously reported in the genus *Botrytis* are highlighted. The bulb symbols next to the species names indicate species that infect monocotyledonous bulbous plants, species without symbol infect dicot hosts.

Analysis of secreted proteins

Secreted proteins are important tools of plant pathogenic fungi to either manipulate the physiology and immune responses of their host plants (effector proteins) or decompose the plant tissue that they colonize in order to acquire carbohydrate nutrients (plant cell wall degrading enzymes, PCWDEs). Orthologous groups of all secreted proteins from 16 *Botrytis* species sequenced in this work, as well as previously published (Valero-Jiménez et al. 2019; van Kan et al. 2017) and *S. cepivorum* were determined using Orthofinder. From a total of 14,838 proteins, 14,326 were assigned to 1,116 orthologous groups. From these, 376 orthologous groups are shared among all 17 species (Supplemental figure 2). Besides orthologous groups shared by all species, 171 groups (columns 2–18 in Supplemental figure 2) are common to all species but one, whereas 454 orthologous groups are unique to a single species (columns 19–37 in Supplemental figure 2). The secretome of *S. cepivorum* lacks 55 secreted proteins that are present in all *Botrytis* species and contains 83 singletons that are unique to *S. cepivorum*, as to be expected for a species from a distinct genus in the same family.

In view of the relevance of secreted effector proteins in fungus–plant interactions, an effector prediction was performed on the set of secreted proteins discussed above. For each of the 16 *Botrytis* species and *S. cepivorum*, a total of 121–152 candidate effector

genes was identified which were assigned to 244 orthologous groups. Among these groups, 25 are represented in all 17 species and another 25 are shared among all but one species. On the other hand, each of the 17 species contains between 8 and 39 predicted effector genes that remained unassigned to orthologous groups, because they are unique for that single species. There were no predicted effectors which are shared among *Allium* pathogens but absent from non-*Allium* pathogens. Furthermore, pairwise comparisons between related *Botrytis* species with distinct hosts did not identify any effector genes that stood out as potential determinants for host specificity.

We also analyzed the secreted proteins that are related to the degradation of plant cell wall carbohydrates (Supplemental table 2). The genomes of 16 *Botrytis* spp. and *S. cepivorum* contain between 109 and 132 PCWDEs. *Sclerotium cepivorum* has fewer PCWDE-encoding genes than the *Botrytis* species. The PCWDEs were further subdivided depending on their substrate: cellulose, hemicellulose, or pectin. The numbers of secreted enzymes capable of degrading cellulose, hemicellulose, and pectin were mostly similar among *Botrytis* spp., with some deviations: *B. sinoallii* has notably fewer genes encoding pectinases (22 vs. 27–38 for other species; Supplemental table 2).

SM gene clusters

Fungi produce a wide array of SMs, usually synthesized by proteins encoded by genes that are physically clustered in the genome, referred to as SM BGCs (Keller et al. 2005). SMs contribute to the adaptation and survival in different environments and in the competition with other (micro)organisms (e.g., (Chatterjee et al. 2016). In a previous study on nine *Botrytis* genomes assembled from short sequence reads, a patchy absence/presence pattern was observed for orthologs to BGCs that were functionally annotated in *B. cinerea* (Valero-Jiménez et al. 2019). Because of the fragmented assemblies resulting from short-read sequencing technology, the latter analysis only considered SM key biosynthetic enzymes, but not the entire gene cluster. In the present study, the analysis of SM gene clusters was extended to all 16 *Botrytis* species (short- and long-read technology based), four related taxa from the family Sclerotiniaceae, and 25 other taxa from the class Leotiomycetes, for which an annotated genome was publicly available (Supplemental table 3). The analysis was conducted by predicting BGCs in all 45 genomes using AntiSMASH, and grouping them by families using BiG-SCAPE. The 45 Leotiomycete genomes each contained between 3 and 67 BGCs. The 1,571 BGCs were grouped over 438 BGC families, which were further categorized based on their phylogenetic distribution. Category 1 contains 342 families of SM BGCs that are distributed among taxa across Leotiomycetes. This category includes a few BGCs that encode enzymes involved in biosynthesis of common metabolites such as melanin and siderophores, however, the exact chemical structures of compounds produced by the vast majority of BGCs in this category remain unknown.

Category 2 contains 36 families of BGCs that are present in Sclerotiniaceae (including the genus *Botrytis*) but not represented in the other 25 Leotiomycete taxa. This category includes the BGCs encoding enzymes involved in production of botcinic acid, and other yet unknown compounds. Category 3 contains 60 families of BGCs that are unique to the genus *Botrytis*, such as the cluster involved in production of botrydial, however, all other SMs produced by the other 59 BGCs in this category are unknown.

BGCs are commonly annotated on the basis of the type of compound that is produced, often a polyketide (PKS), nonribosomal peptide (NRPS), or terpene (TS). The evolutionary trajectory of BGCs can be complex, and the distribution of specific BGCs can be scattered throughout the fungal kingdom (Slot and Gluck-Thaler 2019). Several cases of HGT of BGCs have been documented in fungi (Campbell et al. 2012; Navarro-Muñoz and Collemare 2020; Reynolds et al. 2018; Ropars et al. 2015). We examined the distribution of the predominant classes of BGCs (PKS, NRPS, and TS) over the 45 Leotiomycete species analyzed (Figure 2 for PKS; Supplemental figure 3 for NRPS; Supplemental figure 4 for TS).

The distribution of BGCs is largely consistent with phylogenetic patterns, with related fungal taxa containing a similar distribution. A set of 20 PKS families (as identified by BiG-SCAPE) are most abundant in *Botrytis* species. Six families from this set are exclusive to *Botrytis* (highlighted red in Figure 2), whereas 14 families are also present in other Sclerotiniaceae or in more distantly related Leotiomycete taxa (highlighted in ocher). Conversely, a set of nine PKS clusters that are most abundant in Leotiomycetes outside the family Sclerotiniaceae have sparse and patchy distributions within the genus *Botrytis* (highlighted in blue).

Botrytis species possess at least five (*Botrytis convoluta*) and at most 11 (*B. cinerea*) NRPS clusters (Supplemental figure 3). Five families of NRPS clusters are unique to the genus *Botrytis* (Supplemental figure 3, highlighted in red), whereas eight other families are largely confined to the family Sclerotiniaceae, although two of them (FAM_02547 and FAM_02047) are also shared with the distant taxa *Phialophora hyalina* or *Phialocephala scopiformis* (Supplemental figure 3, highlighted in ocher). Notably, *B. cinerea* contains two NRPS clusters that are not shared with any other *Botrytis* species but have orthologs in several distant Leotiomycetes (Supplemental figure 3, highlighted in blue). The families of terpene cyclase (TS) clusters are relatively simple in pattern, with each *Botrytis* species containing 3–6 TS cluster families (Supplemental figure 4). Eight of the families are exclusively detected in *Botrytis* species (Supplemental figure 4, highlighted in red), whereas four are also present in other Sclerotiniaceae, and two of the TS cluster families are even detected in distant Leotiomycetes (Supplemental figure 4, highlighted in ocher). The family FAM_03197 is conserved in all Sclerotiniaceae, as well as in six other Leotiomycetes, whereas FAM_02531 is present in nine Sclerotiniaceae and six distant Leotiomycetes. Except for the family FAM_02168, involved in the synthesis of the phytoxic metabolite botrydial, the chemical nature of the products of these clusters is unknown.

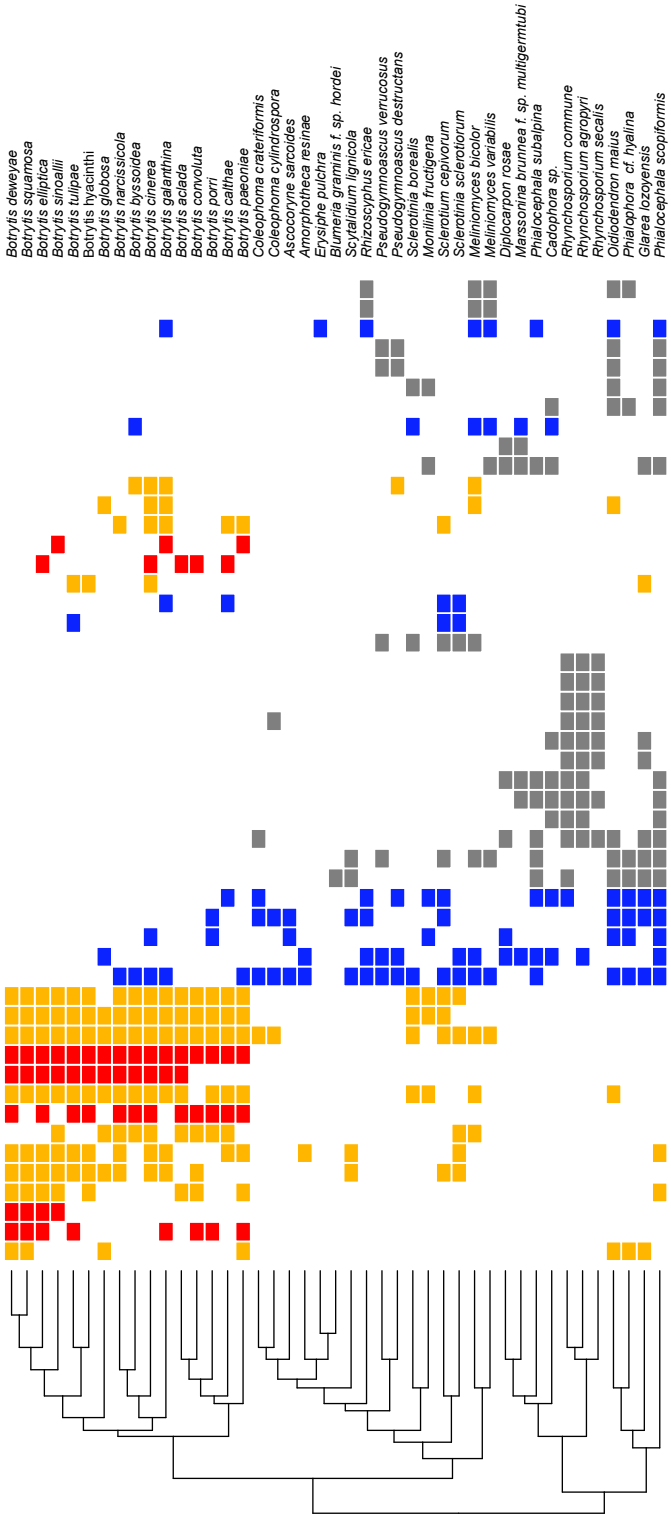

Figure 2. Distribution of polyketide synthase clusters in 45 Leotiomycetes. The 50 clusters that are most abundant among the 45 Leotiomycetes taxa are displayed. Clusters that are exclusively represented in *Botrytis* are marked red; clusters predominantly in *Botrytis* but also in some other taxa are marked ocher; clusters predominantly in other taxa but also in some *Botrytis* species are marked blue; clusters lacking in all *Botrytis* spp. are marked gray.

Ancestral genome reconstruction of the genus *Botrytis* and the family Sclerotiniaceae

The high quality of the long-read assemblies and the previously published *B. cinerea* genome, as well as the extensive manual curation effort of gene models, enabled us to perform a synteny analysis and a reconstruction of the ancestral chromosome configuration of the genus *Botrytis*, in order to understand the extent and nature of chromosomal rearrangements over the course of evolution of the extant species. *Botrytis elliptica* was excluded from the ancestor reconstruction for two reasons: first, the assembly was the most fragmented of all (137 contigs) and second, the phylogenetic relation of *B. elliptica* to its sister taxa *B. squamosa* and *B. deweyae* could not be resolved (Figure 1), which hampered the analysis. The inferred ancestral genome of the entire genus *Botrytis* (AB0) consists of 17 syntenic blocks (Figure 3). Thirteen of the 16 *B. cinerea* core chromosomes are entirely syntenic to the AB0 ancestor, and 17 balanced rearrangements (mostly inversions) are inferred between the ancestor AB0 and the extant *B. cinerea* (Table 2 and Supplemental table 4).

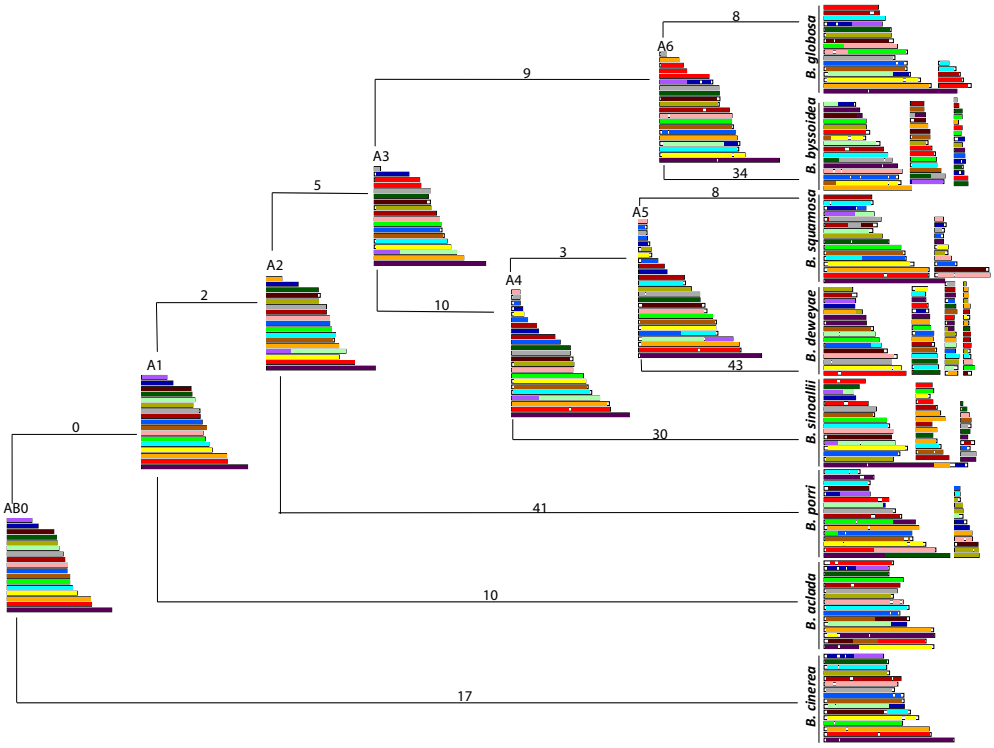

Figure 3. The most parsimonious evolutionary trajectory from the ancestral (A0) configuration toward extant *Botrytis* species. Colored boxes represent syntenic blocks. A1–A6 represent intermediate ancestors. Numbers above the branches represent the total number of balanced rearrangements (interchromosomal translocations and fusions/fissions; intrachromosomal inversions) accumulated between two genomes.

The A1 genome is the inferred ancestor of members of clade 2 in the genus *Botrytis*, whereas *B. cinerea* is the single representative of clade 1 in the analysis (Figure 1). The inferred A1 genome is identical to AB0 (Figure 3). The extant *B. aclada* genome contains ten rearrangements as compared with A1. The A2 intermediate ancestor was inferred to be derived from A1 upon fusion of A1 contigs 13 and 17, and fission of A1 contig 3 (resulting in A2 contigs 5 and 17). Downstream of the A3 intermediate ancestor, the interpretation becomes complex as numbers of contigs increase due to the more fragmented assemblies of some species, for example, *B. deweyae, B. byssoidea*, and *B. sinoallii*. Nonetheless, the number of contigs of intermediate ancestors remains 25 or lower and the number of rearrangements between nodes in the tree ranges from 3 to 43 (Table 2).

Reconstruction of ancestral genomes was extended to the family Sclerotiniaceae using the genomes of *S. cepivorum* (this study) and *Sclerotinia sclerotiorum* (Derbyshire et al. 2017) (Supplemental figure 5). Due to the more fragmented assembly of the *S. cepivorum* genome, the inferred common ancestor AS1 comprised 21 syntenic blocks, five of which were quite small and probably represent only parts of chromosomes. However, the common ancestor ABS0 of the family Sclerotiniaceae contains 16 syntenic blocks, and the configuration of ABS0 differs from the ancestral *Botrytis* genome AB0 by just a single rearrangement (Supplemental figure 5).

Table 2. Numbers of balanced genomic rearrangements between inferred ancestral genomes (AB0-A6) and extant *Botrytis* species, as shown in Figure 3. Note—Further details of the types of rearrangements are provided in Supplemental table 4. BCIN, *B. cinerea*; BACL, *B. aclada*; BSIN, *B. sinoallii*; BSQU, *B. squamosa*; BDEW, *B. deweyae*; BBYS, *B. byssoidea*.

	AB0-BCIN	**AB0-A1**	**A1-BACL**	**A1-A2**	**A2-A3**	**A3-A4**	**A3-A6**	**A4-A5**	**A4-BSIN**	**A5-BSQU**	**A5-BDEW**	**A6-BBYS**
Inversions	15	0	3	0	2	3	6	1	6	2	1	3
Translocations	1	0	1	0	0	0	1	0	2	2	0	4
Transpositions	1	0	1	0	0	0	0	0	1	0	0	0
Fusions	0	0	0	1	2	1	0	1	2	1	2	0
Fissions	0	0	5	1	1	6	2	1	19	3	40	27
Sum	**17**	**0**	**10**	**2**	**5**	**10**	**9**	**3**	**30**	**8**	**43**	**34**

Synteny between *B. aclada* and *B. cinerea*

In order to explore genome rearrangements between individual species in more detail, we further examined the synteny between the genomes of *B. aclada* and *B. cinerea* (the most complete and best annotated) by pairwise alignments. *Botrytis cinerea* minichromosome 18 (BCIN18) was excluded from this analysis because it contains only 13 genes, none of which is orthologous to genes in *B. aclada*. The second minichromosome of *B. cinerea*,

BCIN17, did show some homology to the tip of BACL10 and was therefore included in the analysis. Graphical representation of the alignment (Figure 4) reveals that four chromosomes represent fully syntenic blocks, though some of these blocks contain segmental inversions of ancestral regions on the same chromosome (not visible in the color display). In the remaining 12 chromosomes, the alternation of colored boxes reflects the occurrence of six interchromosomal rearrangements, as well as 13 small translocations or transpositions, of which seven occurred at or close to the telomeres (Figure 4).

Strikingly, we noted that SM BGCs were present in some of these translocated segments. Specifically, BACL05 is almost perfectly syntenic to BCIN07, with the exception of an insertion of a cluster of seven genes (Figure 4, green box marked by an asterisk) representing the BGC for the sesquiterpene metabolite botrydial (Pinedo et al. 2008; Porquier et al. 2016; Siewers et al. 2005), which in *B. cinerea* is located in BCIN12. Conversely, the only difference between BACL12 and BCIN12 is the insertion (in BCIN12) of a segment that exactly contains the BGC for botrydial. Furthermore, BACL9 is entirely syntenic to BCIN11, however, it contains an insertion of the BGC for the phytotoxic metabolite botcinic acid (Dalmais et al. 2011; Porquier et al. 2019) close to the 3'-telomeric region, which in *B. cinerea* is located at the start of BCIN01 (van Kan et al. 2017).

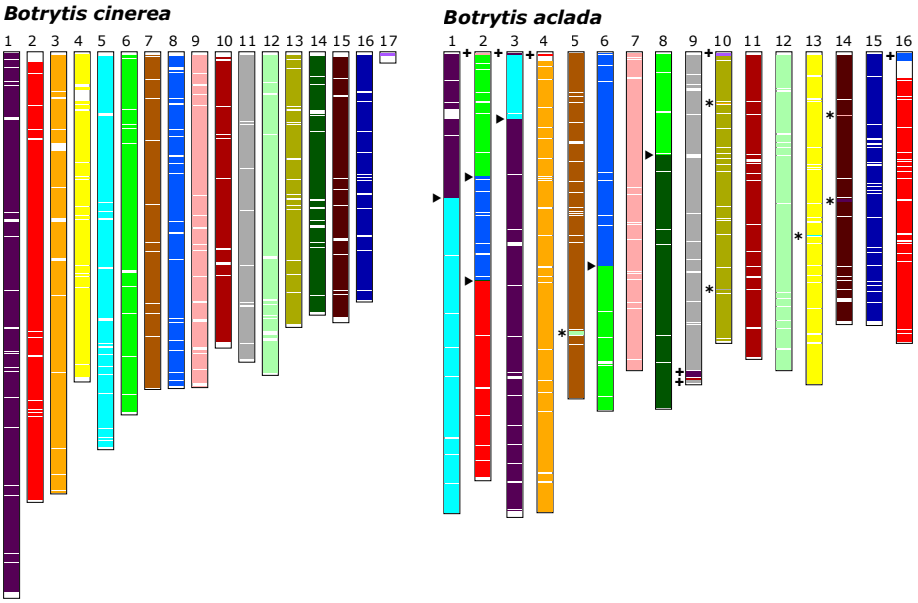

Figure 4. Synteny analysis between *Botrytis aclada* and *Botrytis cinerea*. The 17 chromosomes of *B. cinerea* are color-coded uniformly, the corresponding syntenic regions in *B. aclada* have identical colors. White regions reflect repetitive regions or lack of homology. Arrowheads indicate large reciprocal interchromosomal rearrangements. Asterisks indicate small interchromosomal transpositions. Plus symbols indicate interchromosomal telomeric translocations. Intrachromosomal inversions are not indicated.

Genomic locations of botrydial and botcinic acid BGCs

The synteny analyses described above provided indications that SM BGCs occur in regions that possibly underwent translocation at some moment in the evolution of *Botrytis* species. The distribution of botrydial (BOT) and botcinic acid (BOA) BGCs over the Sclerotiniaceae and the genus *Botrytis* appeared to be patchy. Specifically, the BOT cluster is present in eight *Botrytis* species and absent in other Sclerotiniaceae. We compared the BOT clusters and their flanking sequences in seven species: *B. aclada*, *B. cinerea*, *B. elliptica*, *B. deweyae*, *B. porri*, *B. sinoallii*, and *B. squamosa*. The *B. peaoniae* genome, though containing a BOT cluster, was sequenced by Illumina technology (Valero-Jiménez et al. 2019) and its assembly was too fragmented for synteny analysis. The order of the genes BcBOT1–7 within the cluster was identical in all species, however, the most upstream gene (BcBOT4), was in inverted orientation in *B. aclada* and *B. porri* as compared with the other five species (Figure 5). The BOT clusters were in all cases flanked by gypsy/copia repeats, with lengths up to 160 kb, either on one side (*B. cinerea*, *B. deweyae*, *B. elliptica*, and *B. squamosa*), or on both sides (*B. porri*, *B. aclada*, and *B. sinoallii*) and some species even contained internal transposon repeats within the BOT cluster (*B. aclada*, *B. cinerea*, and *B. sinoallii*; Figure 5). Based on the RNA-Seq reads used for structural annotation, it was observed that all species that do contain intact BOT clusters express all of the seven genes. As these expression data were based on pooled RNAs, representing multiple fungal tissue types and infection stages, it was not possible to compare the expression levels between species or to determine under which conditions the genes were expressed.

The BOA cluster was detected, in whole or in part, in all but one *Botrytis* species (*B. paeoniae*), and in *Sclerotinia sclerotiorum* as well as *S. cepivorum*. In many cases, the BOA cluster in *Botrytis* species is located close to the end of a contig. It was previously reported that in *B. cinerea*, the BOA cluster is at the very start of BCIN01, only 5 kb away from the telomere (van Kan et al. 2017). Alike for the BOT clusters mentioned above, all species that contain intact BOA clusters express all of the 13 genes, however, the use of pooled RNAs prevented us from comparing expression levels between species or determine under which conditions the genes were expressed.

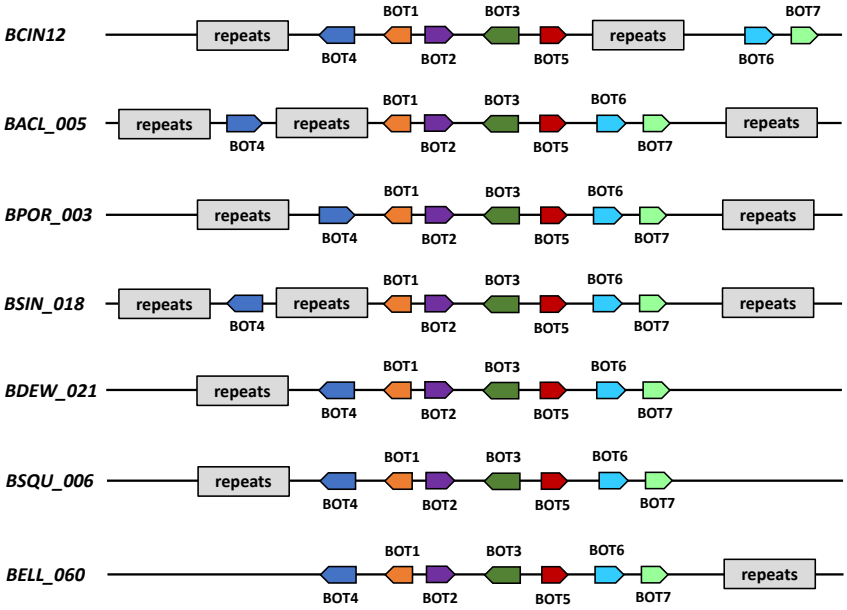

Figure 5. Organization of BOT clusters in seven *Botrytis* species. BCIN, *B. cinerea*; BACL, B. aclada; BPOR, *B. porri*; BSIN, *B. sinoallii*; BSQU, *B. squamosa*; BDEW, *B. deweyae*; BELL, *B. elliptica*. The number of the contig is given behind the species name tag. The seven BOT gene orthologs (not drawn to scale) are color-coded uniformly; the arrow indicates direction of transcription. Repeats are indicated with a gray box. Repeats are not drawn to scale and range in length from 1 to 160 kb.

In view of the high synteny between *Botrytis* species, we examined whether the BOT and BOA clusters in the different species are in syntenic locations as compared with *B. cinerea*. Surprisingly, analysis of flanking genes revealed that BOT clusters are in four distinct genomic regions in the seven *Botrytis* species analyzed. None of the species other than *B. cinerea* contained the BOT cluster in a region syntenic to BCIN12 (Figure 6). The genes directly flanking the BOT cluster in *B. cinerea* (Bcin12g06360 and Bcin12g06440) in all but one of the six species have orthologs that are directly adjacent to one another in these genomes, with intergenic regions ranging from 2 to 5 kb.

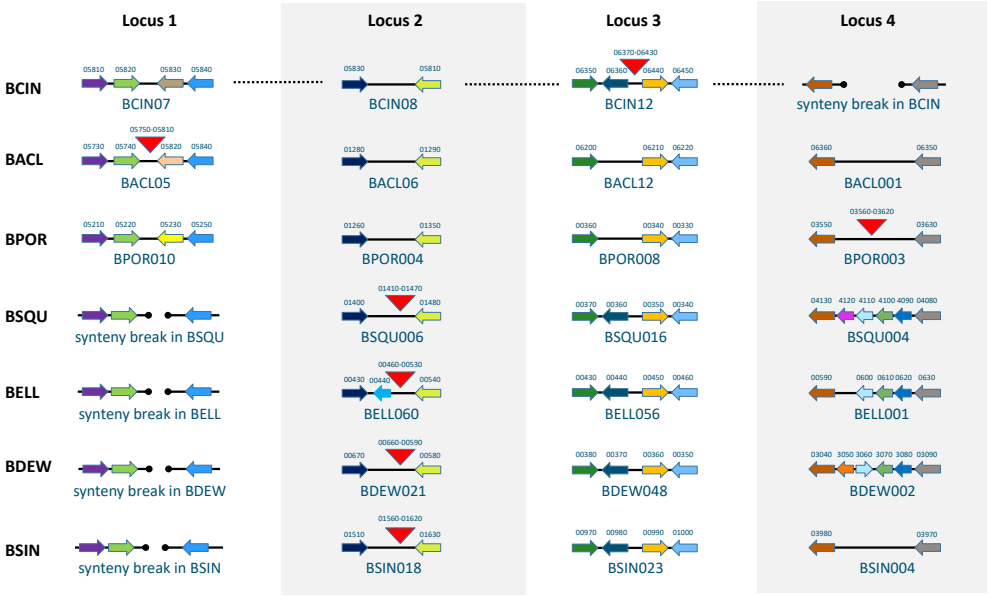

Figure 6. Distinct genomic locations of BOT clusters in seven *Botrytis* species. Four different loci are provided in the columns. Species name tags are in the left hand margin: BCIN, *B. cinerea*; BACL, *B. aclada*; BPOR, *B. porri*; BSIN, *B. sinoallii*; BSQU, *B. squamosa*; BDEW, *B. deweyae*; BELL, *B. elliptica*. Contig numbers in the seven species are provided underneath the locus. In each column, orthologous genes are indicated by identical colors. Gene numbers in the contig are provided above the gene; the arrow indicates direction of transcription. The red triangular blocks represent the location of a BOT cluster. Synteny breaks are shown by interrupted lines with dots marking the break.

No indication was found for the occurrence of truncated remnants of BOT genes at this position in the six genomes. Also in all but one of the other species lacking a BOT cluster, orthologs to Bcin12g06360 and Bcin12g06440 are directly adjacent to one another in these genomes. Through similar analyses and reasoning, the BOT cluster in *B. aclada* is present in a unique position that is syntenic to BCIN07, whereas the BOT cluster in *B. porri* is present in a unique position that is syntenic to positions in five other species (all except in *B. cinerea*, where a synteny break has occurred); lastly, the BOT clusters in *B. squamosa*, *B. deweyae*, *B. elliptica*, and *B. sinoallii* are all located in a syntenic genomic region, which is equivalent to a location between Bcin08g05830 and Bcin08g05810 (Figure 6).

In *Sclerotinia sclerotiorum*, the BOA cluster is dispersed over two chromosomal locations on SSCL05 (genes BOA1 and BOA2) and SSCL15 (genes BOA3-13). A recent study by Graham-Taylor et al. (2020) reported that SSCL can express the 13 BOA genes in a coregulated manner despite their spatial separation. For the largest cluster on SSCL15, its flanking genes on both sides are orthologous to syntenic regions in eight *Botrytis* species (BACL006, BBYS014, BCIN06, BDEW005, BELL059, BGLO010, BSIN006, and BSQU018) that

do not contain any trace of BOA gene remnants. For the smaller cluster on SSCL05, its flanking genes on both sides are orthologous to genes located on BCIN05 (Bcin05g05060 and Bcin05g07100); however, the region is not syntenic, because the genes are far separated in *B. cinerea*.

Inheritance and structural evolution of BOT and BOA clusters

BOT and BOA gene loci were carefully examined for evidence of pseudogenization to infer which of the clusters are fully functional. BOT clusters in *B. sinoallii* and *B. paeoniae* contain one and two pseudogenes, respectively, whereas six species (*B. aclada*, *B. cinerea*, *B. elliptica*, *B. deweyae*, *B. porri*, and *B. squamosa*) have clusters with seven apparently functional genes. Seventeen of the 19 Sclerotiniaceae analyzed contained (parts of) BOA clusters, however only seven species (*B. aclada*, *B. byssoidea*, *B. cinerea*, *B. globosa*, *B. porri*, *B. sinoallii*, and *Sclerotinia sclerotiorum*) appeared to contain a fully functional BGC. The majority of species contain two or more pseudogenes of catalytic enzymes. The most extreme cases of gene loss were in *B. squamosa*, *B. deweyae*, *B. elliptica*, and *B. tulipae*, which lost all but one of the BOA cluster genes. By contrast, *B. calthae*, *B. convoluta*, and *B. narcissicola* contained 2–3 pseudogenes, either in genes encoding accessory enzymes or in the BOA13 gene, which is the transcriptional regulator for the cluster (Porquier et al. 2019). Of the two species outside the genus *Botrytis*, *Sclerotinia sclerotiorum* contains a functional BOA cluster (Graham-Taylor et al. 2020), whereas *S. cepivorum* lacks four genes, including polyketide synthase gene BOA9, and in addition contains two pseudogenes.

Ancestral state reconstructions of genes and pseudogenes (considering HGT events, see below) on the *Botrytis* species tree (Figure 7A) suggest that the BOT cluster was gained in the common ancestor of *Botrytis* and has been lost five times; three times leaving no gene remnants (in *B. calthae*, *B. convolute*, and in the subclade containing *B. galanthina*), and twice leaving a mix of functional genes and pseudogenes (in *B. paeoniae* and *B. sinoallii*). The BOT gene trees are in agreement with the species tree and the clusters are thus inferred to be derived from strictly vertical inheritance. Reconstructions of the BOA clusters (Figure 7B) revealed a more dynamic process involving 12 losses of cluster function after being gained in the common ancestor of *Botrytis* and *Sclerotinia*, and two recent gains by HGT in *B. cinerea* and *B. sinoallii*. HGT of the two clusters is supported by maximum-likelihood gene trees, which suggests that both clusters were acquired from a relative of *B. porri* or *B. aclada*.

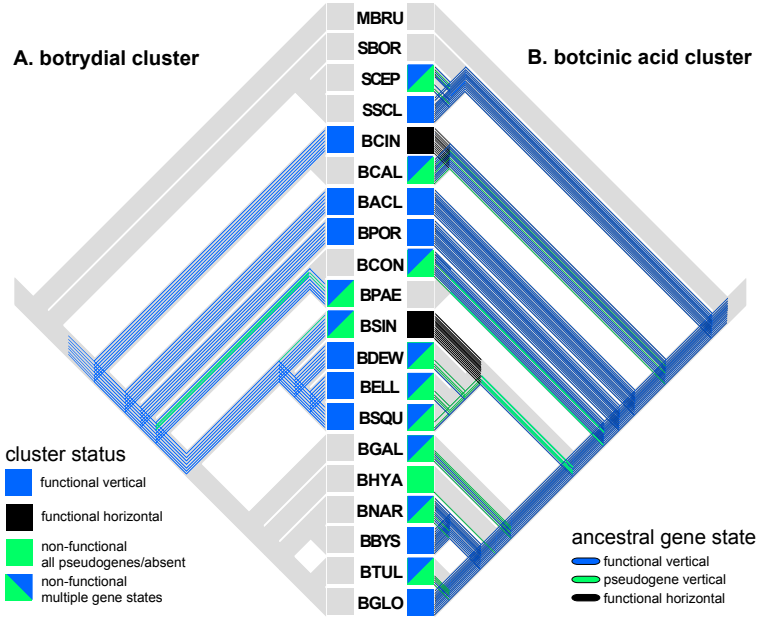

Figure 7. Ancestral state reconstructions of genes and pseudogenes of the BOT cluster (**A**) and the BOA cluster (**B**) on the phylogenetic tree of 20 Sclerotiniaceae species. The status of the cluster is indicated with colored boxes: blue = functional cluster, vertically transmitted; black = functional cluster, horizontally transmitted; green = all cluster genes nonfunctional or absent; green/blue = some genes nonfunctional or absent; gray = total absence of cluster. The ancestral gene states of seven BOT genes and 13 BOA genes are indicated with colored lines in similar way.

Most gene trees became significantly worse than the maximum-likelihood trees, according to Approximately Unbiased tests (Shimodaira 2002), when potential HGT homologs were excluded from the putative donor clade. Strong support for a HGT origin of the functional BOA cluster in *B. sinoallii* comes from two additional observations. First, the inferred HGT cluster is adjoined by a putative amino acid transporter (Bsin003g06700) and alcohol acetyltransferase (Bsin003g06560), which are either adjacent or a few genes removed from the BOA cluster in *B. aclada*; only the homolog of Bsin003g06700 is adjacent to the BOA cluster in *B. porri*. Second, *B. sinoallii* contains an additional, heavily pseudogenized BOA cluster on contig BSIN027, which more closely tracks the species phylogeny and retains flanking genes that are consistent with the species phylogeny. The remnants of the ancestral *B. sinoallii* BOA cluster comprise only three pseudogenes that are embedded in a 330-kb genomic region saturated with transposons.

The HGT of the BOA cluster to *B. cinerea* is supported by the phylogenetic proximity to *B. aclada* and *B. porri* (Figure 7), however, it cannot be corroborated by synteny information, as the *B. cinerea* BOA cluster is located at the start of chromosome 1, and the 25-kb region immediately downstream of the cluster is not syntenic with any *Botrytis* species.

Discussion

Following the efforts to sequence *B. cinerea* isolate B05.10 and nine other *Botrytis* species mainly infecting flower bulb crops (Valero-Jiménez et al. 2019), the present study, focusing on eight species from clade 2 of the genus, brings the number of *Botrytis* genome sequences to 16. This represents about half of the currently recognized species in the genus, though a recent study (Garfinkel et al. 2019) identified at least 15 phylogenetically distinct, new taxa sampled from *Paeonia* in Alaska, which remain to be described and named. There is thus far one single fungal genus, that is, *Verticillium*, for which the genomes of all recognized species have been sequenced (Shi-Kunne et al. 2018). It will take more effort to complete the sequencing of the entire genus *Botrytis.*

The present study aimed to identify genes potentially involved in determining host specificity, by comparing genomes of *Botrytis* species pathogenic on *Allium* with each other and with the genomes of their closest relatives pathogenic on other host plants. Specifically, we compared the genomes of the onion (*Allium cepa*) pathogens *B. squamosa* and *B. sinoallii*, with those of their sister taxa *B. elliptica* and *B. deweyae*, which infect lily and *Hemerocallis*, respectively, and we compared the genomes of *B. aclada* (infecting onion) and *B. porri* (infecting *Allium porri*, leek) with that of *B. paeoniae* (infecting the dicot peony). In order to make a meaningful comparison, the effort was made of manually curating all (>11,000) gene models in the genomes of three species (*B. squamosa*, *B. aclada*, and *S. cepivorum*), and manually curating the gene models of all proteins with a (predicted) signal peptide in the other six species. Comparison of the effector repertoires did not reveal candidate effectors that were shared among all *Allium* pathogens but absent in non-*Allium* pathogens. Each of the species analyzed contained 8–39 predicted effector genes that were unique to the species, however, most had no homologs in other fungi and these genes often had little RNA-Seq support (even in RNA samples from infected onion tissue), questioning the importance of these predicted genes for pathogenicity on onion. The repertoire of cell wall degrading enzymes was also similar between all 16 *Botrytis* species studied, despite the fact that only three species infect dicot hosts, whereas the vast majority infect monocot hosts. Dicots and monocots are considered to have different compositions of cell wall polysaccharides (Jarvis et al. 1988). Thirteen *Botrytis* species in this study infect monocot hosts from the families *Alliaceae*, *Amaryllidaceae*, *Iridiaceae*, and *Liliaceae.* Plants from these families contain high levels of pectin in their cell walls as compared with the *Poaceae* (Jarvis et al. 1988), which are more intensively studied as they comprise major staple crops of global relevance: rice, wheat, and maize. In view of the high pectin content in the monocot hosts of *Botrytis* species in this study, the large repertoire of pectin degrading enzymes in their genomes appears logical. Altogether, we did not identify (sets of) genes that are shared among the *Allium* pathogens and distinguish them from related species with different hosts. The lack of shared genomic features may reflect

the pathology of the *Allium* pathogens, some of which infect the leaves (*B. squamosa*), whereas others infect the bulb (*B. aclada*) or the roots and scale bases (*S. cepivorum*).

Despite the failure to identify host specificity determinants, many interesting features were unraveled by the extensive genome analyses that were performed. The genome of *B. aclada* was assembled into 16 gapless chromosomes, eight of which were full-length (telomere-to-telomere) and six contained telomeric repeats on one end. The *B. aclada* assembly was based on sufficiently high coverage to avoid the requirement for short-read-based correction, nor did it require an optical map or genetic map for assembly verification, as was done for *B. cinerea* (van Kan et al. 2017). Cytogenetic studies on four *Botrytis* species (*B. byssoidea*, *B. cinerea*, *B. squamosa*, and *B. tulipae*) revealed that they each contain 16 mitotic chromosomes, whereas the same study reported 16 or 32 mitotic chromosomes in different isolates of *B. allii* (Shirane et al. 1989). Subsequent studies (Nielsen and Yohalem 2001; Yohalem et al. 2003) revealed that the species earlier named *B. allii* in fact comprised isolates of *B. aclada* (having 16 chromosomes) as well as isolates representing a hybrid of *B. byssoidea* and *B. aclada* (having 32 chromosomes), which is presently still named as *B. allii* (Staats et al. 2005). Strikingly, *Sclerotinia sclerotiorum* also contains 16 chromosomes (Amselem et al. 2011; Derbyshire et al. 2017). These observations suggest a bias for the possession of 16 chromosomes in the genus *Botrytis* and possibly even in related genera. Conservation of chromosome numbers is not commonly observed in fungal genera, especially Ascomycota. As an example, the core chromosome numbers in the genus *Fusarium* vary from four (*Fusarium graminearum*) to 12 (*Fusarium fujikuroi*) (Waalwijk et al. 2018). Could this conservation of chromosome numbers in distant species of the same genus be related to functional constraints for sexual reproduction during the evolution of *Botrytis* species? As sexual reproduction requires chromosome pairing during meiosis, any fusion or fission event that affects core chromosome numbers would have serious repercussion on sexual compatibility and the fertility of offspring. We further explored the conservation of chromosome numbers and architecture by examining synteny and reconstructing ancestral genomes of the genus *Botrytis* and the family Sclerotinaceae.

The ancestral genome reconstruction inferred as few as 17 syntenic blocks for the common ancestor (AB0) of all *Botrytis* species. The inferred ancestral genome of the Sclerotiniaceae (ABS0) consisted of 16 syntenic blocks, and it differed from the AB0 genome by a single rearrangement. Thirteen of the 16 core chromosomes of *B. cinerea* were represented in these blocks, and only three interchromosomal rearrangements were proposed between the ancestor AB0 and the extant *B. cinerea* genome. Moreover, the common ancestor of the entire genus (AB0) was identical to the common ancestor of extant *Botrytis* species in clade 2. Only six interchromosomal rearrangements were proposed between the genome of ancestor A1 and the extant *B. aclada* genome. The genomes of *B. cinerea* and *B. aclada* were thus remarkably syntenic, considering the phylogenetic distance between the two species. Representatives of the two clades within the genus *Botrytis* (Staats et al.

2005) were recently included in molecular clock-based estimates of divergence times for Ascomycota, and these species were estimated to have diverged 5.9 Ma (Shen et al. 2020). The maintenance of 16 chromosomes and the stability of their overall configuration would facilitate chromosome pairing during meiosis. This observation thus suggests the occurrence of a strong selection pressure on sexual reproduction within the genus *Botrytis* over time. The suggestion is further supported by the fact that *Sclerotinia sclerotiorum* also possesses 16 chromosomes (Derbyshire et al. 2017) and that the ancestral genome of the Sclerotiniaceae differs from the ancestral *Botrytis* genome only by a single rearrangement, despite the divergence between the genera *Sclerotinia* and *Botrytis* being estimated to have occurred around 21.5 Ma (Shen et al. 2020). The extent of synteny among *Botrytis* species from distinct clades could only have been retained if sexual reproduction in this genus has been prominent over the course of evolution. Of the 22 *Botrytis* species used in the initial phylogeny of the genus (Staats et al. 2005), 14 were reported to have a sexual stage, whereas eight were not, including *B. aclada*. Population studies may shed more light on the modes of reproduction of *Botrytis* species. Thus far, only *B. cinerea*, *B. pseudocinerea*, *B. tulipae*, and *B. elliptica* have been subject of population analyses (Fournier et al. 2005; Giraud et al. 1999; Mercier et al. 2019; Soltis et al. 2019; Staats et al. 2007a; Walker et al. 2015), whereas other species have received less attention.

Although synteny analyses indicated a strong overall conservation of chromosome architecture between *Botrytis* species, it was striking to detect a substantial number of small translocations between *B. cinerea* and *B. aclada*, both in telomeric and internal chromosomal regions. Telomeric translocations are relatively "safe" rearrangements, as they have limited impact on genome architecture and chromatin organization, minimizing the risk of causing major genome stress. However, such rearrangements have the potential risk of (partial or complete) loss of the telomeric region during the translocation. The BOA clusters that were detected in multiple *Botrytis* species were, with two exceptions, located at the end of contigs, presumably because they were flanked by repetitive sequences. In *Sclerotinia sclerotiorum*, however, the BOA cluster is located internally in chromosome SSCLE15, and it is not flanked by repetitive sequences. Although it seems logical to propose a role of repetitive sequences in the translocation of chromosomal segments (whether telomeric or internal), further studies need to establish such a role. Sequencing multiple isolates of some of the species by long-read technology might reveal the frequency of translocation events within a species.

It was remarkable to note that the BOT clusters appears to be located in four distinct genomic locations in the seven *Botrytis* species in which it was analyzed, and each of the loci was flanked by transposons, and in three cases even interrupted by transposons. It is tempting to speculate that these transposons have played a role in the mobility of the BOT cluster within the genome. The phylogeny of the BOT gene clusters was in full agreement with the species phylogeny, arguing against a horizontal transfer event. Thus,

the data suggest that there have been independent translocations of the BOT gene cluster to distinct chromosomes, culminating in the four distinct genomic locations presently observed in extant fungal isolates. Only within *B. squamosa*, *B. deweyae*, and *B. elliptica* was the BOT cluster in the equivalent genomic location, as could be expected from their phylogenetic proximity within a subclade of clade 2. This suggests a unique transposition event in the lineage toward the common ancestor of species in this subclade (A5 in Figure 4). It is not currently possible to estimate the timing of these translocations, nor could the position of the BOT cluster in the ancestral genome be inferred in the Anchro analysis.

Polymorphism in genomic locations of SM BGCs was recently described within a collection of *Aspergillus fumigatus* isolates, suggesting that mobility of BGCs may occur even within a single species. In this study, there was even one case of two isolates carrying idiomorph BGCs, that is, two distinct clusters residing in the same genomic locations (Lind et al. 2017). It will be interesting to analyze multiple isolates of the different *Botrytis* species and explore whether mobility of BGCs occurs within a single species as well. Long-read sequence technology will be essential for such purpose, to obtain flanking sequence information that permits to infer the correct genomic locations of the various BGCs.

The evolution and dynamics of BOT and BOA clusters

The BGCs involved in the production of phytotoxic SMs BOT and BOA were specifically interesting because they trigger (programmed) cell death in dicots (Rossi et al. 2011) and in monocots (our unpublished results) and contribute to the virulence of *B. cinerea* (Dalmais et al. 2011). The unusual observation of the distinct genomic locations of BOT and BOA clusters encouraged us to explore two distinct evolutionary scenarios: that either clusters were vertically transmitted but were able to excise from their location and reinsert at distinct locations; or that clusters were lost and then regained through HGT. We carefully evaluated the functionality, synteny, and phylogeny of BOT and BOA genes and avoided assuming that vertical gene duplication is the source of multiple paralogs within a lineage. Indeed, half the BOA clusters inferred to be functional in *Botrytis* appear to have been acquired by HGT from other *Botrytis* species, and the functional BOA cluster in *B. sinoallii* is inferred to be a xenolog (horizontally acquired paralog) of the pseudogenized cluster in the same species. The fact that the inferred donor of the BOA cluster in *B. sinoallii* (a taxon closely related to *B. aclada* and *B. porri*), which also is a pathogen of *Allium*, is consistent with host-specific functions selecting for cluster HGT. BGC birth and death processes appear to involve the horizontal replacement of commonly lost clusters; however, the trajectories of BOT and BOA contrast in their evolutionary dynamics. Although BOT is less frequently lost/nonfunctionalized and has not been gained by HGT in this data set, BOA is frequently lost or nonfunctionalized and also replaced by HGT. It is possible that BOT is more readily retained by natural selection due to its role in microbial competition (Vignatti et al. 2020).

This genome comparison has not revealed any host range determinants that enable so many *Botrytis* species (and *S. cepivorum*) to infect *Allium* hosts, likely because fungus–plant interactions may depend on a multitude of factors. Especially the fact that some of these species infect leaf tissue, whereas others infect the bulb or the root, and some species induce blight symptoms, whereas others cause maceration and rot, adds another layer of complexity when comparing species pathogenic on the same host. The high synteny and conservation of chromosome architecture between such distant species across the genus *Botrytis* is remarkable and contrasts with the dynamics of genome evolution in many other plant pathogens.

Acknowledgements

The authors acknowledge Jeff Rollins (University of Florida, Gainesville, USA), Jürgen Köhl (Wageningen Plant Research, the Netherlands), and Jing Zhang and Guoqing Li (Huazhong Agricultural University, Wuhan, China) for providing fungal isolates, as well as Alexander Wittenberg and Harrie Schneiders of Keygene N.V. (Wageningen, the Netherlands) for advice and support in preparing high quality DNA samples for the sequencing. Furthermore, the authors are grateful to Laura Vilanova Torren for her contribution in annotation of the genomes. This work was supported by the Dutch Technology Foundation STW, which is part of the Netherlands Organisation for Scientific Research (NWO), and which is partly funded by the Ministry of Economic Affairs (Project 15003).

Supplemental tables

Supplemental table 1. Information about the strains used in this study.

Botrytis species	Acronym	Isolate	Main host
B. aclada	BACL	633	*Allium cepa*
B. byssoidea	BBYS	MUCL94	*Allium cepa*
B. deweyae	BDEW	B1	*Hemerocallis*
B. elliptica	BELL	Be9612	*Lilium*
B. globosa	BGLO	MUCL444	*Allium ursinum*
B. porri	BPOR	MUCL3234	*Allium porrum*
B. sinoallii	BSIN	Onion Bc23	*Allium cepa*
B. squamosa	BSQU	MUCL31421	*Allium cepa*
S. cepivorum	SCEP	UFL	*Allium cepa*

Supplemental table 2. Comparison of plant cell wall degrading enzymes (PCWDEs) among *Botrytis* spp.. Enzymes were categorized according to their substrate based on information from CAZY database (www.cazy.org). Data taken from this study and earlier studies by van Kan et al. (2017) and Valero-Jiménez et al. (2019).

Species	Cellulose	Hemi-cellulose	Hemicellulose or pectin side chains	Pectin	Plant or Fungal CWDEs	Total	Reference
B. aclada	17	27	13	32	31	120	This study
B. byssoidea	17	29	13	29	31	119	This study
B. calthae	17	30	12	32	21	112	Valero-Jiménez et al. 2019
B. cinerea	20	34	13	38	27	132	van Kan et al. 2017
B. convoluta	18	31	12	34	25	120	Valero-Jiménez et al. 2019
B. deweyae	19	32	13	34	33	131	This study
B. elliptica	19	33	12	33	30	127	This study
B. galanthina	19	35	12	36	23	125	Valero-Jiménez et al. 2019
B. globosa	17	26	12	31	30	116	This study
B. hyacinthi	20	34	13	35	23	125	Valero-Jiménez et al. 2019
B. narcissicola	20	31	11	28	21	111	Valero-Jiménez et al. 2019
B. paeoniae	19	31	12	32	22	116	Valero-Jiménez et al. 2019
B. porri	17	27	12	33	33	122	This study
B. sinoallii	17	28	12	22	28	117	This study
B. squamosa	19	34	12	34	33	132	This study
B. tulipae	18	32	11	29	22	112	Valero-Jiménez et al. 2019
S. cepivorum	15	27	11	27	29	109	This study

Supplemental table 3. The 45 Leotiomycete genomes used for orthogroup analysis of secondary metabolite biosynthetic gene clusters (SM BGCs).

Species	Genus	Family	NCBI accession
A. resinae	*Amorphotheca*	Myxotrichaceae	MADK00000000
A. sarcoides	*Ascocoryne*	Helotiaceae	AIAA00000000
B. graminis f. sp. *hordei*	*Blumeria*	Erysiphaceae	CAUH00000000
B. graminis f. sp. *tritici*	*Blumeria*	Erysiphaceae	ANZE00000000
B. aclada	*Botrytis*	Sclerotiniaceae	RCSV00000000
B. byssoidea	*Botrytis*	Sclerotiniaceae	RCSW00000000
B. calthae	*Botrytis*	Sclerotiniaceae	PHWZ00000000
B. cinerea	*Botrytis*	Sclerotiniaceae	CP009805-CP009822
B. convoluta	*Botrytis*	Sclerotiniaceae	PQXN00000000
B. deweyae	*Botrytis*	Sclerotiniaceae	RCSX00000000
B. elliptica	*Botrytis*	Sclerotiniaceae	RCSY00000000
B. galanthina	*Botrytis*	Sclerotiniaceae	PQXL00000000
B. globosa	*Botrytis*	Sclerotiniaceae	RCSZ00000000
B. hyacinthi	*Botrytis*	Sclerotiniaceae	PQXK00000000
B. narcissicola	*Botrytis*	Sclerotiniaceae	PQXJ00000000
B. paeoniae	*Botrytis*	Sclerotiniaceae	PQXI00000000
B. porri	*Botrytis*	Sclerotiniaceae	RCTA00000000
B. sinoallii	*Botrytis*	Sclerotiniaceae	RCTB00000000
B. squamosa	*Botrytis*	Sclerotiniaceae	RCTC00000000
B. tulipae	*Botrytis*	Sclerotiniaceae	PQXH00000000
Cadophora sp.	*Cadophora*	Helotiales incertae sedis	PCYN00000000
C. crateriformis	*Coleophoma*	Helotiales incertae sedis	PDLN00000000
C. cylindrospora	*Coleophoma*	Helotiales incertae sedis	PDLM00000000
D. rosae	*Diplocarpon*	Dermateaceae	MVNX00000000
E. necator	*Erysiphe*	Erysiphaceae	JNVN00000000
E. pulchra	*Erysiphe*	Erysiphaceae	PEDP00000000
G. lozoyenzis	*Glarea*	Helotiaceae	ALVE00000000
M. brunnea f. sp. *multigermtubi*	*Marssonina*	Dermateaceae	AFXC00000000
M. bicolor	*Meliniomyces*	Hyaloscyphaceae	LXPI00000000
M. variabilis	*Meliniomyces*	Hyaloscyphaceae	LXPR00000000
M. fructigena	*Monilinia*	Sclerotiniaceae	QGLU00000000
O. maius	*Oidiodendron*	Myxotrichaceae	JMDP00000000
P. subalpina	*Phialocephala*	Helotiales incertae sedis	FJOG00000000
P. scopiformis	*Phialocephala*	Helotiales incertae sedis	LKNI00000000
Phialophora cf. *hyalina*	*Phialophora*	Leotiomycetes incertae sedis	NPIC00000000
P. destructans	*Pseudogymnoascus*	Pseudeurotiaceae	LAJJ00000000
P. verrucosus	*Pseudogymnoascus*	Pseudeurotiaceae	LAJO00000000
R. ericae	*Rhizoscyphus*	Ericaceae	LYBP00000000
R. agropyri	*Rhynchosporium*	Helotiales incertae sedis	FJUX00000000
R. commune	*Rhynchosporium*	Helotiales incertae sedis	FJUW00000000

Species	Genus	Family	NCBI accession
R. secalis	*Rhynchosporium*	Helotiales incertae sedis	FJVC00000000
S. borealis	*Sclerotinia*	Sclerotiniaceae	AYSA00000000
S. sclerotiorum	*Sclerotinia*	Sclerotiniaceae	CP017814-CP017829
S. cepivorum	*Sclerotium*	Sclerotiniaceae	RCTD00000000
S. lignicola	*Scytalidium*	Leotiomycetes incertae sedis	NCSJ00000000

Supplemental table 4. Details of chromosomal rearrangements in the genus *Botrytis*. Details of balanced genomic rearrangements between inferred ancestral genomes (AB0-A6) and extant *Botrytis* species, as provided in simplified form in Table 2. Inferences were made using the tool Anchro.

Type of rearrangement	AB0-BCIN	AB0-A1	A1-BACL	A1-A2	A2-A3	A3-A4	A3-A6	A4-A5	A4-BSIN	A5-BSQU	A5-BDEW	A6-BBYS	A6-BGLO
Terminal Inversion of one block	2	0	0	0	0	0	1	0	0	0	0	0	0
Inversions of one block (ex: (AB,BC)->(A-B,-BC) or (-CB,B-A))	9	0	2	0	2	3	5	1	6	2	1	3	1
Terminal Inversion of several blocks (because on same chr)	2	0	0	0	0	0	0	0	0	0	0	0	0
Inversions of several blocks (ex: (AB,CD)->(A-C,-BD) or (A-C,-DB)	2	0	1	0	0	0	0	0	0	0	0	0	1
Non-reciprocal translocation of one block	0	0	0	0	0	0	0	0	0	1	0	1	0
Translocations of two blocks	0	0	0	0	0	0	0	0	0	1	0	2	0
Terminal Translocations	1	0	0	0	0	0	0	0	1	0	0	1	0
Translocation	0	0	1	0	0	0	1	0	0	0	0	0	1
Inversions/Translocations (for long cycles)	0	0	0	0	0	0	0	0	1	0	0	0	0
Terminal Transpositions (ex: (0A,AB,EF)->(0B,EA,AF))	0	0	0	0	0	0	0	0	0	0	0	0	0
Transpositions (ex: (CA,AB,EF)->(CB,EA,AF))	1	0	1	0	0	0	0	0	1	0	0	0	0
Fusions	0	0	0	1	2	1	0	1	2	1	2	0	2
Fissions	0	0	5	1	1	6	2	1	19	3	40	27	3
Sum	**17**	**0**	**10**	**2**	**5**	**10**	**9**	**3**	**30**	**8**	**43**	**34**	**8**

Supplemental figures

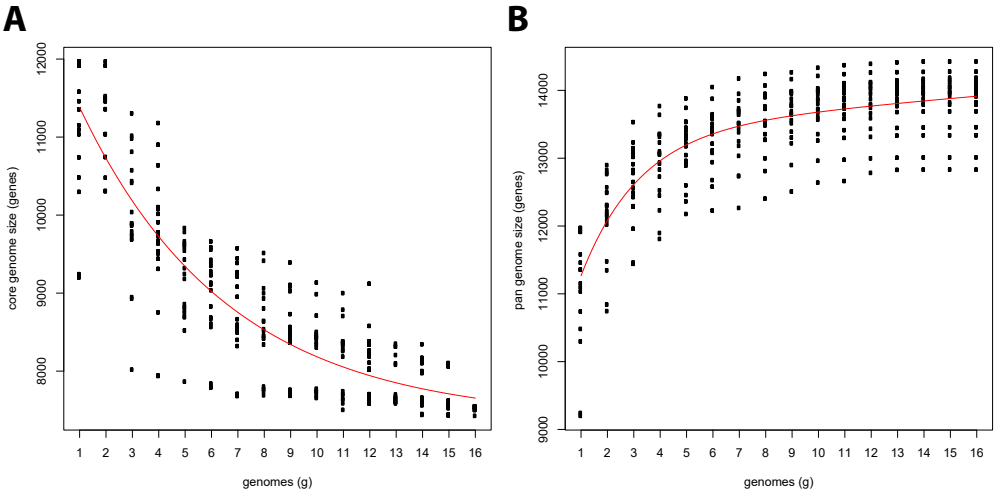

Supplemental figure 1. Core genome and pan-genome analysis of 16 *Botrytis* species. (**A**) Estimation of *Botrytis* spp. core genome, in which the number of shared genes is plotted as a function of the number of species sequentially added. (**B**) Estimation of *Botrytis* spp. pan-genome size, in which the number of all genes is plotted as a function of the number of species sequentially added.

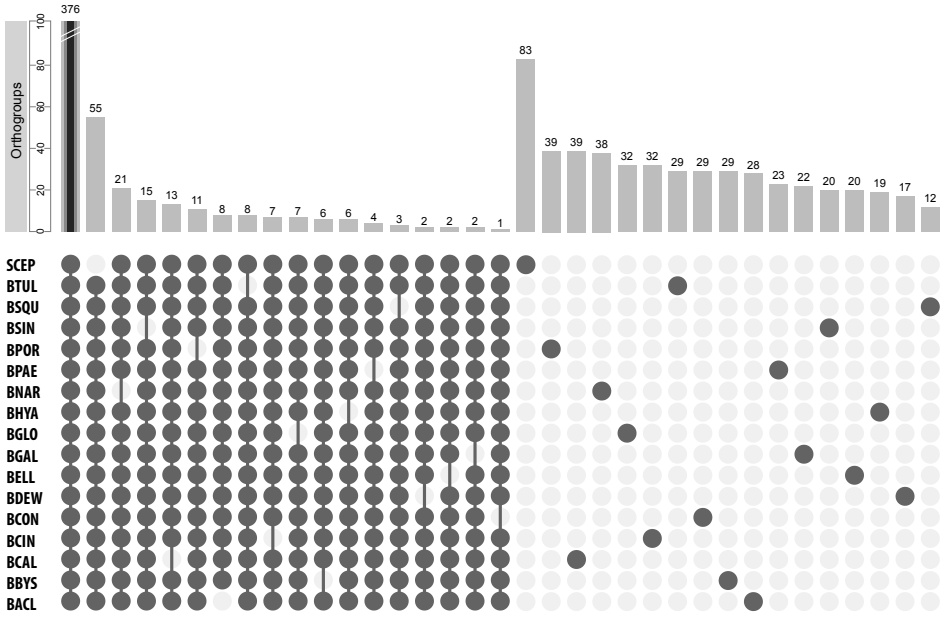

Supplemental figure 2. Presence/absence of orthologous groups of secreted proteins among 16 *Botrytis* species and *S. cepivorum* (species listed in descending alphabetical order). Dark circles indicate the presence of different subgroups in each species, while white circles indicate absence. The number of orthologous groups for each subgroup is shown above the bars.

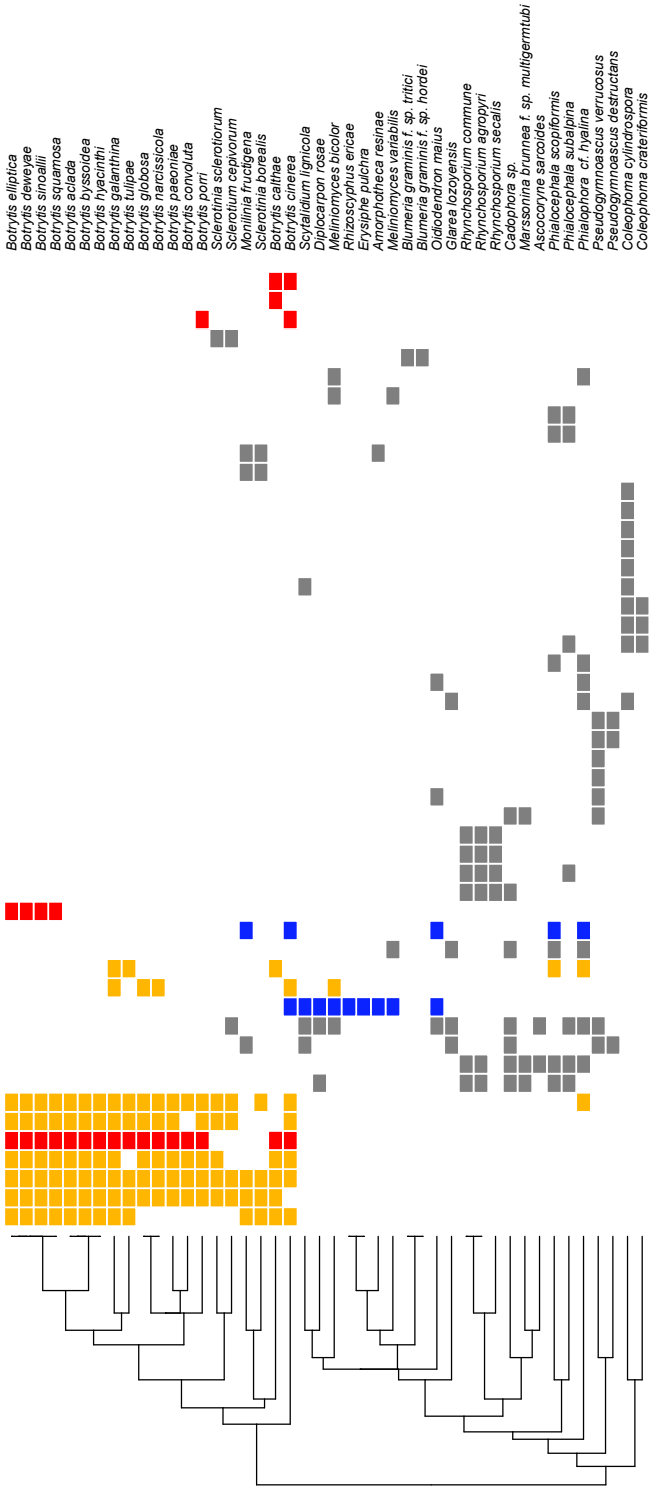

Supplemental figure 3. Distribution of orthogroups of Non-Ribosomal Peptide Synthase clusters in 45 Leotiomycetes. The 50 clusters that are most abundant among the 45 Leotiomycetes taxa are displayed. Clusters that are exclusively represented in *Botrytis* are marked red; clusters predominantly in *Botrytis* but also in some other taxa are marked as ochre; clusters predominantly in other taxa but also in some *Botrytis* species are marked as blue; clusters lacking in all *Botrytis* species are marked as grey.

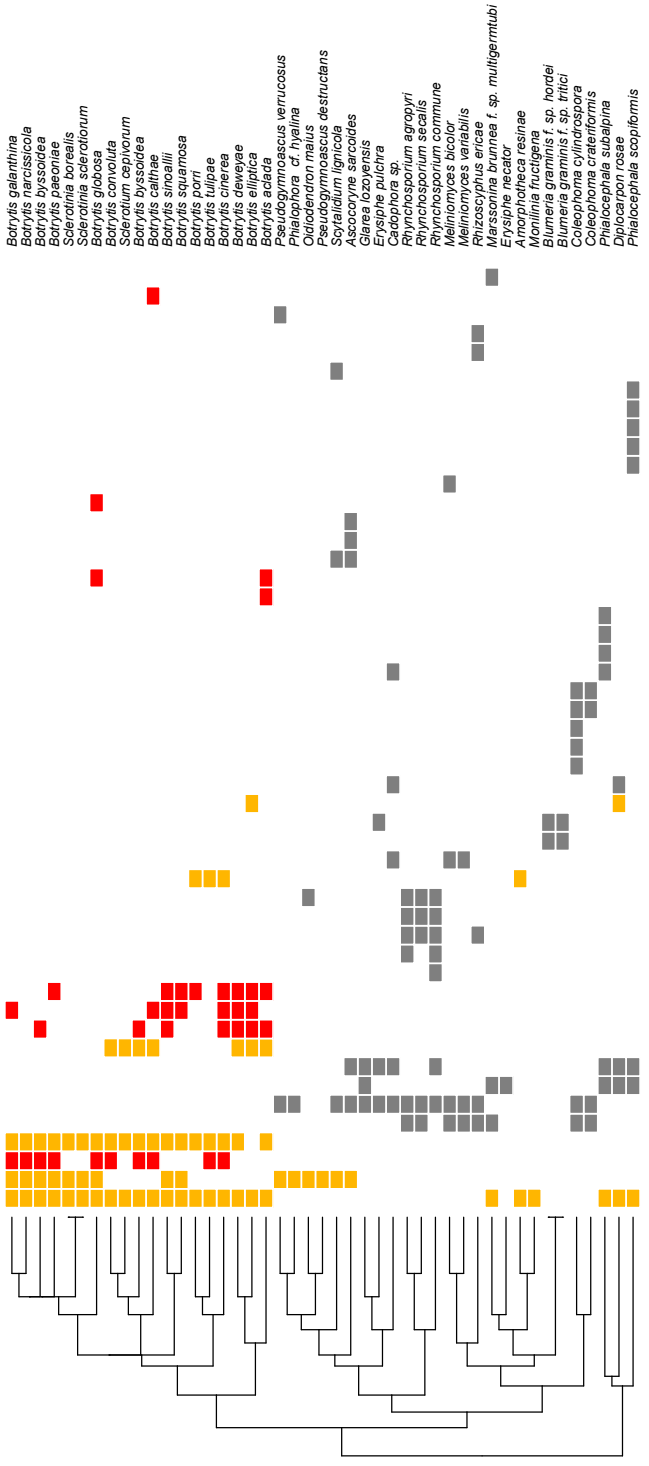

Supplemental figure 4. Distribution of orthogroups of Terpene Synthase clusters in 45 Leotiomycetes. The 50 clusters that are most abundant among the 45 Leotiomycetes taxa are displayed. Clusters that are exclusively represented in *Botrytis* are marked red; clusters predominantly in *Botrytis* but also in some other taxa are marked as ochre; clusters predominantly in other taxa but also in some *Botrytis* species are marked as blue; clusters lacking in all *Botrytis* species are marked as grey.

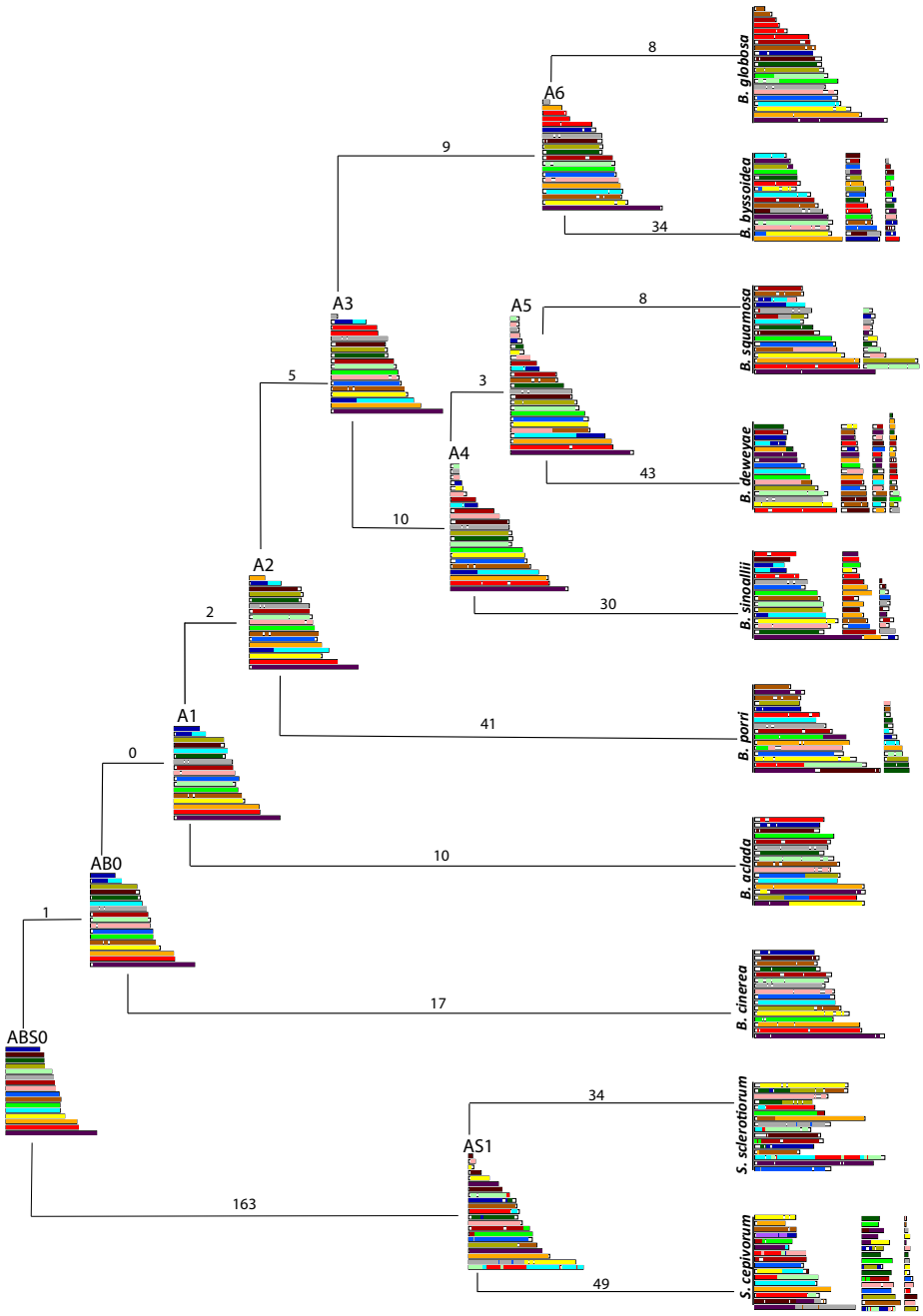

Supplemental figure 5. The most parsimonious evolutionary trajectory from the ancestral (ABS0) configuration towards extant Sclerotiniaceae. Coloured boxes represent syntenic blocks. A1-A6 represent intermediate ancestors. Numbers above the branches represent the total number of balanced rearrangements (interchromosomal translocations and fusions/fissions; intrachromosomal inversions) accumulated between two genomes.

Chapter 5

Identification and validation of effector proteins of *Botrytis squamosa*

Maikel B. F. Steentjes [1]
Andrea L. Herrera Valderrama [1]
Claudio A. Valero-Jiménez [1]
Christiaan Bootsma [1]
Sjef Boeren [2]
Thomas Leisen [3]
Matthias Hahn [3]
Olga E. Scholten [4]
Jan A. L. van Kan [1]

[1] Laboratory of Phytopathology, Wageningen University, Wageningen 6708 PB, The Netherlands
[2] Laboratory of Biochemistry, Wageningen University, Wageningen 6708 PB, The Netherlands
[3] Department of Biology, University of Kaiserslautern, Kaiserslautern 67663, Germany
[4] Plant Breeding, Wageningen University, Wageningen 6708 PB, The Netherlands

Abstract

Fungal plant pathogens secrete effector proteins that manipulate the host in order to facilitate colonization. Necrotrophs have evolved specialized effector proteins that actively induce plant cell death by co-opting the programmed cell death machinery of the host. In this study we aimed to identify and validate cell death-inducing effectors of the onion pathogen *Botrytis squamosa*. Using a combination of proteomics and genome-wide effector prediction, we identified candidate effector genes. The cell death-inducing activity of effector proteins was tested by transient expression via *Agrobacterium tumefaciens*-mediated transformation of *Nicotiana benthamiana*. Additionally, we produced a subset of effector proteins in *Pichia pastoris* which allowed us test the cell death-inducing activity on onion. To evaluate if the effectors had been subject to diversifying selection, the genetic diversity of protein coding sequences was compared among seven *B. squamosa* isolates. Finally, the contribution of two effector proteins to the virulence of *B. squamosa* on onion was assessed using knockout mutants obtained by CRISPR-Cas9-mediated transormation. Identifying effector proteins of *B. squamosa* might provide insights in their contribution to host specificity of *Botrytis* species.

Introduction

Botrytis squamosa is a member of the fungal genus *Botrytis* and is the causal agent of onion leaf blight. The disease poses a serious threat for onion cultivation in all major production areas worldwide and control measures mainly involve fungicide sprays (Carisse et al. 2011; Steentjes et al. 2021a). The disease is characterized by small necrotic spots on the onion foliage, often surrounded by a chlorotic halo. In a later stage of the infection, the lesions expand and leaves start to blight, resulting in reduced plant growth and decreased bulb development (Lacy and Lorbeer 2008a; Lorbeer et al. 2007). On necrotic leaf parts, *B. squamosa* produces conidia that are dispersed by wind to initiate a new disease cycle (Lorbeer 1992).

For a long time, fungi with a necrotrophic lifestyle have been considered to invade their hosts in a rather unsophisticated manner. Using lytic and degradative enzymes, the fungus first kills and subsequently grows into host cells and eventually colonizes host tissue. In the past decades however, evidence has been accumulating that the interaction between necrotrophs and their hosts is more subtle and sophisticated than previously appreciated. Necrotrophs actively induce plant cell death by co-opting the programmed cell death machinery of the host using specialized effector proteins, to a certain extent similar to biotrophs (Dickman et al. 2001; van Kan 2006). The induction of plant cell death using effectors is vital for the success of infection (Stergiopoulos et al. 2013; Tan et al. 2010; Veloso and van Kan 2018). Moreover, for some necrotrophic effectors the corresponding plant receptor proteins required for effector recognition and for triggering of the cell death response have been identified (Abeysekara et al. 2009; Gao et al. 2015; Schürch et al. 2004). The cell death response to necrotrophic effectors is based on similar mechanisms as the recognition of effectors from biotrophic pathogens, but leads to disease susceptibility instead of disease resistance as is the case for biotrophs (Lorang et al. 2007; Tan et al. 2010).

The role of necrotrophic effectors in plant-pathogens interactions is best studied in Septoria nodorum blotch (SNB) in wheat, caused by the Ascomycete fungus *Parastagonospora nodorum*. The first identified effector from *P. nodorum* was SnTox1, a small, secreted protein that induced necrosis upon infiltration in wheat lines carrying the sensitivity gene *Snn1* (Liu et al. 2004). SnTox1 knockout mutants lost virulence on *Snn1*-carrying wheat lines, and introduction of SnTox1 into an avirulent *P. nodorum* strain rendered pathogenicity on wheat lines harbouring *Snn*1 (Liu et al. 2012). By genetic analysis, more *P. nodorum* effectors and corresponding wheat sensitivity genes were identified such as SnToxA-*Tsn1*, SnTox4-*Snn4*, and SnTox6-*Snn6* (Abeysekara et al. 2009; Faris et al. 2010; Gao et al. 2015; Tan et al. 2012). To date, nine necrotrophic effectors and corresponding host sensitivity genes have been identified in the *P. nodorum*-wheat pathosystem (Cowger et al. 2020; Duba et al. 2018). The severity of infection depends in a quantitative manner on the number and

identity of pathogen effectors and corresponding wheat sensitivity genes (Haugrud et al. 2019; Oliver et al. 2012; Phan et al. 2016; Ruud et al. 2017).

The broad host range model necrotroph *Botrytis cinerea* is also known to secrete proteins that induce cell death upon recognition by the host. *B. cinerea* endopolygalacturonases (PGs) induce necrosis upon infiltration in *Arabidopsis thaliana*, but only in lines harbouring leucine-rich repeat (LRR) receptor-like protein RBPG1 (Zhang et al. 2014). Other proteinaceous virulence factors that function as cell death-inducing proteins identified in *B. cinerea* are BcXyl11a and BcXyl1, xylanases that induce necrosis in plant tissue independent from their catalytic activity (Noda et al. 2010; Yang et al. 2018). Also a xyloglucanase, BcXYG1, was found to induce cell death, but not with its enzymatic activity (Zhu et al. 2017). Xylanases are recognized by the LRR receptor-like proteins *LeEix1* and *LeEix2* and the cell death response to BcXyl1 and BcXYG1 requires the LRR receptor-like kinases BAK1 and SOBIR1 (Ron and Avni 2004; Yang et al. 2018; Zhu et al. 2017). In addition to the cell wall degrading enzymes with cell death-inducing activity, often considered as PAMPs or catalytic necrosis-inducing proteins (NIPs), *B. cinerea* also secretes cell death-inducing proteins that lack a known enzymatic domain and are referred to as effectors. Amongst others BcNep1, BcNep2, BcSpl1 and BcIEB1 have been heterologously produced and induced cell death upon infiltration in dicot plants (Arenas et al. 2010; Frías et al. 2011; Frías et al. 2016).

Since *B. squamosa* is a host-specific necrotrophic pathogen of onion, we hypothesize that during infection *B. squamosa* secretes effector proteins that induce cell death specifically in its host plant onion. In this study, we aimed to identify such effectors of *B. squamosa* and validate their cell death-inducing activity. A combination of genome-wide effector predictions and proteomics approaches provided a list of candidate effector genes. By heterologous production of several proteins in *Pichia pastoris* or transient expression via *Agrobacterium tumefaciens*-mediated transformation, we were able to test the plant cell death-inducing activity of the candidate effectors. Genetic diversity of candidate effectors in *B. squamosa* isolates was assessed to check for diversifying selection, a characteristic often observed for effector genes. For two candidate effectors, *B. squamosa* knock-out mutants were made using a CRISPR-Cas9-mediated transformation. Here, we present the result of attempts to characterize *B. squamosa* effector proteins and study their role in virulence.

Material and methods

Fungal strains, culture conditions and transformation procedure

B. squamosa isolate MUCL31421 was used for RNA isolation and sequencing and as recipient strain for transformation. Spores of *B. squamosa* were obtained by growth on autoclaved onion leaves on water agar and exposure to UV light as described in (Steentjes et al. 2021b). Spores were kept in 15% glycerol at -80°C for long term storage. To obtain *B. squamosa* P11 and E14 knockout mutants, we used the CRISPR-Cas9-mediated protoplast transformation protocol optimized for *B. cinerea* as described by Leisen et al. (2020). Protoplasting conditions were optimized for *B. squamosa* by using $5x10^6$ spores to inoculate the liquid culture and allow growth for 24 hours. Mutants were selected using an initial concentration of 17.5 µg/ml hygromycin B. Knockout mutants were confirmed by PCR and sequencing of the gene fragment and obtained mutants were tested for their *in vitro* growth rate and ability to produce sclerotia and conidia.

Proteomics approach to identify effectors

Liquid cultures of *B. squamosa* were made by adding $5x10^6$ spores to 50 mL PDB (24g/L) in a round bottom flask. The culture was incubated at 22°C for 4 days while shaking at 100 RPM. After 4 days of growth, the culture was filtered over 22µm nylon mesh and filter sterilized (0.45 µm, Millipore). To test for proteinaceous origin of necrotic activity, culture filtrate was boiled in a heating block at 99°C for 1 and 5 minutes, or treated with 10 mM DTT at room temperature. To fractionate the proteinaceous content, the culture filtrate was subjected to both cation and anion chromatography using streamline SP XL (GE Healthcare) at pH 5.5 and streamline Q XL (GE Healthcare) at pH 8.0, respectively. Proteins were eluted from the resin using eluents with 0, 20, 100, 200, 500 and 1000 mM NaCl. Crude extracts and protein fractions were subjected to mass spectrometry. Peptides were mapped to the annotated *B. squamosa* genome (Valero-Jiménez et al. 2020).

Genome-wide effector prediction

The genome of *B. squamosa* was analysed for secreted proteins using Signal-P and the secretome was assessed for predicted effector genes using effectorP as described in Valero-Jiménez et al. (2020). Predicted effector genes that were represented by fewer than 6 reads in all transcriptome libraries were discarded. Subsequently, all predicted effectors that had a domain with a known function not related to effector activity were removed, as well as effectors that had orthologous in many Ascomycete fungi outside *Botrytis*. Finally, effectors that were predicted to possess a GPI anchor by TMHMM were eliminated.

Agrobacterium-mediated expression

Mature protein coding sequences of candidate effectors were amplified from cDNA of *B. squamosa* infected onion leaves. Amplicons were inserted into digested expression vector pAJ21. Ligation of the fragment was checked by PCR and sequencing, and correctly ligated plasmids were transformed into *Agrobacterium tumefaciens* strain GV3101 by electroporation. Cultures of transformed *A. tumefaciens* were suspended in MMAi infiltration buffer. This suspension was mixed 1:1 with *A. tumefaciens* cultures expressing P19 to suppress post-transcriptional gene silencing, to a final OD of 1.6. Bacterial suspensions were infiltrated into leaves of 4-6 weeks old *N. benthamiana* plants using needleless syringes and plant responses were assessed at 3 DPI. For apoplastic fluid isolation, agroinfiltrated *N. benthamiana* leaves were submerged under water using a vacuum. Release of the vacuum allows water to fill up the apoplast, and subsequent centrifugation yields the apoplastic fluid. Concentration of apoplastic fluid was performed using centrifugal concentrators (Pierce) with a 3.5 kDa cutoff threshold.

Protein production and purification

The mature protein coding sequences of Nep1, Spl1, P11, P12 and E14 were amplified from cDNA and cloned into the vector pPIC9k (Invitrogen) via restriction enzymes *Eco*RI and *Not*I. After confirmation of the insert by PCR and sequencing, the plasmids were transformed into *Pichia pastoris* strain GS115 by electroporation. Fermentation was performed on a large scale using a BioFlo 120 fermentor (Eppendorf) applying the fermentation protocol described in Schouten et al. (2008). Briefly, approximately 3 L of *P. pastoris* culture was grown at 30°C for 5 days, including 3 days on methanol as sole carbon source to induce protein production. After 5 days the supernatant was separated by centrifugation and concentrated to 200 mL via diafiltration using a VivaFlow 200 Cassette MWCO 5000 Dalton (Sartorius, VF20P4). This concentrated supernatant was desalted, washed twice with 10 mM KPO_4 pH 7.0, and filter-sterilized.

Protein purification was performed by affinity chromatography. Briefly, 5 mL of resin was equilibrated with 3 volumes of 10 mM KPO_4, in a glass Econo-column (Biorad 7371012), and transferred to a 50 mL tube containing 40 mL of concentrated crude protein sample. Proteins were allowed to bind by agitation on a horizontal rotor at 4°C for 90 min, and the glass column was filled again with the protein bound-resin. The resin was rinsed by flushing the column twice with two column volumes 10 mM KPO_4, and the bound proteins were recovered by eluting with an increasing salt concentration. The eluted fractions were pooled, desalted, and concentrated using Amicon Ultra-15 PLBC filters. Protein concentrations were quantified using Bradford assays (Biorad). Purified protein was analyzed by polyacrylamide gel electrophoresis.

For Nep1, resin Streamline SP XL (GE Healthcare) at pH 7.0 was used as described in Schouten et al. (2008). Nep1 was recovered by eluting with an increasing salt concentration between 0.1 M and 0.3 M NaCl. Spl1 was bound to resin Streamline Q XL (GE Healthcare) at pH 5.5 and eluted with increasing salt concentration between 0.05 M and 1 M NaCl. The majority of Spl1 was obtained with the eluent corresponding to 0.05 M NaCl and no additional desalting was performed. For both protein P11 and P12, resin Streamline Q XL was used at pH 7.0. Proteins were eluted from the resin using salt concentration between 0.05 M and 1M NaCl. The majority of protein was eluted on by 0.05M and 0.1M NaCl. Fractions were pooled and no additional desalting was performed. Protein E14 was bound to resin Streamline SP XL at pH 5.5. Also here, the majority of Bs14 was eluted on fractions with 0.05 M and 0.1 M NaCl and fractions were pooled but not desalted.

Plant material and protein infiltration

N. benthamiana (WT) used for *Agrobacterium*-mediated expression and protein infiltration and eight onion genotypes for protein infiltration were grown from seed under greenhouse conditions. In addition, proteins were infiltrated in parental lines *A. cepa*, *A. fistulosum*, *A. roylei*, and the F1 (*A. roylei* x *A. fistulosum*), as well as a subset of six F2 (*A. cepa* x ((*A. roylei* x *A. fistulosum*)) offspring lines of the tri-hybrid population as described in Scholten et al. (2016). The tri-hybrid population as well as the parental genotypes were maintained in tissue culture and plants of all genotypes were transferred to the greenhouse, transplanted in potting soil and grown for several weeks before infiltration. Plants were infiltrated using a syringe on the abaxial side of their leaves (where possible) with purified protein samples or with buffer, and plant responses were assessed at 3 DPI. Proteins were infiltrated in a range of pH from 5.5 to 7.0 in 10 mM KPO_4 buffer, as well as a range of concentrations. The highest protein concentrations that could be tested were dependent on initial protein yield and purification efficiency. The maximum concentrations tested for Nep1, Spl1, P11, P12 and E14 were 50, 175, 400, 60 and 300 µg/mL, respectively.

Infection assays and RNA isolation for expression analysis

For inoculation of *B. squamosa*, young but fully grown leaves of 2-4 month onion plants were used. For testing the virulence of the P11 knockout mutant, onion genotypes 'Centurion' and '2012-19' were used for infection assays 1 and 2, respectively. To assess the virulence of the E14 knockout mutant onion genotype 'Centurion' was used for infection assays. For expression analysis onion genotype DH was used. Detached leaves were placed in humid boxes and the cuticle of leaves was gently wiped with tissue paper to facilitate inoculation. Leaves were inoculated with 2 µl droplets *B. squamosa* spores at 10^6 spores/mL in 12 g/L PDB. To assess the virulence, lesion sizes were measured at three consecutive days and the area under the diseases progression curve was calculated for inoculations

with a secondary lesion growth. For RNA isolation, 16, 24 and 48 hour after inoculation plant tissue was sampled in three replicates and also the used inoculum at 0 hours was sampled. Samples were frozen in liquid nitrogen, freeze dried and grinded to powder. For RNA extraction, samples were incubated in Trizol (Ambion, Life Technologies) and treated with chloroform. Ethanol was added to the aqueous phase and the mixture was further purified using an RNeasy Plant Mini Kit (Qiagen). This RNA was sent for sequencing. Reads were mapped to the annotated genome of *B. squamosa* (Valero-Jiménez et al. 2020).

Analysis of genetic diversity

B. squamosa isolates MUCL_31421, MUCL_9112, MUCL_3812, 026, 1306, BS_878 and BS_1126 were grown on a cellophane layer on top of PDA. Mycelium was harvested, frozen in liquid nitrogen and freeze dried before it was grinded to powder. The mycelial power was used to extract genomic DNA by incubation in cell lysis solution (Qiagen) followed by protein precipitation solution (Qiagen). DNA was precipitated using 100% isopropanol and washed with 70% ethanol and finally eluted in $T_{10}E_1$. Genes encoding Nep1, Spl1, P11, P12, E14 and E28 were amplified by PCR and the amplicons were sequenced. 5'UTR, 3'UTR and introns were removed and the mature protein coding sequences were aligned using MEGA-X.

Statistical analysis

Differences in virulence between *B. squamosa* WT and knockout mutants were statistically assessed in SPSS Statistics 25.0 (IBM) using independent samples *t*-tests. Differences were considered to be statistically significant with two-tailed P values <0.05.

Results

Liquid cultures of *B. squamosa* contain cell death-inducing proteins

The potential effector activity of *B. squamosa* was tested with culture filtrates of *B. squamosa* grown in liquid medium. The culture filtrate appeared to induce strong cell death responses upon infiltration into two onion cultivars and the non-host *Nicotiana benthamiana* (Figure 1A). The cell death-inducing activity of the filtrate was reduced upon heat treatment and upon reduction of disulphide bonds by DTT, suggesting that at least part of the cell death-inducing activity of the culture filtrate was from proteinaceous origin (Supplemental figure 1A). To investigate the protein composition of the filtrate, we fractionated the sample using cation and anion exchange chromatography yielding fractions with different combinations of proteins (Supplemental figure 1B). Infiltration of these protein fractions into onion cultivars caused necrosis only for specific fractions, suggesting that they contained one or more active proteins from the *B. squamosa* culture filtrate. For the protein fractions obtained by cation exchange chromatography, infiltration of solely fraction 3 caused a necrotic plant response in onion cultivar DH, but not in onion cultivar Centurion nor in *N. benthamiana* (Figure 1B), suggesting the presence of a cultivar-specific cell death-inducing protein in this fraction.

To reveal the identity of proteins present in the culture filtrate and in the fractions that showed cell death-inducing activity, protein fractions were analysed using mass spectrometry. By matching the detected peptides to predicted proteins of the annotated *B. squamosa* genome (Valero-Jiménez et al. 2020), the identity of proteins present in the culture filtrate and in several ion exchange chromatography fractions was determined (Supplemental table 1).

All of the identified *B. squamosa* proteins had orthologs in *B. cinerea* and *B. aclada*. Two proteins were specifically present in cation exchange fraction 3, that caused cell death in onion cultivar DH, and 13 proteins were specifically present in the active anion exchange fractions 4 and 5. Since protein concentrations differed between samples and were sometimes low, some proteins may have escaped detection. Therefore, the conclusion that only proteins identified specifically in the active cation and/or anion fractions possess cell death-inducing activity is invalid. Moreover, some proteins identified in ion exchange chromatography fractions were not detected in the crude culture filtrate, demonstrating that the list with identified genes cannot be used to pinpoint which protein is responsible for the cell death-inducing activity of a protein fraction, but rather as a collection of proteins that needs further validation.

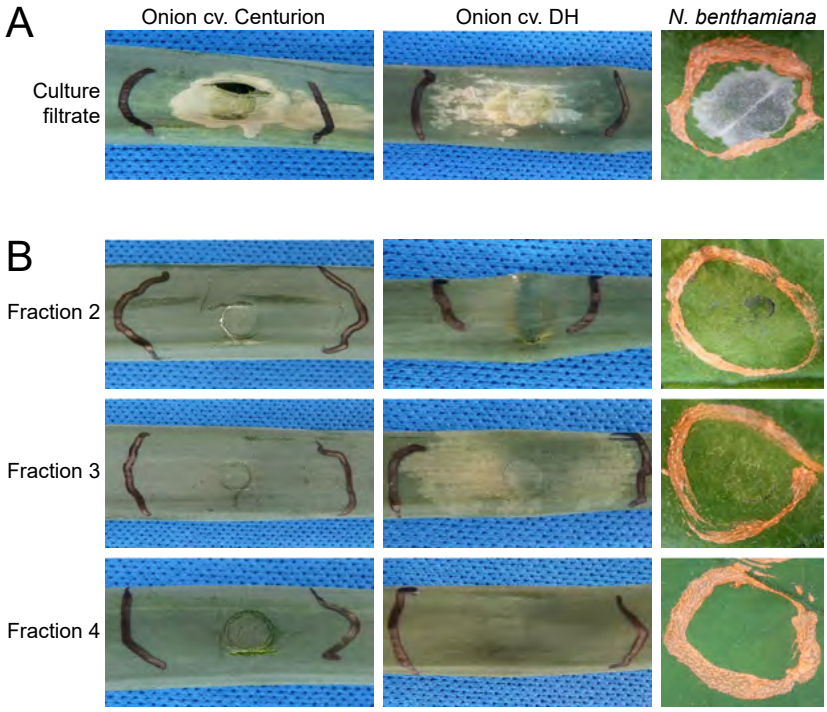

Figure 1. Cell death responses of two onion cultivars and *N. benthamiana* upon infiltration of (**A**) culture filtrate of *B. squamosa* and (**B**) different protein fractions of the culture filtrate obtained by cation exchange chromatography.

Genome-wide effector prediction yields candidates that are not unique to *B. squamosa*

In addition to identifying effector genes by a proteomics-based approach, we also used a genome-wide effector prediction approach to identify putative effectors in the genome of *B. squamosa*. First the sequenced and annotated genome of *B. squamosa* was filtered for secreted proteins and subsequently the probability of genes being effectors was predicted using EffectorP (Valero-Jiménez et al. 2020). The secretome of *B. squamosa* contained 897 genes (7.5%) and the total repertoire of predicted effectors was 132 genes. To prioritize these candidates, genes were discarded that were either expressed to extremely low levels, had a protein domain with a known (enzymatic) function unrelated to effector activity, were predicted to have a glycosylphosphatidylinositol (GPI) cell surface anchor, or that had homologues in many fungi outside the genus *Botrytis*. These filtering steps yielded a list with 52 remaining candidate effectors (Supplemental table 2). All 52 candidates had homologues in related *Botrytis* species. Furthermore, none of the effector candidates was exclusively present in *Allium*-infecting *Botrytis* species (*B. squamosa*, *B.*

aclada, *B. globosa*, *B. byssoidea*, *B. sinoallii* and *B. porri*), suggesting that these candidates likely not function as host specificity determinants. None of the candidates identified using genome-wide effector prediction was detected in the cell death-inducing protein fractions from *B. squamosa* culture filtrates.

Heterologous expression of candidate effector genes by agroinfiltration in *Nicotiana benthamiana*

From the two lists of candidate effector genes, a number of candidates was selected for further characterization. For candidates identified by the proteomics-based approach, genes were prioritized based on classical effector characteristics such as small size and high number of cysteines, as well as absence of known enzymatic domains. Also the amount of peptides of a specific protein detected in samples was taken into consideration. Furthermore, to prioritize candidates from both effector prediction and proteomics approaches, expression data of early infection timepoints of *B. squamosa* on onion leaves was used. Effector genes that play an important role during infection are thought to be highly expressed during the early stages of infection. Expression levels of *B. squamosa* genes from infected leaf tissue 16, 24 and 48 hours after inoculation as well as in spores were analyzed using RNAseq (Figure 2A). In addition to candidate effectors identified by genomic prediction and proteomics, homologues of characterized effector genes of *B. cinerea* (Spl1, Nep1 and CND1), as well as the negative control α-Tubulin were included in the validation of *B. squamosa* effectors.

In total 18 *B. squamosa* genes were cloned into expression vectors and transformed into *Agrobacterium tumefaciens* (Table 1). To analyze their cell death-inducing activity, the candidate effector constructs were agroinfiltrated into *N. benthamiana* and infiltrated areas were assessed for cell death at 3 DPI. Agroinfiltration with negative controls α-Tubulin (Tub) and GFP, as well as the empty vector did not cause any visible plant response (Supplemental figure 2). Infiltration with *B. squamosa* Nep1 resulted in a strong necrotic plant response that covered the complete infiltrated area (Figure 2B). Infiltration of most candidate effectors as well as homologues of effectors from *B. cinerea* did not cause any visible plant response (Supplemental figure 2), whereas candidates P11 and E14 caused small necrotic spots dispersed over the infiltrated area (Figure 2B). The agroinfiltration of candidate E28 resulted in slight discoloration of the infiltrated area, however this response was not consistently observed over multiple infiltrations (Supplemental figure 2). To test the activity of candidate effector genes on onion, we could not perform agroinfiltrations since the *A. tumefaciens*-mediated expression system is not functional in onion. Instead, we isolated apoplastic fluid of agroinfiltrated *N. benthamiana* leaves and infiltrated this fluid, either crude or concentrated, into onion leaves. No plant response was observed upon infiltration of the apoplastic fluid of any of the agroinfiltrated candidate effectors. Also re-infiltration of the apoplastic fluid into *N. benthamiana* did not cause any visible

plant responses. For Nep1, we could not verify its activity in onion using this method, since agroinfiltration rapidly resulted in dry necrotic tissue which constrained the isolation of apoplastic fluid.

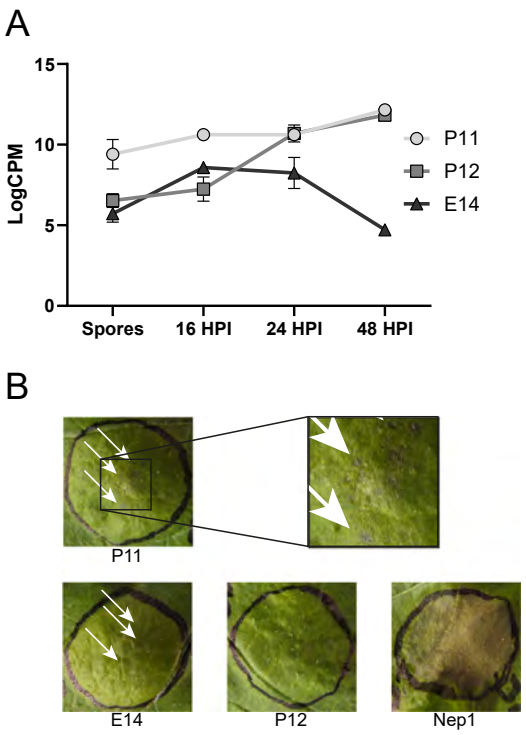

Figure 2. (**A**) Expression of three candidate effector genes during early stages of onion leaf infection by *B. squamosa* analyzed in spores, at 16, 24 and 48 HPI. (**B**) Plant response upon infiltration of *A. tumefaciens* expressing candidate effector genes assessed at 3 DPI, arrows indicate small necrotic spots.

Table 1. List of candidate effector genes that were cloned and transformed into *A. tumefaciens* to test their *in planta* activity. Column source indicates how the candidate effector was identified and columns size and cysteines show respectively the total number of amino acids and the number of cysteines in the protein including signal peptide.

Name	Protein ID	Source	Size	Cysteines
Tub	BSQU_002g00810	Control α-Tubulin	450	14
P1	BSQU_002g06800	Proteomics	540	14
Spl1	BSQU_003g00420	Prot. / Homol. BcSpl1	137	4
P3	BSQU_003g01170	Proteomics	175	6
P4	BSQU_003g05450	Proteomics	607	38
P5	BSQU_003g05460	Proteomics	155	4
E33	BSQU_004g02520	Effector prediction	61	4
E34	BSQU_004g04600	Effector prediction	183	3
P7	BSQU_005g00770	Proteomics	380	8
CND1	BSQU_006g01720	Homologue BcCND1	249	2

Name	Protein ID	Source	Size	Cysteines
E36	BSQU_006g06210	Effector prediction	95	10
P11	BSQU_008g05540	Proteomics	189	4
P12	BSQU_009g00250	Proteomics	160	2
P13	BSQU_011g02090	Proteomics	390	2
E14	BSQU_012g04030	Effector prediction	147	8
Nep1	BSQU_015g03410	Homologue BcNep1	246	3
E28	BSQU_018g01640	Effector prediction	175	4
E31	BSQU_020g00110	Effector prediction	152	2

Activity of candidate effectors produced in *Pichia pastoris*

To test the cell death-inducing activity of candidate effectors on onion, we produced the proteins in the heterologous expression system *Pichia pastoris*. After cloning of candidate effector genes into expression vectors and transformation, *P. pastoris* was grown in a bioreactor to allow optimal control over growth conditions and methanol-induced gene expression. Obtained proteins were purified by ion exchange chromatography. For the majority of produced candidate effectors a relatively pure protein could be obtained, as exemplified by the purification of Spl1 (Figure 3A). In total 5 proteins were successfully produced and purified; Spl1, P11, P12, E14 and Nep1. Purified protein samples were infiltrated into onion as well as *N. benthamiana,* a non-host for *B. squamosa*. Infiltration of Nep1 into *N. benthamiana* resulted in a strong necrotic response, similar as observed for the agroinfiltration of Nep1. However, infiltration of Nep1 into onion also caused a strong and consistent necrotic response (Figure 3B). Candidate effector E14 did not induce any visible symptoms in either *N. benthamiana,* nor in onion (Figure 3B). For all three other tested candidate effectors (Spl1, P11, and P12) some responses could be observed in onion leaves, but they were weak and variable in consistency, particularly when compared to Nep1. For P12, some infiltrated areas showed slight discoloration at the border of infiltration or close to the syringe mark, but only in a minority of infiltrated leaves (Figure 3B). All purified candidate effector samples were infiltrated in buffers with a pH range from 5.5 to 7.0, and in a range of concentrations (dependent on initial protein yield and purification efficiency). Infiltrations were performed in a set of eight onion genotypes, but none of the tested samples and conditions induced a consistent plant response, except for Nep1. In addition to different cultivars of onion (*Allium cepa*), the proteins were also infiltrated in leaves of an interspecific tri-hybrid population of *A. cepa* with *A. roylei* x *A. fistulosum* that shows a segregating resistance to *B. squamosa* (Scholten et al. 2016). The parental lines *A. cepa*, *A. fistulosum*, *A. roylei*, and the F1 (*A. roylei* x *A. fistulosum*), as well as a subset of six F2 (*A. cepa* x ((*A. roylei* x *A. fistulosum*)) offspring lines were used to test

their response to these candidate effectors. None of the infiltrated plants showed visible symptoms upon infiltration of any of the candidate effectors, except for Nep1.

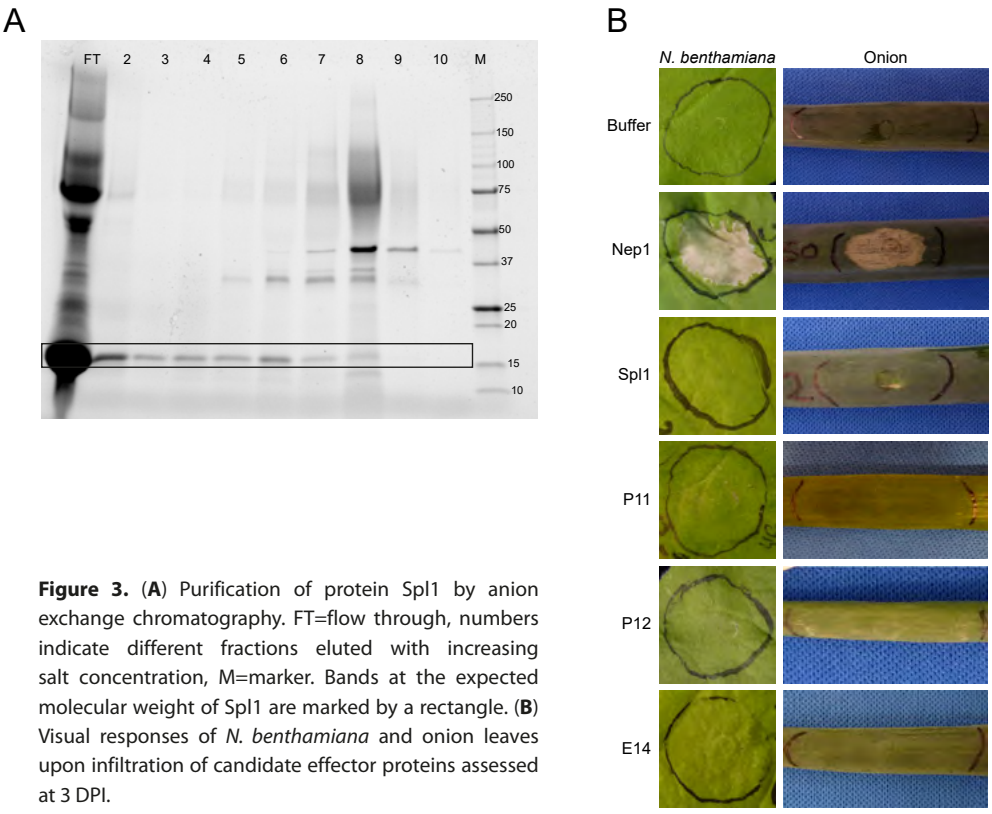

Figure 3. (**A**) Purification of protein Spl1 by anion exchange chromatography. FT=flow through, numbers indicate different fractions eluted with increasing salt concentration, M=marker. Bands at the expected molecular weight of Spl1 are marked by a rectangle. (**B**) Visual responses of *N. benthamiana* and onion leaves upon infiltration of candidate effector proteins assessed at 3 DPI.

Genetic diversity of candidate effectors

Effector genes are suggested to display genetic diversity since their protein products are in contact with the environment, in this case the host plant. There are many reports of microbial effector genes that are under diversifying selection. We sequenced the candidate effector genes Nep1, Spl1, P11, P12, E14 and E28 in seven *B. squamosa* isolates. Five isolates (MUCL_31421, MUCL_9112, MUCL_3812, 026 and 1306) originated from a culture collection and two isolates (BS_878 and BS_1126) were field isolates sampled from infected onions. Candidate effector genes Spl1, P11, P12, E14 and E28 did not show any sequence polymorphism in the seven tested *B. squamosa* isolates. Only Nep1 showed polymorphisms, with in total six SNPs of which five were exclusively present in isolate BS_1126. The sixth SNP was shared between isolates BS_878, BS_1126 and MUCL_9112 (Figure 4). All identified SNPs were synonymous and therefore did not affect the amino acid sequence of Nep1 in the different *B. squamosa* isolates.

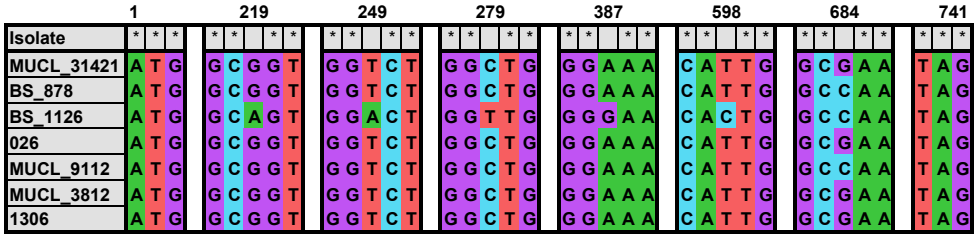

Figure 4. Genetic diversity of Nep1 among seven *B. squamosa* isolates. Selected parts of the sequence show (from left to right) the start codon, the six identified SNPs, and the stop codon with numbers indicating nucleotide positions of the mature protein coding sequence.

Role of candidate effectors in virulence of *B. squamosa* on onion leaves

To assess the role of candidate effectors P11 and E14 in the virulence of *B. squamosa*, knock-out mutants of these genes in *B. squamosa* were made using a CRIPSR-Cas9-mediated transformation. Although candidate effectors P11 and E14 did not induce clear cell death responses upon infiltration of the protein into onion, it cannot be excluded that these genes play a role during infection. The knock-out mutants and WT strain were inoculated on onion leaves and lesion diameters were measured at consecutive days in order to calculate the area under the disease progression curve (AUDPC). The ΔP11 mutant was not significantly reduced in virulence compared to WT in either of the two performed infection assays (Figure 5A). For the ΔE14 mutant the first infection assay suggested a slight increase in virulence and in the second infection assay a slight decrease in virulence was observed as compared to WT. The differences in both experiments were not statistically significant.

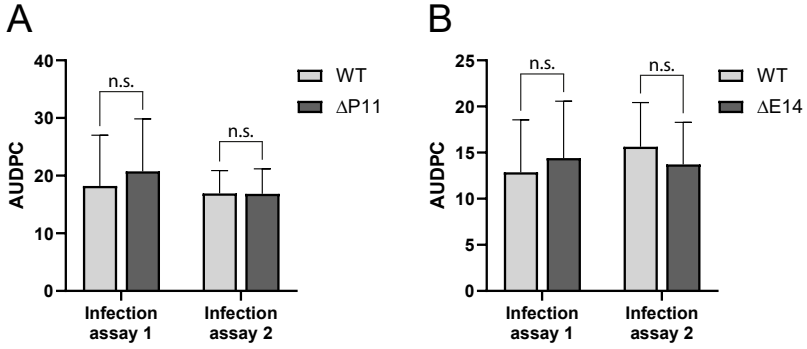

Figure 5. Virulence of WT and knock out mutants of (**A**) candidate effector P11 and (**B**) candidate effector E14 measured as AUDPC. Two infection assays per knockout strain were performed (P11 n=83 and n=80, E14 n=81 and n=96). Differences were statistically assessed with an independent samples *t*-test, and error bars represent standard error.

Discussion

In this study, we identified candidate effector proteins of *B. squamosa* and tested these proteins for their cell death-inducing activity. In total 52 candidate effector proteins were identified by genome-wide effector predictions and another 14 proteins were identified in culture filtrate-derived protein fractions that caused cell death upon infiltration in onion leaves. By heterologous production, we tested the cell death-inducing activity of 17 different candidate effectors via *A. tumefaciens*-mediated transformation, and subsequently six of those via production in *P. pastoris*. Hence, many candidate effectors remain unexplored, some of which showed relatively high expression during early stages of infection, that are worth studying in more detail.

Heterologous expression of candidate effectors using *A. tumefaciens*-mediated transformation was functional in *N. benthamiana*. Since many monocotyledonous plants including onion are notoriously difficult to be transformed by *A. tumefaciens* (Koetle et al. 2015; Sood et al. 2011), candidate effectors could not be transiently expressed in onion leaves. In order to test the activity of candidate effectors in onion, we isolated the apoplastic fluid of agroinfiltrated *N. benthamiana* leaves, and subsequently infiltrated the apoplastic fluid. No plant response was observed for any of the 17 candidates tested, whether infiltrated into onion or re-infiltrated into *N. benthamiana*. The amount of effector candidate protein that eventually reached the apoplast of the infiltrated leaf using this method is difficult to assess, since expression levels of transiently transformed leaves are difficult to control and protein stability might be affected by proteases present in the apoplast (Grosse-Holz et al. 2018; Jutras et al. 2020). Moreover, once an effector protein triggers cell death, as observed upon agroinfiltration of Nep1, isolation of apoplastic fluid becomes impossible because the apoplast collapses in the cell death process.

As an alternative to testing the cell death-inducing activity of candidate effectors via *A. tumefaciens*-mediated transformation, we produced candidate effectors using the heterologous expression system *P. pastoris*. Infiltration of the purified proteins Spl1, P11 and P12 in onion resulted in weak and inconsistent plant responses. The observed variation may be a result of impurity of the infiltrated protein samples. Endogenous *P. pastoris* proteins might have co-eluted during ion exchange chromatography purification and ended up in protein samples. Candidate effectors were produced without a purification tag to avoid the risk of an altered charge, structure and activity of the relatively small effector proteins. However, adding a C-terminal epitope tag would have allowed affinity-based purification and likely have resulted in more pure protein samples (Walls and Loughran 2011; Yadav et al. 2016). Only for Nep1 we observed a rapid and strong cell death response in all replicate infiltrations, both in *N. benthamiana* and onion. The cell death-inducing activity of Nep1-like proteins (NLPs) from other plant pathogens on dicot

plants has been extensively studied and fits our observation of the necrotic response in *N. benthamiana* upon infiltration of *B. squamosa* Nep1. The cell death-inducing activity of Nep1 on onion, however, is striking since NLPs supposedly do not induce cell death on monocotyledonous plants (Lenarčič et al. 2017; Seidl and Van den Ackerveken 2019). These observations raised the question whether *B. squamosa* Nep1 might function differently from other characterized NLPs or whether the sensitivity of onion to NLPs is different from other monocotyledonous plants. A more detailed study of the activity of *B. squamosa* Nep1 on onion is presented in chapter 6 of this thesis.

In addition to testing the cell death-inducing activity of candidate effectors, we also assessed the genetic diversity of candidate effectors among seven different *B. squamosa* isolates. Effector genes are often observed to display genetic diversity within pathogen populations as a result of diversifying selection imposed by the host (Stergiopoulos and de Wit 2009). Indeed many effectors, including those of necrotrophic plant pathogens, show a variety of haplotypes in population studies. Effectors SnToxA, SnTox1 and SnTox3 of *P. nodorum* were all found to display different haplotypes and to be under diversifying selection (Hafez et al. 2020; Richards et al. 2019; Stukenbrock and McDonald 2007). In our analysis of *B. squamosa* candidate effectors, we did not observe any SNPs, except for Nep1. The absence of polymorphisms, although only assessed in seven isolates, suggests that there is no diversifying selection exerted on these genes. The genetic diversity of NLPs on a species level in the genus *Botrytis* has been studied before. Several protein positions appeared to be under diversifying selection, which is congruent with our observation of polymorphisms between isolates of *B. squamosa* (Staats et al. 2007c).

Despite the absence of cell death-inducing activity of the tested candidate effectors, these genes can still play important roles during infection and function as virulence factors without being involved in killing of host cells. To assess the role of P11 and E14 in virulence we made knockout mutants of these genes in *B. squamosa* using CRISPR-Cas9-mediated transformation. According to literature, this is the first report of the use of CRISPR-Cas9 in any *Botrytis* spp. other than *B. cinerea*. The functionality of this technique allows rapid and efficient molecular gene characterization in *B. squamosa* and likely other *Botrytis* species as well. Knockout mutants of P11 and E14 were not reduced in lesion size on onion, suggesting that these genes do not have an essential contribution in virulence. Due to functional redundancy in the effector repertoire, disruption of individual genes does not necessarily lead to a reduction in virulence. For example, *B. cinerea* strains disrupted in cell death inducing proteins Nep1, Nep2, or IEB1 were not affected in virulence (Arenas et al. 2010; Frías et al. 2016). However, since P11 and E14 did not have cell death-inducing activity, were genetically uniform, and did not contribute to virulence, we can exclude them as effectors.

Concluding, we have made a start in the identification and validation of effector proteins of *B. squamosa*. The obtained list with putative effectors provides a resource for future validation of cell death-inducing activity and contribution to virulence. The identification of effectors of *B. squamosa* will provide insights in their role as host determinants and furthermore, the identification of corresponding onion sensitivity genes might have implications for onion resistance breeding against *Botrytis* leaf blight.

Acknowledgements

Authors are thankful to Javier Veloso (University of A Coruña, Spain) for providing plasmid pAJ21 and GFP-expressing *A. tumefaciens*, as well as to Anneke Kroes (Bejo Zaden B.V., The Netherlands) for providing *B. squamosa* isolates. This work was financially supported by the Dutch Technology Foundation STW, which is part of the Netherlands Organisation for Scientific Research (NWO), and which is partly funded by the Ministry of Economic Affairs (Project 15003).

Supplemental tables

Supplemental table 1. List of proteins detected by mass spectrometry in culture filtrate and ion exchange chromatography-based protein fractions. Proteins that are detected specifically in the active cell death-inducing fraction of the cation or anion exchange chromatography are indicated. Columns size and cysteines show, respectively, the total number of amino acids and the number of cysteines of the protein including signal peptide. Secretion signal indicates whether the gene has a predicted secretion signal and PFAM shows the known domains of the detected proteins.

Protein ID	Specific for active fraction cation	Specific for active fraction anion	Size	Cysteines	Secretion signal	PFAM
BSQU_001g00680	No	Yes	714	11	Yes	Multicopper oxidase
BSQU_001g01150	No	Yes	372	6	Yes	Common central domain of tyrosinase
BSQU_001g09360	No	Yes	593	7	Yes	Multicopper oxidase
BSQU_002g06800	No	Yes	540	14	Yes	X8 domain
BSQU_003g00420	No	No	137	4	Yes	Cerato-platanin
BSQU_003g01170	No	No	175	6	Yes	None
BSQU_003g03140	No	No	248	2	Yes	Glycosyl hydrolase family 12
BSQU_003g05350	No	Yes	442	4	Yes	Phosphoesterase family
BSQU_003g05450	No	Yes	607	38	Yes	Polysaccharide deacetylase/ Chitin recognition protein
BSQU_003g05460	No	No	155	4	Yes	None
BSQU_005g00520	No	No	371	9	Yes	Glycosyl hydrolases family 28
BSQU_005g00770	No	No	380	8	Yes	Glycosyl hydrolases family 28
BSQU_005g00780	Yes	Yes	327	3	Yes	Pectinesterase
BSQU_007g02910	No	No	676	10	No	Glycosyl hydrolases family 15/Starch binding domain
BSQU_008g02230	No	Yes	415	1	Yes	Phosphoesterase family
BSQU_008g05540	No	No	189	4	Yes	None
BSQU_011g02090	Yes	No	390	2	Yes	Eukaryotic aspartyl protease
BSQU_012g04570	No	Yes	888	11	No	Pectate lyase superfamily protein
BSQU_013g00020	No	No	591	8	No	Berberine and berberine like/ FAD binding domain
BSQU_013g04240	No	Yes	529	10	No	Histidine phosphatase superfamily (branch 2)
BSQU_014g03460	No	No	450	2	Yes	Glycosyl hydrolases family 17
BSQU_015g00480	No	Yes	456	6	Yes	Glucanosyltransferase
BSQU_015g02090	Yes	Yes	321	2	Yes	Glycosyl hydrolase family 62
BSQU_016g03170	No	Yes	355	3	Yes	None
BSQU_026g00140	No	No	423	13	Yes	None

Supplemental table 2. List of selected candidate effector genes predicted by EffectorP. Column effectorP shows the predicted probability of genes to be effectors, columns size and cysteines show, respectively, the total number of amino acids and the number of cysteines of proteins including signal peptide. Column blast hits shows to which genomes the candidate effector has a blast hit, with subject genomes being all sequenced *Botrytis* spp. and *Sclerotium cepivorum* as described in (Valero-Jiménez et al. 2020).

Protein ID	EffectorP	Size	Cysteines	Blast hits
BSQU_001g03530	1	91	5	Ex. SCEP
BSQU_001g04100	0.527	225	2	Only BELL, BDEW & BSIN
BSQU_001g05780	0.857	228	13	All *Botrytis* spp.
BSQU_001g07210	0.75	82	0	Ex. BCAL, BNAR, BHYA, BPAE & BTUL
BSQU_002g00710	1	89	0	Ex. SCEP & BBYS
BSQU_002g01130	0.847	141	8	All *Botrytis* spp.
BSQU_002g02180	0.981	120	6	Ex. BCAL
BSQU_002g02320	0.895	102	0	All *Botrytis* spp.
BSQU_002g03900	0.966	371	32	All *Botrytis* spp.
BSQU_002g03920	0.504	235	13	All *Botrytis* spp.
BSQU_002g04240	0.977	162	6	Ex. SCEP
BSQU_002g06930	0.996	280	0	Ex. SCEP
BSQU_002g07810	0.853	111	8	All *Botrytis* spp.
BSQU_003g03100	0.997	233	4	All *Botrytis* spp.
BSQU_003g03520	0.996	246	7	Ex. SCEP
BSQU_004g02520	0.71	61	4	All *Botrytis* spp.
BSQU_004g04600	0.792	183	3	All *Botrytis* spp.
BSQU_004g06110	0.981	321	0	Ex. SCEP, BACL
BSQU_005g00320	0.667	377	40	All *Botrytis* spp.
BSQU_005g04110	0.66	143	0	All *Botrytis* spp.
BSQU_006g00280	0.856	128	7	All *Botrytis* spp.
BSQU_006g05020	0.86	164	6	Ex. BCON, BHYA, BTUL, BNAR & BPAE
BSQU_006g06170	0.985	82	8	All *Botrytis* spp.
BSQU_006g06210	0.835	95	10	All *Botrytis* spp.
BSQU_007g03200	1	213	5	Ex. SCEP
BSQU_007g04500	0.831	105	13	All *Botrytis* spp.
BSQU_007g04610	0.643	175	8	All *Botrytis* spp.
BSQU_008g00440	1	148	6	Ex. BSIN
BSQU_008g00850	0.949	184	2	Ex. SCEP
BSQU_008g02380	0.605	87	8	Only BCAL, BCIN, BGAL, BTUL
BSQU_008g02390	0.99	116	4	Only BCIN, BCAL, BGAL
BSQU_008g03270	0.932	220	0	Ex. BCAL, SCEP
BSQU_009g02370	0.854	145	7	Ex. BHYA
BSQU_009g02900	1	170	6	Ex. SCEP, BGAL, BNAR, BPOR & BTUL
BSQU_010g00470	0.671	283	0	Ex. SCEP & BACL
BSQU_010g02260	0.789	170	8	All *Botrytis* spp.
BSQU_011g01650	0.986	97	6	All *Botrytis* spp.
BSQU_011g03360	0.999	201	4	Only BELL, BDEW & BSIN

Protein ID	EffectorP	Size	Cysteines	Blast hits
BSQU_012g00270	1	153	3	All *Botrytis* spp.
BSQU_012g00830	0.982	242	0	All *Botrytis* spp.
BSQU_012g03700	0.715	82	1	Only BDEW, BTUL, BGLO
BSQU_013g02760	0.956	147	4	All *Botrytis* spp.
BSQU_015g02590	0.976	316	6	All *Botrytis* spp.
BSQU_016g00040	0.889	104	8	Ex. SCEP & BNAR
BSQU_017g00230	0.687	247	0	Ex. B0510, BCAL, BGLO & SCEP
BSQU_017g04470	0.995	178	9	All *Botrytis* spp.
BSQU_018g00730	0.991	181	4	All *Botrytis* spp.
BSQU_018g01640	0.992	175	4	Ex. BPOR & BACL
BSQU_018g04130	0.55	252	0	All *Botrytis* spp.
BSQU_020g00110	0.926	152	2	All *Botrytis* spp.
BSQU_021g00930	0.929	165	4	Ex. SCEP
BSQU_025g00170	1	154	8	All *Botrytis* spp.

Supplemental figures

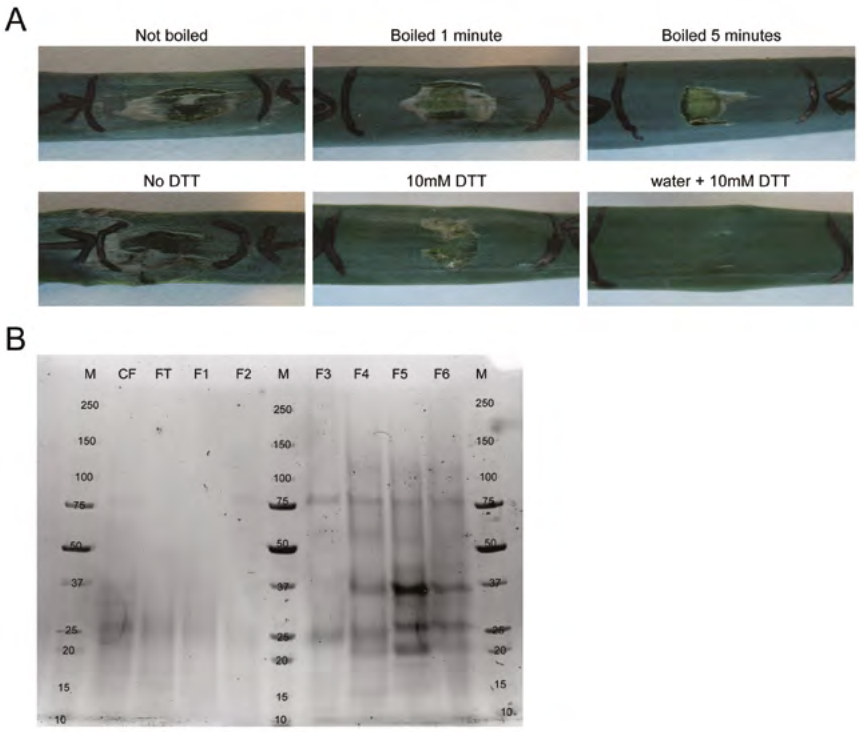

Supplemental figure 1. (**A**) Effects of treatment of *B. squamosa* culture filtrate with heat and with DTT on its cell death-inducing activity upon infiltration in onion. First row: untreated culture filtrate, boiled for 1 minute and boiled for 5 minutes. Second row: untreated culture filtrate, culture filtrate with 10mM DTT, and water with 10mM DTT. (**B**) Protein gel showing different fractions obtained by anion exchange chromatography of the culture filtrate. CF=culture filtrate, FT=flow through of proteins that did not bind to ion exchange column, F=fraction and M=marker.

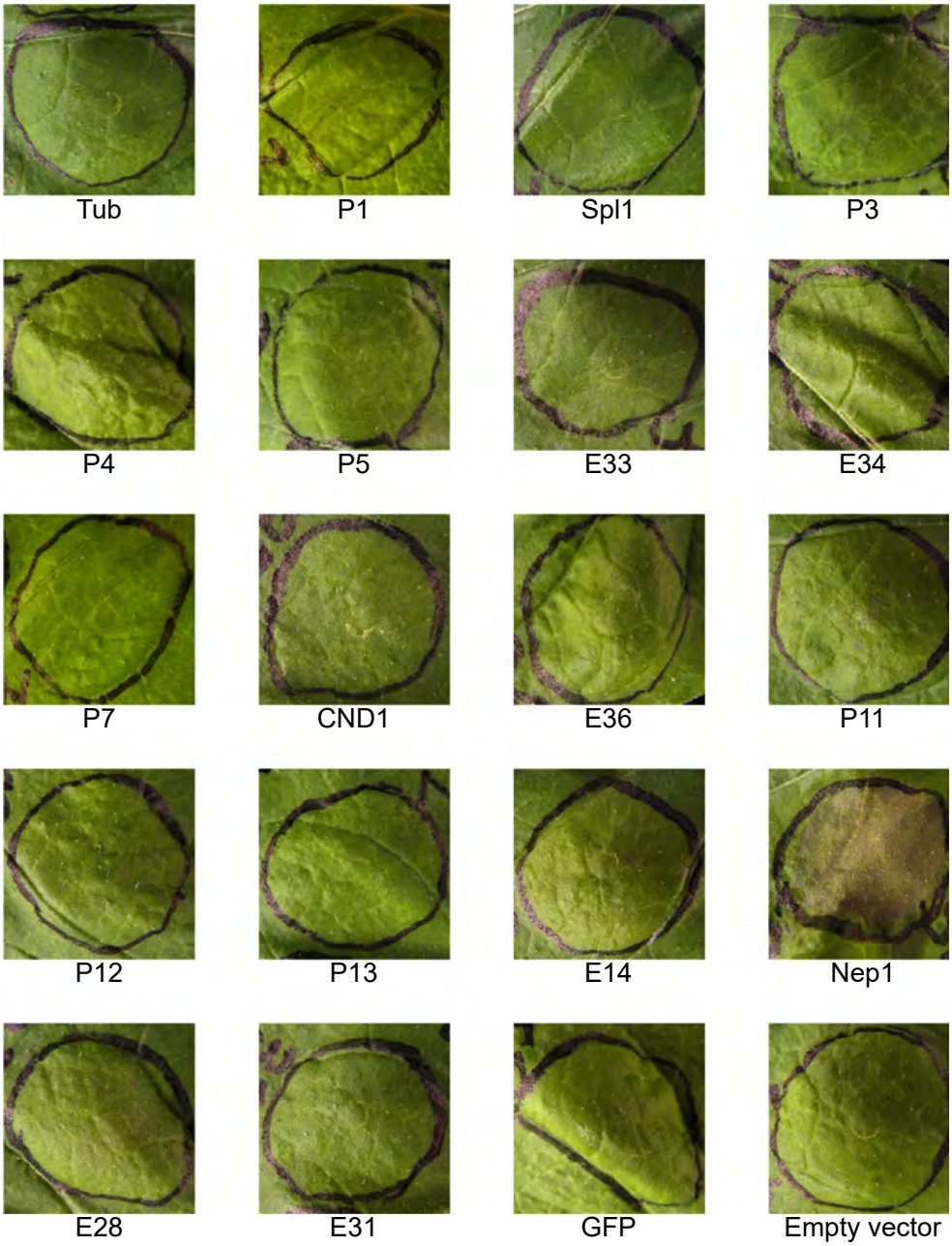

Supplemental figure 2. Plant responses of *N. benthamiana* agroinfiltrated with candidate effectors assessed at 3 DPI. In addition to *B. squamosa* candidate effectors, agroinfiltration of GFP and empty vector were included as extra controls.

Chapter 6

Cytolytic activity of NLPs on the monocot *Allium cepa*

Maikel B. F. Steentjes [1]
Andrea L. Herrera Valderrama [1]
Christiaan Bootsma [1]
Laetitia Fouillen [2]
Delphine Bahammou [2]
Sébastien Mongrand [2]
Olga E. Scholten [3]
Jan A. L. van Kan [1]

[1] Laboratory of Phytopathology, Wageningen University, Wageningen 6708 PB, The Netherlands
[2] Laboratoire de Biogènese Membranaire, UMR 5200, CNRS, University of Bordeaux, Bordeaux, France
[3] Plant Breeding, Wageningen University, Wageningen 6708 PB, The Netherlands

Abstract

Necrosis- and ethylene inducing peptide 1 (Nep1)-like proteins (NLPs) are found throughout several plant-associated microbial taxa and are known to possess cytolytic activity exclusively on dicot plant species. Despite the dicot-specific activity, cytolytic NLPs also are present in pathogens of monocot plants such as the onion pathogen *Botrytis squamosa*. In this study, we assessed *B. squamosa Bs*Nep1, as well as other previously characterized NLPs for their cytolytic activity on various monocot plant species including onion. Leaf infiltration of NLPs showed that onion genotypes are differentially sensitive to NLPs and analysis of their sphingolipid content revealed that the GIPC composition did not correlate to NLP sensitivity. Infiltration of *Bs*Nep1 in the tri-hybrid population CCxRF derived from a cross between onion (*Allium cepa*) and an interspecific F1 hybrid (*Allium roylei* x *Allium fistulosum*) showed that there is variation in NLP sensitivity within the population. QTL mapping revealed a QTL for NLP insensitivity that co-localized with a previously identified QTL for *B. squamosa* resistance. *B. squamosa* knockout mutants in the *BsNep1* gene were not reduced in their virulence on onion leaves. Our results on the cytolytic activity of NLPs on several monocot plant species contravenes the dogma of dicot-specific NLP activity.

Introduction

Microbial plant pathogens are dependent on their host as a source of nutrients that are required for proliferation and reproduction. Pathogens with a necrotrophic lifestyle, as well as hemibiotrophs that initially interact with their host as biotrophs but in a later stage of infection switch to necrotrophy, kill host cells to obtain nutrients and colonize host tissue. The killing of host cells is effectuated by the secretion of toxic molecules, referred to as effectors, that are able to induce host cell death responses. Some of the necrotic effector genes are uniquely present in certain pathogens and have host-specific activity, while other effector genes are widely dispersed over several microbial taxa and are active in a broad range of hosts. One of the most notorious broad host range effectors is necrosis- and ethylene-inducing peptide 1 (Nep1), that was originally identified in culture filtrates of *Fusarium oxysporum* pathogenic on coca plants. Infiltration of Nep1 into leaves of coca, as well as other dicot plant species, resulted in necrosis and ethylene production, which clarifies the etymology of Nep1 (Bailey 1995). Since the discovery of Nep1, Nep1-like proteins (NLPs) have been identified in many plant pathogenic fungi as well as other plant-associated microbes such as bacteria and oomycetes (Seidl and Van den Ackerveken 2019). Not all identified NLPs are able to induce necrosis, though the function of these proteins, classified as noncytolytic NLPs, remains to be discovered (Baxter et al. 2010; Dong et al. 2012; Lenarčič et al. 2019). All functionally characterized cytolytic NLPs however, are able to induce necrosis upon leaf infiltration in dicot plant species, but not in monocots (Gijzen and Nürnberger 2006; Seidl and Van den Ackerveken 2019).

The dicot-specific activity of NLPs was resolved relatively recently by the elucidation of the NLP plant target (Lenarčič et al. 2017). NLPs interact with glycosylinositol phosphorylceramide (GIPC), sphingolipids which are integral plant plasma membrane components. More specifically, NLPs bind to the terminal hexose residues of GIPCs which results in a conformational change that brings a loop with a hydrophobic amino acid residue in close contact with the plasma membrane. It is proposed that the interaction between the plasma membrane and the loop of NLPs results in the formation of a pore with subsequent cytoplasmic leakage, ultimately causing cell death (Lenarčič et al. 2017). In dicot plants, GIPCs possess two terminal hexoses while in monocot plants they contain three hexoses (Cacas et al. 2013). Although NLPs can bind to GIPCs of both dicots and monocots and in both cases undergo conformational change, the third hexose residue of monocot GIPCs was proposed to create a physical distance between the protruded loop and the plasma membrane that prevents their interaction and the subsequent pore formation (Lenarčič et al. 2017).

Apart from its necrotic activity, NLPs play an additional role in plant-pathogen interactions by triggering plant innate immune responses (Qutob et al. 2006). Leucine-rich repeat

receptor protein (LRR-RP) RLP23 was shown to recognize NLPs and trigger immunity in *Arabidopsis thaliana* (Albert et al. 2015). Both cytolytic and noncytolytic NLPs can trigger immunity, and the recognition is thus independent from the necrotic activity (Oome et al. 2014). Moreover, recognition did not require the full length protein, as a conserved fragment of only 20 amino acids found in most NLPs could trigger immunity as well (Böhm et al. 2014). Overexpression of RLP23 in potato conferred enhanced immunity against the NLP secreting pathogens *Phytophthora infestans* and *Sclerotinia sclerotiorum* (Albert et al. 2015).

Although the necrotic activity of NLPs is considered to be exclusively effective on dicots, cytolytic NLPs also occur in the genomes of plant pathogens that are host-specific on monocots. The lily pathogen *Botrytis elliptica* for example has two NLPs that could induce necrosis upon infiltration in dicot plants, but not in the monocot host plant lily (Staats et al. 2007b). The presence of NLPs with dicot-specific cytolytic activity in microbial pathogens of monocot plants has for a long time been enigmatic. In this study, we aimed to analyze the biological activity of NLPs of the onion pathogen *Botrytis squamosa* and elucidate the role of cytolytic NLPs in the interaction between pathogens and monocot plants. *B. squamosa* is the causal agent of onion (*Allium cepa*) leaf blight and is considered to use effector proteins to induce host cell death (Lorbeer et al. 2007; Steentjes et al. 2021a). Here, we report cytolytic activity of NLPs on several monocot plant species, and demonstrate that onion genotypes show differential sensitivity to NLPs. Furthermore, we were able to map a QTL for NLP insensitivity in an interspecific *Allium* hybrid population.

Material and methods

Fungal strains, culture conditions and transformation procedure

B. squamosa isolate MUCL31421 was used to inoculate onion leaves for RNA isolation and sequencing, and as recipient strain for transformation. Spores of *B. squamosa* were obtained by growth on autoclaved onion leaves on top of water agar and exposure to UV light as described in Steentjes et al. (2021b). For long term storage spores were kept in 15% glycerol at -80°C. To obtain *B. squamosa BsNep1* knockout mutants, we used the CRISPR-Cas9-mediated protoplast transformation protocol optimized for *B. cinerea* as described by Leisen et al. (2020). Protoplasting conditions were optimized for *B. squamosa* by using $5x10^6$ spores to inoculate the liquid culture and allow growth for 24 hours. Mutants were selected using an initial concentration of 17.5 µg/ml hygromycin B. Knockout mutants were confirmed by PCR and sequencing of the gene fragment and obtained mutants were tested for their *in vitro* growth rate and ability to produce sclerotia and conidia.

Plant material and NLP infiltration

Plant material used for NLP infiltration was as following: *N. benthamiana* (WT), *A. thaliana* (Col-0), Maize (Golden Bantam), Wheat (Tadinia), Leek (Toledo), Lily (Asiatic), Onion (*Allium cepa* genotype 1-8). Plant material from the *Allium* interspecific hybrid population (*A. cepa* x (*A. roylei* x *A. fistulosum*)) was selected as described in Scholten et al. (2016). The population as well as the parental genotypes were maintained in tissue culture and plants of all genotypes were transferred to the greenhouse, transplanted in potting soil and grown for several weeks before infiltration. Plants were infiltrated using a syringe on the abaxial side of their leaves (where possible) with one of the four NLP proteins *Bs*NLP, *Bc*NLP, *Pya*NLP, *Pp*NLP or with buffer. NLP proteins were dissolved in 10mM KPO_4 buffer with a pH of 6.0. The final concentration of NLP proteins infiltrated in assays depicted in figure 2 is 1 µM, while for assays depicted in figures 4, 5 and supplemental figures 3 and 5 the final concentration was 0.5 µM. Plant responses were assessed at 3 DPI, either by evaluation of symptoms or by measuring cell death intensity as described in Villanueva et al. (2021).

Onion leaf infection assays and RNA isolation for expression analysis

For inoculation of *B. squamosa*, young but fully grown leaves of 2-4 month onion plants were used. For testing the virulence of *BsNep1* knockout mutants, onion genotype 'Centurion' was used for infection assay 1, 3 and 4, and for infection assay 2 onion genotype '2012-19' was used. For expression analysis onion genotype DH was used. Detached leaves

were placed in humid boxes and the cuticle of leaves was gently wiped with tissue paper to facilitate inoculation. Leaves were inoculated with 2 µl droplets *B. squamosa* spores at 10^6 spores/mL in 12 g/L PDB. To assess the virulence, lesion sizes were measured at three consecutive days and the area under the diseases progression curve was calculated for inoculations with a secondary lesion growth. For RNA isolation, 16, 24 and 48 hour after inoculation plant tissue was sampled in three replicates and also the used inoculum at 0 hours was sampled. Samples were frozen in liquid nitrogen, freeze dried and grinded to powder. For RNA extraction, samples were incubated in Trizol (Ambion, Life Technologies) and treated with chloroform. Ethanol was added to the aqueous phase and the mixture was used as input for an RNeasy Plant Mini Kit (Qiagen). This RNA was sent for sequencing. Reads were mapped to the annotated genome of *B. squamosa* (Valero-Jiménez et al. 2020).

Production and purification of *Bs*Nep1

The mature protein coding sequence of *Bs*Nep1 was amplified from cDNA and cloned into the vector pPIC9k (Invitrogen) via restriction enzymes EcoRI and NotI. After confirmation of the insert by PCR and sequencing, the plasmid was transformed into *Pichia pastoris* strain GS115 by electroporation. Fermentation was performed on a large scale using a BioFlo 120 fermentor (Eppendorf) applying the fermentation protocol described in Schouten et al. (2008). Briefly, approximately 3 L of P. pastoris culture was grown at 30°C for 5 days. After 5 days the supernatant was separated by centrifugation and concentrated to 200 mL via diafiltration using a VivaFlow 200 Cassette MWCO 5000 Dalton (Sartorius, VF20P4). This concentrated supernatant was desalted and washed twice with 10 mM potassium phosphate pH 7.0, and filter-sterilized.

Protein purification was performed by affinity chromatography using Streamline SP XL (GE Healthcare) at pH 7.0 as described in Schouten et al. (2008). Briefly, 5 mL of resin SP was equilibrated with 3 volumes of 10 mm KPi, pH 7.0 in a glass Econo-column (Biorad 7371012), and transferred to a 50 mL tube containing 40 mL of concentrated crude protein sample. Proteins were allowed to bind by agitation on a horizontal rotor at 4°C for 90 min, and the glass column was filled again with the protein bound-resin. The resin was rinsed by flushing the column 2 times with two column volumes 10 mm KPi, pH 7.0, and the bound proteins were recovered by eluting with an increasing salt concentration between 0.1M and 0.3M NaCl in 10mM Kpi. The eluted fractions were pooled, desalted, and concentrated using Amicon Ultra-15 PLBC filters. *Bs*Nep1 concentrations were quantified using Bradford assays (Biorad). Purified protein was analyzed by polyacrylamide gel electrophoresis.

GIPC composition analysis

Young but fully grown leaves of onion genotypes 3-7 were used to analyse GIPC composition. GIPC extraction and determination of terminal hexoses using mass spectrometry was performed as described in Lenarčič et al. (2017). GIPC ratios are an average of three independent measurements.

Protein sequence alignment and structure modelling

Mature protein sequences of *Bs*Nep1, *Bs*Nep2, *Bc*Nep1, *BcNep2* and *Pya*NLP were used as input for a clustal W alignment and visualized using ESPript (Robert and Gouet 2014). The tertiary structure of *Bs*Nep1 was predicted by Raptor X (Källberg et al. 2012). The 3GNZ protein model of *Pya*NLP was used as structure template for the prediction. Both models were compared using 3D-Match (Softberry) and visualized using Cn3D (Wang et al. 2000).

Reactive oxygen species measurements

Leaves of 4-6 week old *A. thaliana* Col-0 and ΔRLP23 (Albert et al. 2015) were used to perform ROS measurements. Leaf disks were obtained using a disposable biopsy punch and were placed on water in a 96-well plate and were incubated overnight. After the water was removed, disks were treated with 50 µl assay solution containing 10 µg/ml horseradish peroxidase (Sigma) and 50 µM luminol L-012 (Fujifilm). Immunity responses were triggered by the synthesized peptides nlp20 (1 µM) as described in Böhm et al. (2014), nlp27 (1 µM) from *Bs*Nep1 and *Bc*Nep1 (GIMYAWYFPKDQPAAGNVVGGHRHDWE), or with flg22 (0.1 µM) as a positive control or water as a negative control. Luminescence was measured by a microplate reader for 4 hours.

Statistical analysis

Statistical analysis of cell death intensity quantified by red light emission, as well as alteration in virulence of *BsNep1* knockout mutants was performed in SPSS Statistics 25.0 (IBM). To assess cell death intensities, a one-way ANOVA with Tukey Post Hoc analysis for multiple comparisons was performed per NLP. To test the significance of the differences between the two independent *BsNep1* knockout mutants and WT, independent samples *t*-tests were performed. Differences were considered to be statistically significant with two-tailed P values <0.05. QTL mapping for NLP insensitivity was performed in MapQTL® 6 using interval mapping and mean values of red light emission per genotype as input, and the QTL was visualized on chromosome 6 using MapChart (Voorrips 2002).

Results

Botrytis squamosa contains two NLP genes that are expressed during onion leaf infection.

All species in the genus *Botrytis* are reported to possess two NLP genes (Staats et al. 2007c). In the genome of *B. squamosa* (Valero-Jiménez et al. 2020), genes BSQU_015g03410 and BSQU_002g07590 encode orthologs of previously characterized proteins Nep1 and Nep2 from *B. cinerea* (Arenas et al. 2010). The protein sequences of Nep1 and Nep2 display respectively 95% and 91% amino acid identity between *B. squamosa* and *B. cinerea* (Supplemental figure 1).

Analysis of RNA-sequencing data from *B. squamosa*-infected onion leaves indicated that both genes are expressed during infection at different levels and with different temporal dynamics. *BsNep1* transcript levels gradually increased from the moment of inoculation until 24 hours post inoculation (HPI), and declined at 48 HPI. The *BsNep*2 transcript levels slightly increased at 16 HPI and then remained steady over the course of the experiment, but were always at lower levels than the *BsNep*1 transcript (Figure 1).

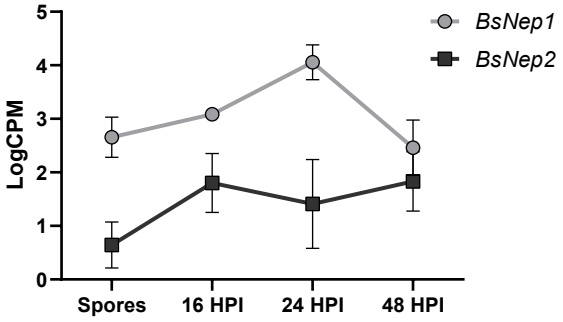

Figure 1. Expression levels of *B. squamosa BsNep1* and Bs*Nep2* genes (in counts per million) in spores and during the infection of onion leaves at 16, 24 and 48 HPI. Values represent the average of three biological replicates, with error bars representing standard deviation.

*Bs*Nep1 induces necrosis in a subset of monocot plant species and onion genotypes are differentially sensitive

We cloned the mature protein coding sequence of *BsNep1* in vector pPIC9k and produced the *Bs*Nep1 protein using the heterologous expression system *Pichia pastoris*. Ion-exchange chromatography-based purification yielded a protein of ~25kDa (Supplemental figure 2). To evaluate its cytolytic activity, *Bs*Nep1 was infiltrated into leaves of the dicot plants *Arabidopsis thaliana* and *Nicotiana benthamiana* which induced clear necrotic

responses. Infiltration in leaves of the monocot plants onion, maize and lily, however, also resulted in necrotic leaf tissue, while leek and wheat did not show cell death response upon infiltration of *Bs*Nep1, indicating a differential response to *Bs*Nep1 between monocots (Figure 2A).

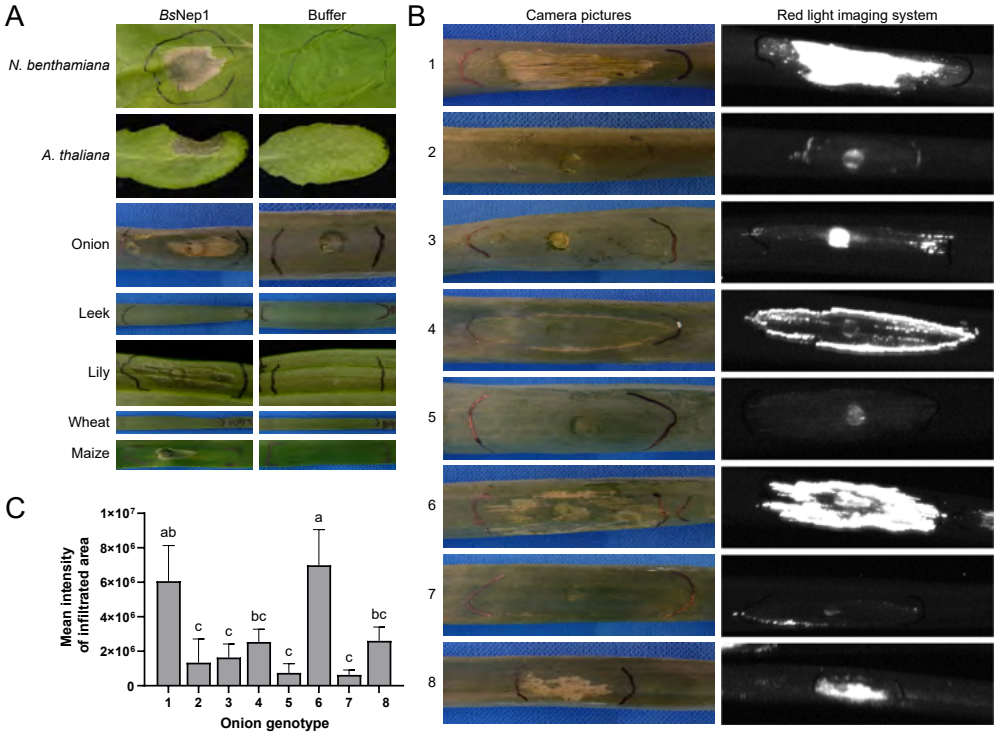

Figure 2. Plant responses upon infiltration of *Bs*Nep1. (**A**) Infiltration of *Bs*Nep1 and buffer into the dicot plants *N. benthamiana* and *A. thaliana* and the monocots onion, leek, lily, wheat and maize. Displayed infiltrated areas are a representative of three replicate infiltrations that yielded similar plant responses and were assessed at 3 DPI. (**B**) Cell death response of 8 onion cultivars upon infiltration of *Bs*Nep1. Left column shows symptoms as seen by eye and right column shows the cell death intensity as observed by red light imaging. Displayed infiltrated areas and red light images are a representative of three replicate infiltrations and were assessed at 3 DPI. (**C**) Quantification of cell death intensity of eight onion genotypes infiltrated with *Bs*Nep1 as measured by red light imaging at 3 DPI. Values are averages of three replicates and error bars represent standard deviation with significant differences being indicated by different letters (Tukey Post Hoc analysis).

Because of the unexpected necrotic activity of *Bs*Nep1 on onion and other monocots, we verified the *Bs*Nep1 activity on monocots by infiltrating a set of eight onion genotypes. A variation in response was observed between the genotypes ranging from strong necrosis in genotypes 1 and 6 to almost no visible symptoms in genotypes 5 and 7 (Figure 2B). In order to objectively quantify the plant responses, we used a red light imaging system that allows quantification of cell death intensity of the infiltrated area (Villanueva et al.

2021). Cell death signal intensities correlated to visual scoring of necrosis (Figure 2B). Quantification of the red light emission yielded significant differences between onion genotypes that corresponded to the severity of visible symptoms (Figure 2C).

Structural modeling of *Bs*Nep1

The unprecedented observation of NLP activity on monocots by *Bs*Nep1 evokes the hypothesis that *Bs*Nep1 functions in a different manner than previously characterized NLPs. Comparison of the protein structures of *Bs*Nep1 and the well-characterized NLP of *Pythium aphanidermatum* (*Pya*NLP), of which the protein structure was dissolved by crystallography (Ottmann et al. 2009), may provide insight in the mechanisms underpinning the cytolytic activity of *Bs*Nep1 on monocot plants. Aligning the amino acid sequences of *Bs*Nep1 and *Pya*NLP yielded a sequence identity of 43% (Supplemental figure 1). The protein structure of *Bs*Nep1 was predicted using *Pya*NLP as a template. The modelled structure of *Bs*Nep1 very much resembled the structure of *Pya*NLP and contained identical loops and sheets (Figure 3). One substantial difference between the two protein structures is the elongation of loop 2 (L2) in *Bs*Nep1, which is a consequence of the insertion of three hydrophobic amino acids. Loop 3 (L3) is considered to be required for the interaction of NLPs with the plasma membrane and the subsequent insertion and pore formation. It could be hypothesized that the elongated L2 of *Bs*Nep1 may be able to take over or accompany the function of L3 and bridge the physical distance between the NLP and the plasma membrane when bound to monocot GIPCs, and therefore effectuate cytolytic activity on monocot plants.

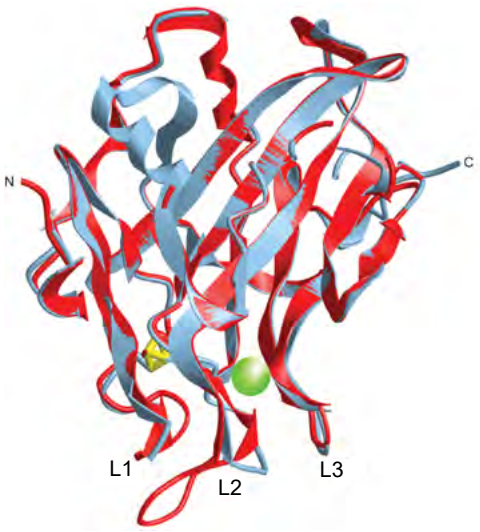

Figure 3. Predicted protein structure of *Bs*Nep1 (red) using *Pya*NLP (gray) as a template. Loops 1-3 are marked at the lower part of the structures as L1, L2, and L3 and disulfide bonds are represented as yellow triangles. The proposed GIPC binding site is indicated by a green sphere.

Necrotic activity of NLPs on monocots is not specific for *Bs*Nep1 and variation in sensitivity cannot be explained by GIPC composition

To assess whether the predicted differences in protein structure between *Bs*Nep1 and *Pya*NLP lead to differential activity, we compared the necrotic effect of *Bs*Nep1 with the well-characterized NLPs from *B. cinerea* (*Bc*Nep1), *Phytophthora parasitica* (*Pp*NLP) and PyaNLP in a set of monocot plant species. Surprisingly, all tested NLPs induced necrosis upon infiltration in onion (Figure 4A). Moreover, in all monocot plant species in which *Bs*Nep1 induced necrosis (onion, maize and lily), also all other NLPs were active, suggesting no difference in activity between *Bs*Nep1 and other NLPs (Supplemental figure 3). Also the ability of *Bs*Nep1 to trigger immunity by RLP23-mediated recognition in *A. thaliana* was similar to other NLPs. Both the nlp20 peptide (derived from *Pya*NLP) and a corresponding *Bs*Nep1 peptide fragment of 27 amino acids (nlp27) were equally able to induce a ROS-burst in *A. thaliana* WT but not in RLP23-defective mutant lines (Supplemental figure 4).

In addition to testing the necrotic activity of the four NLPs in monocot plants, we also infiltrated the proteins in a set of onion genotypes (3-7) that showed variation in response to *Bs*Nep1 infiltration before (Supplemental figure 5). Quantification of the cell death intensity by red light imaging yielded differences in NLP sensitivity between onion genotypes (Figure 4B). The differences in plant response had the same trend as observed upon infiltration of *Bs*Nep1, with genotype 6 being relatively sensitive and genotype 5 and 7 being relatively insensitive. Although there was variation in cell death intensity upon infiltration of different NLPs in the same onion genotype, the differences in NLP sensitivity between genotypes were seemingly independent of which of the four NLPs was infiltrated.

To examine a correlation between the variation in NLP sensitivity and the membrane sphingolipid composition, we assessed the GIPC composition of the different onion genotypes. The heretofore assumed dicot-specific activity of NLPs was considered to rely on a difference in the ratio of terminal hexose residues of GIPCs between monocots and dicots. Dicots were shown to contain predominantly GIPCs with two hexose residues (Series A) and monocots purportedly had a majority of GIPCs with three hexoses (Series B), that structurally prevent NLPs from exerting their cytolytic activity (Lenarčič et al. 2017). GIPCs were extracted from leaf material of onion genotypes 3-7 and the ratio series A : series B GIPCs was determined using liquid chromatography-mass spectrometry. All five analyzed onion genotypes showed a similar GIPC composition with a series A content varying between 50 and 62% (Figure 4C). There was no correlation between GIPC ratios of the five onion genotypes and their sensitivity to NLPs.

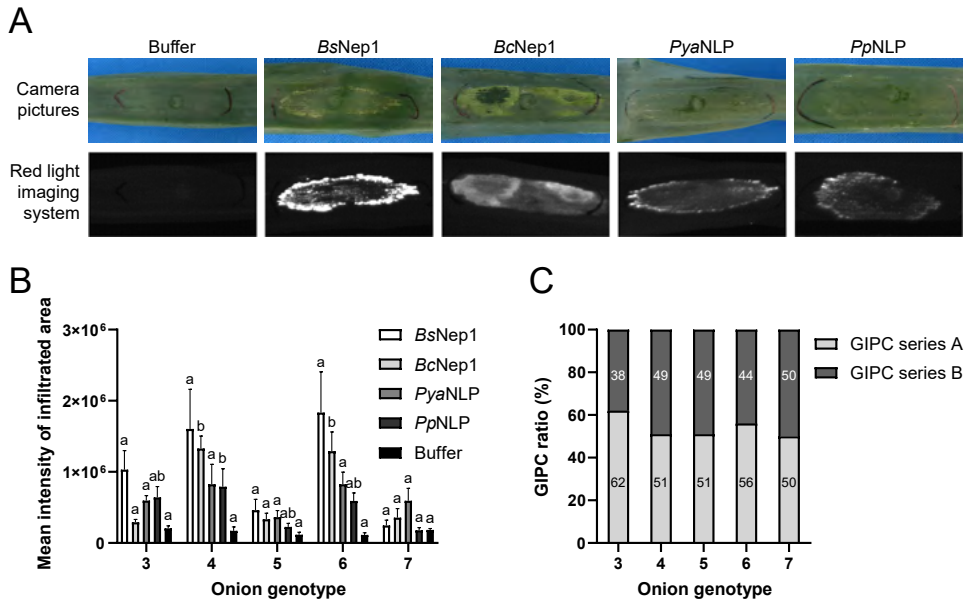

Figure 4. Cell death responses of onion genotypes upon infiltration with NLPs and their GIPC composition. (**A**) Cell death response of onion genotype 6 upon infiltration of buffer and the four different NLPs *Bs*Nep1, *Bc*Nep1, *Pya*NLP and *Pp*NLP. Upper row shows symptoms as seen by eye and lower row shows the cell death intensity as observed by the red light imaging system. Displayed infiltrated areas and red light images are a representative of six replicate infiltrations and were assessed at 3 DPI. (**B**) Quantification of cell death intensity of five onion genotypes (3-7) infiltrated with buffer and four different NLPs as measured by red light imaging at 3 DPI. Values are averages of six replicates and error bars represent standard error. Different letters per NLP indicate significant differences (Tukey Post Hoc analysis). (**C**) GIPC quantification of onion genotypes with Series A representing two hexose moieties (Hex(R1)-HexA-IPC), and Series B representing three hexose moieties (Hex-Hex(R1)-HexA-IPC). Ratios are averages of three technical replicates.

6

*Bs*Nep1 sensitivity segregates as quantitative trait in an interspecific *Allium* hybrid population

In view of the observed variation in sensitivity to *Bs*Nep1 between onion genotypes that are known to be susceptible to *B. squamosa*, we decided to test the sensitivity to *Bs*Nep1 in the tri-hybrid population CCxRF that was derived from a cross between onion (*Allium cepa*) and an interspecific F1 hybrid (*Allium roylei* x *Allium fistulosum*). The CCxRF population segregates for resistance to *B. squamosa* with a QTL on Chromosome 6 from *A. roylei* (Scholten et al. 2016). *Bs*Nep1 was infiltrated into leaves of 140 individual genotypes of the CCxRF population, as well as into the parental species *A. cepa, A. roylei, A. fistulosum*, and the hybrid plant *A. roylei* x *A. fistulosum* in three replicates. The response to the protein was quantified using the red light imaging system. Responses to *Bs*Nep1 infiltration varied between progeny lines of the population as well as between the parental genotypes with

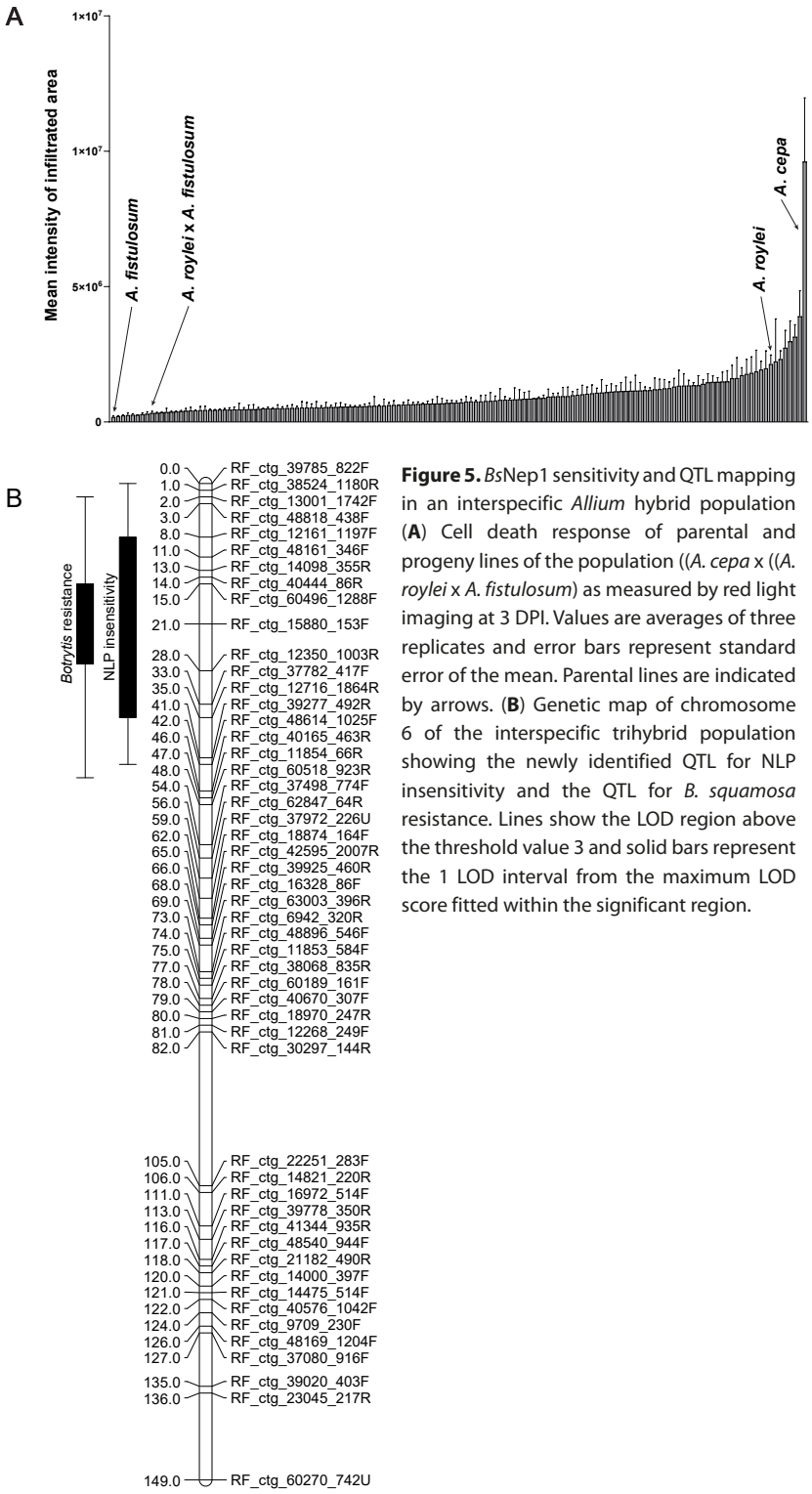

Figure 5. *Bs*Nep1 sensitivity and QTL mapping in an interspecific *Allium* hybrid population (**A**) Cell death response of parental and progeny lines of the population ((*A. cepa* x ((*A. roylei* x *A. fistulosum*) as measured by red light imaging at 3 DPI. Values are averages of three replicates and error bars represent standard error of the mean. Parental lines are indicated by arrows. (**B**) Genetic map of chromosome 6 of the interspecific trihybrid population showing the newly identified QTL for NLP insensitivity and the QTL for *B. squamosa* resistance. Lines show the LOD region above the threshold value 3 and solid bars represent the 1 LOD interval from the maximum LOD score fitted within the significant region.

the most intensive cell death observed for *A. cepa* and *A. roylei* and the least for *A. fistulosum* (Figure 5A). The mean values of red light emission per genotype were used for QTL mapping. A QTL region originating from *A. fistulosum* was identified on Chromosome 6. This region fully co-localized with the QTL region earlier discovered for resistance to *B. squamosa* from *A. roylei* (Figure 5B).

*Bs*Nep1 does not contribute to virulence of *B. squamosa* on onion leaves

In view of the cytolytic activity of *Bs*Nep1 in onion leaves and the observation of cell death and tissue collapse during *B. squamosa* infection, we studied the contribution of *Bs*Nep1 to the induction of disease symptoms and the virulence of the fungus. *BsNep1* knockout mutants were generated using the CRISPR-Cas9 protocol developed for *B. cinerea* (Leisen et al. 2020). Two homokaryotic mutants with the desired gene deletion were assessed for their virulence on onion leaves, in four separate infection assays. A small, statistically significant difference in area under the disease progression curve (AUDPC) was observed between Δ*BsNep1*-1 and the wild type only in infection assay 2 (Figure 7). In the other three assays, the virulence of Δ*BsNep1*-1 was not reduced as compared to WT. Also another, independent mutant, Δ*BsNep1*-2, did not show a difference in AUDPC compared to WT, suggesting that *BsNep1* does not play a role in the virulence of *B. squamosa* on onion leaves.

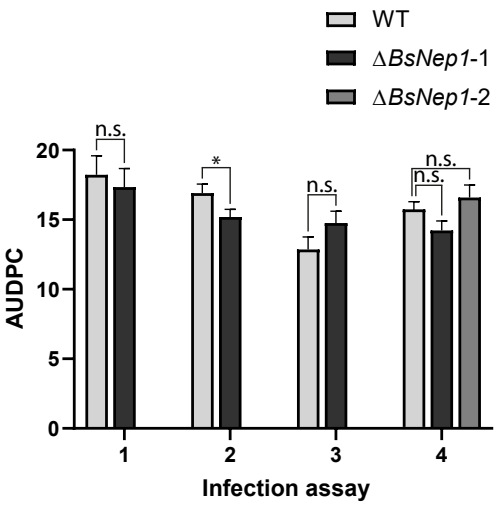

Figure 6. Virulence of *B. squamosa* WT and two independent *BsNep1* knockout mutants measured as AUDPC. Error bars represent standard error with n=82, n=79, n=80 and n=155 in order of infection assay. Differences that are statistically significant are indicated with an asterisk while differences that are not statistically significant are indicated by n.s. (independent samples *t*-test).

Discussion

Since the first discovery of a necrosis- and ethylene-inducing peptide 1 (Nep1) in 1995, many Nep1-like proteins (NLPs) have been described in fungi, bacteria and oomycetes. To date, all functionally characterized cytolytic NLPs were reported to have an extremely broad host activity that is solely delimited to dicot plant species (Bailey 1995; Seidl and Van den Ackerveken 2019). One exception to this discrepancy is the ornamental plant species *Phalaenopsis amabilis*, a member of the monocot family Orchidaceae, that was shown to be sensitive to *Pya*NLP (Lenarčič et al. 2017). In this study, we show cytolytic activity on a diverse set of monocot plant species for NLPs that were previously reported to be dicot-specific. It remains elusive why the dogmatic discrepancy in host range of NLP activity has been sustained for over 25 years. Studies that involve plant-microbe interaction on monocots often focus on crop species such as rice and wheat, of which the latter was indeed found to be insensitive to NLPs in our study. By contrast, the related *Poaceae* crop species maize did develop necrosis upon NLP infiltration. Studies on the lily pathogen *Botrytis elliptica*, a close relative of *B. squamosa*, showed that NLPs of that species were not able to induce necrosis in lily (Staats et al. 2007b), whereas we did observe lilies to be sensitive to NLPs. Possibly, the use of different hybrid types of lily underlies the contrasting observations, similar to the differences in NLP sensitivity between different onion genotypes.

We showed that onion genotypes varied in their sensitivity to NLPs, independent of which of the four tested NLPs was infiltrated. GIPC composition analysis of the same set of onion genotypes revealed that all roughly had a similar content of series A : series B GIPCs of approximately 50%. The GIPC composition thus could not explain the observed differences in NLP sensitivity. Possibly, differences in tissue structure or leaf morphology such as leaf thickness may underly the observed variation in sensitivity between genotypes. To test whether the observed variation in NLP sensitivity depends on differences in tissue structure, or whether it is a characteristic of the membrane composition, sensitivity to NLPs can be assessed on onion protoplasts or plasma membrane vesicles (Ottmann et al. 2009).

In addition to different onion genotypes, also an interspecific *Allium* hybrid population (*A. cepa* x (*A. roylei* x *A. fistulosum*) showed variation in sensitivity upon infiltration of *Bs*Nep1. We identified a QTL for NLP insensitivity that co-localized with a previously identified QTL for *B. squamosa* resistance (Scholten et al. 2016). It would be interesting to examine whether the identified QTL for NLP insensitivity can be correlated to the GIPC composition of the parental lines and progeny. Remarkably, a closely related crop species of onion, leek (*A. porrum*) was insensitive to NLPs and was previously reported to contain predominantly series B GIPCs (Cacas et al. 2013; Lenarčič et al. 2017), suggesting that there can be

variation in GIPC composition even between species of the same genus. Whether or not the differences in NLP sensitivity between the parental *Allium* species of the population are based on GIPC content and whether the identified QTL for NLP insensitivity is based on genetic diversity in the regulatory or biosynthetic genes for GIPCs remains to be determined. Alternatively, the cytolytic activity of NLPs on monocots might require the involvement of receptor proteins or secondary target molecules, which could determine the differences in NLP sensitivity observed between onion genotypes with similar GIPC compositions.

The QTL for NLP insensitivity present in *A. fistulosum* explained approximately 16% of the phenotypic variation and co-localized with the previously identified QTL for *B. squamosa* leaf blight resistance present in *A. roylei* that explained 27-54% of the phenotypic variation in the same population (Scholten et al. 2016). The observation that both a disease resistance allele and a NLP insensitivity allele might originate from the same chromosomal location of one parental (interspecific hybrid) plant line is enigmatic. As the QTLs cover over 40 cM on the chromosome it is clear that a wide region is involved that contains many genes. Therefore, it is conceivable that the NLP insensitivity and leaf blight resistance are separate traits that happen to be localized in a similar genomic region. So far, we did not obtain any evidence that *Bs*Nep1 contributes to virulence of *B. squamosa*. Knockout mutants of *Bs*Nep1 were not consistently affected in lesion size as compared to WT when tested in onion plants. In order to further clarify the correlation between NLP sensitivity and susceptibility to *B. squamosa*, we could inoculate several onion genotypes that differ in sensitivity to NLPs and monitor disease development. If *Bs*Nep1 indeed contributes to virulence of the fungus, NLP-sensitive plant lines would be predicted to be more susceptible than NLP-insensitive plant lines to *B. squamosa* wild type, but equally susceptible to the *BsNep1* mutant strain. Earlier studies on NLPs of *B. cinerea* and *B. elliptica* showed that knockout mutants in either Nep1 or Nep2 did not display reduced virulence (Arenas et al. 2010; Staats et al. 2007b). The absence of one NLP gene in single knockout mutants could potentially be compensated by the other gene, and double knockout mutants in both NLP genes are required to assess the contribution of cytolytic NLP activity to virulence of *Botrytis* species.

Altogether, we show the functionality of cytolytic NLPs on monocot plant species and legitimize the presence of cytolytic NLPs in monocot-specific pathogens. The identification of a QTL for NLP insensitivity might help to track the genes involved in this trait and enable to further elucidate the functionality of NLPs in plant-microbe interactions.

Acknowledgements

We thank Isabel Albert and Thorsten Nurnberger (University of Tübingen, Germany) for kindly providing *PyaNLP* and *Pp*NLP and Sander Schouten (Wageningen University, The Netherlands) for providing *Bc*Nep1. Authors are thankful to Guido van den Ackerveken (Utrecht University, The Netherlands) for sharing mutant RLP23 *A. thaliana* seed and thank Thomas Leisen and Matthias Hahn (University of Kaiserslautern, Germany) for their assistance in optimizing CRISPR-Cas9-mediated transformation protocols for *B. squamosa*. Furthermore, authors are grateful to Karin Burger-Meijer (Wageningen Plant Research, Plant Breeding) for excellent plant care of the *Allium* hybrid population. This work was financially supported by the Dutch Technology Foundation STW, which is part of the Netherlands Organisation for Scientific Research (NWO), and which is partly funded by the Ministry of Economic Affairs (Project 15003).

Supplemental figures

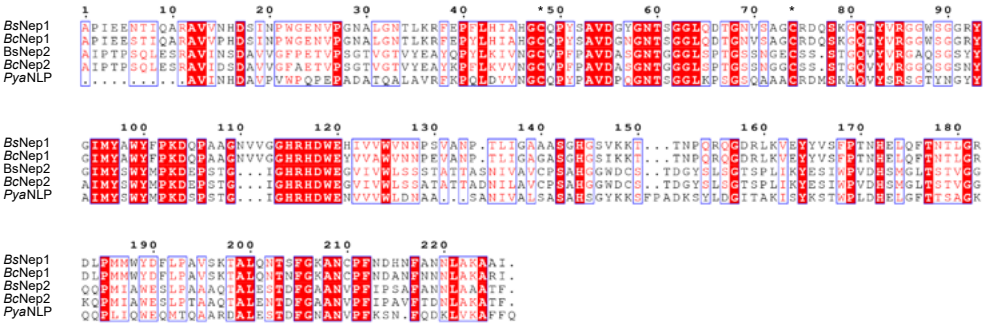

Supplemental figure 1. Amino acid alignment of mature Proteins *Bs*Nep1, *Bs*Nep2, *Bc*Nep1, *Bc*Nep2 and *Pya*NLP. Amino acids highlighted in red indicate 100% identity between all proteins and blue squares indicate conservative replacement. Conserved cysteines are marked with asterisks.

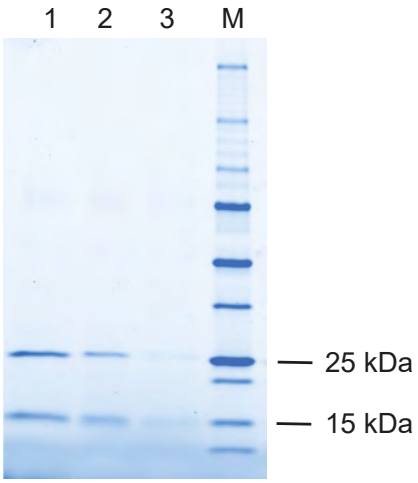

Supplemental figure 2. Protein gel of ion exchange chromatography-based purification of *P. pastoris* produced *Bs*Nep1. Lanes 1-3 contain eluents with purified BsNep1 protein with a size of ~25 kDa. A second protein that could not be eliminated in the purification is observed at ~15 kDa (M=marker).

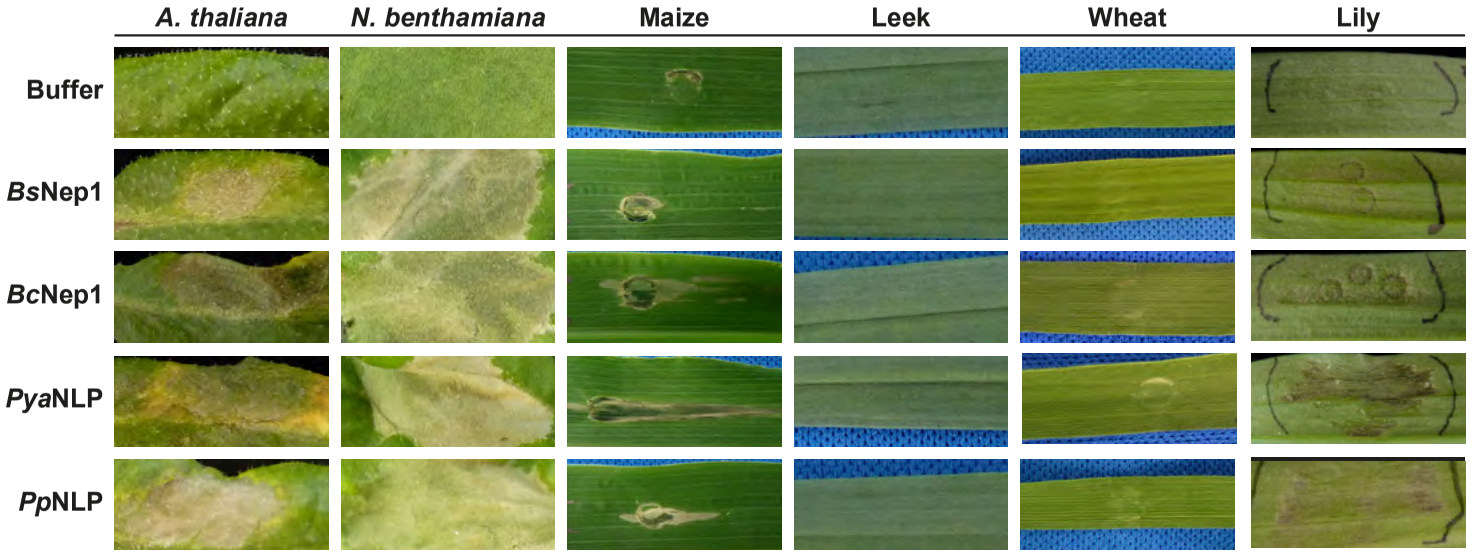

Supplemental figure 3. Infiltration of buffer and the four different NLPs *Bs*Nep1, *Bc*Nep1, *Pya*NLP and *Pp*NLP into the dicot plants *N. benthamiana* and *A. thaliana* and the monocots maize, leek, wheat and lily. Displayed infiltrated areas are a representative of three replicate infiltrations that yielded similar plant responses and were assessed at 3 DPI.

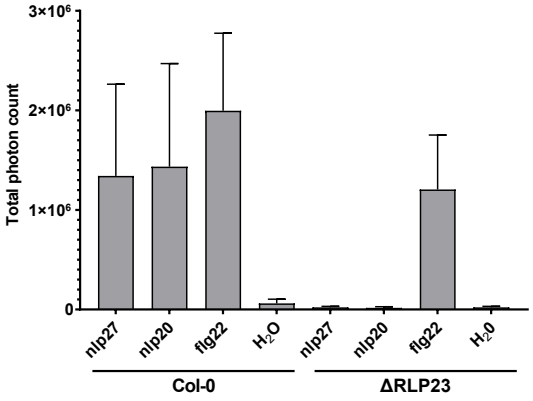

Supplemental figure 4. Reactive oxygen species burst triggered by nlp20 (*PyaNLP*), nlp27 (*Bs*Nep1), flg22 as a positive control, or water as negative control in *A. thaliana* Col-0 and rlp-23 defective mutant lines. Values are averages of measurements for 12 leaf disks per sample and error bars represent standard deviation.

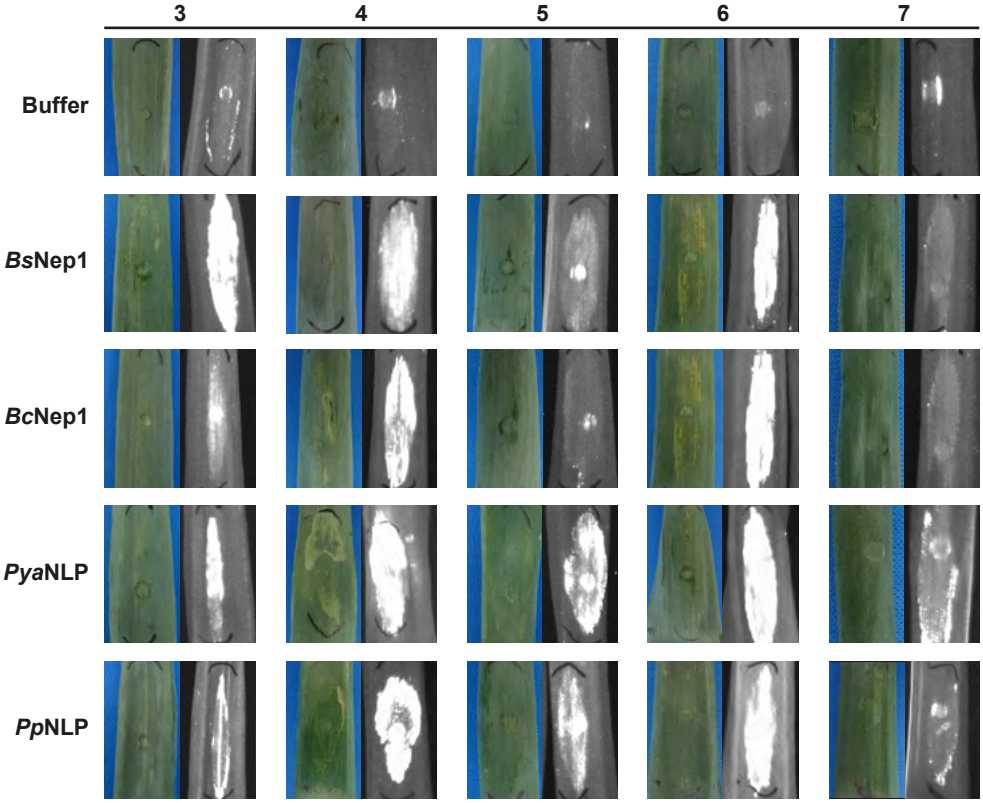

Supplemental figure 5. Cell death response of onion genotypes 3-7 upon infiltration of buffer and the four different NLPs *Bs*Nep1, *Bc*Nep1, *Pya*NLP and *Pp*NLP. Pictures on the left side shows symptoms as seen by eye and on the right side cell death intensity as observed by the red light imaging system. Displayed infiltrated areas and red light images are a representative of six replicate infiltrations and were assessed at 3 DPI.

Chapter 7

General discussion

Introduction

Onion is an important vegetable crop that is cultivated for its edible bulbs. The vast diversity of onion cultivars and varieties allows worldwide cultivation. Some varieties are processed and consumed directly after harvest while others are well suited for storage, making onion available year-round.

Botrytis leaf blight, neck rot, and white rot are three diseases that pose a major threat to onion cultivation. *Botrytis* leaf blight is a foliar disease caused by the fungus *Botrytis squamosa*. After air-borne spores land on the surface of an onion leaf, the fungus penetrates and colonizes tissue resulting in necrotic spots and later blighting of the leaf. Eventually new spores are produced on necrotic leaf tissue (Carisse et al. 2011; Lorbeer et al. 2007). *Botrytis* neck rot is a postharvest disease that occurs in stored onions without displaying symptoms during the growing season (Lacy and Lorbeer 2008b). In total three *Botrytis* species are associated with neck rot; *B. aclada*, *B. allii*, and *B. byssoidea* (Chilvers and du Toit 2006). White rot is a soil-borne disease of onion caused by *Sclerotium cepivorum*. This fungus infects the plant via its roots and grows towards bulbs that become covered in white mycelium. *S. cepivorum* forms sclerotia that can stay dormant in the soil for many years until a host plant grows nearby after which the sclerotium germinates and starts the new infection cycle (Crowe 2008; Sammour et al. 2011).

In an attempt to gain a better understanding of the interaction between these fungal pathogens and their host plant onion, we aimed to identify the mechanisms of virulence of these pathogens. In this thesis we studied a variety of aspects of the plant-pathogen interaction, including infection biology, detoxification of an antifungal onion metabolite, genomic composition of the pathogens, and the cell-death inducing activity of effector proteins of *B. squamosa*, specifically effector *Bs*Nep1.

Host specificity determinants of *Botrytis* species pathogenic on onion

The causal agents of *Botrytis* leaf blight, neck rot and white rot are all considered host-specific pathogens of onion. In the field, these species are exclusively found on onion or closely related *Allium* species, although under laboratory conditions some are capable of colonizing other plant species as well. Despite the fact that these fungi share the same host, they are not each other's closest relatives (Staats et al. 2005). In the genus *Botrytis*, all species pathogenic on onion, and even all species pathogenic on *Allium spp*., are dispersed over clade 2 of the phylogenetic tree, that contains species pathogenic on a single host or a few taxonomically related hosts (Figure 1). For example *B. squamosa's* closest sister species are *B. deweyae* and *B.* elliptica, which are host-specific to daylily and lily, respectively. Only few species of *Botrytis* are generalist, broad host range plant pathogens and these species are present in clade 1. The notorious and well-studied *B. cinerea* is capable of infecting over 1400 plant species including the majority of cultivated crops (Elad et al. 2016). The more recently defined species *B. pseudocinerea* also has a broad host range (Walker et al. 2011). The scattered distribution of species pathogenic on onion over the phylogenetic tree suggests that either the ability to infect onion has been gained several times independently during the speciation of the genus, or the common ancestor was able to infect onion and several contemporary species have lost this ability and specialized on other hosts. In the latter case, genetic elements that contribute to onion pathogenicity are likely to be shared between the species of *Botrytis* pathogenic on onion. One of the goals of this thesis was to identify genetic determinants of host specificity. Our aim was to find genetic differences between *Botrytis* spp. that could underpin pathogenicity on onion and therefore could explain the scattered host specificity over the genus. This approach was also considered to possibly reveal genetic clues that elucidate the discrepancy between the extremely broad host range of two *Botrytis* species, versus the specificity towards single plant species of other *Botrytis* species.

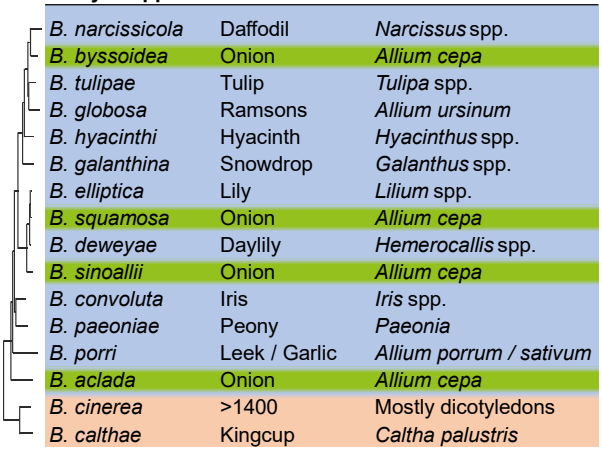

Botrytis spp.	Common host name	Scientific host name
B. narcissicola	Daffodil	*Narcissus* spp.
B. byssoidea	Onion	*Allium cepa*
B. tulipae	Tulip	*Tulipa* spp.
B. globosa	Ramsons	*Allium ursinum*
B. hyacinthi	Hyacinth	*Hyacinthus* spp.
B. galanthina	Snowdrop	*Galanthus* spp.
B. elliptica	Lily	*Lilium* spp.
B. squamosa	Onion	*Allium cepa*
B. deweyae	Daylily	*Hemerocallis* spp.
B. sinoallii	Onion	*Allium cepa*
B. convoluta	Iris	*Iris* spp.
B. paeoniae	Peony	*Paeonia*
B. porri	Leek / Garlic	*Allium porrum / sativum*
B. aclada	Onion	*Allium cepa*
B. cinerea	>1400	Mostly dicotyledons
B. calthae	Kingcup	*Caltha palustris*

Figure 1. Phylogeny of species in the genus *Botrytis* and the names of their corresponding host plants. Only species with a sequenced genome as described in Valero-Jiménez et al. (2020) are included in the phylogeny, which is based on 4746 conserved core genes. Clade 1 and 2 are highlighted in orange and blue, respectively, and species pathogenic on onion are highlighted in green.

Genome architecture

In this thesis, we described the sequencing, assembly and annotation of the genomes of seven *Botrytis* species and *S. cepivorum* (Chapter 4). In a comparative genomics approach using the newly obtained genomes, together with seven previously sequenced *Botrytis* species (Valero-Jiménez et al. 2019), we analyzed genetic elements that could potentially underlie host specificity such as chromosome architecture, gene content and the presence of secondary metabolite biosynthetic gene clusters (SM BGCs). Comparative genomic analyses have been used in the past to unravel determinants of host specificity in other fungal taxa. Isolates of *Fusarium oxysporum* with different host specificity were found to contain unique lineage-specific chromosomes that are essential for pathogenicity on a specific host (Armitage et al. 2018; Ma et al. 2010; van Dam et al. 2017). In *Verticillium dahliae*, lineage-specific regions embedded in core chromosomes were discovered that contained effector genes required for virulence on specific hosts (Chen et al. 2018; de Jonge et al. 2013; Faino et al. 2016). In our analysis of *Botrytis* genomes, however, we did not find any indications of genomic elements or chromosomal organisation that were associated with host specificity. Moreover, synteny analysis revealed that the number of chromosomes and the chromosome architecture of all analysed *Botrytis* genomes was highly conserved. Since we did not identify obvious structural genomic elements that could be linked to host specificity, we analysed the gene content to find potential determinants of host specificity.

Effector proteins

Fungal plant pathogens secrete effectors that manipulate the host in favour of colonization. Many effectors have been reported to contribute to virulence on certain hosts, but some effectors are determinants of host range. The *V. dahliae* effector Tom1 is required for pathogenicity on tomato and introduction of Tom1 into a non-pathogenic isolate rendered the ability to cause disease on tomato (Li et al. 2019). Similarly, the presence of the necrotrophic effector ToxA renders isolates of *Pyrenophora tritici-repensis* pathogenic on wheat (Ciuffetti et al. 2010; Ciuffetti et al. 1997). To identify effectors that could putatively determine host range of *Botrytis* species and be determinants of onion pathogenicity, we assessed their effector repertoire. Analysis of predicted effectors of all sequenced *Botrytis* species showed that there are no effectors shared exclusively by species pathogenic on onion or *Allium*. Yet, for each individual *Botrytis* species between 8 and 37 effector genes were predicted that were unique to that single species. As described in chapter 5, we extensively searched for effectors of *B. squamosa* and tested their cell death-inducing activity as putative host specificity determinants. However, all eight predicted effector genes that are unique for *B. squamosa* were expressed to extremely low levels during the early stages of onion leaf infection. Therefore, we concluded that these genes cannot play important roles in virulence, let alone be determinants of host specificity. Altogether, we did not find any indications that presence/absence polymorphisms of effector genes in *Botrytis* species contribute to pathogenicity on onion. Allelic variation of commonly shared effectors may possibly result in host-specific functionality. However, before studying the effect of haplotypes, the functional characterization of the activity of such a commonly shared effector on onion would be required.

Secondary metabolites

Besides proteins, *Botrytis* also secretes secondary metabolites, produced by secondary metabolite biosynthetic gene clusters (SM BGCs), that contribute to virulence. In *B. cinerea*, over 40 SM BGCs have been identified, but only few metabolites produced by these clusters have been chemically characterized (Collado and Viaud 2016). The two best characterized metabolites are botrydial and botcinic acid, phytotoxic metabolites with necrotic activity on host plant tissue (Cutler et al. 1996; Dalmais et al. 2011; Pinedo et al. 2008; Rossi et al. 2011). Perhaps, gene clusters for as yet unidentified secondary metabolites can contribute to the host specificity of *Botrytis* species. If SM BGCs are shared exclusively by *Botrytis* species infecting onion, then such BGCs may play a role as host determinant. Analysis of the distribution of gene clusters however, revealed that the presence/absence pattern of most clusters were largely congruent with the genus phylogeny. Some clusters were distributed in a more patchy pattern, similar to findings of a previous analysis of *Botrytis* SM BGCs (Valero-Jiménez et al. 2019), but we did not find a correlation between the presence

of any particular cluster and the capacity to infect onion. In another pathogen of onion, a secondary metabolite has been associated to host specificity on onion. In the bacterium *Pantoea ananatis*, causal agent of onion center rot, the HiVir gene cluster was identified as essential for virulence on onion (Asselin et al. 2018). This gene cluster is responsible for the biosynthesis of a phosphanate metabolite and its presence was significantly associated with isolates of *P. ananatis* originating from onion (Stice et al. 2021).

Tolerance to antimicrobial compounds

In the search for host specificity factors, characteristics of the pathogen involved in host invasion and attack were considered good candidates. However, also fungal molecules that are involved in counteracting plant defence responses can contribute to host specificity. Plants defend themselves against pathogen attack, amongst others by the production of antimicrobial compounds that prevent or slow down infection. Pathogens in their turn, have developed mechanisms to overcome the antimicrobial effect of these plant toxins. Several studies on plant antimicrobial metabolites called saponins have demonstrated how antifungal activity and subsequent detoxification of host metabolites determines fungal host specificity. The best studied saponins in this context are avenacin and α-tomatine from wheat and tomato, respectively (Bowyer et al. 1995; You and van Kan 2021). In this thesis, we focussed on onion-specific antimicrobial saponins called ceposides (Chapter 3). Although we did not find direct evidence for the detoxification of ceposides by the onion pathogens *B. aclada* and *S. cepivorum*, yet I think that the importance of antifungal compounds in onion and the ability of onion pathogens to detoxify or tolerate such compounds should still be considered as potential determinants of host specificity. Onion is known to contain a wide variety of antimicrobial compounds of diverse chemical classes, such as thiosulfinates and saponins, and this feature affects onion as a host plant (Lanzotti et al. 2012a; Lanzotti et al. 2014; Sobolewska et al. 2016). Only specialized pathogens that are able to deal with the combination of onion-specific antimicrobial compounds will be able to infect onion.

Overall, in our search for determinants of host specificity of *Botrytis* species, we did not identify genetic elements that could be related to onion pathogenicity. In addition, a remarkable level of synteny and conservation of chromosome architecture between the different *Botrytis* species was observed, which distinguishes *Botrytis* from several other fungal taxa for which a flexibility of genomes was observed (Waalwijk et al. 2018). The genetic elements assessed (effectors, SM BGCs and detoxification of antimicrobial compounds) did not reveal any clues about host specificity. However, in this thesis many effector genes and secondary metabolites have remained uncharacterized yet and may potentially contribute to onion pathogenicity and host specificity. Similarly, the effects of several antimicrobial compounds of onion on *Botrytis* species have remained unknown

and are worth exploring. An alternative hypothesis is that the ability of certain *Botrytis* species to specifically infect onion is a polygenic trait that results from a combination of few or more of the elements discussed above. It may even be possible that other *Botrytis* species that are considered not to be onion pathogens have the same combination of traits and are therefore able to infect onion, but are not recognized as onion pathogens due to ecological or geographical constraints that prevent their accumulation or detection in onion cultivation. The combination of effector proteins and secondary metabolites with necrotic activity, and mechanisms conferring tolerance to antimicrobial compounds are likely to contribute quantitatively to host specificity of *Botrytis* species.

Perspectives for resistance breeding against onion leaf blight, neck rot and white rot

Leaf blight, neck rot and white rot are three diseases of onion that pose a serious threat to onion cultivation and bulb production. Because of the fast progression of leaf blight, onion growers use preventative fungicide sprays to control the disease (Carisse et al. 2011). The active ingredients of these fungicides are often simultaneously effective against multiple *Botrytis* species, such as the causal agents of neck rot. Since white rot is a soil-borne disease, spraying the above ground plant parts with fungicides is not effective method to prevent or inhibit infection. The emergence of fungicide-resistant *B. squamosa* and *B. allii* strains, together with the increasing awareness of the negative effects of fungicides on the environment and a reduction in the number of admitted fungicides, require a more durable strategy to combat or prevent these diseases (Carisse and Tremblay 2007; Tremblay et al. 2003; Viljanen-Rolinson et al. 2007). Efforts have been made to breed onion cultivars with quantitative resistance against leaf blight using a wild relative of onion as a source of resistance (De Vries et al. 1992; Hyde et al. 2015; Scholten et al. 2016). Here, I discuss what additional strategies might be exploited to breed for resistant onion cultivars and how insights in the plant-pathogen interactions can be incorporated in future efforts to find sources of resistance and exploit suitable germplasm to control leaf blight, neck rot and white rot.

Effectors as tools in resistance breeding

One example of a breeding strategy that might be exploited in onion resistance breeding against leaf blight is effector-based screening of wheat germplasm against Septoria nodorum blotch (SNB). *Parastagonospora nodorum* is a necrotrophic Ascomycete fungus and is the causal agent of SNB on wheat. This fungus uses effector proteins to induce host cell death and infect wheat leaves for successful colonization (Oliver et al. 2012).

The effectors of *P. nodorum* are recognized by corresponding wheat sensitivity genes that initiate a programmed cell death response upon recognition. To date, nine pairs of *P. nodorum* effectors and corresponding wheat sensitivity genes have been identified (Haugrud et al. 2019). The number and identity of effectors of *P. nodorum* contribute in a quantitative manner to the virulence of the pathogen. Conversely, the susceptibility of wheat genotypes to SNB depends in a quantitative manner on the number and identity of sensitivity genes (Cowger et al. 2020; Haugrud et al. 2019; Phan et al. 2016). The fewer effectors a plant genotype is able to recognize, the higher the resistance of the genotype and the slower disease will progress. Screening for the presence of sensitivity genes in wheat genotypes is relatively simple because infiltration of wheat leaves with pure effector proteins yields a cell death response upon recognition of the effector (Abeysekara et al. 2009; Gao et al. 2015). By contrast, cell death is not observed if the sensitivity gene is absent. Breeders have used such pure effectors, individually, to screen for insensitivity and combined insensitivity traits from different wheat lines to obtain higher levels of quantitative resistance in new cultivars (Cowger et al. 2020; Downie et al. 2018; Downie et al. 2020; Ruud et al. 2018; Ruud et al. 2017; Tan et al. 2015).

Since *Botrytis* species also use effector proteins to induce host cell death (Mbengue et al. 2016), a similar effector-based strategy as used for SNB in wheat might be successful to identify resistance in host plants of *Botrytis* species. Upon identification of effector proteins of *B. squamosa*, we tested their cell death-inducing activity by infiltration of these proteins in leaves of onion cultivars (Chapter 5). Effector proteins with necrotic activity in onion may be valuable to screen onion cultivars and *Allium* germplasm to search for insensitivity to the effector. Like in wheat breeding for resistance to *P. nodorum*, breeding onions with combined insensitivities to distinct *B. squamosa* effectors might result in decreased susceptibility to leaf blight. However, such breeding strategy will only work if the effectors that are used to screen for insensitivity contribute to the virulence of the pathogen, analogous to the contribution of individual *P. nodorum* effectors to pathogenicity (Liu et al. 2012; Tan et al. 2015). In *B. cinerea* for example, several cell death-inducing effectors were reported, such as BcNep1, BcNep2, and BcIEB1, that did not contribute to virulence (Arenas et al. 2010; Frías et al. 2016). After studying knockout mutants of these effectors, it was hypothesised that *B. cinerea* has extensive redundancy in its effector repertoire and therefore the loss of activity of a single effector could be compensated by other effectors without compromising virulence. If a *B. squamosa* effector also does not contribute to virulence on a specific onion cultivar, then removing the corresponding sensitivity gene from that cultivar would not result in an increased resistance to *B. squamosa*.

Presuming that also *B. squamosa* shows a redundancy in effectors, the strategy to breed for less susceptible onion cultivars by using effector insensitivity genes might only work if multiple insensitivities are combined, equivalently to double or triple knockout mutants of effector genes that do show a reduced virulence in contrast to single knockout

mutants. As discussed above, effectors of *B. squamosa* are likely to be shared with other *Botrytis* species and might not necessarily contribute to host specificity. In principle, the common occurrence of an effector does not have to be a direct issue for the screening for insensitivities using this effector. As long as the effector contributes to virulence, whether only in *B. squamosa* or also in other *Botrytis* species that possess the effector, the insensitive host genotype is likely to be less susceptible to *B. squamosa*. However, the presence of an effector in many *Botrytis* species that infect different hosts, might be an indication that the target of the effector is widely shared between all host plants. Such commonly shared targets possibly have other, rather elemental functions than recognizing effectors and functioning as sensitivity genes. Therefore, when screening with effectors shared between fungal pathogens of distinct host plants, it might be challenging to find insensitive plant lines, cultivars or species. Deleting the effector target might have detrimental effect for the host, similar to pleiotrophic effects that are sometimes observed after deleting susceptibility genes in other plant species (Pavan et al. 2010). However, the absence of SNB sensitivity genes in wheat lines does not have any detrimental effects for plant growth and yield, demonstrating the potential of effectors as tools in resistance breeding.

The potential of *Bs*Nep1 insensitivity for resistance breeding against leaf blight

In chapter 6, we tested the necrotizing activity of effector Nep1 of *B. squamosa* on onion. We observed that different onion genotypes varied in sensitivity to the protein, suggesting that the cell death response did not depend on a presence/absence polymorphism of a *Bs*Nep1 sensitivity gene, but rather behaved like a quantitative trait. Infiltration of *Bs*Nep1 in the tri-hybrid population CCxRF derived from a cross between onion (*Allium cepa*) and an interspecific F1 hybrid (*Allium roylei* x *Allium fistulosum*) (Khrustaleva and Kik 1998), also resulted in a variation of cell death intensities. QTL mapping for *Bs*Nep1 insensitivity revealed one dominant QTL region originating from *A. fistulosum*, that co-localized with a previously identified QTL for *B. squamosa* resistance from *A. roylei* (Scholten et al. 2016). The different origin of *Bs*Nep1 insensitivity and *B. squamosa* resistance in combination with the co-localization of the QTLs for both features is enigmatic. Potentially, instead of a dominant QTL for *Bs*Nep1 insensitivity from *A. fistulosum*, we identified a recessive trait for *Bs*Nep1 sensitivity originating from *A. roylei*. The potential value of the newly identified QTL for resistance breeding depends on the genetic correlation with *B. squamosa* resistance. Despite the co-localization of both QTLs, it remains to be confirmed whether *Bs*Nep1 contributes to virulence of *B. squamosa* on *Bs*Nep1 sensitive lines, and whether *Bs*Nep1 sensitive lines are more susceptible to *B. squamosa*. NLPs are known to target a specific GIPC, a plasma membrane component that can vary in chemical composition between plant species (Cacas et al. 2013; Lenarčič et al. 2017). The analysis of the GIPC content of onion genotypes that varied in *Bs*Nep1 sensitivity revealed that the genotypes

had equal GIPC compositions, and thus could not explain the differences in *Bs*Nep1 sensitivity. Analysis of GIPC content of the genotypes from the hybrid population, as well as the parental lines, will reveal if the *Bs*Nep1 insensitivity QTL might be associated to GIPC composition, or whether other mechanisms are underpinning the insensitivity.

Antimicrobial plant metabolites as a source of resistance

Plants produce metabolites with antimicrobial activity that prevent or slow down pathogen infection. Some plant metabolites, such as avenacin, can completely prevent infection of a specific pathogen species and can therefore be considered as host-specific resistance determinants (Bowyer et al. 1995). Plant pathogens, especially host-specific microbes, have evolved methods to overcome the antimicrobial effect of plant metabolites, often involving detoxification (You and van Kan 2021). As a strategy to increase the resistance of plants, the production or accumulation of metabolites could be enhanced, or new antimicrobial metabolites can be introduced. The potency of plant metabolites as a source of resistance in onion is exemplified by the saponin Alliospiroside A from shallot (*Allium cepa* var. *aggregatum*) (Abdelrahman et al. 2017; Teshima et al. 2013; Vu et al. 2012). This saponin has antifungal properties and inhibits growth of the onion basal rot causing fungus *Fusarium oxysporum* f.sp. *cepa*. Shallot plants naturally produce Alliospiroside A and thereby show a higher level of resistance to *F. oxysporum* f.sp. *cepa* than lines of onion (*Allium cepa*) and Japanese bunching onion (*Allium fistulosum*) that do not produce Alliospiroside A. The addition of chromosome 2A of shallot, that contains the biosynthetic and regulatory genes responsible for the production of Alliospiroside A, to monosomic lines of Japanese bunching onion allowed these lines to produce Alliospiroside A. Extracts of roots of these lines had an increased growth inhibitory effect on *F. oxysporum* f.sp. *cepa*. Moreover, these plants also showed an increased resistance to basal bulb rot.

Exploiting close relatives of onion as a genetic resource for introducing antimicrobial metabolites might be a feasible strategy in breeding for resistance against leaf blight, neck rot and white rot. The effect of metabolites can easily be assessed by fungal growth assays using purified metabolites. If the antimicrobial activity of the metabolite inhibits fungal growth and the fungi are unable to detoxify or tolerate the compound, then introducing these new metabolites will likely enhance the resistance to these fungi. Although crosses between onion and wild relatives can be challenging because of variation in genome size and composition with subsequent low fertility of progeny, there are examples of successful crosses made in the past (Khrustaleva and Kik 1998; Scholten et al. 2007). Alternatively to introducing new secondary metabolites, also increasing the levels of endogenous metabolites may have a beneficial effect on pathogen resistance.

Although introducing new antimicrobial toxins into onion or increasing the production of endogenous metabolites might increase pathogen resistance, the possible detrimental

effects on the plant itself, and on onion bulbs as a commodity for consumption should be taken into consideration. Some saponins for instance, are known to have a bitter taste, and the introduction of new saponins, or the increased accumulation of endogenous ones may affect the taste of onion bulbs (Oleszek and Oleszek 2020). Similarly, certain thiosulphinates are responsible for the pungent flavor of onion and upon cutting of the bulb act as a chemical eye irritant and induce tears (Kato et al. 2016). Thus caution is required when breeding onions purely for a metabolite repertoire with stronger antifungal activity, although it also provides opportunities to obtain onion cultivars with new aromas.

Another consideration on the introduction of new metabolites into onion as a source of resistance is the durability of such a trait. Pathogens that specialized on onion are likely unable to tolerate or detoxify metabolites from other *Allium* species. However, pathogens of the plant species from which the metabolite originates likely are able to deal with such compounds. The introduction of new metabolites into onion will put selection pressure on onion-specific pathogens to evolve mechanisms to circumvent the antimicrobial effect of the newly introduced metabolite. The genes or gene clusters required for tolerance might be acquired by horizontal gene transfer from pathogens on the plant species from which the metabolite originates. The intensity of the selection pressure to evolve tolerance and the possibility of horizontal gene transfer as a source of tolerance was illustrated by a *Pseudomonas fluorescens* strain isolated from garlic. A gene cluster conferring tolerance to the garlic metabolite allicin was identified in this *P. fluorescens* strain and was shown to be acquired by horizontal gene transfer (Borlinghaus et al. 2020).

The consequence of differences in pathogen biology for resistance breeding strategies

Leaf blight, neck rot and white rot are three diseases of onion that are all three caused by Ascomycetes. Despite the close phylogenetic relation of these fungi, the diseases that they cause are very different. *Botrytis squamosa*, *B. aclada* as a representative of the species causing neck rot, and *S. cepivorum* have a very different infection biology with adaptations to different host tissues and distinct ecological niches (Figure 2). *B. squamosa* infects onion leaves with a classic necrotrophic behavior in which it kills host cells and subsequently colonizes the dead tissue. *B. aclada* shows a completely different lifestyle and infection biology than *B. squamosa*. We did not obtain any evidence that *B. aclada* truly infects onion leaves. Instead, we observed that this fungus grows over the surface of the onion leaf without ever entering the leaf mesophyll. *B. aclada* even produced new conidia on the surface of the onion leaf, but also on plants that are considered as non-host plants (Chapter 2). How *B. aclada* ends up in the neck area of the onion, and why

symptoms only develop during storage still remains to be discovered. Based on these findings, we should reconsider whether *B. aclada*, and also *B. allii* and *B. byssoidea,* should be classified as necrotrophic fungi. One other *Botrytis* species, *B. deweyae,* was shown to behave predominantly as an endophyte and occasionally switches to classic necrotrophic behaviour (Grant-Downton et al. 2014). Next to *B. squamosa* and *B. aclada*, *S. cepivorum* has yet another lifestyle since it is a soil-borne pathogen that does not form spores to spread and establish disease, but infects the roots of onion plants and produces sclerotia that can last in the soil for decades.

Figure 2. Schematic representation of leaf blight, neck rot, and white rot on an onion plant. Symptoms of leaf blight are visible as characteristic necrotic spots and eventually blighted leaves. Neck rot symptoms can be seen on the inside of the bulb as brown discoloration of scales around the neck area. It should be noted that neck rot symptoms normally develop only after onion bulbs have been harvested and stored. White rot is represented by white hyphae growing out of sclerotia, first colonizing the root system and eventually forming mycelium that is covering the outside of the lower part of the bulb.

The difference in lifestyle and infection biology of these closely related fungi has consequences for the resistance breeding strategies targeting these fungi, and an effective resistance against leaf blight might not be functional against neck rot or white rot. Identification of leaf blight resistance using effectors of *B. squamosa* to screen for insensitivities is a putatively viable strategy, as demonstrated by the work on the *B. squamosa* effector *Bs*Nep1. This approach however, will likely not be equally applicable to identify resistance against other species. Since *B. aclada* appears to behave at least for part of its life cycle as an epiphyte, it will likely not secrete cell death-inducing effectors. To assess potential effector activity of *B. squamosa* we produced liquid culture filtrates that showed clear necrotizing activity upon infiltration in onion. The same approach, however, did not reveal any detectable cell death-inducing activity in culture filtrates of *B. aclada*, endorsing the difference in secreted proteins and thus in lifestyles between *B. squamosa* and *B. aclada*. Breeding for neck rot resistance will require alternative strategies, but will be problematic by the lack of a suitable quantitative infection assay and the lack of evidence for genetic variation for susceptibility among onion cultivars.

For *S. cepivorum*, we visualized the early phases of infection on onion and on the non-host tomato as described in chapter 2. In the first contact between *S. cepivorum* and its potential host plant, the fungus produced an infection cushion that attached to the root, or root hair surface of the plant. Interestingly, we observed that *S. cepivorum* formed these infection structures on both onion and the non-host tomato. On onion, the infection cushion achieved a successful entry and growth of invasive hyphae inside the root, but on tomato the infection structure died within 12 to 24 hours after the initial contact. Since the outcome of the interaction between plant and pathogen is determined by the infection cushion and its invasion attempt into the host root, it would be interesting to study what causes the cell death in the infection cushion on the roots of a non-host. Insights into this process might provide new leads for developing control strategies or approaches for resistance breeding against white rot.

Concluding, our findings provide insights in onion-pathogen interactions that could potentially be exploited in breeding strategies for resistance. The fundamental differences in infection biology of *B. squamosa*, *B. aclada* and *S. cepivorum* should be taken into consideration when developing approaches to identify resistance. Continued efforts to understand the molecular, cellular and biochemical interaction between these pathogens and their host onion, are essential to provide leads for resistance breeding as a durable solution against leaf blight, neck rot and white rot in onion cultivation.

References

A

Abd-El-Razik, A., Shatla, M., and Rushdi, M. 1973. Studies on the infection of onion plants by *Sclerotium cepivorum* Berk. Phytopathologische Zeitschrift 76:108-116.

Abd El-Razik, A., Shatla, M., and Rushdi, M. 1974. Relationship of pectolytic enzyme production by isolates of *Sclerotium cepivorum* Berk to their pathogenicity. Zentralblatt für Bakteriologie, Parasitenkunde, Infektionskrankheiten und Hygiene. Zweite Naturwissenschaftliche Abteilung: Allgemeine, Landwirtschaftliche und Technische Mikrobiologie 129:253-258.

Abdelrahman, M., Hirata, S., Sawada, Y., Hirai, M. Y., Sato, S., Hirakawa, H., Mine, Y., Tanaka, K., and Shigyo, M. 2019. Widely targeted metabolome and transcriptome landscapes of *Allium fistulosum–A. cepa* chromosome addition lines revealed a flavonoid hot spot on chromosome 5A. Scientific reports 9:1-15.

Abdelrahman, M., El-Sayed, M., Sato, S., Hirakawa, H., Ito, S.-i., Tanaka, K., Mine, Y., Sugiyama, N., Suzuki, M., and Yamauchi, N. 2017. RNA-sequencing-based transcriptome and biochemical analyses of steroidal saponin pathway in a complete set of *Allium fistulosum—A. cepa* monosomic addition lines. Plos one 12:e0181784.

Abeysekara, N. S., Friesen, T. L., Keller, B., and Faris, J. D. 2009. Identification and characterization of a novel host–toxin interaction in the wheat–*Stagonospora nodorum* pathosystem. Theoretical and applied genetics 120:117-126.

Ahmed, A., and Tribe, H. 1977. Biological control of white rot of onion (*Sclerotium cepivorum*) by *Coniothyrium minitans*. Plant pathology 26:75-78.

Albert, I., Böhm, H., Albert, M., Feiler, C. E., Imkampe, J., Wallmeroth, N., Brancato, C., Raaymakers, T. M., Oome, S., and Zhang, H. 2015. An RLP23–SOBIR1–BAK1 complex mediates NLP-triggered immunity. Nature plants 1:1-9.

Alderman, S., and Lacy, M. 1983. Influence of dew period and temperature on infection of onion leaves. Phytopathology 73:1020-1023.

Alderman, S., Lacy, M., and Everts, K. 1985. Influence of interruptions of dew period on numbers of lesions produced on onion by *Botrytis squamosa*. Phytopathology 75:808-810.

Ali, A., and El Shabrawy, A. 1979. Effect of some cultural practices and some chemicals on the control of neck rot disease caused by *Botrytis allii* during storage and in the field for seed onion production in ARE. Agricultural research review 57:103-114.

Allen, J., and Young, J. 1968. Soil fungistasis and *Sclerotium cepivorum* berk. Plant and soil 29:479-480.

Amin, M., Tadele, S., and Selvaraj, T. 2014. White rot (*Sclerotium cepivorum* Berk) an aggressive pest of onion and garlic in Ethiopia: An overview. Journal of agricultural biotechnology and sustainable development 6:6-15.

Amselem, J., Cuomo, C. A., van Kan, J. A., Viaud, M., Benito, E. P., Couloux, A., Coutinho, P. M., de Vries, R. P., Dyer, P. S., and Fillinger, S. 2011. Genomic analysis of the necrotrophic fungal pathogens *Sclerotinia sclerotiorum* and *Botrytis cinerea*. Plos genetics 7:e1002230.

Ankri, S., and Mirelman, D. 1999. Antimicrobial properties of allicin from garlic. Microbes and infection 1:125-129.

Araújo, E. R., Alves, D. P., and Higashikawa, F. S. 2018. Cultivar resistance and chemical, biological and fertilizer treatments for controling *Botrytis* leaf blight of onion. Tropical plant pathology 43:160-164.

Arenas, Y. C., Kalkman, E. R., Schouten, A., Dieho, M., Vredenbregt, P., Uwumukiza, B., Ruiz, M. O., and van Kan, J. A. 2010. Functional analysis and mode of action of phytotoxic Nep1-like proteins of *Botrytis cinerea*. Physiological and molecular plant pathology 74:376-386.

Armitage, A. D., Taylor, A., Sobczyk, M. K., Baxter, L., Greenfield, B. P., Bates, H. J., Wilson, F., Jackson, A. C., Ott, S., and Harrison, R. J. 2018. Characterisation of pathogen-specific regions and novel effector candidates in *Fusarium oxysporum* f. sp. *cepae*. Scientific reports 8:1-15.

Ashton, P., Thanh, L., Trieu, P., van Anh, D., Trinh, N., Beardsley, J., Kibengo, F., Chierakul, W., Dance, D., and Rattanavong, S. 2019. Three phylogenetic groups have driven the recent population expansion of *Cryptococcus neoformans*. Nature communications 10:1-10.

Asselin, J. A. E., Bonasera, J. M., and Beer, S. V. 2018. Center rot of onion (*Allium cepa*) caused by *Pantoea ananatis* requires *pepM*, a predicted phosphonate-related gene. Molecular plant-microbe interactions 31:1291-1300.

B

Backhouse, D., and Stewart, A. 1987. Anatomy and histochemistry of resting and germinating sclerotia of *Sclerotium cepivorum*. Transactions of the British mycological society 89:561-567.

Bailey, B. A. 1995. Purification of a protein from culture filtrates of *Fusarium oxysporum* that induces ethylene and necrosis in leaves of *Erythroxylum coca*. Phytopathology 85:1250-1255.

Bakonyi, J., Vajna, L., Szeredi, A., Tímár, E., Kovács, G., Csősz, M., and Varga, A. 2011. First report of *Sclerotium cepivorum* causing white rot of garlic in Hungary. New disease reports 23.

Banks, E., and Edgington, L. 1989. Effect of integrated control practices on the onion white rot pathogen in organic soil. Canadian journal of plant pathology 11:268-272.

Bansal, R., and Broadhurst, P. 1992. An evaluation of *Allium* germplasm for resistance to white rot caused by *Sclerotium cepivorum* Berk. New Zealand journal of crop and horticultural science 20:361-365.

Baxter, L., Tripathy, S., Ishaque, N., Boot, N., Cabral, A., Kemen, E., Thines, M., Ah-Fong, A., Anderson, R., and Badejoko, W. 2010. Signatures of adaptation to obligate biotrophy in the *Hyaloperonospora arabidopsidis* genome. Science 330:1549-1551.

Bergquist, R., and Lorbeer, J. 1971. Reaction of *Allium* spp. and *Allium cepa* to *Botryotinia* (*Botrytis*) *squamosa*. Plant disease reporter 55:394-398.

Bergquist, R., and Lorbeer, J. 1972. Apothecial production, compatibility and sex in *Botryotinia squamosa*. Mycologia 64:1270-1281.

Bertazzoni, S., Williams, A. H., Jones, D. A., Syme, R. A., Tan, K.-C., and Hane, J. K. 2018. Accessories make the outfit: accessory chromosomes and other dispensable DNA regions in plant-pathogenic fungi. Molecular plant-microbe interactions 31:779-788.

Böhm, H., Albert, I., Oome, S., Raaymakers, T. M., van den Ackerveken, G., and Nürnberger, T. 2014. A conserved peptide pattern from a widespread microbial virulence factor triggers pattern-induced immunity in *Arabidopsis*. Plos pathogens 10:e1004491.

Borlinghaus, J., Albrecht, F., Gruhlke, M. C., Nwachukwu, I. D., and Slusarenko, A. J. 2014. Allicin: chemistry and biological properties. Molecules 19:12591-12618.

Borlinghaus, J., Bolger, A., Schier, C., Vogel, A., Usadel, B., Gruhlke, M. C., and Slusarenko, A. J. 2020. Genetic and molecular characterization of multicomponent resistance of *Pseudomonas* against allicin. Life science alliance 3:e202000670.

Bowyer, P., Clarke, B., Lunness, P., Daniels, M., and Osbourn, A. 1995. Host range of a plant pathogenic fungus determined by a saponin detoxifying enzyme. Science 267:371-374.

Brix, H., and Zinkernagel, V. 1992. Screening for resistance of *Allium* species to *Sclerotium cepivorum* with special reference to non-stimulatory resistance. Plant pathology 41:308-316.

C

Cacas, J.-L., Buré, C., Furt, F., Maalouf, J.-P., Badoc, A., Cluzet, S., Schmitter, J.-M., Antajan, E., and Mongrand, S. 2013. Biochemical survey of the polar head of plant glycosylinositolphosphoceramides unravels broad diversity. Phytochemistry 96:191-200.

Campbell, M. A., Rokas, A., and Slot, J. C. 2012. Horizontal transfer and death of a fungal secondary metabolic gene cluster. Genome biology and evolution 4:289-293.

Cantarel, B. L., Korf, I., Robb, S. M., Parra, G., Ross, E., Moore, B., Holt, C., Alvarado, A. S., and Yandell, M. 2008. MAKER: an easy-to-use annotation pipeline designed for emerging model organism genomes. Genome research 18:188-196.

Capella-Gutiérrez, S., Silla-Martínez, J. M., and Gabaldón, T. 2009. trimAl: a tool for automated alignment trimming in large-scale phylogenetic analyses. Bioinformatics 25:1972-1973.

Carisse, K. X., Burnett, P., Tewari, J., Chen, M., Turkington, T., and Helm, J. 2000. Histopathological study of barley cultivars resistant and susceptible to *Rhynchosporium secalis*. Phytopathology 90:94-102.

Carisse, O., and Tremblay, D. 2007. Incidence and significance of iprodione-insensitive isolates of *Botrytis squamosa*. Plant disease 91:41-46.

Carisse, O., Savary, S., and Willocquet, L. 2008. Spatiotemporal relationships between disease development and airborne inoculum in unmanaged and managed *Botrytis* leaf blight epidemics. Phytopathology 98:38-44.

Carisse, O., Levasseur, A., and van der Heyden, H. 2012. A new risk indicator for *Botrytis* leaf blight of onion caused by *Botrytis squamosa* based on infection efficiency of airborne inoculum. Plant pathology 61:1154-1164.

Carisse, O., McCartney, H., Gagnon, J., and Brodeur, L. 2005. Quantification of airborne inoculum as an aid in the management of leaf blight of onion caused by *Botrytis squamosa*. Plant disease 89:726-733.

Carisse, O., Tremblay, D.-M., McDonald, M. R., Brodeur, L., and McRoberts, N. 2011. Management of *Botrytis* leaf blight of onion: the Québec experience of 20 years of continual improvement. Plant disease 95:504-514.

Chakraborty, M., Baldwin-Brown, J. G., Long, A. D., and Emerson, J. 2016. Contiguous and accurate de novo assembly of metazoan genomes with modest long read coverage. Nucleic acids research 44:e147-e147.

Chatterjee, S., Kuang, Y., Splivallo, R., Chatterjee, P., and Karlovsky, P. 2016. Interactions among filamentous fungi *Aspergillus niger*, *Fusarium verticillioides* and *Clonostachys rosea*: fungal biomass, diversity of secreted metabolites and fumonisin production. BMC microbiology 16:1-13.

Chen, J. Y., Liu, C., Gui, Y. J., Si, K. W., Zhang, D. D., Wang, J., Short, D. P., Huang, J. Q., Li, N. Y., and Liang, Y. 2018. Comparative genomics reveals cotton-specific virulence factors in flexible genomic regions in *Verticillium dahliae* and evidence of horizontal gene transfer from *Fusarium*. New phytologist 217:756-770.

Chilvers, M. I., and du Toit, L. J. 2006. Detection and identification of *Botrytis* species associated with neck rot, scape blight, and umbel blight of onion. Plant health progress 7:38.

Chilvers, M. I., Hay, F., and Wilson, C. 2004. Survey for *Botrytis* species associated with onion bulb rot in northern Tasmania, Australia. Australasian plant pathology 33:419-422.

Chilvers, M. I., du Toit, L. J., Akamatsu, H., and Peever, T. L. 2007. A real-time, quantitative PCR seed assay for *Botrytis* spp. that cause neck rot of onion. Plant disease 91:599-608.

Chin, C.-S., Alexander, D. H., Marks, P., Klammer, A. A., Drake, J., Heiner, C., Clum, A., Copeland, A., Huddleston, J., and Eichler, E. E. 2013. Nonhybrid, finished microbial genome assemblies from long-read SMRT sequencing data. Nature methods 10:563.

Ciuffetti, L. M., Tuori, R. P., and Gaventa, J. M. 1997. A single gene encodes a selective toxin causal to the development of tan spot of wheat. The plant cell 9:135-144.

Ciuffetti, L. M., Manning, V. A., Pandelova, I., Betts, M. F., and Martinez, J. P. 2010. Host-selective toxins, Ptr ToxA and Ptr ToxB, as necrotrophic effectors in the *Pyrenophora tritici-repentis*–wheat interaction. New phytologist 187:911-919.

Clark, C., and Lorbeer, J. 1973a. Reaction of onion cultivars to *Botrytis* brown stain. Plant disease reporter 57:210-214.

Clark, C., and Lorbeer, J. 1973b. Symptomatology, etiology, and histopathology of *Botrytis* brown stain of onion. Phytopathology 63:1231-1235.

Clark, C., and Lorbeer, J. 1976. Comparative histopathology of *Botrytis squamosa*. Phytopathology 66:1279-1289.

Coley-Smith, J. 1960. Studies of the biology of *Sclerotium cepivorum* Berk. IV. Germination of sclerotia. Annals of applied biology 48:8-18.

Coley-Smith, J. 1986. A comparison of flavour and odour compounds of onion, leek, garlic and *Allium fistulosum* in relation to germination of sclerotia of *Sclerotium cepivorum*. Plant pathology 35:370-376.

Coley-Smith, J., and Holt, R. 1966. The effect of species of *Allium* on germination in soil of sclerotia of *Sclerotium cepivorum* Berk. Annals of applied biology 58:273-278.

Coley-Smith, J., and King, J. 1969. The production by species of *Allium* of alkyl sulphides and their effect on germination of sclerotia of *Sclerotium cepivorum* Berk. Annals of applied biology 64:289-301.

Coley-Smith, J., Mitchell, C. M., and Sansford, C. E. 1990. Long-term survival of sclerotia of *Sclerotium cepivorum* and *Stromatinia gladioli*. Plant pathology 39:58-69.

Coley-Smith, J., Parfitt, D., Taylor, I., and Reese, R. 1987. Studies of dormancy in sclerotia of *Sclerotium cepivorum*. Plant pathology 36:594-599.

Coley-Smith, J. R., and Parfitt, D. 1986. Some effects of diallyl disulphide on sclerotia of *Sclerotium cepivorum*: Possible novel control method for white rot disease of onions. Pesticide science 17:587-594.

Collado, I. G., and Viaud, M. 2016. Secondary metabolism in *Botrytis cinerea*: combining genomic and metabolomic approaches. Pages 291-313 in: *Botrytis*–The fungus, the pathogen and its management in agricultural systems. Fillinger S., and Elad Y. (eds) Springer, Cham, Switzerland.

Contreras-Moreira, B., and Vinuesa, P. 2013. GET_HOMOLOGUES, a versatile software package for scalable and robust microbial pangenome analysis. Applied and environmental microbiology 79:7696-7701.

Coolong, T. W., Walcott, R. R., and Randle, W. M. 2008. A quantitative real-time polymerase chain reaction assay for *Botrytis aclada* in onion bulb tissue. HortScience 43:408-413.

Couch, B., and Kohn, L. 2000. Clonal spread of *Sclerotium cepivorum* in onion production with evidence of past recombination events. Phytopathology 90:514-521.

Cowger, C., Ward, B., Brown-Guedira, G., and Brown, J. 2020. Role of effector-sensitivity gene interactions and durability of quantitative resistance to Septoria nodorum blotch in Eastern US wheat. Frontiers in plant science 11:155.

Cramer, C. S. 2000. Breeding and genetics of *Fusarium* basal rot resistance in onion. Euphytica 115:159-166.

Crowe, F. 2008. White rot. Pages 22-26 in: Compendium of onion and garlic diseases, second edition. Schwartz H. F., and Mohan S. F. (eds) American Phytopathological Society, St. Paul, MN, USA.

Crowe, F., and Hall, D. 1980a. Vertical distribution of sclerotia of *Sclerotium cepivorum* and host root systems relative to white rot of onion and garlic. Phytopathology 70:70-73.

Crowe, F., and Hall, D. 1980b. Soil temperature and moisture effects on sclerotium germination and infection of onion seedlings by *Sclerotium cepivorum*. Phytopathology 70:74-78.

Crowe, F., Hall, D., Greathead, A., and Baghott, K. 1980. Inoculum density of *Sclerotium cepivorum* and the incidence of white rot of onion and garlic. Phytopathology 70:64-69.

Crowe, F. J., Carlson, H., Kirby, D., and Simmons, R. B. 2005. Further investigtion of flooding as a means of *Allium* white rot control. Central Oregon Agricultural Research Center 2004 Annual report:10.

Currah, L., and Maude, R. 1984. Laboratory tests for leaf resistance to *Botrytis squamosa* in onions. Annals of applied biology 105:277-283.

Cutler, H. G., Parker, S. R., Ross, S. A., Crumley, F. G., and Schreiner, P. R. 1996. Homobotcinolide: a biologically active natural homolog of botcinolide from *Botrytis cinerea*. Bioscience, biotechnology, and biochemistry 60:656-658.

D

Dalmais, B., Schumacher, J., Moraga, J., Le Pecheur, P., Tudzynski, B., Collado, I. G., and Viaud, M. 2011. The *Botrytis cinerea* phytotoxin botcinic acid requires two polyketide synthases for production and has a redundant role in virulence with botrydial. Molecular plant pathology 12:564-579.

Davis, R., Hao, J., Romberg, M., Nunez, J., and Smith, R. 2007. Efficacy of germination stimulants of sclerotia of *Sclerotium cepivorum* for management of white rot of garlic. Plant Disease 91:204-208.

de Jonge, R., Bolton, M. D., Kombrink, A., van den Berg, G. C., Yadeta, K. A., and Thomma, B. P. 2013. Extensive chromosomal reshuffling drives evolution of virulence in an asexual pathogen. Genome research 23:1271-1282.

De Silva, D. D., Crous, P. W., Ades, P. K., Hyde, K. D., and Taylor, P. W. 2017. Life styles of *Colletotrichum* species and implications for plant biosecurity. Fungal biology reviews 31:155-168.

de Visser, C. 1996. Field evaluation of a supervised control system for *Botrytis* leaf blight in spring sown onions in the Netherlands. European journal of plant pathology 102:795-805.

de Vries, J., Wietsma, W., and de Vries, T. 1992. Introgression of leaf blight resistance from *Allium roylei* Stearn into onion (*A. cepa* L.). Euphytica 62:127-133.

de Vries, R., Riley, R., Wiebenga, A. et al. 2017. Comparative genomics reveals high biological diversity and specific adaptations in the industrially and medically important fungal genus *Aspergillus*. Genome biology 18:28.

Derbyshire, M., Denton-Giles, M., Hegedus, D., Seifbarghy, S., Rollins, J., van Kan, J., Seidl, M. F., Faino, L., Mbengue, M., and Navaud, O. 2017. The complete genome sequence of the phytopathogenic fungus *Sclerotinia sclerotiorum* reveals insights into the genome architecture of broad host range pathogens. Genome biology and evolution 9:593-618.

Dickman, M., Park, Y., Oltersdorf, T., Li, W., Clemente, T., and French, R. 2001. Abrogation of disease development in plants expressing animal antiapoptotic genes. Proceedings of the national academy of sciences 98:6957-6962.

Dong, S., Raffaele, S., and Kamoun, S. 2015. The two-speed genomes of filamentous pathogens: waltz with plants. Current opinion in genetics & development 35:57-65.

Dong, S., Kong, G., Qutob, D., Yu, X., Tang, J., Kang, J., Dai, T., Wang, H., Gijzen, M., and Wang, Y. 2012. The NLP toxin family in *Phytophthora sojae* includes rapidly evolving groups that lack necrosis-inducing activity. Molecular plant-microbe interactions 25:896-909.

Downie, R. C., Lin, M., Corsi, B., Ficke, A., Lillemo, M., Oliver, R. P., Phan, H., Tan, K.-C., and Cockram, J. 2020. Septoria nodorum blotch of wheat: disease management and resistance breeding in the face of shifting disease dynamics and a changing environment. Phytopathology in press.

Downie, R. C., Bouvet, L., Furuki, E., Gosman, N., Gardner, K. A., Mackay, I. J., Campos Mantello, C., Mellers, G., Phan, H. T., and Rose, G. A. 2018. Assessing European wheat sensitivities to *Parastagonospora nodorum* necrotrophic effectors and fine-mapping the *Snn3-B1* locus conferring sensitivity to the effector SnTox3. Frontiers in plant science 9:881.

du Toit, L. J., Derie, M. L., and Pelter, G. Q. 2004. Prevalence of *Botrytis* spp. in onion seed crops in the Columbia basin of Washington. Plant disease 88:1061-1068.

Duba, A., Goriewa-Duba, K., and Wachowska, U. 2018. A review of the interactions between wheat and wheat pathogens: *Zymoseptoria tritici*, *Fusarium* spp. and *Parastagonospora nodorum*. International journal of molecular sciences 19:1138.

Dunn, N. A., Unni, D. R., Diesh, C., Munoz-Torres, M., Harris, N. L., Yao, E., Rasche, H., Holmes, I. H., Elsik, C. G., and Lewis, S. E. 2019. Apollo: Democratizing genome annotation. Plos computational biology 15:e1006790.

E

Edgar, R. C. 2010. Search and clustering orders of magnitude faster than BLAST. Bioinformatics 26:2460-2461.

El-Samra, I., El-Faham, Y., and Kamara, A. 1981. Selective induction of infection cushions by *Rhizoctonia solani* in relation to host responses. Journal of phytopathology 102:122-126.

Elad, Y., Pertot, I., Prado, A. M. C., and Stewart, A. 2016. Plant hosts of *Botrytis* spp. Pages 413-486 in: *Botrytis*–The fungus, the pathogen and its management in agricultural systems. Fillinger S., and Elad Y. (eds). Springer, Cham, Switzerland.

Ellerbrock, L., and Lorbeer, J. 1977a. Sources of primary inoculum of *Botrytis squamosa*. Phytopathology 67:363-372.

Ellerbrock, L., and Lorbeer, J. 1977b. Survival of sclerotia and conidia of *Botrytis squamosa*. Phytopathology 67:219-225.

Emanuelsson, O., Brunak, S., Von Heijne, G., and Nielsen, H. 2007. Locating proteins in the cell using TargetP, SignalP and related tools. Nature protocols 2:953.

Emms, D. M., and Kelly, S. 2015. OrthoFinder: solving fundamental biases in whole genome comparisons dramatically improves orthogroup inference accuracy. Genome biology 16:1-14.

Entwistle, A., Clarkson, J., Munasinghe, H., and Mead, A. 1991. Microbial and integrated control of *Allium* white rot. Pages 415-420 in: Developments in Agricultural and Managed Forest Ecology, Volume 23. Beemster A. B. R., Bollen G. J., Gerlagh M., Ruissen M. A., Schippers B., and Tempel A. (eds) Elsevier, Amsterdam, The Netherlands.

Esler, G., and Coley-Smith, J. 1983. Flavor and odour characteristics of species of *Allium* in relation to their capacity to stimulate germination of sclerotia of *Sclerotium cepivorum*. Plant pathology 32:13-22.

F

Faino, L., Seidl, M. F., Shi-Kunne, X., Pauper, M., van den Berg, G. C., Wittenberg, A. H., and Thomma, B. P. 2016. Transposons passively and actively contribute to evolution of the two-speed genome of a fungal pathogen. Genome research 26:1091-1100.

FAOSTAT. 2020. Food and Agriculture Organization of the United Nations. Statistical Database.

Faris, J. D., Zhang, Z., Lu, H., Lu, S., Reddy, L., Cloutier, S., Fellers, J. P., Meinhardt, S. W., Rasmussen, J. B., and Xu, S. S. 2010. A unique wheat disease resistance-like gene governs effector-triggered susceptibility to necrotrophic pathogens. Proceedings of the national academy of sciences 107:13544-13549.

Fletcher, J., Knight, B., Bate, E., and Cragg, I. 1971. The control of white rot (*Sclerotium cepivorum* Berk.) in salad onions with dicloran. Plant pathology 20:88-92.

Fournier, E., Giraud, T., Albertini, C., and Brygoo, Y. 2005. Partition of the *Botrytis cinerea* complex in France using multiple gene genealogies. Mycologia 97:1251-1267.

Frías, M., González, C., and Brito, N. 2011. BcSpl1, a cerato-platanin family protein, contributes to *Botrytis cinerea* virulence and elicits the hypersensitive response in the host. New phytologist 192:483-495.

Frías, M., González, M., González, C., and Brito, N. 2016. BcIEB1, a *Botrytis cinerea* secreted protein, elicits a defense response in plants. Plant science 250:115-124.

Friesen, T. L., Stukenbrock, E. H., Liu, Z., Meinhardt, S., Ling, H., Faris, J. D., Rasmussen, J. B., Solomon, P. S., McDonald, B. A., and Oliver, R. P. 2006. Emergence of a new disease as a result of interspecific virulence gene transfer. Nature genetics 38:953-956.

G

Gao, Y., Faris, J., Liu, Z., Kim, Y., Syme, R., Oliver, R., Xu, S., and Friesen, T. 2015. Identification and characterization of the SnTox6-*Snn6* interaction in the *Parastagonospora nodorum*–wheat pathosystem. Molecular plant-microbe interactions 28:615-625.

Gardan, L., Bella, P., Meyer, J.-M., Christen, R., Rott, P., Achouak, W., and Samson, R. 2002. *Pseudomonas salomonii* sp. nov., pathogenic on garlic, and *Pseudomonas palleroniana* sp. nov., isolated from rice. International journal of systematic and evolutionary microbiology 52:2065-2074.

Garfinkel, A. R., Lorenzini, M., Zapparoli, G., and Chastagner, G. A. 2017. *Botrytis euroamericana*, a new species from peony and grape in North America and Europe. Mycologia 109:495-507.

Garfinkel, A. R., Coats, K. P., Sherry, D. L., and Chastagner, G. A. 2019. Genetic analysis reveals unprecedented diversity of a globally-important plant pathogenic genus. Scientific reports 9:1-14.

Gent, D. H., du Toit, L. J., Fichtner, S. F., Mohan, S. K., Pappu, H. R., and Schwartz, H. F. 2006. Iris yellow spot virus: an emerging threat to onion bulb and seed production. Plant Disease 90:1468-1480.

Gijzen, M., and Nürnberger, T. 2006. Nep1-like proteins from plant pathogens: recruitment and diversification of the NPP1 domain across taxa. Phytochemistry 67:1800-1807.

Gill, H. K., Garg, H., Gill, A. K., Gillett-Kaufman, J. L., and Nault, B. A. 2015. Onion thrips (Thysanoptera: *Thripidae*) biology, ecology, and management in onion production systems. Journal of integrated pest management 6.

Gindro, C., and L'Hoste, G. 1997. Germination and infectious potential of microconidia of *Sclerotium cepivorum*. Journal of phytopathology 145:171-175.

Giraud, T., Fortini, D., Levis, C., Lamarque, C., Leroux, P., LoBuglio, K., and Brygoo, Y. 1999. Two sibling species of the *Botrytis cinerea* complex, transposa and vacuma, are found in sympatry on numerous host plants. Phytopathology 89:967-973.

Gladders, P., Carter, M., and Owen, W. 1994. Resistance to benomyl in *Botrytis allii* from shallots. Plant pathology 43:410-411.

Gluck-Thaler, E., and Slot, J. C. 2018. Specialized plant biochemistry drives gene clustering in fungi. The ISME journal 12:1694-1705.

Graham-Taylor, C., Kamphuis, L. G., and Derbyshire, M. C. 2020. A detailed in silico analysis of secondary metabolite biosynthesis clusters in the genome of the broad host range plant pathogenic fungus *Sclerotinia sclerotiorum*. BMC genomics 21:1-20.

Grant-Downton, R. T., Terhem, R. B., Kapralov, M. V., Mehdi, S., Rodriguez-Enriquez, M. J., Gurr, S. J., van Kan, J. A., and Dewey, F. M. 2014. A novel *Botrytis* species is associated with a newly emergent foliar disease in cultivated *Hemerocallis*. Plos one 9:e89272.

Grinstein, A., Elad, Y., Temkin-Gorodeiski, N., Rivan, Y., and Frankel, H. 1992. Reduced volume application of fungicides for the control of onion rots. Phytoparasitica 20:293.

Grosse-Holz, F., Kelly, S., Blaskowski, S., Kaschani, F., Kaiser, M., and van der Hoorn, R. A. 2018. The transcriptome, extracellular proteome and active secretome of agroinfiltrated *Nicotiana benthamiana* uncover a large, diverse protease repertoire. Plant biotechnology journal 16:1068-1084.

Gunkel, W., Lorbeer, J., Kaufman, J., and Smith, H. 1971. Artificial drying-a method for control of *Botrytis* neck rot in bulk stored onions. NY Farm Elec Counc Progr Rep.

Gupta, M., and Bharat, N. K. 2017. Occurrence of white rot disease of garlic in Himachal Pradesh. International journal of farm sciences 7:47-50.

H

Hafez, M., Gourlie, R., Despins, T., Turkington, T. K., Friesen, T. L., and Aboukhaddour, R. 2020. *Parastagonospora nodorum* and related species in western Canada: genetic variability and effector genes. Phytopathology 110:1946-1958.

Hancock, J., and Lorbeer, J. 1963. Pathogenesis of *Botrytis cinerea*, *B. squamosa*, and *B. allii* on onion leaves. Phytopathology 53:669-673.

Hancock, J., Lorbeer, J., and Millar, R. 1964. Role of pectolytic and cellulolytic enzymes in *Botrytis* leaf blight of onion. Phytopathology 54:932-935.

Haralampidis, K., Bryan, G., Qi, X., Papadopoulou, K., Bakht, S., Melton, R., and Osbourn, A. 2001. A new class of oxidosqualene cyclases directs synthesis of antimicrobial phytoprotectants in monocots. Proceedings of the national academy of sciences 98:13431-13436.

Harrow, K., and Harris, S. 1969. Artificial curing of onions for control of neck rot (*Botrytis allii* Munn). New Zealand journal of agricultural research 12:592-604.

Haugrud, A. R. P., Zhang, Z., Richards, J. K., Friesen, T. L., and Faris, J. D. 2019. Genetics of variable disease expression conferred by inverse gene-for-gene interactions in the wheat-*Parastagonospora nodorum* pathosystem. Plant physiology 180:420-434.

Have, A. t., Mulder, W., Visser, J., and van Kan, J. A. 1998. The endopolygalacturonase gene *Bcpg1* is required for full virulence of *Botrytis cinerea*. Molecular plant-microbe interactions 11:1009-1016.

Hennebert, G. 1973. *Botrytis* and *Botrytis*-like genera. Persoonia 7:183-204.

Hickman, C., and Ashworth, D. 1943. The occurrence of *Botrytis* spp. on onion leaves with special reference to *B. squamosa*. Transactions of the British mycological society 26:153-157.

Hirschi, K., and VanEtten, H. 1996. Expression of the pisatin detoxifying genes (*PDA*) of *Nectria haematococca* in vitro and in planta. Molecular plant-microbe interactions 9:483-491.

Hoff, K. J., Lange, S., Lomsadze, A., Borodovsky, M., and Stanke, M. 2016. BRAKER1: unsupervised RNA-Seq-based genome annotation with GeneMark-ET and AUGUSTUS. Bioinformatics 32:767-769.

Hovius, M., and McDonald, M. 2002. Management of *Allium* white rot [*Sclerotium cepivorum*] in onions on organic soil with soil-applied diallyl disulfide and di-*N*-propyl disulfide. Canadian journal of plant pathology 24:281-286.

Hovius, M. H., and Goldman, I. L. 2004. Evaluation of long-day onions for resistance to white rot infection using greenhouse and laboratory techniques. Journal of the American society for horticultural science 129:258-265.

Huang, D., Bhairi, S., and Staples, R. 1989. A transformation procedure for *Botryotinia squamosa*. Current genetics 15:411-414.

Hwang, S. K., Lee, S. Y., Back, C. G., Kang, I. K., Lee, H. B., Jung, H. Y., and Ohga, S. 2016. No reported species, *Botrytis aclada* causing gray mold neck rot disease on onion bulbs in Korea. Journal of the faculty of agriculture, Kyushu university 61:263-266.

Hyde, K. D., Nilsson, R. H., Alias, S. A., Ariyawansa, H. A., Blair, J. E., Cai, L., de Cock, A. W., Dissanayake, A. J., Glockling, S. L., and Goonasekara, I. D. 2014. One stop shop: backbones trees for important phytopathogenic genera: I. Fungal diversity 67:21-125.

Hyde, P. T., Leckie, B. M., Carpenter, S. C., Lorbeer, J. W., Hoepting, C. A., Ullrich, M. R., and Mutschler, M. A. 2015. Evaluation of onion (*Allium cepa* L.) lines and hybrids possessing *Bs1* for resistance against multiple isolates of *Botrytis squamosa*. Crop science 55:136-145.

I

Ito, S.-i., Ihara, T., Tamura, H., Tanaka, S., Ikeda, T., Kajihara, H., Dissanayake, C., Abdel-Motaal, F. F., and El-Sayed, M. A. 2007. α-Tomatine, the major saponin in tomato, induces programmed cell death mediated by reactive oxygen species in the fungal pathogen *Fusarium oxysporum*. FEBS letters 581:3217-3222.

J

Jarvis, M. C., Forsyth, W., and Duncan, H. J. 1988. A survey of the pectic content of nonlignified monocot cell walls. Plant physiology 88:309-314.

Jutras, P. V., Dodds, I., and van der Hoorn, R. A. 2020. Proteases of *Nicotiana benthamiana*: an emerging battle for molecular farming. Current opinion in biotechnology 61:60-65.

K

Källberg, M., Wang, H., Wang, S., Peng, J., Wang, Z., Lu, H., and Xu, J. 2012. Template-based protein structure modeling using the RaptorX web server. Nature protocols 7:1511-1522.

Kars, I., and van Kan, J. A. 2007. Extracellular enzymes and metabolites involved in pathogenesis of *Botrytis*. Pages 99-118 in: *Botrytis*: Biology, pathology and control. Elad Y., Williamson B., Tudzynski P., and Delen N. (eds) Springer, Dordrecht, The Netherlands.

Kato, M., Masamura, N., Shono, J., Okamoto, D., Abe, T., and Imai, S. 2016. Production and characterization of tearless and non-pungent onion. Scientific reports 6:1-9.

Katoh, K., and Standley, D. M. 2013. MAFFT multiple sequence alignment software version 7: improvements in performance and usability. Molecular biology and evolution 30:772-780.

Keller, N. P., Turner, G., and Bennett, J. W. 2005. Fungal secondary metabolism-from biochemistry to genomics. Nature reviews microbiology 3:937-947.

Khan, M. I., Marroni, V., Keenan, S., Scott, I. A., Viljanen-Rollinson, S. L., and Bulman, S. 2013. Enhanced molecular identification of *Botrytis* spp. from New Zealand onions. European journal of plant pathology 136:495-507.

Khrustaleva, L., and Kik, C. 1998. Cytogenetical studies in the bridge cross *Allium cepa*×(*A. fistulosum*× *A. roylei*). Theoretical and applied genetics 96:8-14.

Kik, C. 2002. Exploitation of wild relatives for the breeding of cultivated *Allium* species. Pages 81-98 in: *Allium* crop science: recent advances. Rabinowitch H. D., and Currah L. (eds) CABI, Wallingford, UK.

Koetle, M., Finnie, J., Balázs, E., and van Staden, J. 2015. A review on factors affecting the *Agrobacterium*-mediated genetic transformation in ornamental monocotyledonous geophytes. South African journal of botany 98:37-44.

Köhl, J., Krijger, M., and Kessel, G. 1992. Drought tolerance of *Botrytis squamosa*, *B. aclada* and potential antagonists. Pages 206-210 in: Advances in *Botrytis* Research. Verhoeff K., Malathrakis N. E., and Williamson B. (eds) Pudoc Scientific Publishers, Wageningen, The Netherlands.

Köhl, J., Belanger, R., and Fokkema, N. 1997. Interaction of four antagonistic fungi with *Botrytis aclada* in dead onion leaves: a comparative microscopic and ultrastructural study. Phytopathology 87:634-642.

Köhl, J., van der Plas, C. H., Molhoek, W. M., and Fokkema, N. J. 1995. Effect of interrupted leaf wetness periods on suppression of sporulation of *Botrytis allii* and *B. cinerea* by antagonists on dead onion leaves. European journal of plant pathology 101:627-637.

Köhl, J., Molhoek, W., Goossen-van de Geijn, H., and van der Plas, C. L. 2003. Potential of *Ulocladium atrum* for biocontrol of onion leaf spot through suppression of sporulation of *Botrytis* spp. BioControl 48:349-359.

Köhl, J., Lombaers-van der Plas, C., Molhoek, W., Kessel, G., and Goossen-van der Geijn, H. 1999. Competitive ability of the antagonists *Ulocladium atrum* and *Gliocladium roseum* at temperatures favourable for *Botrytis* spp. development. BioControl 44:329-346.

Koren, S., Walenz, B. P., Berlin, K., Miller, J. R., Bergman, N. H., and Phillippy, A. M. 2017. Canu: scalable and accurate long-read assembly via adaptive k-mer weighting and repeat separation. Genome research 27:722-736.

Kritzman, G. 1983. Studies on the fungicidal control of bulb rot caused by *Botrytis allii* in onions for the production of seeds. The journal of agricultural science 100:519-525.

Kritzman, G., and Netzer, D. 1978. A selective medium for isolation and identification of *Botrytis* spp. from soil and onion seed. Phytoparasitica 6:3-7.

Krogh, A., Larsson, B., Von Heijne, G., and Sonnhammer, E. L. 2001. Predicting transmembrane protein topology with a hidden Markov model: application to complete genomes. Journal of molecular biology 305:567-580.

Kyung, K. H. 2012. Antimicrobial properties of *Allium* species. Current opinion in biotechnology 23:142-147.

L

Labani, R., and Elkington, T. 1987. Nuclear DNA variation in the genus *Allium* L. (Liliaceae). Heredity 59:119-128.

Lacy, M., and Pontius, G. Prediction of weather-mediated release of conidia of *Botrytis squamosa* from onion leaves in the field. Phytopathology 73:670-676.

Lacy, M., and Lorbeer, J. 2008a. *Botrytis* leaf blight. Pages 26-29 in: Compendium of onion and garlic diseases, second edition. Schwartz H. F., and Mohan S. F. (eds) American Phytopathological Society, St. Paul, MN, USA.

Lacy, M., and Lorbeer, J. 2008b. Neck rot. Pages 47-49 in: Compendium of onion and garlic diseases, second edition. Schwartz H. F., and Mohan S. F. (eds) American Phytopatholigical Society, St. Paul, MN, USA.

Lanzotti, V. 2006. The analysis of onion and garlic. Journal of chromatography A 1112:3-22.

Lanzotti, V., Scala, F., and Bonanomi, G. 2014. Compounds from *Allium* species with cytotoxic and antimicrobial activity. Phytochemistry reviews 13:769-791.

Lanzotti, V., Romano, A., Lanzuise, S., Bonanomi, G., and Scala, F. 2012a. Antifungal saponins from bulbs of white onion, *Allium cepa* L. Phytochemistry 74:133-139.

Lanzotti, V., Barile, E., Antignani, V., Bonanomi, G., and Scala, F. 2012b. Antifungal saponins from bulbs of garlic, *Allium sativum* L. var. Voghiera. Phytochemistry 78:126-134.

Leggett, M., and Rahe, J. 1985. Factors affecting the survival of sclerotia of *Sclerotium cepivorum* in the Fraser Valley of British Columbia. Annals of applied biology 106:255-263.

Leisen, T., Bietz, F., Werner, J., Wegner, A., Schaffrath, U., Scheuring, D., Willmund, F., Mosbach, A., Scalliet, G., and Hahn, M. 2020. CRISPR/Cas with ribonucleoprotein complexes and transiently selected telomere vectors allows highly efficient marker-free and multiple genome editing in *Botrytis cinerea*. Plos pathogens 16:e1008326.

Lenarčič, T., Pirc, K., Hodnik, V., Albert, I., Borišek, J., Magistrato, A., Nürnberger, T., Podobnik, M., and Anderluh, G. 2019. Molecular basis for functional diversity among microbial Nep1-like proteins. Plos pathogens 15:e1007951.

Lenarčič, T., Albert, I., Böhm, H., Hodnik, V., Pirc, K., Zavec, A. B., Podobnik, M., Pahovnik, D., Žagar, E., and Pruitt, R. 2017. Eudicot plant-specific sphingolipids determine host selectivity of microbial NLP cytolysins. Science 358:1431-1434.

Leontiev, R., Hohaus, N., Jacob, C., Gruhlke, M. C., and Slusarenko, A. J. 2018. A comparison of the antibacterial and antifungal activities of thiosulfinate analogues of allicin. Scientific reports 8:1-19.

Li, C., Schmidt, N. E., and Gitaitis, R. 2011. Detection of onion postharvest diseases by analyses of headspace volatiles using a gas sensor array and GC-MS. LWT-food science and technology 44:1019-1025.

Li, J., Faino, L., and Thomma, B. P. 2019. A single effector mediates pathogenicity of *Verticillium dahliae* on tomato. Identification of host-specific effectors mediating pathogenicity of the vascular wilt pathogen *Verticillium dahliae*. Dissertation Wageningen University:59-81.

Li, L., Stoeckert, C. J., and Roos, D. S. 2003. OrthoMCL: identification of ortholog groups for eukaryotic genomes. Genome research 13:2178-2189.

Lin, M.-W., Watson, J. F., and Baggett, J. R. 1995. Inheritance of resistance to neck-rot disease incited by *Botrytis allii* in bulb onions. Journal of the American society for horticultural science 120:297-299.

Lind, A. L., Wisecaver, J. H., Lameiras, C., Wiemann, P., Palmer, J. M., Keller, N. P., Rodrigues, F., Goldman, G. H., and Rokas, A. 2017. Drivers of genetic diversity in secondary metabolic gene clusters within a fungal species. Plos biology 15:e2003583.

Linfield, C. A., Kenny, S. R., and Lyons, N. F. 1995. A serological test for detecting *Botrytis allii*, the cause of neck rot of onion bulbs. Annals of applied biology 126:259-268.

Liu, Z., Faris, J., Meinhardt, S., Ali, S., Rasmussen, J., and Friesen, T. 2004. Genetic and physical mapping of a gene conditioning sensitivity in wheat to a partially purified host-selective toxin produced by *Stagonospora nodorum*. Phytopathology 94:1056-1060.

Liu, Z., Faris, J. D., Oliver, R. P., Tan, K.-C., Solomon, P. S., McDonald, M. C., McDonald, B. A., Nunez, A., Lu, S., and Rasmussen, J. B. 2009. SnTox3 acts in effector triggered susceptibility to induce disease on wheat carrying the *Snn3* gene. Plos pathogens 5:e1000581.

Liu, Z., Zhang, Z., Faris, J. D., Oliver, R. P., Syme, R., McDonald, M. C., McDonald, B. A., Solomon, P. S., Lu, S., and Shelver, W. L. 2012. The cysteine rich necrotrophic effector SnTox1 produced by *Stagonospora nodorum* triggers susceptibility of wheat lines harboring *Snn1*. Plos Pathogens 8:e1002467.

Lorang, J. M., Sweat, T. A., and Wolpert, T. J. 2007. Plant disease susceptibility conferred by a "resistance" gene. Proceedings of the national academy of sciences 104:14861-14866.

Lorbeer, J. 1992. *Botrytis* leaf blight of onion. Pages 186-211 in: Plant diseases of international importance. Volume II. Diseases of vegetables and oil seed crops. Chaube H., Kumar J., Mukhopadhyay A., and Singh U. (eds) Pretice-Hall, Inc., Englewood Cliffs, NJ, USA.

Lorbeer, J., and Tichelaar, G. 1970. A selective medium for the assay of *Botrytis allii* in organic and mineral soils. Phytopathology 60:1301.

Lorbeer, J. W., Seyb, A. M., de Boer, M., and van den Ende, J. E. 2007. *Botrytis* species on bulb crops. Pages 273-294 in: *Botrytis*: Biology, pathology and control. Elad Y., Williamson B., Tudzynski P., and Delen N. (eds) Springer, Dordrecht, The Netherlands.

Love, J. et al. 2019. nextgenusfs/funannotate: funannotate Version 1.5.3. Available from: https://github.com/nextgenusfs/funannotate. Accessed June 2018.

Lupien, S. L., Hellier, B. C., Dugan, F. M., Skoglund, L. G., and Ward, K. F. 2013. White rot of garlic and onion (causal agent, *Sclerotium cepivorum*): A status report from the Pacific Northwest. Plant health progress 14:33.

M

Ma, L.-J., van der Does, H. C., Borkovich, K. A., Coleman, J. J., Daboussi, M.-J., Di Pietro, A., Dufresne, M., Freitag, M., Grabherr, M., and Henrissat, B. 2010. Comparative genomics reveals mobile pathogenicity chromosomes in *Fusarium*. Nature 464:367-373.

Maddison, W. P., and Maddison, D. R. 2019. Mesquite: a modular system for evolutionary analysis. Version 3.61. Available from: http://www.mesquiteproject.org. Accessed July 2020.

Mansfield, J. 2000. Antimicrobial compounds and resistance. Pages 325-370 in: Mechanisms of resistance to plant diseases. Slusarenko A. J., Fraser R. S. S., and van Loon L.C. (eds) Springer, Dordrecht, The Netherlands.

Mansfield, J., and Richardson, A. 1981. The ultrastructure of interactions between *Botrytis* species and broad bean leaves. Physiological plant pathology 19:41-48.

Martin-Hernandez, A., Dufresne, M., Hugouvieux, V., Melton, R., and Osbourn, A. 2000. Effects of targeted replacement of the tomatinase gene on the interaction of *Septoria lycopersici* with tomato plants. Molecular plant-microbe interactions 13:1301-1311.

Maude, R. 1983. The correlation between seed-borne infection by *Botrytis allii* and neck rot development in store. Seed science and technology 11:829-834.

Maude, R., and Presly, A. 1977a. Neck rot (*Botrytis allii*) of bulb onions: I. Seed-borne infection and its relationship to the disease in the onion crop. Annals of applied biology 86:163-180.

Maude, R., and Presly, A. 1977b. Neck rot (*Botrytis allii*) of bulb onions: II. Seed-borne infection in relationship to the disease in store and the effect of seed treatment. Annals of applied biology 86:181-188.

Maude, R., Shipway, M., Presly, A., and O'connor, D. 1984. The effects of direct harvesting and drying systems on the incidence and control of neck rot (*Botrytis allii*) in onions. Plant pathology 33:263-268.

Mbengue, M., Navaud, O., Peyraud, R., Barascud, M., Badet, T., Vincent, R., Barbacci, A., and Raffaele, S. 2016. Emerging trends in molecular interactions between plants and the broad host range fungal pathogens *Botrytis cinerea* and *Sclerotinia sclerotiorum*. Frontiers in plant science 7:422.

McDonald, M. C., Taranto, A. P., Hill, E., Schwessinger, B., Liu, Z., Simpfendorfer, S., Milgate, A., and Solomon, P. S. 2019. Transposon-mediated horizontal transfer of the host-specific virulence protein ToxA between three fungal wheat pathogens. MBio 10:e01515-19.

McLean, K., Swaminathan, J., and Stewart, A. 2001. Increasing soil temperature to reduce sclerotial viability of *Sclerotium cepivorum* in New Zealand soils. Soil biology and biochemistry 33:137-143.

Medema, M. H., Kottmann, R., Yilmaz, P., Cummings, M., Biggins, J. B., Blin, K., De Bruijn, I., Chooi, Y. H., Claesen, J., and Coates, R. C. 2015. Minimum information about a biosynthetic gene cluster. Nature chemical biology 11:625-631.

Mercier, A., Carpentier, F., Duplaix, C., Auger, A., Pradier, J. M., Viaud, M., Gladieux, P., and Walker, A. S. 2019. The polyphagous plant pathogenic fungus *Botrytis cinerea* encompasses host-specialized and generalist populations. Environmental microbiology 21:4808-4821.

Metcalf, D., and Wilson, C. 1999. Histology of *Sclerotium cepivorum* infection of onion roots and the spatial relationships of pectinases in the infection process. Plant pathology 48:445-452.

Metcalf, D., and Wilson, C. 2001. The process of antagonism of *Sclerotium cepivorum* in white rot affected onion roots by *Trichoderma koningii*. Plant pathology 50:249-257.

Metcalf, D., Dennis, J., and Wilson, C. 1997. First report of the large sclerotial form of *Sclerotium cepivorum* in Australia. Australasian plant pathology 26:203-203.

Mikhail, S., Stewart, D., El Haggagy, M. K., and Wilkinson, R. 1974. The role of grazing animals in the dissemination of the onion white-rot pathogen in Egypt. FAO plant protection bulletin 22:37-41.

Min, B., Grigoriev, I. V., and Choi, I.-G. 2017. FunGAP: Fungal Genome Annotation Pipeline using evidence-based gene model evaluation. Bioinformatics 33:2936-2937.

Miñambres, G. G., Conles, M. Y., Lucini, E. I., Verdenelli, R. A., Meriles, J. M., and Zygadlo, J. A. 2010. Application of thymol and iprodione to control garlic white rot (*Sclerotium cepivorum*) and its effect on soil microbial communities. World journal of microbiology and biotechnology 26:161-170.

Misawa, T., and Takeuchi, M. 2015. Species composition of *Botrytis* leaf blight pathogens of Chinese chives and their seasonal and annual changes in Hokkaido, Japan. Journal of general plant pathology 81:218-225.

Möller, M., and Stukenbrock, E. H. 2017. Evolution and genome architecture in fungal plant pathogens. Nature reviews microbiology 15:756.

Morris, R., and Lane, S. 1990. Further observations on the interaction between *Trichoderma viride* and *Botrytis* species. Mycologist 4:195-197.

N

Navarro-Muñoz, J. C., and Collemare, J. 2020. Evolutionary histories of type III polyketide synthases in fungi. Frontiers in microbiology 10:3018.

Navarro-Muñoz, J. C., Selem-Mojica, N., Mullowney, M. W., Kautsar, S. A., Tryon, J. H., Parkinson, E. I., De Los Santos, E. L., Yeong, M., Cruz-Morales, P., and Abubucker, S. 2020. A computational framework to explore large-scale biosynthetic diversity. Nature chemical biology 16:60-68.

Nguyen, L.-T., Schmidt, H. A., Von Haeseler, A., and Minh, B. Q. 2015. IQ-TREE: a fast and effective stochastic algorithm for estimating maximum-likelihood phylogenies. Molecular biology and evolution 32:268-274.

Nielsen, K., and Yohalem, D. S. 2001. Origin of a polyploid *Botrytis* pathogen through interspecific hybridization between *Botrytis aclada* and *B. byssoidea*. Mycologia 93:1064-1071.

Nielsen, K., Yohalem, D. S., and Jensen, D. F. 2002. PCR detection and RFLP differentiation of *Botrytis* species associated with neck rot of onion. Plant disease 86:682-686.

Nielsen, K., Justesen, A. F., Jensen, D. F., and Yohalem, D. S. 2001. Universally primed polymerase chain reaction alleles and internal transcribed spacer restriction fragment length polymorphisms distinguish two subgroups in *Botrytis aclada* distinct from *B. byssoidea*. Phytopathology 91:527-533.

Noda, J., Brito, N., and González, C. 2010. The *Botrytis cinerea* xylanase Xyn11A contributes to virulence with its necrotizing activity, not with its catalytic activity. BMC plant biology 10:1-15.

O

Ökmen, B., Etalo, D. W., Joosten, M. H., Bouwmeester, H. J., de Vos, R. C., Collemare, J., and de Wit, P. J. 2013. Detoxification of α-tomatine by *Cladosporium fulvum* is required for full virulence on tomato. New phytologist 198:1203-1214.

Oleszek, M., and Oleszek, W. 2020. Saponins in Food. In: Handbook of Dietary Phytochemicals. Xiao J., Sarker S., and Asakawa J. (eds) Springer, Singapore.

Oleszek, W., Kapusta, I., and Stochmal, A. 2008. TLC of Triterpenes (Including Saponins). Pages 519-542 in: Thin Layer Chromatography in Phytochemistry. Waksmundzka-Hajnos M., Sherma J., and Kowalska T. (eds) Taylor & Francis Group, Boca Raton, Gl, USA.

Oliver, R. P., Friesen, T. L., Faris, J. D., and Solomon, P. S. 2012. *Stagonospora nodorum*: from pathology to genomics and host resistance. Annual review of phytopathology 50:23-43.

Oome, S., Raaymakers, T. M., Cabral, A., Samwel, S., Böhm, H., Albert, I., Nürnberger, T., and van den Ackerveken, G. 2014. Nep1-like proteins from three kingdoms of life act as a microbe-associated molecular pattern in *Arabidopsis*. Proceedings of the national academy of sciences 111:16955-16960.

Osbourn, A. E. 1996. Preformed antimicrobial compounds and plant defense against fungal attack. The plant cell 8:1821.

Ottmann, C., Luberacki, B., Küfner, I., Koch, W., Brunner, F., Weyand, M., Mattinen, L., Pirhonen, M., Anderluh, G., and Seitz, H. U. 2009. A common toxin fold mediates microbial attack and plant defense. Proceedings of the national academy of sciences 106:10359-10364.

Owen, J., Walker, J., and Stahmann, M. 1950. Variability in onion neck rot fungi. Phytopathology 40:749-768.

P

Page, O. 1953. *Botrytis* spot of onion leaves in Ontario. Plant disease reporter 37:513-514.

Papadopoulou, K., Melton, R., Leggett, M., Daniels, M., and Osbourn, A. 1999. Compromised disease resistance in saponin-deficient plants. Proceedings of the national academy of sciences 96:12923-12928.

Pareja-Jaime, Y., Roncero, M. I. G., and Ruiz-Roldán, M. C. 2008. Tomatinase from *Fusarium oxysporum* f. sp. *lycopersici* is required for full virulence on tomato plants. Molecular plant-microbe interactions 21:728-736.

Pavan, S., Jacobsen, E., Visser, R. G., and Bai, Y. 2010. Loss of susceptibility as a novel breeding strategy for durable and broad-spectrum resistance. Molecular breeding 25:1-12.

Pedro, H., Yates, A. D., Kersey, P. J., and De Silva, N. H. 2019. Collaborative annotation redefines gene sets for crucial phytopathogens. Frontiers in microbiology 10:2477.

Perez-Moreno, L., Olalde-Portugal, V., Sanchez-Pale, J., and Entwistle, A. 1999. Characteristics of *Sclerotium cepivorum* Berk. sclerotia from a single infested field in Mexico. Phyton-International journal of experimental botany 65:131-141.

Petersen, T. N., Brunak, S., Von Heijne, G., and Nielsen, H. 2011. SignalP 4.0: discriminating signal peptides from transmembrane regions. Nature methods 8:785-786.

Pfaffl, M. W. 2001. A new mathematical model for relative quantification in real-time RT–PCR. Nucleic acids research 29:e45-e45.

Pfaffl, M. W., Horgan, G. W., and Dempfle, L. 2002. Relative expression software tool (REST©) for group-wise comparison and statistical analysis of relative expression results in real-time PCR. Nucleic acids research 30:e36-e36.

Phan, H. T., Rybak, K., Furuki, E., Breen, S., Solomon, P. S., Oliver, R. P., and Tan, K. C. 2016. Differential effector gene expression underpins epistasis in a plant fungal disease. The plant journal 87:343-354.

Pinedo, C., Wang, C.-M., Pradier, J.-M., Dalmais, B., Choquer, M., Le Pêcheur, P., Morgant, G., Collado, I. G., Cane, D. E., and Viaud, M. 2008. Sesquiterpene synthase from the botrydial biosynthetic gene cluster of the phytopathogen *Botrytis cinerea*. ACS chemical biology 3:791-801.

Podila, G. K., Rogers, L. M., and Kolattukudy, P. E. 1993. Chemical signals from avocado surface wax trigger germination and appressorium formation in *Colletotrichum gloeosporioides*. Plant physiology 103:267-272.

Porquier, A., Moraga, J., Morgant, G., Dalmais, B., Simon, A., Sghyer, H., Collado, I. G., and Viaud, M. 2019. Botcinic acid biosynthesis in *Botrytis cinerea* relies on a subtelomeric gene cluster surrounded by relics of transposons and is regulated by the Zn_2Cys_6 transcription factor BcBoa13. Current genetics 65:965-980.

Porquier, A., Morgant, G., Moraga, J., Dalmais, B., Luyten, I., Simon, A., Pradier, J.-M., Amselem, J., Collado, I. G., and Viaud, M. 2016. The botrydial biosynthetic gene cluster of *Botrytis cinerea* displays a bipartite genomic structure and is positively regulated by the putative $Zn(II)_2Cys_6$ transcription factor BcBot6. Fungal genetics and biology 96:33-46.

Presly, A. 1984. Retention of iprodione on salad onion leaves in relation to the control of *Botrytis* spp. Plant pathology 33:571-580.

Presly, A. 1985. Studies on *Botrytis* spp. occurring on onions (*Allium cepa*) and leeks (*Allium porrum*). Plant pathology 34:422-427.

Presly, A., and Maude, R. 1982. Tolerance in *Botrytis squamosa* to iprodione. Annals of applied biology 100:117-127.

Presti, L. L., and Kahmann, R. 2017. How filamentous plant pathogen effectors are translocated to host cells. Current opinion in plant biology 38:19-24.

Prithiviraj, B., Vikram, A., Kushalappa, A., and Yaylayan, V. 2004. Volatile metabolite profiling for the discrimination of onion bulbs infected by *Erwinia carotovora* ssp. *carotovora*, *Fusarium oxysporum* and *Botrytis allii*. European journal of plant pathology 110:371-377.

Q

Quidde, T., Osbourn, A., and Tudzynski, P. 1998. Detoxification of α-tomatine by *Botrytis cinerea*. Physiological and molecular plant pathology 52:151-165.

Qutob, D., Kemmerling, B., Brunner, F., Küfner, I., Engelhardt, S., Gust, A. A., Luberacki, B., Seitz, H. U., Stahl, D., and Rauhut, T. 2006. Phytotoxicity and innate immune responses induced by Nep1-like proteins. The plant cell 18:3721-3744.

R

Ramakers, C., Ruijter, J. M., Deprez, R. H. L., and Moorman, A. F. 2003. Assumption-free analysis of quantitative real-time polymerase chain reaction (PCR) data. Neuroscience letters 339:62-66.

Reynolds, H. T., Vijayakumar, V., Gluck-Thaler, E., Korotkin, H. B., Matheny, P. B., and Slot, J. C. 2018. Horizontal gene cluster transfer increased hallucinogenic mushroom diversity. Evolution letters 2:88-101.

Richards, J. K., Stukenbrock, E. H., Carpenter, J., Liu, Z., Cowger, C., Faris, J. D., and Friesen, T. L. 2019. Local adaptation drives the diversification of effectors in the fungal wheat pathogen *Parastagonospora nodorum* in the United States. Plos genetics 15:e1008223.

Rivera-Mendez, W., Obregón, M., Moran-Diez, M. E., Hermosa, R., and Monte, E. 2020. *Trichoderma asperellum* biocontrol activity and induction of systemic defenses against *Sclerotium cepivorum* in onion plants under tropical climate conditions. Biological control 141:104145.

Robert, X., and Gouet, P. 2014. Deciphering key features in protein structures with the new ENDscript server. Nucleic acids research 42:W320-W324.

Rod, J. 1984. Antagonistic effects of some fungi on fungal pathogens causing storage rots of onion (*Allium cepa*)[*Botrytis*, *Sclerotium*, *Fusarium*, *Gliocladium*, *Trichothecium*, *Trichoderma*, *Penicillium*, *Acremoniella*]. Ceska Mykologie 38:235-239.

Ron, M., and Avni, A. 2004. The receptor for the fungal elicitor ethylene-inducing xylanase is a member of a resistance-like gene family in tomato. The plant cell 16:1604-1615.

Ropars, J., de la Vega, R. C. R., López-Villavicencio, M., Gouzy, J., Sallet, E., Dumas, É., Lacoste, S., Debuchy, R., Dupont, J., and Branca, A. 2015. Adaptive horizontal gene transfers between multiple cheese-associated fungi. Current biology 25:2562-2569.

Rossi, F. R., Gárriz, A., Marina, M., Romero, F. M., Gonzalez, M. E., Collado, I. G., and Pieckenstain, F. L. 2011. The sesquiterpene botrydial produced by *Botrytis cinerea* induces the hypersensitive response on plant tissues and its action is modulated by salicylic acid and jasmonic acid signaling. Molecular plant-microbe interactions 24:888-896.

Roulston, S., and Lane, S. 1988. Observations on the interaction between *Trichoderma viride* and three *Botrytis* species. Mycologist 2:176-177.

Ruud, A. K., Dieseth, J. A., and Lillemo, M. 2018. Effects of three *Parastagonospora nodorum* necrotrophic effectors on spring wheat under Norwegian field conditions. Crop science 58:159-168.

Ruud, A. K., Windju, S., Belova, T., Friesen, T. L., and Lillemo, M. 2017. Mapping of SnTox3–*Snn3* as a major determinant of field susceptibility to Septoria nodorum leaf blotch in the SHA3/CBRD × Naxos population. Theoretical and applied genetics 130:1361-1374.

S

Sammour, R. H., Yehia, A.-G. M., Mustafa, A., and Alhoziem, R. 2011. Biology, controlling and genetic variability in *Sclerotium cepivorum* Berk; the causal agent of *Allium* white rot disease. Microbiology 7:101-111.

Scholten, O., van Heusden, A., Khrustaleva, L., Burger-Meijer, K., Mank, R., Antonise, R., Harrewijn, J., Oost, E., Peters, R., and Kik, C. 2007. The long and winding road leading to the successful introgression of downy mildew resistance into onion. Euphytica 156:345-353.

Scholten, O. E., van Kaauwen, M. P., Shahin, A., Hendrickx, P. M., Keizer, L. P., Burger, K., van Heusden, A. W., van der Linden, C. G., and Vosman, B. 2016. SNP-markers in *Allium* species to facilitate introgression breeding in onion. BMC plant biology 16:187.

Schouten, A., van Baarlen, P., and van Kan, J. A. 2008. Phytotoxic Nep1-like proteins from the necrotrophic fungus *Botrytis cinerea* associate with membranes and the nucleus of plant cells. New phytologist 177:493-505.

Schouten, A., Wagemakers, L., Stefanato, F. L., van der Kaaij, R. M., and van Kan, J. A. 2002. Resveratrol acts as a natural profungicide and induces self-intoxication by a specific laccase. Molecular microbiology 43:883-894.

Schumacher, J. 2012. Tools for *Botrytis cinerea*: new expression vectors make the gray mold fungus more accessible to cell biology approaches. Fungal genetics and biology 49:483-497.

Schürch, S., Linde, C. C., Knogge, W., Jackson, L. F., and McDonald, B. A. 2004. Molecular population genetic analysis differentiates two virulence mechanisms of the fungal avirulence gene *NIP1*. Molecular plant-microbe interactions 17:1114-1125.

Schwartz, H. F., and Mohan, S. K. 2008. Compendium of onion and garlic diseases and pests, second edition. American Phytopathological Society, St. Paul, MN, USA.

Seidl, M. F., and van den Ackerveken, G. 2019. Activity and phylogenetics of the broadly occurring family of microbial Nep1-like proteins. Annual review of phytopathology 57:367-386.

Shannon, P., Markiel, A., Ozier, O., Baliga, N. S., Wang, J. T., Ramage, D., Amin, N., Schwikowski, B., and Ideker, T. 2003. Cytoscape: a software environment for integrated models of biomolecular interaction networks. Genome research 13:2498-2504.

Shen, X.-X., Steenwyk, J. L., LaBella, A. L., Opulente, D. A., Zhou, X., Kominek, J., Li, Y., Groenewald, M., Hittinger, C. T., and Rokas, A. 2020. Genome-scale phylogeny and contrasting modes of genome evolution in the fungal phylum Ascomycota. Science advances 6:eabd0079.

Shi-Kunne, X., Faino, L., van den Berg, G. C., Thomma, B. P., and Seidl, M. F. 2018. Evolution within the fungal genus *Verticillium* is characterized by chromosomal rearrangement and gene loss. Environmental microbiology 20:1362-1373.

Shi, G., Friesen, T. L., Saini, J., Xu, S. S., Rasmussen, J. B., and Faris, J. D. 2015. The wheat *Snn7* gene confers susceptibility on recognition of the *Parastagonospora nodorum* necrotrophic effector SnTox7. The plant genome 8:1-10.

Shi, G., Zhang, Z., Friesen, T. L., Bansal, U., Cloutier, S., Wicker, T., Rasmussen, J. B., and Faris, J. D. 2016. Marker development, saturation mapping, and high-resolution mapping of the Septoria nodorum blotch susceptibility gene *Snn3-B1* in wheat. Molecular genetics and genomics 291:107-119.

Shimodaira, H. 2002. An approximately unbiased test of phylogenetic tree selection. Systematic biology 51:492-508.

Shirane, N., Masuko, M., and Hayashi, Y. 1989. Light microscopic observation of nuclei and mitotic chromosomes of *Botrytis* species. Phytopathology 79:728-730.

Shlezinger, N., Minz, A., Gur, Y., Hatam, I., Dagdas, Y. F., Talbot, N. J., and Sharon, A. 2011. Anti-apoptotic machinery protects the necrotrophic fungus *Botrytis cinerea* from host-induced apoptotic-like cell death during plant infection. Plos Pathogens 7:e1002185.

Shoemaker, P., and Lorbeer, J. 1977a. Timing initial fungicide application to control *Botrytis* leaf blight epidemics on onions. Phytopathology 67:409-414.

Shoemaker, P., and Lorbeer, J. 1977b. The role of dew and temperature in the epidemiology of *Botrytis* leaf blight of onion. Phytopathology 67:1267-1272.

Siewers, V., Viaud, M., Jimenez-Teja, D., Collado, I. G., Gronover, C. S., Pradier, J.-M., Tudzynsk, B., and Tudzynski, P. 2005. Functional analysis of the cytochrome P450 monooxygenase gene *bcbot1* of *Botrytis cinerea* indicates that botrydial is a strain-specific virulence factor. Molecular plant-microbe interactions 18:602-612.

Simão, F. A., Waterhouse, R. M., Ioannidis, P., Kriventseva, E. V., and Zdobnov, E. M. 2015. BUSCO: assessing genome assembly and annotation completeness with single-copy orthologs. Bioinformatics 31:3210-3212.

Sipos, G., Prasanna, A. N., Walter, M. C., O'Connor, E., Bálint, B., Krizsán, K., Kiss, B., Hess, J., Varga, T., and Slot, J. 2017. Genome expansion and lineage-specific genetic innovations in the forest pathogenic fungi *Armillaria*. Nature ecology & evolution 1:1931-1941.

Slot, J. C., and Gluck-Thaler, E. 2019. Metabolic gene clusters, fungal diversity, and the generation of accessory functions. Current opinion in genetics & development 58:17-24.

Sobolewska, D., Michalska, K., Podolak, I., and Grabowska, K. 2016. Steroidal saponins from the genus *Allium*. Phytochemistry reviews 15:1-35.

Soltis, N. E., Atwell, S., Shi, G., Fordyce, R., Gwinner, R., Gao, D., Shafi, A., and Kliebenstein, D. J. 2019. Interactions of tomato and *Botrytis cinerea* genetic diversity: parsing the contributions of host differentiation, domestication, and pathogen variation. The plant cell 31:502-519.

Sood, P., Bhattacharya, A., and Sood, A. 2011. Problems and possibilities of monocot transformation. Biologia plantarum 55:1-15.

Spatafora, J. W., Aime, M. C., Grigoriev, I. V., Martin, F., Stajich, J. E., and Blackwell, M. 2017. The fungal tree of life: from molecular systematics to genome-scale phylogenies. The fungal kingdom:1-34.

Sperschneider, J., Gardiner, D. M., Dodds, P. N., Tini, F., Covarelli, L., Singh, K. B., Manners, J. M., and Taylor, J. M. 2016. EffectorP: predicting fungal effector proteins from secretomes using machine learning. New phytologist 210:743-761.

Staats, M., van Baarlen, P., and van Kan, J. A. 2005. Molecular phylogeny of the plant pathogenic genus *Botrytis* and the evolution of host specificity. Molecular biology and evolution 22:333-346.

Staats, M., van Baarlen, P., and van Kan, J. A. 2007a. AFLP analysis of genetic diversity in populations of *Botrytis elliptica* and *Botrytis tulipae* from the Netherlands. European journal of plant pathology 117:219-235.

Staats, M., van Baarlen, P., Schouten, A., and van Kan, J. A. 2007b. Functional analysis of NLP genes from *Botrytis elliptica*. Molecular plant pathology 8:209-214.

Staats, M., van Baarlen, P., Schouten, A., van Kan, J. A., and Bakker, F. T. 2007c. Positive selection in phytotoxic protein-encoding genes of *Botrytis* species. Fungal genetics and biology 44:52-63.

Stamatakis, A. 2014. RAxML version 8: a tool for phylogenetic analysis and post-analysis of large phylogenies. Bioinformatics 30:1312-1313.

Stanke, M., Schöffmann, O., Morgenstern, B., and Waack, S. 2006. Gene prediction in eukaryotes with a generalized hidden Markov model that uses hints from external sources. BMC bioinformatics 7:1-11.

Steentjes, M. B., Scholten, O. E., and van Kan, J. A. 2021a. Peeling the onion: Towards a better understanding of *Botrytis* diseases of onion. Phytopathology 111:464-473.

Steentjes, M. B., Tonn, S., Coolman, H., Langebeeke, S., Scholten, O. E., and van Kan, J. A. 2021b. Visualization of three sclerotiniaceae species pathogenic on onion reveals distinct biology and infection strategies. International journal of molecular sciences 22:1865.

Stergiopoulos, I., and de Wit, P. J. 2009. Fungal effector proteins. Annual review of phytopathology 47:233-263.

Stergiopoulos, I., Collemare, J., Mehrabi, R., and De Wit, P. J. 2013. Phytotoxic secondary metabolites and peptides produced by plant pathogenic *Dothideomycete* fungi. FEMS microbiology reviews 37:67-93.

Stewart, A., and Mansfield, J. 1984. Fungal development and plant response in detached onion, onion bulb scales and leaves inoculated with *Botrytis allii*, *B. cinerea*, *B. fabae* and *B. squamosa*. Plant pathology 33:401-409.

Stewart, A., and Franicevic, S. 1994. Infected seed as a source of inoculum for *Botrytis* infection of onion bulbs in store. Australasian plant pathology 23:36-40.

Stewart, A., Fullerton, R., and Sutherland, P. 1989a. Infection of onion by the white rot pathogen, *Sclerotium cepivorum*. Journal of phytopathology 126:33-42.

Stewart, A., Backhouse, D., Sutherland, P., and Fullerton, R. 1989b. The Development of Infection Structures of *Sderotium cepivorum* on Onion. Journal of phytopathology 126:22-32.

Stice, S. P., Thao, K. K., Khang, C. H., Baltrus, D. A., Dutta, B., and Kvitko, B. H. 2020. Thiosulfinate tolerance is a virulence strategy of an atypical bacterial pathogen of onion. Current biology 30:3130-3140. e3136.

Stice, S. P., Yoon Shin, G., De Armas, S., Koirala, S., Galván, G. A., Siri, M. I., Severns, P. M., Coutinho, T. A., Dutta, B., and Kvitko, B. H. 2021. The distribution of onion virulence gene clusters among *Pantoea* spp. Frontiers in plant science 12:384.

Stukenbrock, E. H., and McDonald, B. A. 2007. Geographical variation and positive diversifying selection in the host-specific toxin *SnToxA*. Molecular plant pathology 8:321-332.

Sutton, J., Swanton, C., and Gillespie, T. 1978. Relation of weather variables and host factors to incidence of airborne spores of *Botrytis squamosa*. Canadian journal of botany 56:2460-2469.

Sutton, J., James, T., and Rowell, P. 1983. Relation of weather and host factors to an epidemic of *Botrytis* leaf blight in onions. Canadian journal of plant pathology 5:256-265.

Sutton, J., Rowell, P., and James, T. 1984. Effects of leaf wax, wetness duration and temprature on infection of onion leaves by *Botrytis squamosa*. Phytoprotection 65:65-68.

Sutton, J., James, T., and Rowell, P. 1986. BOTCAST: a forecasting system to time the initial fungicide spray for managing *Botrytis* leaf blight of onions. Agriculture, ecosystems & environment 18:123-143.

T

Tan, K.-C., Oliver, R. P., Solomon, P. S., and Moffat, C. S. 2010. Proteinaceous necrotrophic effectors in fungal virulence. Functional plant biology 37:907-912.

Tan, K.-C., Phan, H. T., Rybak, K., John, E., Chooi, Y. H., Solomon, P. S., and Oliver, R. P. 2015. Functional redundancy of necrotrophic effectors–consequences for exploitation for breeding. Frontiers in plant science 6:501.

Tan, K.-C., Ferguson-Hunt, M., Rybak, K., Waters, O. D., Stanley, W. A., Bond, C. S., Stukenbrock, E. H., Friesen, T. L., Faris, J. D., and McDonald, B. A. 2012. Quantitative variation in effector activity of ToxA isoforms from *Stagonospora nodorum* and *Pyrenophora tritici-repentis*. Molecular plant-microbe interactions 25:515-522.

Tanović, B., Koščica, M., Hrustić, J., Mihajlović, M., Trkulja, V., and Delibašić, G. 2019. *Botrytis squamosa*: The causal agent of onion leaf blight in Bosnia and Herzegovina. Pesticidi i fitomedicina 34:9-17.

Teshima, Y., Ikeda, T., Imada, K., Sasaki, K., El-Sayed, M. A., Shigyo, M., Tanaka, S., and Ito, S.-i. 2013. Identification and biological activity of antifungal saponins from shallot (*Allium cepa* L. Aggregatum group). Journal of agricultural and food chemistry 61:7440-7445.

Tichelaar, G. 1967. Studies on the biology of *Botrytis allii* on *Allium cepa*. Netherlands journal of plant pathology 73:157-160.

Tiku, A. R. 2020. Antimicrobial compounds (phytoanticipins and phytoalexins) and their role in plant defense. Pages 845-868 in: Co-evolution of secondary metabolites. Mérillon J.-M., and Ramawat K. G. (eds) Springer, Cham, Switzerland.

Tremblay, D., Talbot, B., and Carisse, O. 2003. Sensitivity of *Botrytis squamosa* to different classes of fungicides. Plant disease 87:573-578.

Tsuba, M., Katagiri, C., Takeuchi, Y., Takada, Y., and Yamaoka, N. 2002. Chemical factors of the leaf surface involved in the morphogenesis of *Blumeria graminis*. Physiological and molecular plant pathology 60:51-57.

Tyson, J., Fullerton, R., Elliott, G., and Reynolds, P. 2000. Use of diallyl disulphide for the commercial control of *Sclerotium cepivorum*. New Zealand plant protection 53:393-397.

U

Utkhede, R., and Rahe, J. 1978. Screening commercial onion cultivars for resistance to white rot. Phytopathology 68:1080-1083.

Utkhede, R., and Rahe, J. 1984. Resistance to white rot infections in bulb onion seed lots. Scientia horticulturae 22:315-320.

Utkhede, R., Rahe, J., Smith, J. C.-., Meer, Q. V. d., Brewer, J., and Criscola, V. 1982. Genotype-environment interactions for resistance to onion white rot. Canadian journal of plant pathology 4:269-271.

V

Vakirlis, N., Sarilar, V., Drillon, G., Fleiss, A., Agier, N., Meyniel, J.-P., Blanpain, L., Carbone, A., Devillers, H., and Dubois, K. 2016. Reconstruction of ancestral chromosome architecture and gene repertoire reveals principles of genome evolution in a model yeast genus. Genome research 26:918-932.

Valero-Jiménez, C. A., Veloso, J., Staats, M., and van Kan, J. A. 2019. Comparative genomics of plant pathogenic *Botrytis* species with distinct host specificity. BMC genomics 20:1-12.

Valero-Jiménez, C. A., Steentjes, M. B., Slot, J. C., Shi-Kunne, X., Scholten, O. E., and van Kan, J. A. 2020. Dynamics in secondary metabolite gene clusters in otherwise highly syntenic and stable genomes in the fungal genus *Botrytis*. Genome biology and evolution 12:2491-2507.

van Dam, P., Fokkens, L., Ayukawa, Y., van der Gragt, M., ter Horst, A., Brankovics, B., Houterman, P. M., Arie, T., and Rep, M. 2017. A mobile pathogenicity chromosome in *Fusarium oxysporum* for infection of multiple cucurbit species. Scientific reports 7:1-15.

van der Meer, Q., and de Vries, J. 1990. An interspecific cross between *Allium roylei* Stearn and *Allium cepa* L., and its backcross to *A. cepa*. Euphytica 47:29-31.

van der Meer, Q., van Bennekom, J., and van der Giessen, A. 1983. Screening for resistance to white rot caused by *Sclerotium cepivorum* Berk. in onions (*Allium cepa* L.) and leeks (*Allium porrum* L.). Euphytica 32:697-701.

van Kan, J. A. 2006. Licensed to kill: the lifestyle of a necrotrophic plant pathogen. Trends in plant science 11:247-253.

van Kan, J. A., Stassen, J. H., Mosbach, A., van der Lee, T. A., Faino, L., Farmer, A. D., Papasotiriou, D. G., Zhou, S., Seidl, M. F., and Cottam, E. 2017. A gapless genome sequence of the fungus *Botrytis cinerea*. Molecular plant pathology 18:75-89.

van Raamsdonk, L., Ensink, W., van Heusden, A., Vrielink-van Ginkel, M., and Kik, C. 2003. Biodiversity assessment based on cpDNA and crossability analysis in selected species of *Allium* subgenus *Rhizirideum*. Theoretical and applied genetics 107:1048-1058.

Veloso, J., and van Kan, J. A. 2018. Many shades of grey in *Botrytis*–host plant interactions. Trends in plant science 23:613-622.

Vignatti, P., Gonzalez, M. E., Jofré, E. C., Bolívar-Anillo, H. J., Moraga, J., Viaud, M., Collado, I. G., and Pieckenstain, F. L. 2020. Botrydial confers *Botrytis cinerea* the ability to antagonize soil and phyllospheric bacteria. Fungal biology 124:54-64.

Vik, J., and Aastveit, K. 1984. Breeding for resistance to neck rot (*Botrytis allii*) in onions (*Allium cepa*). Euphytica 33:257-262.

Viljanen-Rolinson, S., Maroni, M., and Butler, R. 2007. Reduced sensitivity to carbendazim in isolates of *Botrytis allii*. New Zealand plant protection 60:108-113.

Villanueva, S. L., Malvestiti, M. C., Joosten, M. H., van Ieperen, W., and van Kan, J. A. 2021. Red-light imaging for programmed cell death visualization and quantification in plant-pathogen interactions. Molecular plant pathology:22:361-372.

Vincelli, P., and Lorbeer, J. 1989. BLIGHT-ALERT: A weather-based predictive system for timing fungicide applications on onion before infection periods of *Botrytis squamosa*. Phytopathology 79:493-498.

Voorrips, R. 2002. MapChart: software for the graphical presentation of linkage maps and QTLs. Journal of heredity 93:77-78.

Vu, H. Q., El-Sayed, M. A., Ito, S.-I., Yamauchi, N., and Shigyo, M. 2012. Discovery of a new source of resistance to *Fusarium oxysporum*, cause of *Fusarium* wilt in *Allium fistulosum*, located on chromosome 2 of *Allium cepa* Aggregatum group. Genome 55:797-807.

W

Waalwijk, C., Taga, M., Zheng, S.-L., Proctor, R. H., Vaughan, M. M., and O'Donnell, K. 2018. Karyotype evolution in *Fusarium*. IMA fungus 9:13-26.

Walcott, R., Gitaitis, R., and Langston, D. 2004. Detection of *Botrytis aclada* in onion seed using magnetic capture hybridization and the polymerase chain reaction. Seed Science and Technology 32:425-438.

Walker, A.-S., Gautier, A., Confais, J., Martinho, D., Viaud, M., Le Pêcheur, P., Dupont, J., and Fournier, E. 2011. *Botrytis pseudocinerea*, a new cryptic species causing gray mold in French vineyards in sympatry with *Botrytis cinerea*. Phytopathology 101:1433-1445.

Walker, A. S., Gladieux, P., Decognet, V., Fermaud, M., Confais, J., Roudet, J., Bardin, M., Bout, A., C. Nicot, P., and Poncet, C. 2015. Population structure and temporal maintenance of the multihost fungal pathogen *Botrytis cinerea*: causes and implications for disease management. Environmental microbiology 17:1261-1274.

Walker, J. 1925a. Two undescribed species of *Botrytis* associated with the neck rot disease of onion bulbs. Phytopathology 15:708-713.

Walker, J. C. 1925b. Control of mycelial neck rot of onion by artificial curing. Journal of agricultural research 30:365-373.

Walls, D., and Loughran, S. T. 2011. Tagging recombinant proteins to enhance solubility and aid purification. Protein chromatography:151-175.

Wang, Y., Geer, L. Y., Chappey, C., Kans, J. A., and Bryant, S. H. 2000. Cn3D: sequence and structure views for Entrez. Trends in biochemical sciences 25:300-302.

Ward, M., Wilson, L., Carmona, C., and Turner, G. 1988. The *oliC3* gene of *Aspergillus niger*: isolation, sequence and use as a selectable marker for transformation. Current genetics 14:37-42.

Weber, T., Blin, K., Duddela, S., Krug, D., Kim, H. U., Bruccoleri, R., Lee, S. Y., Fischbach, M. A., Müller, R., and Wohlleben, W. 2015. antiSMASH 3.0–a comprehensive resource for the genome mining of biosynthetic gene clusters. Nucleic acids research 43:W237-W243.

Wong, W., and Hughes, I. 1986. *Sclerotium cepivorum* Berk. in onion (*Allium cepa* L.) crops: isolation and characterization of bacteria antagonistic to the fungus in Queensland. Journal of applied bacteriology 60:57-60.

X

Xu, Z., Harrington, T. C., Gleason, M. L., and Batzer, J. C. 2010. Phylogenetic placement of plant pathogenic *Sclerotium* species among teleomorph genera. Mycologia 102:337-346.

Y

Yadav, D. K., Yadav, N., Yadav, S., Haque, S., and Tuteja, N. 2016. An insight into fusion technology aiding efficient recombinant protein production for functional proteomics. Archives of biochemistry and biophysics 612:57-77.

Yanai, T., and Sato, M. 2000. Purification and characterization of an α-L-rhamnosidase from *Pichia angusta* X349. Bioscience, biotechnology, and biochemistry 64:2179-2185.

Yang, Y., Yang, X., Dong, Y., and Qiu, D. 2018. The *Botrytis cinerea* xylanase BcXyl1 modulates plant immunity. Frontiers in microbiology 9:2535.

Yeats, T. H., and Rose, J. K. 2013. The formation and function of plant cuticles. Plant physiology 163:5-20.

Yohalem, D. S., Nielsen, K., and Nicolaisen, M. 2003. Taxonomic and nomenclatural clarification of the onion neck rotting *Botrytis* species. Mycotaxon 85:175-182.

Yohalem, D. S., Nielsen, K., Green, H., and Funck Jensen, D. 2004. Biocontrol agents efficiently inhibit sporulation of *Botrytis aclada* on necrotic leaf tips but spread to adjacent living tissue is not prevented. FEMS microbiology ecology 47:297-303.

You, Y., and van Kan, J. A. 2021. Bitter and sweet make tomato hard to (b)eat. New phytologist 230:90-100.

Z

Zhang, J., Zhang, L., Li, G.-Q., Yang, L., Jiang, D.-H., Zhuang, W.-Y., and Huang, H.-C. 2010. *Botrytis sinoallii*: a new species of the grey mould pathogen on *Allium* crops in China. Mycoscience 51:421-431.

Zhang, L., Kars, I., Essenstam, B., Liebrand, T. W., Wagemakers, L., Elberse, J., Tagkalaki, P., Tjoitang, D., van den Ackerveken, G., and van Kan, J. A. 2014. Fungal endopolygalacturonases are recognized as microbe-associated molecular patterns by the *Arabidopsis* receptor-like protein RESPONSIVENESS TO BOTRYTIS POLYGALACTURONASES1. Plant physiology 164:352-364.

Zhu, W., Ronen, M., Gur, Y., Minz-Dub, A., Masrati, G., Ben-Tal, N., Savidor, A., Sharon, I., Eizner, E., and Valerius, O. 2017. BcXYG1, a secreted xyloglucanase from *Botrytis cinerea*, triggers both cell death and plant immune responses. Plant physiology 175:438-456.

Summary

Onion is a vegetable crop that is consumed and cultivated worldwide. The production of bulbs, however, is threatened by pathogens and pests that infect onion plants and cause yield losses. Three severe diseases of onion are leaf blight, neck rot and white rot and all three are caused by fungi of the family Sclerotiniaceae. In **chapter 1**, the long history of Sclerotiniaceae diseases of onion is discussed, and an overview of the disease etiology and current status of control strategies is given. Leaf blight is a foliar disease of onion caused by *Botrytis squamosa* that can lead to serious yield losses due to its fast progression and air-borne conidia that can easily spread. Neck rot is a post-harvest disease that manifests in bulbs after storage and which can be caused by either of three *Botrytis* species: *B. aclada*, *B. allii* and *B. byssoidea*. The symptomless infection of onion plants in the field makes it difficult to predict the incidence of neck rot in storage. White rot is a soil-borne disease of onion bulbs caused by *Sclerotium cepivorum* and is devastating to continued onion cultivation in production fields. Sclerotia of *S. cepivorum* can survive in soil for decades, making it difficult to develop control strategies. In this thesis project, I studied several aspects of the plant-pathogen interaction with the aim to unravel the biology of *Botrytis* species and *S. cepivorum* pathogenic on onion. New fundamental insights into the genetic, biochemical, molecular and cellular aspects of the interaction of *Botrytis* species and *S. cepivorum* with their host onion are essential to develop new breeding strategies for resistant onion cultivars as a durable solution to leaf blight, neck rot and white rot.

To get a better understanding of the infection biology of the fungal pathogens of onion, visualisation of the infection process is very informative. In **chapter 2**, we transformed *B. squamosa*, *B. aclada* and *S. cepivorum* with a fluorescent label that allowed to visualize and trace the fungi in their first contact with host tissue. *B. squamosa* entered onion leaves by penetrating the leaf surface through stomata or by growth into anticlinal walls of onion epidermis cells. *B. aclada* did not penetrate the leaf surface but instead formed superficial colonies. These superficial colonies produced new conidia that might contribute to the spread of the disease and potentially infect the neck area of bulb during harvest. *S. cepivorum* entered onion roots via infection cushions and appressorium-like structures. In the non-host tomato, *S. cepivorum* also produced these infection structures, but upon prolonged contact with the tomato root the structures died. The visualization of the infection of all three fungi helped to better understand the development of the disease and the infection strategy of the pathogens.

Onion plants defend themselves against pathogens by producing several compounds with antimicrobial activity. A previous study identified metabolites that belong to the class of saponins, called ceposides, that were specifically present in onion and had antifungal activity. We tested the effect of ceposides on *B. aclada* and *S. cepivorum* and showed a

growth inhibitory activity in a concentration-dependent manner in **chapter 3**. Since *B. aclada* and *S. cepivorum* are specialized pathogens of onion bulbs, we hypothesized that they likely have evolved mechanism to tolerate ceposides. In the genomes of both species, we identified genes that are potentially involved in the detoxification of ceposides. These genes, encoding enzymes that can possibly hydrolyse the terminal sugar residues rhamnose and xylose, were tested for their involvement in ceposide detoxification. Expression analysis and experiments with knockout mutants did not provide evidence that these sugar hydrolases could provide tolerance against ceposides, neither in *B. aclada* nor in *S. cepivorum*.

In **chapter 4**, we attempted to pinpoint the genetic determinants of host specificity in the genus *Botrytis*. We sequenced, assembled and annotated the genomes of onion pathogenic *Botrytis* species and *S. cepivorum*, as well as genomes of *Botrytis* species pathogenic on other hosts. Using a comparative genomics approach, we searched for genes underlying pathogenicity and host specificity for onion. The distribution of genes encoding secreted proteins and secondary metabolite gene clusters was analysed among all sequenced species, and did not reveal any genes that were exclusively present in pathogens of onion or other *Allium* species. Using the newly obtained genomes, we were able to reconstruct the evolution of the genus *Botrytis* and found that chromosomal architecture had remained remarkably similar between species that diverged millions of years ago. In addition, evidence was provided for horizontal transfer of the gene cluster responsible for the production of the phytotoxic metabolite botcinic acid.

In the comparative genomics approach that aimed to resolve specificity of *Botrytis* species infecting onion, we analysed their effector repertoire. Necrotrophic pathogens such as *B. squamosa* use effector proteins that actively induce plant cell death by co-opting the programmed cell death machinery of the host. In **chapter 5**, we aimed to investigate the cell death-inducing activity of effector proteins of *B. squamosa*. In addition to studying the effectors identified by comparative genomics, we assessed the protein composition of a *B. squamosa* liquid culture filtrate that caused necrosis upon infiltration in onion leaves. The cell death-inducing activity of 17 effector proteins was tested by transient expression via *Agrobacterium tumefaciens*-mediated transformation. Also, we produced several effector proteins in *Pichia pastoris* and tested their cell death-inducing activity on onion. Besides the ability of effectors to induce cell death, we also assessed their role in virulence of *B. squamosa* on onion and their genetic diversity among seven *B. squamosa* isolates. One effector, Nep1, was able to rapidly induce a severe cell death response upon infiltration in onion.

The effector Nep1 is not unique for *B. squamosa* since many Nep1-like proteins (NLPs) have been identified in other plant pathogenic microbes. NLPs were reported to have cytolytic activity exclusively on dicot plant species. Since we observed cell death in the

monocot plant onion upon infiltration of *B. squamosa* Nep1, we studied the cytolytic activity of NLPs on monocots in more detail in **chapter 6**. We showed that also NLPs other than *B. squamosa* Nep1 were able to induce cell death in the monocot onion, as well as in maize and lily. A set of eight onion genotypes appeared to be differentially sensitive to NLPs. Analysis of the GIPC sphingolipid composition, a trait that allegedly determines the hitherto assumed dicot-specific NLP activity, revealed that GIPC composition of the onion genotypes did not correlate with their NLP sensitivity. By infiltrating Nep1 protein in an interspecific *Allium* hybrid population, we were able to identify a QTL for *Bs*Nep1 insensitivity that co-localized with a previously identified QTL for *B. squamosa* resistance.

In **chapter 7**, all aspects of the interaction of *Botrytis* species and *S. cepivorum* with their host onion assessed in this thesis are discussed. By integrating the genetic, biochemical, molecular and cellular insights, I describe our attempts to decipher what makes some *Botrytis* species host-specific pathogens of onion. Furthermore, I discuss how the different aspects of onion pathogenicity studied in this thesis can help to identify sources of resistance. Lastly, I describe my vision about the consequences of differences in pathogen biology for developing resistance breeding strategies as a durable solution against leaf blight, neck rot and white rot.

Samenvatting

Ui is een gewas dat wereldwijd wordt geconsumeerd en geteeld. De productie van uien wordt echter bedreigd door pathogenen en plagen die uienplanten infecteren met oogstverliezen tot gevolg. Drie ernstige ziektes van ui zijn bladvlekkenziekte, koprot en witrot, en alle drie worden veroorzaakt door schimmels die behoren tot de familie Sclerotiniaceae. In **hoofdstuk 1** wordt de lange geschiedenis van uienziekten veroorzaakt door Sclerotiniaceae beschreven, en wordt een overzicht gegeven van de etiologie en de huidige status van bestrijdingsstrategieën. Bladvlekkenziekte is een ziekte aan het loof van ui en wordt veroorzaakt door *Botrytis squamosa*. De snelle progressie van de ziekte en de sporen die eenvoudig door de lucht kunnen verspreiden kunnen serieuze oogstverliezen tot gevolg hebben. Koprot is een na-oogst ziekte die zich na bewaring manifesteert in de bol en kan worden veroorzaakt door één van de drie volgende *Botrytis* soorten: *B. aclada*, *B. allii* en *B. byssoidea*. De symptoomloze infectie van uienplanten in het veld maakt het moeilijk om de incidentie van nekrot tijdens bewaring te voorspellen. Witrot is een bodemgebonden uienziekte die wordt veroorzaakt door *Sclerotium cepivorum* en is verwoestend voor productievelden van continue uienteelt. Omdat sclerotia van *S. cepivorum* decennia in de bodem kunnen overleven, is het moeilijk om bestrijdingsstrategieën te ontwikkelen. In dit proefschift heb ik verschillende aspecten van de plant-pathogeen interactie bestudeerd met als doel om inzicht te geven in de biologie van *Botrytis* soorten en *S. cepivorum* pathogeen op ui. Nieuwe fundamentele inzichten in de genetische, biochemische, moleculaire en cellulaire aspecten van de interactie tussen *Botrytis* soorten en *S. cepivorum*, en hun waardplant ui zijn essentieel om nieuwe veredelingsstrategieën voor resistente uienrassen te ontwikkelen als een duurzame oplossing voor bladvlekkenziekte, koprot en witrot.

Om een beter begrip te krijgen van de infectiebiologie van de schimmels pathogeen op ui kan visualisatie van het infectieproces erg informatief zijn. In **hoofdstuk 2** hebben we *B. squamosa*, *B. aclada* en *S. cepivorum* getransformeerd met een fluorescent label dat het mogelijk maakte om de schimmels te visualiseren en traceren tijdens het eerste contact met de waardplant. *B. squamosa* drong het uienblad binnen door de bladoppervlakte te penetreren door huidmondjes, of door tussen anticlinale celwanden van de uienepidermis te groeien. *B. aclada* penetreerde het bladoppervlak niet, maar vormde kolonies op het bladoppervlak. Deze kolonies produceerden nieuwe sporen die zouden kunnen bijdragen aan de verspreiding van de ziekte en potentieel de kop van de bol kunnen infecteren tijdens de oogst. *S. cepivorum* ging wortels van de uienplant binnen via infectiekussens en appressoriumachtige structuren. In tomaat, dat geen waardplant is, produceerde *S. cepivorum* dezelfde infectiestructuren, maar naarmate het contact met de tomatenwortel langer duurde gingen de infectiestructuren dood. De visualisatie van de infectie van alle

drie de schimmels helpt om een beter inzicht te krijgen in de ontwikkeling van de ziekten en de infectiestrategie van de pathogenen.

Uienplanten verdedigen zichzelf tegen pathogenen door verschillende stoffen met antimicrobiële activiteit te produceren. Een voorgaand onderzoek identificeerde metabolieten die behoren tot de klasse van saponinen, genaamd ceposiden, die specifiek in ui aanwezig waren en schimmelwerende activiteit vertoonden. Wij testten het effect van ceposiden op *B. aclada* en *S. cepivorum* en toonden een groeiremmende activiteit in een concentratieafhankelijke manier in **hoofdstuk 3**. Omdat *B. aclada* en *S. cepivorum* gespecialiseerde pathogenen van uienbollen zijn, hypothetiseerden we dat deze schimmels waarschijnlijk tolerantiemechanismen tegen ceposides hebben geëvolueerd. In de genomen van beide soorten hebben we genen geïdentificeerd die potentieel betrokken zijn bij de detoxificatie van ceposiden. Deze genen, die coderen voor enzymen die mogelijk de terminale suikergroepen rhamnose en xylose kunnen hydrolyseren, werden getest op hun betrokkenheid bij de detoxificatie van ceposiden. Expressieanalyse en experimenten met knockout mutanten leverden geen bewijs dat deze suiker hydrolases tolerantie tegen ceposiden konden bieden in *B. aclada* en *S. cepivorum*.

In **hoofdstuk 4** hebben we geprobeerd om de genetische factoren voor waardplant specificiteit in het genus *Botrytis* te bepalen. We sequenceten, assembleerden en annoteerden de genomen van *Botrytis* soorten pathogeen op ui en *S. cepivorum*, evenals de genomen van *Botrytis* soorten pathogeen op andere planten. Met een comparative genomics benadering hebben we gezocht naar genen die ten grondslag liggen aan de pathogeniteit en de waardplant specificiteit voor ui. De verspreiding van genen die coderen voor uitgescheiden eiwitten en secundaire metaboliet genclusters werd geanalyseerd voor alle gesequencende soorten, maar er werden geen genen gevonden die exclusief aanwezig waren in pathogenen van ui of andere *Allium* soorten. Door gebruik te maken van de nieuw verkregen genomen konden we de evolutie van het genus *Botrytis* reconstrueren en achterhaalden we dat de chromosomale architectuur opmerkelijk hetzelfde was gebleven tussen soorten die miljoenen jaren geleden opsplitsten. Daarnaast werd er bewijs geleverd voor horizontale overdracht van het gencluster verantwoordelijk voor de productie van het fytotoxische metaboliet botcinic acid.

Als onderdeel van de comparative genomics benadering om de specificiteit van *Botrytis* soorten pathogeen op ui te verklaren, analyseerden we ook hun effector repertoire. Necrotrofe pathogenen zoals *B. squamosa* gebruiken effector eiwitten die actief celdood in de plant induceren door het geprogrammeerde celdood mechanisme van de waardplant over te nemen. In **hoofdstuk 5** onderzochten we de celdood inducerende activiteit van effector eiwitten van *B. squamosa*. Naast het bestuderen van effectoren die geïdentificeerd waren door comparative genomics, onderzochten we ook de eiwitsamenstelling van *B. squamosa* vloeistof cultuurfiltraat dat necrose veroorzaakte na infiltratie in uienbladeren.

De celdood inducerende activiteit van 17 effector eiwitten werd getest door tijdelijke expressie via *Agrobacterium tumefaciens* transformatie. Daarnaast produceerden we verschillende effector eiwitten in *Pichia pastoris* en testten we de celdood inducerende activiteit van deze eiwitten in ui. Naast het vermogen van effectoren om celdood te induceren hebben we ook hun rol in virulentie van *B. squamosa* op ui getest en hebben we de genetische diversiteit in zeven *B. squamosa* isolaten onderzocht. Eén effector, Nep1, was in staat om snel een sterke celdood reactie te induceren wanneer deze werd geïnfiltreerd in ui.

De effector Nep1 is niet uniek voor *B. squamosa* en er zijn al veel Nep1-achtige eiwitten (NLPs) geïdentificeerd in andere plant pathogene microben. NLPs hebben cytolytische activiteit exclusief op dicotyle plantensoorten. Omdat infiltratie van *B. squamosa* Nep1 een celdood reactie veroorzaakte in de monocotyle plant ui, bestudeerden we de cytolytische activiteit van NLPs op monocotylen in meer detail in **hoofdstuk 6**. We toonden aan dat ook andere NLPs dan *B. squamosa* Nep1 in staat waren om celdood te induceren in de monocotyl ui, evenals in mais en lelie. Een set van acht ui genotypes was differentieel gevoelig voor NLPs. Analyse van de GIPC sfingolipide samenstelling, een eigenschap die naar verluidt de tot nu toe veronderstelde dicotyl specifieke NLP activiteit bepaalt, onthulde dat de GIPC samenstelling van de ui genotypes niet correleerde met hun NLP gevoeligheid. Door het Nep1 eiwit te infiltreren in een interspecifieke *Allium* populatie waren we in staat om een QTL voor *Bs*Nep1 ongevoeligheid te identificeren, die colokaliseerde met een eerder geïdentificeerd QTL voor *B. squamosa* resistentie.

In **hoofdstuk 7** worden alle aspecten van de interactie tussen *Botrytis* soorten en *S. cepivorum*, en hun waardplant ui die aan bod kwamen in dit proefschrift bediscussieerd. Door het integreren van genomische, biochemische, moleculaire en cellulaire inzichten, beschrijf ik onze pogingen om te achterhalen wat sommige *Botrytis* soorten waardplant specifieke pathogenen van ui maakt. Bovendien bediscussieer ik hoe de verschillende aspecten van ui pathogeniteit bestudeerd in dit proefschift kunnen helpen om bronnen van resistentie te identificeren. Ten slotte beschrijf ik mijn visie over de gevolgen van de verschillen in pathogeen biologie voor het ontwikkelen van resistentieveredelingsstrategieën als duurzame oplossing voor bladvlekkenziekte, koprot en witrot.

Acknowledgements

All good things come to an end. I have enjoyed my time as a PhD candidate a lot, and this is the moment to acknowledge all the kind people that I had the privilege to work with during my PhD. I would like to emphasize that a PhD thesis is the result of the shared efforts of many different people, whom I would like to thank.

First I would like to acknowledge my promotor, supervisor and mentor Jan. Whether I needed help regarding laboratory procedures, organizational issues, experimental advice or manuscript writing, your valuable experience and relentless effort and support has always been deeply appreciated! In addition to the excellent supervision and guidance in all aspects of the PhD, I would also like to thank you for inspiring me how to be a great teacher. With your enthusiasm and your inspirational *Botrytis*-storytelling you get people enthusiastic for phytopathology in the most passionate way!

Secondly, I would like to thank my co-promotor and second supervisor Olga. I truly enjoyed our update meetings and your valuable ideas and advice from a plant breeding perspective was always much appreciated.

One of the reasons why I enjoyed my PhD that much was because it was part of a bigger research project. Claudio, you started on the onion project one and a half month before I arrived in the lab. It has been a great pleasure to collaborate with such a friendly person and I want to thank you for all the things I got to learn from you.

Lorena, you arrived at the time when we were in desperate need of some helping hands to support the onion project and I am so happy that you were willing to dive into the deep and had the courage to go for it. With your enthusiasm, humor, music preferences, and open personality, you made the long days in the lab or the transplanting of thousands of onion seedlings so much more fun!

During my PhD, I have had the privilege of supervising six talented students. Michele, Sebastian, Jyotsna, Hilde, Sander, and Christiaan, thank you for all the hard work and efforts which really contributed to this thesis. It was such a pleasure to work with you and I thank all of you for the nice time we have spent together in the lab.

Laura, once you arrived in the lab we teamed up and I am really grateful for your presence and the professional and personal things I have learned from you. Also thank you for being the perfect travel buddy together with Claudio during our trip to the Fungal Genetics Conference in the USA.

Si, I surely want to thank you for being such a nice lab colleague and I could not wish for any other person to share the lab bench with. I really appreciate all the times when I was in need of someone to talk to after experiencing unexpected results and you were open for

discussing the smallest experimental details. Our CRISPR adventure trip to Kaiserslautern together with Laura was very memorable because of the extreme long days of hard work as well as all the fun we had together.

I would also like to thank all other past and current *Botrytis* group members: Henriek, Javier, Michele, Sander, and Yaohua. Thank you for all the great work discussion and the collaborations in the lab, but also for all the nice dinners, dumpling evenings, and barbecues.

If it was not for the PhD students and postdocs in the lab, my time at phytopathology would not have been so much enjoyable. Special thanks to Carolina, Gabriel, Hui, Katharina, Martin and Nick, for all the fun at the coffee table and for your support in the lab.

In addition, I would like to thank all former and present staff members for their support and advice, and for making the laboratory such an enjoyable place to work. Special thanks to Laurens for not only being readily available for technical support, but also for representing De Achterhoek in the lab.

Some people have had a great influence on my career path and without them I probably would never have started the PhD adventure. Meneer Schoemaker, thank you for enthusing me for biology and for sharing your Wageningen experiences in the classroom. André van Lammeren, your enthusiasm for plant cell biology in all BSc courses was really inspiring and sparked my interest into plant cell research. Tijs Ketelaar, thank you for being a great supervisor during my time at the Laboratory of Cell Biology and for giving me the courage to persevere a PhD.

Naast de mensen die op professioneel gebied hebben bijgedragen aan dit proefschrift wil ik ook de belangrijkste personen bedanken die altijd voor me klaarstaan en die me de afgelopen vier jaar hebben gesteund en gemotiveerd. Pap en mam, bedankt voor jullie steun en aanmoediging en voor jullie interesse in mijn onderzoek. Jullie hebben me altijd gemotiveerd om eruit te halen wat erin zit en daarmee hebben jullie zeker bijgedragen aan de totstandkoming van dit proefschrift. Tot slot, dankjewel Kristel voor je onvoorwaardelijke steun en liefde. Ook al was het voor jou af en toe lastig te snappen waar ik me soms zo druk over maakte, jij was degene die altijd voor me klaarstond. Dankzij jou heb ik het doen van een PhD kunnen relativeren en in het juiste perspectief kunnen plaatsen, en samen hebben we dit avontuur tot een succes gemaakt.

About the author

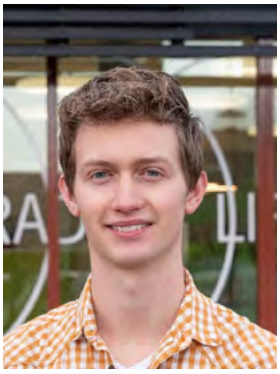

Maikel Steentjes was born on June 29th, 1993 in Gendringen, the Netherlands. After he completed VWO at the Almende Isala College in Silvolde, he went to Wageningen for his BSc studies Biology at the Wageningen University. His interest was aroused by the molecular and genetic aspects of his studies, and therefore he decided to select a major in cell and molecular biology and perform his thesis at the Laboratory of Molecular Biology. After completion of his BSc, Maikel continued with a MSc program in Biology with a specialization in molecular development and gene regulation at the Wageningen University. After his thesis at the Laboratory of Cell Biology under the supervision of Dr Tijs Ketelaar, he got the opportunity to write a grant proposal for a PhD project shared between the Laboratories of Cell Biology and Phytopathology in the framework of the Graduate Program of the Graduate School Experimental Plant Sciences. Since his first encounter with the research field of phytopathology, Maikel was intrigued to find out more about the cellular and molecular interplay between plants and pathogens. As a result, he decided to perform his MSc internship at the breeding company Rijk Zwaan where he worked on downy mildew of lettuce. After completion of the MSc program, Maikel started his PhD at the Laboratory of Phytopathology under the supervision of Dr Jan van Kan. During his PhD, Maikel focused on the molecular aspects of three important fungal pathogens of onion, and the outcome of his research is presented in this thesis.

List of Publications

Steentjes, M.B.F., Scholten, O.E., and van Kan, J.A.L. (2021). Peeling the onion: Towards a better understanding of *Botrytis* diseases of onion. *Phytopathology*, *111*(3), 464-473.

Steentjes, M.B.F., Tonn, S., Coolman, H., Langebeeke, S., Scholten, O.E., and van Kan, J.A.L. (2021). Visualization of three Sclerotiniaceae species pathogenic on onion reveals distinct biology and infection strategies. *International journal of molecular sciences*, *22*(4), 1865.

Valero-Jiménez, C.A., **Steentjes, M.B.F.**, Slot, J.C., Shi-Kunne, X., Scholten, O.E., and van Kan, J.A.L. (2020). Dynamics in secondary metabolite gene clusters in otherwise highly syntenic and stable genomes in the fungal genus *Botrytis*. *Genome biology and evolution*, *12*(12), 2491-2507.

Steentjes, M.B.F., Valderrama, A.L.H., Fouillen, L., Bahammou, D., Leisen, T., Hahn, M., Mongrand, S., Scholten, O.E., and van Kan, J.A.L. Cytolytic activity of NLPs on the monocot *Allium cepa*. *In preparation*.

Tang, H., de Keijzer, J., Overdijk, E.J.R., Sweep, E., **Steentjes, M.B.F.**, Vermeer, J.E. M., Janson, M.E., and Ketelaar, T. (2019). Exocyst subunit Sec6 is positioned by microtubule overlaps in the moss phragmoplast prior to cell plate membrane arrival. *Journal of cell science*, *132*(3).

Education Statement of the Graduate School Experimental Plant Sciences

Issued to: Maikel B. F. Steentjes

Date: 28 June 2021

Group: Laboratory of Phytopathology

University: Wageningen University & Research

1) Start-Up Phase	date	cp
► **First presentation of your project**		
Identifying effector proteins in necrotrophic onion pathogens	03 Nov 2017	1,5
► **Writing or rewriting a project proposal**		
► **MSc courses**		
Subtotal Start-Up Phase		1,5

2) Scientific Exposure	date	cp
► **EPS PhD student days**		
EPS PhD student days 'Get2Gether', Soest, NL	15-16 Feb 2018	0,6
EPS PhD student days 'Get2Gether', Soest, NL	11-12 Feb 2019	0,6
EPS PhD student days 'Get2Gether', Soest, NL	10-11 Feb 2020	0,6
► **EPS theme symposia**		
EPS theme 2 symposium & Willie Commelin Scholten Day 'Interactions between plants and biotic agents', Amsterdam, NL	24 Jan 2018	0,3
EPS theme 2 symposium & Willie Commelin Scholten Day 'Interactions between plants and biotic agents', Wageningen, NL	01 Feb 2019	0,3
EPS theme 2 symposium & Willie Commelin Scholten Day 'Interactions between plants and biotic agents', Utrecht, NL	04 Feb 2020	0,3
EPS theme 2 symposium & Willie Commelin Scholten Day 'Interactions between plants and biotic agents', online	09 Feb 2021	0,2
► **Lunteren Days and other national platforms**		
Annual Meeting 'Experimental Plant Sciences', Lunteren, NL	09-10 Apr 2018	0,6
Annual Meeting 'Experimental Plant Sciences', Lunteren, NL	08-09 Apr 2019	0,6
Annual Meeting 'Experimental Plant Sciences', online	12-13 Apr 2021	0,5
► **Seminars (series), workshops and symposia**		
Symposia		
Host-Microbe Genetics Meeting, Wageningen, NL	27 Oct 2017	0,3
Mini-symposium 'Cell biology of biotic interactions', Wageningen, NL	17 Oct 2019	0,2
Seminars		
Asaf Levy - 'Bacteria and the future of agriculture: from sequence to function'	22 Feb 2018	0,1

Timothy Friesen - 'Genome wide association as a tool for identifying fungal effectors important in virulence'	18 Apr 2018	0,1
Mary Wildermuth - 'Salicylic acid and cell cycle control of plant-microbe interactions'	25 Jun 2018	0,1
Melvin Bolton - 'Sugarbeet pathology - from fungi to viruses'	07 Sep 2018	0,1
Yan Wang - 'A leucine-rich repeat receptor-like protein as PAMP receptor recognising XEG1, a Phytophthora glycoside hydrolase 12'	10 Sep 2018	0,1
Volker Lipka - 'Live and let die or live and let live - Interactions of *Arabidopsis* with fungal pathogens'	14 Sep 2018	0,1
Tom Wood - 'Nanopath: utilising Nanopore sequencing for *Septoria* surveillance'	14 Sep 2018	0,1
Andrea Gust - 'Receptor-like proteins and their adaptor kinase SOBIR1 – just a mimic of receptor kinases'	21 Sep 2018	0,1
Antonio Di Pietro - 'Host adaptation in the fungal cross-kingdom pathogen *Fusarium oxysporum*'	17 Oct 2018	0,1
David Geiser - 'A phylogenomic view of *Fusarium oxysporum* taxonomy and evolution'	30 Oct 2018	0,1
Theo van der Lee - 'From genomes to function: bioinformatics to disclose the obligate biotrophic soilborne fungus *Synchytrium endobioticum*'	18 Jan 2019	0,1
Daniela Sueldo - 'Mining the plant-pathogen interface using activity-based proteomics'	08 Feb 2019	0,1
Ronnie de Jonge - 'Microbial small molecules – weapons of plant subversion'	20 Feb 2019	0,1
Andrea Sanchez-Vallet - 'Competition ability of fungal pathogens'	20 Feb 2019	0,1
Luigi Faino - 'Insights into Nanopore MinION sequencing'	22 Feb 2019	0,1
Nick Talbot - 'Investigating the biology of plant infection by rice blast fungus'	02 Apr 2019	0,1
Yuling Bai - 'Activities and perspectives of the research group Breeding for resistance in *Solanaceae*'	05 Apr 2019	0,1
Daniel Croll - 'Parasites within parasites: how transposable elements drive the evolution of plant pathogenic fungi'	21 Jun 2019	0,1
Rays Jiang - 'Using cutting-edge genomics tools to study host-microbe interactions'	05 Jul 2019	0,1
Eva Stukenbrock - 'Causes and consequences of chromosome instability in a fungal plant pathogen'	13 Dec 2019	0,1
Thorsten Nürnberger - 'Microbial virulence and plant immunity-stimulating activities of microbial cytolysin'	03 Feb 2020	0,1
Peter Solomon - 'How the study of necrotrophic effectors advanced our understanding of the enigmatic PR-1 protein'	20 Apr 2020	0,1
Gert Kema - 'The ongoing pandemic of Tropical Race 4 threatens global banana production'	30 April 2020	0,1
Luigi Faino - 'Evolution of mini-chromosomes in *Fusarium*'	25 May 2020	0,1
Evelien Snelders - 'Evolution of antifungal resistance'	12 Jun 2020	0,1
Duur Aanen - 'Somatic deficiency causes reproductive parasitism in a fungus'	06 Nov 2020	0,1
Xiao Lin - 'Dissect late blight resistance of *Solanum americanum*'	13 Nov 2020	0,1
Sarah Gurr - 'The movement of fungal pathogens: perils and predictions'	15 Jan 2021	0,1
José Lozano - 'Proline-rich extension-like receptor kinases mediate damage-triggered immune responses to nematode infections'	12 Feb 2021	0,1
James Brown - 'Genomic insights into fungicide activities and evolution of resistance'	05 Mar 2021	0,1
Harrold van den Burg - 'Hydathodes: overpressure valves, passive barriers, or devoted immune organelles protecting the plant interior'	19 Mar 2021	0,1

▶	**Seminar plus**		
	Nick Talbot - PhD students Laboratory of Phytopathology	02 Apr 2019	0,1
	Eva Stukenbrock - PhD students Laboratory of Phytopathology	13 Dec 2019	0,1
	Thorsten Nürnberger - PhD students Botrytis group	03 Feb 2020	0,1
	Sarah Gurr - PhD students Laboratory of Phytopathology	15 Jan 2021	0,1
	Harrold van den Burg - PhD students Laboratory of Phytopathology	25 Mar 2021	0,1
▶	**International symposia and congresses**		
	10th European Plant Science Retreat (EPSR), Utrecht, NL	03-06 Jul 2018	1,0
	30th Fungal Genetics Conference, Pacific Grove, CA, USA	12-17 Mar 2019	1,5
	International Society for Molecular Plant-Microbe Interactions (IS-MPMI) XVII Congress, Glasgow, Scotland	14-18 Jul 2019	1,5
	Nep1-like protein (NLP) symposium, Paris, France	12 Feb 2020	0,3
▶	**Presentations**		
	Talk: Kick-off meeting STW user committee	22 Jun 2017	1,0
	Talk: Insect and nonhost resistance group, Plant Breeding	16 Nov 2017	1,0
	Poster: European Plant Science Retreat, Utrecht, NL	05 Jul 2018	1,0
	Poster: Fungal Genetics Conference, Pacific Grove, CA, USA	13 Mar 2019	1,0
	Talk: Insect and nonhost resistance group, Plant Breeding	18 Apr 2019	1,0
	Poster: IS-MPMI Congress, Glasgow, Schotland	17 Jul 2019	1,0
	Talk: EPS theme 2 & Willie Commelin Scholten Day, Utrecht, NL	04 Feb 2020	1,0
	Talk: NLP Symposium, Paris, France	12 Feb 2020	1,0
	Talk: Insect and nonhost resistance group, Plant Breeding	26 Nov 2020	1,0
	Talk: Progress meeting STW user committee	03 Dec 2020	1,0
▶	**3rd year interview**		
▶	**Excursions**		
	Bejo Seeds open days, Warmenhuizen, NL	28 Sep 2017	0,3
	KeyGene, EPS PhD council, Wageningen, NL	12 Oct 2017	0,2
	Research group Barbara Blanco, University of California (UC) Davis, CA, USA	11 Mar 2019	0,3
		Subtotal Scientific Exposure	23,8

3) In-Depth Studies		*date*	*cp*
▶	**Advanced scientific courses & workshops**		
	Workshop: Plants & Patents, GeneSprout Initiative, Wageningen, NL	21 Oct 2019	0,2
	Workshop translational science: Taking MPMI Discoveries to the Field, online	02 Dec 2020	0,2
▶	**Journal club**		
	Botrytis group literature discussion sessions	2018-2021	1,5
	Laboratory of Phytopathology expert meetings literature sessions	2020-2021	1,0
▶	**Individual research training**		
	Research group Matthias Hahn, CRISPR-Cas9 in Botrytis, Technische Universität Kaiserslautern, Germany	19-23 Aug 2019	1,5
		Subtotal In-Depth Studies	4,4

4) Personal Development		date	cp
►	**General skill training courses**		
	EPS PhD Introduction Course, Wageningen, NL	26 Sep 2017	0,3
	Wageningen Graduate Schools PhD Workshop Carousel, Wageningen, NL	25 May 2018	0,3
	The Essentials of Scientific Writing & Presenting, Wageningen, NL	10-20 May 2019	1,2
	Wageningen Graduate Schools PhD Workshop Carousel, Wageningen, NL	24 May 2019	0,3
	Workshop: Scientific paper writing Sheba Agarwal-Jans, Wageningen, NL	24 Oct 2019	0,1
	Workshop: Applying for a Marie Skłodowska-Curie Fellowship: from proposal to project, Wageningen, NL	16 Dec 2019	0,2
►	**Organisation of meetings, PhD courses or outreach activities**		
	Member of the Laboratory of Phytopathology Management Team	Oct 2019-Oct 2020	1,5
►	**Membership of EPS PhD Council**		
	Subtotal Personal Development		3,9

5) Teaching & Supervision Duties		date	cp
►	**Courses**		
	Cell Biology CBI-10306	Nov-Dec 2017	3,0
	Cell Biology CBI-10306	Nov-Dec 2018	
	Cell Biology CBI-10306	Nov-Dec 2019	
	Ecological Aspects of Bio-interactions ENT-30306	Sep-Oct 2017	
	Ecological Aspects of Bio-interactions ENT-30306	Sep-Oct 2018	
	Ecological Aspects of Bio-interactions ENT-30306	Sep-Oct 2019	
►	**Supervision of BSc/MSc students**		
	MSc thesis Michele Malvestiti	Jul 2017-Dec 2017	3,0
	MSc thesis Sebastian Tonn	Jan 2018-Aug 2018	
	MSc thesis Jyotsna Nepal	Mar 2018-Sep 2018	
	MSc thesis Sander Langebeeke	Jan 2019-Aug 2019	
	MSc thesis Hilde Coolman	Jan 2019-Aug 2019	
	BSc thesis Christiaan Bootsma	Nov 2019-Jan 2020	
	Subtotal Teaching & Supervision Duties		6,0

TOTAL NUMBER OF CREDIT POINTS*	**39,6**

Herewith the Graduate School declares that the PhD candidate has complied with the educational requirements set by the Educational Committee of EPS with a minimum total of 30 ECTS credits.

** A credit represents a normative study load of 28 hours of study.*

The research described in this thesis was financially supported by the Dutch Technology Foundation STW, which is part of the Netherlands Organisation for Scientific Research (NWO), and which is partly funded by the Ministry of Economic Affairs, as well as by BASF Vegetable Seeds, Bejo Zaden, Hazera Seeds, Takii Europe and Holland Onion Association (project number 15003).

Financial support from STW for printing this thesis is gratefully acknowledged.

Cover design: Maikel Steentjes & Iliana Boshoven-Gkini | AgileColor.com
Layout design: Iliana Boshoven-Gkini | AgileColor.com
Printed by: GVO drukkers & vormgevers, gvo.nl